DOCTOR OF PHILOSOPHY

microRNA expression in colorectal tumours identification of novel mechanisms of gene regulation

Amankwatia, Edward Bobie

Award date:
2014

DOCTOR OF PHILOSOPHY

microRNA expression in colorectal tumours

identification of novel mechanisms of gene regulation

Edward Bobie Amankwatia

2014

University of Dundee

microRNA expression in colorectal tumours: identification of novel mechanisms of gene regulation

Edward Bobie Amankwatia

Thesis submitted for the degree of PhD

August 2014

University of Dundee

Table of Contents

List of Figures

List of Tables

List of abbreviations

2-DG	2-deoxy-D-glucose	**dNTP(s)**	Deoxyribonucleotide triphosphate(s)
3'UTR	3' untranslated region	**DPYD**	Dihydropyrimidine dehydrogenase
5-FU	5-Fluorouracil	**ds cDNA**	Double-stranded copy DNA
AMPK	5' adenosine monophosphate-activated protein kinase	**DSB**	Double-stranded breaks
APS	Ammonium persulfate	**ECAR**	Extracellular acidification rate
Asp	Aspartic acid	**EDTA**	Ethylenediaminetetraacetic acid
ATM	Ataxia telangiectasia mutated	**EGR**	Epidermal growth factor
ATP	Adenosine triphosphate	**EGFR**	Epidermal growth factor receptor
Bad	Bcl-2-associated death promoter	**ELISA**	Enzyme-linked immunosorbent assay
Bax	Bcl-2-associated X protein	**EMT**	Epithelial-to-mesenchymal transition
Bcl-2	B-cell lymphoma 2	**ERCC1**	Excision repair cross-complementing 1
BMM	Basement membrane matrix	**ERK**	Extracellular-signal-regulated kinase
BSA	Bovine serum albumin	**ERM**	External response monitor
CDK	Cyclin dependent kinase	**f.T.P**	Factor for temperature and pressure
cDNA	Complementary DNA	**FACS**	Fluorescence-activated cell sorting
CIN	Chromosomal instability	**FAP**	Familial adenomatous polyposis
CLL	Chronic lymphocytic leukaemia	**FBS**	Foetal bovine serum
CRUK	Cancer Research UK	**FDHU**	5-fluorodihydrouracil
Ct	Cycle threshold	**FdUMP**	Fluorodeoxyuridine monophosphate
CTC	Circulating cancer cells	**FdUTP**	Fluoro-deoxyuridine triphosphate
DAC	5-aza-2'-deoxycytidine	**FFPE**	Formalin-fixed, paraffin-embedded
DMEM	Dulbecco's Modified Eagle's Medium	**FRET**	Fluorescence Resonance Energy Transfer
DNMT	DNA methyltransferase	**FSC**	Forward scatter
DMSO	Dimethyl sulfoxide	**FUTP**	Fluorouridine triphosphate

G13D	Guanine to aspartic acid substitution (Codon 13)	**mTOR**	Mammalian target of rapamycin
GAP	GTPase activating protein	**MTT**	Thiazolyl Blue Tetrazolium Bromide
GDP	Guanosine disphosphate	**nC**	Nano Coulombs
GST	Glutathione-S-transferase	**NCI**	National Cancer Institute
GTP	Guanosine triphosphate	**NER**	Nucleotide excision repair
Gy	Gray	**NF-KB**	Nuclear factor kappa-light-chain-enhancer of activated B cells
HCC	Hepatocellular carcinoma	**OCR**	Oxygen consumption rate
HDAC	histone deacetylase	**Phe**	Phenylalanine
HGA	High grade adenoma	**PI**	Propidium iodide
HNPCC	Hereditary non-polyposis colorectal cancer	**PI3K**	Phosphoinositide 3-kinase
HRP	Horseradish peroxidise	**PMSF**	Phenylmethylsulfonyl fluoride
HSP27	Heat shock protein 27	**PRAS40**	Proline-rich Akt substrate of 40 kDa
IORT	Intraoperative radiotherapy	**pre-miRNA**	Precursor-microRNA
ITP	Inosine triphosphate	**pri-miRNA**	Primary-microRNA
LGA	Low grade adenoma	**PRS**	Photon radio-surgery system
MAPK	Mitogen-activated protein kinase	**qRT-PCR**	Quantitative real time polymerase chain reaction
MCM2	Minichromosome maintenance complex component 2	**RBD**	Raf-like Ras-binding domain
MEK	Mitogen-activated protein kinase kinase	**RFU**	Relative fluorescence units
miRNA(s)	microRNA(s)	**RIN**	RNA integrity number
MMP	Matrix mellatoprotease	**RISC**	RNA induced silencing complex
MMR	DNA mismatch repair	**RKIP**	Raf kinase inhibitory protein
mRNA	Messenger RNA	**RLU**	Relative luminescence units
MSI	Microsatellite instability	**RMA**	Robust Multi-array Average
MSS	Microsatellite stable	**rRNA**	Ribosomal RNA

RT	Reverse transcription
SAPK/JNK	Stress-activated protein kinase/c-Jun N-terminal kinase
SD	Standard deviation
SDS	Sodium dodecyl sulphate
SDS-PAGE	SDS-Polyacrylamide gel electrophoresis
SEM	Standard error of mean
Ser	Serine
SIGN	Scottish Intercollegiate Guidelines Network
SNP	Single nucleotide polymorphisms
snRNA	Small nuclear RNA
SSC	Side scatter
Stat1	Signal Transducers and Activators of Transcription-1
Stat3	Signal Transducers and Activators of Transcription-3
TEMED	Tetramethylethylenediamine
TGF- βR2	TGF-β receptor 2
TGF-β	Transforming growth factor beta
Thr	Threonine
TLDA	Taqman Low Density Array
TNM	Cancer Node Metastasis
TOPO1	Topoisomerase 1
Tyr	Tyrosine
TTP	Thymidine triphosphate
TYMP	Thymidine phosphorylase
TYMS	Thymidylate synthase
VE-cadherin	Vascular endothelial cadherin
VEGF	Vascular endothelial growth factor
WT	Wild type
ZEB	Zinc finger E-box binding homeobox

Acknowledgements

I would like to firstly thank my supervisors Dr Gillian Smith and Professor Roland Wolf for giving me the opportunity to pursue this research and for all their support and guidance throughout my PhD. I am also grateful for the clinical support and expertise provided by Professors Frank Carey, Alastair Munro and Robert Steele. I also thank the past and present members of the Smith laboratory for their kind support and their contribution to a pleasant working atmosphere.

I very much appreciate the following for the time they took to contribute to my work: Probir Chakravarty (CRUK Bioinformatics and Biostatistics Service, London) for his assistance with bioinformatics analysis, Dr Ian Sanders (Ninewells Hospital, Dundee) for teaching me how to operate the laboratory irradiator, Dr Michael Boylan for technical advice on the use of FACS analysis, Professor Julian Blow and colleagues (University of Dundee) for their assistance with some of my flow cytometry work, Professor Mike Ashford and Alison Milne (University of Dundee) for allowing me to use the Seahorse Bioanalyzer, the staff at the Wellcome Trust Clinical Research Facility (Edinburgh) for performing the Illumina HT-12 BeadChip mRNA expression arrays and Tayside Tissue Bank for providing the clinical samples necessary for this research.

I am thankful for the encouragement I received from my Thesis Monitoring Committee - Dr Frances Fuller-Pace, Professor Stewart Fleming and Dr Norman Pratt - and from all staff and students at the Division of Cancer Research (University of Dundee).

I am ever grateful to my family, who have always been loving and supportive throughout my studies.

Finally, this work would not have been possible without the funding received from the Medical Research Council and the Anonymous Trust (University of Dundee).

Declaration

I declare that the work presented in this thesis is, unless otherwise stated, entirely my own; that all references cited herein have been consulted by myself; and that this work has not been previously accepted for a higher degree

Edward B. Amankwatia

I certify that Edward Amankwatia has carried out research under my supervision, and has fulfilled the conditions of the relevant ordinance and regulation for the completion of a PhD

Professor Roland Wolf

Dr Gillian Smith

Abstract

Colorectal cancer is a major cause of cancer-related death in the UK, in part as a consequence of a failure to detect the disease at its early stages and also to treatment failure due to the development of drug and radiation resistance. MicroRNAs (miRNAs), small non-coding RNAs, regulate the expression of tumour suppressor genes and oncogenes including *KRAS* and may influence cancer development and drug and radiation response in colorectal cancer. MiRNAs therefore have potential as biomarkers of disease progression and treatment response.

Quantitative real time PCR analysis, in the form of Taqman Low Density Array (TLDA) miRNA cards, was firstly used to prolife colorectal adenomas, cancers and matched normal mucosae and isogenic *KRAS* mutant and wild-type colorectal cancer cell lines to identify potential candidate miRNAs that regulate KRAS signalling and are involved in colorectal cancer progression.

The over-expression of miR-224 was identified to be an early and persistent event in colorectal cancer as it was increased in colorectal adenomas and cancers compared to patient-matched normal tissue. MiR-224 expression was also increased in *KRAS* WT cells compared to mutant cells and in *KRAS/BRAF* WT colorectal cancers compared to *BRAF* mutant cancers. MiR-224 knockdown in *KRAS* WT cells increased the amount of GTP-bound activated KRAS, increased ERK 1/2 phosphorylation and also increased cellular 5-FU sensitivity thus mimicking a *KRAS* mutant phenotype. MiR-224 knockdown also reduced cell

invasion *in vitro* and miR-224 expression was additionally increased in liver metastases compared to patient-matched primary colorectal cancers.

To identify novel mechanisms of drug resistance, two colorectal cancer cell lines HCT116 and DLD-1 were made resistant to 5-FU or oxaliplatin, following continuous incremental drug selection, and chemosensitivity to the colorectal cancer drugs 5-FU, oxaliplatin and irinotecan were compared using MTT cytotoxicity assays. MiRNA and messenger RNA (mRNA) expression differences in paired drug sensitive and resistant cells were identified using TLDA miRNA cards and Illumina HT-12 BeadChip mRNA expression arrays. To identify miRNAs involved in KRAS-mediated radiation resistance, isogenic *KRAS* WT and mutant colorectal cancer cell lines were treated with 5 Gy of ionising radiation and profiled using TLDA miRNA cards.

MiRNA target prediction databases (mirDB, miRANDA, miRBase, TargetMiner and TargetScan) identified common candidate target genes for each differentially expressed miRNA, and Metacore analysis predicted key processes and pathways involved in drug and radiation resistance.

In the paired drug sensitive and resistant cell lines, miRNA and mRNA profiling and bioinformatics analysis predicted cancer-related pathways and processes involved with cell invasion, cell cycle regulation and glycolysis as drug resistance mechanisms, which were then experimentally validated. I identified candidate drug resistance genes (*ACTB, TUBB, ANGPTL4, MCM4, ALDOA, PGAM1, and AKR1C3*) involved in the aforementioned cancer-related pathways and processes

as well as candidate drug resistance miRNAs predicted to regulate the expression of my candidate drug resistance genes.

In radiation treated *KRAS* WT and mutant cells, the pathways and processes involved in radiation response were similar to those predicted in acquired drug resistance. I also identified a number of miRNAs, including miR-224, that were differentially expressed in irradiated *KRAS* WT and mutant cells and that may modulate KRAS-mediated radiation resistance.

My data suggests that miR-224 could be a useful disease progression biomarker, in conjunction with other markers, to aid in determining patient prognosis. Furthermore, this study has identified novel candidate drug and radiation resistance signatures that could aid as additional markers of treatment response.

Chapter 1

General Introduction

1.1. Introduction

1.1.1. The nature of colorectal cancer

Colorectal cancer is a disease characterised by cancerous growths within the colon and rectum. Initially, colorectal cancer presents as benign polyps (adenomas), some of which progress to colorectal adenocarcinomas and invade and metastasise to secondary sites within the body. Cases predominate in the left side of the bowel, with cancers in the sigmoid colon, recto-sigmoid junction and rectum accounting for 60% of colorectal cancer cases (CRUK, 2014; Figure 1.1). Colorectal cancer can be categorised into sporadic and familial, the latter of which accounts for less than 10% of colorectal cancer cases (Söreide *et al*, 2006).

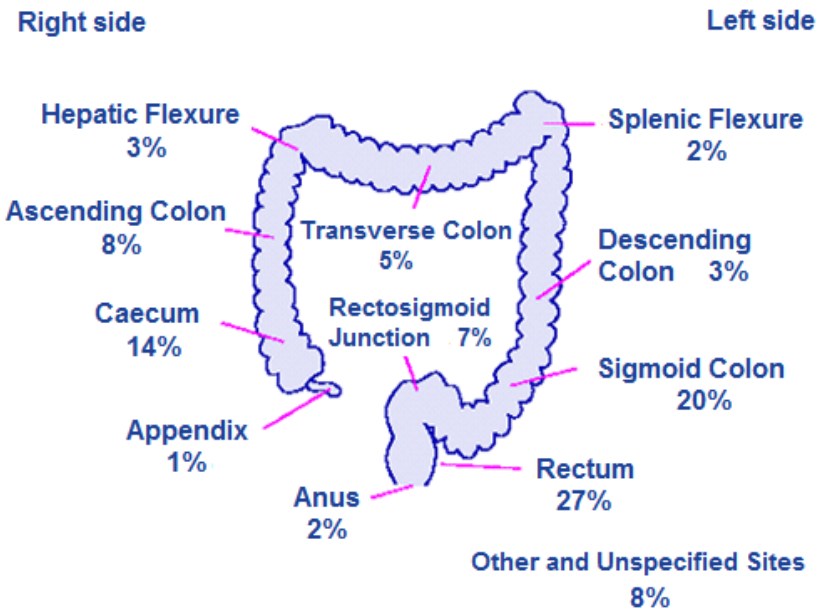

Figure 1.1: ***The anatomical distribution of colorectal cancer cases****. Data collected in the United Kingdom between 2007 and 2009 show that 60% of colorectal cancer cases were diagnosed on the left side of the bowel; namely in the descending colon, sigmoid colon, recto-sigmoid junction, rectum and anus (CRUK, 2014).*

According to Cancer Research UK (2014), colorectal cancer is the fourth most common type of cancer in the UK, with approximately 41,500 new cases diagnosed and about 16,000 deaths each year. The high number of deaths is attributed to the fact that patients tend to present with their cancers at advanced stages, thus reducing the 5 year survival success rate of current treatment (Wang & DuBois, 2009) and highlighting the importance of early detection and treatment of this disease.

The incidence of colorectal cancer has been shown to increase with age, with 84% of cases arising in people who are 60 years of age or older. Diet is also another major risk factor in the development of colorectal cancer. Countries such as Japan have recently seen an increase in the rate of colorectal cancers as they adopt a more 'westernised' lifestyle and diet rich in red meat and abandon the more traditional staple diets rich in fibre, fruit and vegetables (Tominaga & Kuroishi, 1997). It has also been shown that immigrants develop the same risk for colorectal cancer of their new country, often within one generation, most probably due to the adoption of the lifestyle and diet (Le Marchand, 1999). Furthermore, a meta-analysis by Ma *et al* (2013) of 54 studies reported a positive association with obesity (defined by body mass index or waist circumference) and a higher risk of developing colorectal cancer.

This brings into question, amongst other factors, the link between diet, lifestyle and the development of cancer. Additionally, patients with pre-existing chronic inflammatory diseases such as ulcerative and Crohn's colitis have a 70% higher

risk of developing colorectal cancer compared to the general population (Lutgens *et al*, 2013).

1.1.2. The development of colorectal cancer

As previously mentioned, some colorectal adenomas are precursors to the development of colorectal adenocarcinomas, although many remain benign. Colorectal adenomas histologically present as either tubular, tubulovillous or villous and increasingly change from displaying low to intermediate to high grades of dysplasia during colorectal cancer progression (Konishi & Morson, 1982).

Vogelstein *et al* (1988) initially proposed colorectal carcinogenesis to be driven by a progressive acquisition of genetic mutations and chromosomal deletions. Their initial study in 172 colorectal specimens at different stages of cancer development proposed that a mutation in the *KRAS* gene and allelic losses or mutations in chromosomes 5q, 17p and 18q which correspond to, among others, mutations in the *APC*, *TP53* and *DCC* genes respectively were required for the transition from normal colorectal epithelium to colorectal adenocarcinomas.

However, a number of groups have since shown that this proposed model does not represent the majority of colorectal cancers (Smith *et al*, 2002; Frattini *et al*, 2004; Samowitz *et al*, 2007). Smith *et al* (2002), for example, found in a cohort of 106 colorectal cancers, that there was variability in mutation burden. For instance, the *TP53* gene was mutated in 61.3% of all cancers, whilst 56% and 27.4% of the cancers had mutations in the *APC* and *KRAS* genes respectively.

Importantly, only 6% of all cancers had mutations in the *KRAS*, *TP53* and *APC* genes whilst approximately 11% contained no mutations in the aforementioned genes. Interestingly, mutations in *KRAS* and *TP53* were found to rarely occur together, suggesting that they were involved in different pathways that lead to cancer development. Thus the study concluded that the original colorectal cancer model proposed by Vogelstein in 1988 may not actually represent the vast majority of sporadic colorectal cancer cases as the progressive accumulation of multiple mutations in these genes is not a prerequisite for cancer development.

Microsatellite instability (MSI) is an alternative mechanism of colorectal cancer development (Kinzler & Vogelstein, 1996), in addition to chromosomal instability (CIN) which accounts for approximately 85% of colorectal cancer cases and is characterised by allelic losses, chromosomal amplification and translocations. MSI occurs as a result of frame-shift mutations or base pair substitutions in microsatellites, short tandem-repeated nucleotide sequences present within the genome (Söreide *et al*, 2006). MSI is caused by failure of the mismatch repair mechanism, either because of germline mutations in one of the mismatch repair genes such as *MLH1* (causing hereditary non-polyposis colorectal cancer; HNPCC) or through its epigenetic silencing (contributing to sporadic colorectal cancer; de la Chappelle, 2004). Colorectal cancers with MSI have also been shown to have mutations in a number of genes, including those coding for TGF-βR2 and the pro-apoptotic protein BAX (Fernández-Peralta *et al*, 2005), as well as β-catenin (Kim *et al*, 2003; Figure 1.2). In contrast, mutations in *KRAS* and

TP53 are inversely associated with MSI (Samowitz *et al*, 2001). Familial adenomatous polyposis (FAP), another type of familial colorectal cancer in addition to HPNCC, develops as a result of inherited alterations in the *APC* gene (de la Chapelle, 2004).

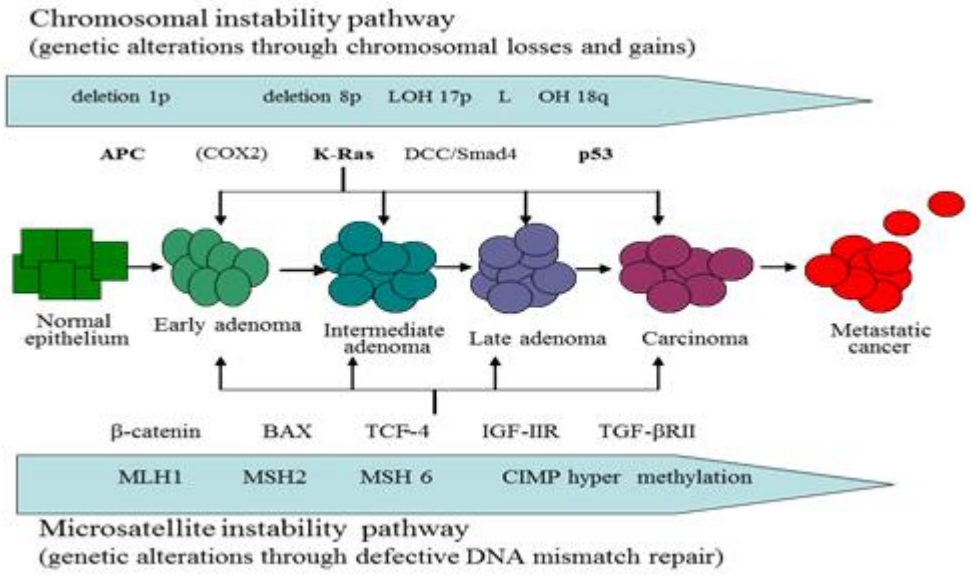

Figure 1.2: ***The genetic alterations in colorectal cancer.*** *The genetic alterations characterised by chromosomal changes and mutations in key genes in the chromosomal instability (microsatellite stable) pathway and the genetic alterations characterised by defects in DNA mismatch repair in the microsatellite instability pathway that contribute to colorectal cancer development as depicted in Söreide et al (2006). As discussed, not all mutations are required for colorectal cancer development.*

1.1.3. Limitations of current prognostic approaches to colorectal cancer

The current methods of determining the staging of colorectal cancer is through the TNM classification (Edge *et al*, 2010), although the Dukes' staging system is still used to a lesser extent and is referred to in earlier colorectal cancer studies.

This staging system describes the size of a primary cancer (T), whether the cancer has spread to any lymph nodes (N) and whether the cancer has spread to another part of the body or metastasised (M). Additionally, pathologists determine the grade (low grade, intermediate grade, high grade) of cancers by defining the extent of cancer differentiation and therefore aggressiveness. Tables 1.1 and 1.2 describe how colorectal cancers are classified or staged using the TNM classification system and Dukes' staging respectively.

Table 1.1: The TNM classification system (Edge *et al*, 2010)

Stage	Description	
Stage 1	Cancer has grown through the inner lining of the bowel, or into the muscle wall but no further. There is no cancer in the lymph nodes (T1, N0, M0 or T2, N0, M0).	
Stage 2	a	No cancer cells in the lymph nodes, but the cancer has broken through the outer covering of the bowel (T3, N0, M0)
	b	Cancer has grown through the outer covering of the bowel wall and into tissues or organs (T4) next to the bowel. But no lymph nodes are affected (N0) and the cancer has not spread to another area of the body (M0).
Stage 3	a	Cancer is still in the inner layer of the bowel wall or has grown into the muscle layer, and between 1 and 3 nearby lymph nodes contain cancer cells (T1, N1, M0 or T2, N1, M0)
	b	Cancer has grown through the bowel wall or into surrounding body tissues or organs and between 1 and 3 nearby lymph nodes contain cancer cells (T3, N1, M0 or T4, N1, M0)
	c	Cancer can be any size, has spread to 4 or more nearby lymph nodes, but there is no cancer spread to any other part of the body (any T, N2, M0)
Stage 4	Cancer has spread to other parts of the body (such as the liver or lungs) through the lymphatic system or bloodstream (any T, any N, M1).	

Table 1.2: The Dukes' staging (Dukes, 1932)

Stage	Description
Dukes A	Cancer only affects the innermost lining of the colon or rectum or slightly growing into the muscle layer
Dukes B	Cancer has grown through the muscle layer of the colon or rectum
Dukes C	Cancer has spread to at least one lymph node in the area
Dukes D	Cancer has spread to somewhere else in the body, like the liver or lung

These methods are problematic as they only correspond to the anatomical nature of the disease and, to a lesser extent, may be subjective depending on the assessing clinician. The current classification system is, however, important for determining the prognosis of patients. Figures from England between 1996 and 2002 show that patients who were diagnosed at the earliest stage of colorectal cancer had a 93% five-year relative survival rate. This is vastly in contrast to patients who were diagnosed at the most advanced stages of colorectal cancer who were shown to have a 7% five-year relative survival rate (CRUK, 2014). This therefore highlights the importance of early detection and treatment of this disease. National screening programmes are in place where people in higher risk age groups (between 50 and 74 in Scotland) are sent faecal occult blood tests every two years to test for blood in their stool. These programmes aim to detect colorectal polyps or early stage colorectal

adenocarcinomas and, in Scotland, are reported to prevent at least 150 deaths from colorectal cancer each year (Scottish Bowel Screening Programme, 2014).

However, despite these programmes, there is a need for molecular determinants that can further stratify patients into different risk categories and aid with prognosis and response to treatment.

1.1.4. Current drug therapeutic approaches to colorectal cancer

The first line of treatment for colorectal cancer patients is surgical resection, although this is only curative if the cancer is diagnosed at its early stages (Walther *et al*, 2009). In cases where the cancer has metastasised, neo-adjuvant (before surgery) or adjuvant (after surgery) chemotherapy is administered to patients in addition to surgical resection (Walther *et al*, 2009). Additionally, radiotherapy may also be administered, usually for the treatment of rectal cancer.

5-Fluorouracil (5-FU) has been the mainstay treatment in colorectal cancer for over 50 years (Longley *et al*, 2003). 5-FU exerts its cytotoxic effects through its active metabolites (Figure 1.3). The main mechanism of action of 5-FU is through the active metabolite (FdUMP), which forms an irreversible complex with thymidine synthase (TYMS). This results in the depletion of thymidine triphosphate (TTP), one of the four nucleotide triphosphates used in the *in vivo* synthesis of DNA (Longley *et al*, 2003). Additionally, fluoro-deoxyuridine triphosphate (FdUTP) and fluorouridine triphosphate (FUTP) are active metabolites that are misincorporated into DNA and RNA (replacing uracil)

respectively, thus inhibiting DNA and RNA synthesis and consequently cell growth (Longley *et al*, 2003; Figure 1.3).

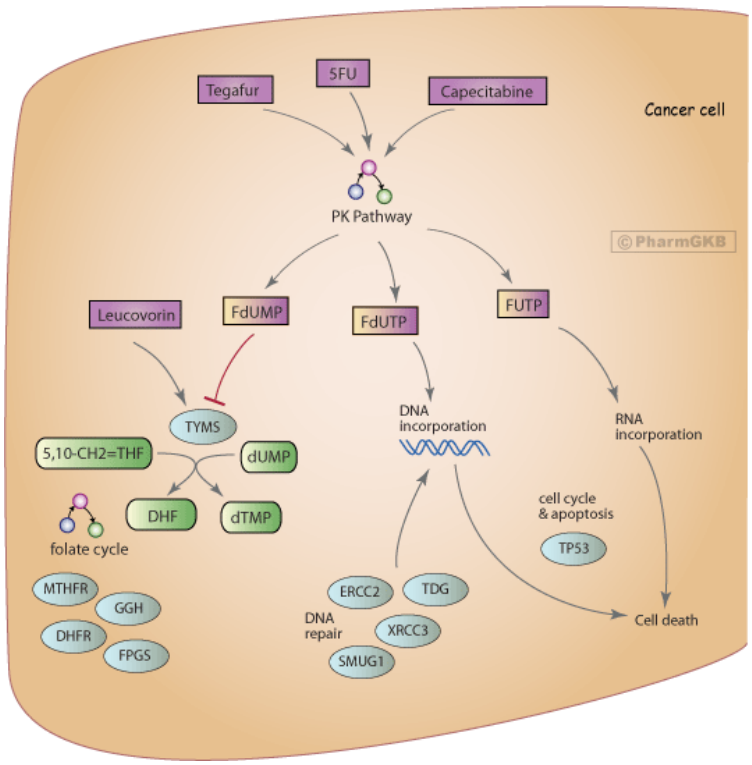

Figure 1.3: ***The mechanisms of action of the active metabolites of 5-FU.*** *5-FU is metabolised to FdUMP, FdUTP and FUTP which respectively inhibits the action of TYMS, incorporates into DNA and incorporates into RNA (http://www.pharmgkb.org/pathway/PA165291507).*

5-FU or its pro-drug capecitabine is administered, either as bolus injections or by continuous infusion, with leucovorin (folinic acid). Leucovorin is co-administered to strengthen the binding of FdUMP to TYMS and thus potentiate the effect of 5-FU. 5-FU or capecitabine are also co-administered with other drugs to increase efficacy in patients. The FOLFOX regimen consists of 5-FU, oxaliplatin and leucovorin whereas XELOX consists of capecitabine and oxaliplatin. Additionally, FOLFIRI consists of the administration of 5-FU, irinotecan and leucovorin. Current treatment guidelines in Scotland suggest that oxaliplatin should be used

as second line therapy following first line irinotecan therapy and *vice versa* (Scottish Intercollegiate Guidelines Network (SIGN), 2011). Response to 5-FU in colorectal cancer patients as monotherapy has been shown to be approximately 10-15% (Johnston & Kaye, 2001). However, response rate has been shown to improve to up to 50% when 5-FU and folinic acid is co-administered with oxaliplatin or irinotecan (de Gramont *et al*, 2000; Douillard *et al*, 2000).

Oxaliplatin is a platinum-based agent which binds preferentially to the guanine and cytosine moieties of DNA, leading to cross-linking of DNA and thus inhibiting DNA synthesis and function (Di Francesco *et al*, 2002). The active metabolite of irinotecan, SN-38 (Figure 1.4), inhibits DNA Topoisomerase I (TOPO1), a nuclear enzyme which functions by unwinding DNA for replication and prevents DNA strand breaks (Pommier *et al*, 2010).

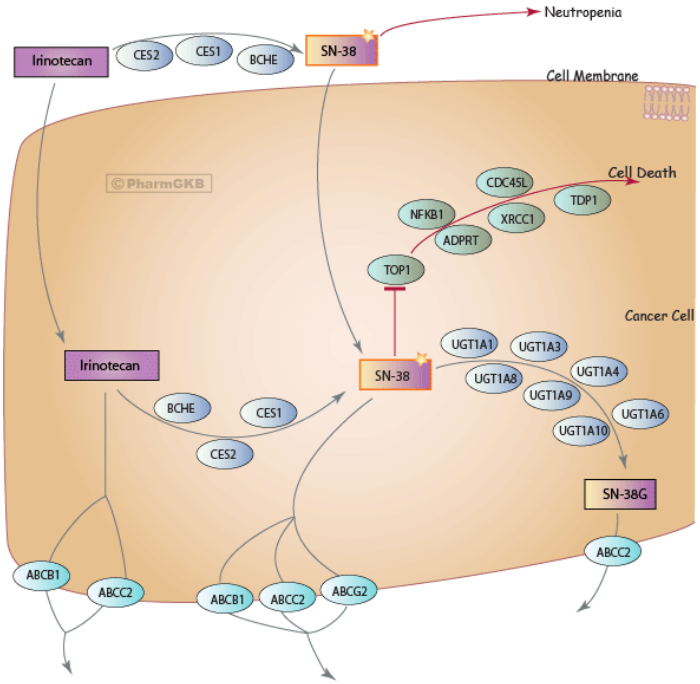

Figure 1.4: ***The mechanism of action of irinotecan****. Irinotecan is metabolised to SN-38 by butyrylcholinesterase (BCHE) and liver carboxylesterases (CES1 and CES2) and inhibits the action of topoisomerase 1 (TOP1). SN-38 thus prevents DNA unwinding (by inhibiting TOP1) and causes DNA damage leading to cell death. The action of SN-38 is deactivated by the action of UDP-glucuronosyltransferase enzymes (e.g. UGT1A1; http://www.pharmgkb.org/pathway/PA2029).*

Recently, biological treatment such as humanised targeted monoclonal antibodies towards the epidermal growth factor receptor (EGFR) have been approved to treat colorectal cancer patients with metastatic disease, in combination with standard chemotherapy (SIGN, 2014). Studies have shown an improved efficacy for cetuximab in *KRAS* WT colorectal cancer patients (Lievre *et al*, 2006; Bokemeyer *et al*, 2008; Amado *et al*, 2008) compared to *KRAS* mutant patients.

The inter-patient differences in response to chemotherapeutic drugs and biological therapy highlights the importance of identifying prognostic molecular

markers which may be used to select the most appropriate patients for adjuvant chemotherapy or to identify colorectal cancer patients at increased risk of disease progression.

1.1.5. Molecular therapeutic biomarkers

There is considerable interest in how somatic mutations and genetic alterations previously mentioned to play key roles in colorectal cancer development and progression could affect patient survival and response to treatment. *KRAS* mutation status, as previously mentioned, has been shown to play a role in patient response to anti-EGFR therapy.

KRAS is one of three human RAS genes (the others being *NRAS* and *HRAS*) that code for small $p21^{RAS}$ G proteins which transduce signals across the plasma membrane and mainly activate the RAS/MAPK signalling pathway (Barbacid, 1990). The proteins thus play key roles in the control of cell growth and differentiation through their intrinsic GTPase activity (Downward *et al*, 2003).

KRAS in its active form binds guanosine triphosphate (GTP) allowing it to affect downstream signalling pathways. However, GTPase activating protein (GAP) triggers the hydrolysis of GTP to guanosine disphosphate (GDP), resulting in the inactivation of KRAS (Figure 1.5; Ellis & Clarke, 2000). The mutant form of KRAS is constantly activated as it is less sensitive to the hydrolysing action of GAP (Downward *et al*, 2003). Therefore, in its constitutively active form, KRAS induces unregulated cellular proliferation leading to malignant transformation.

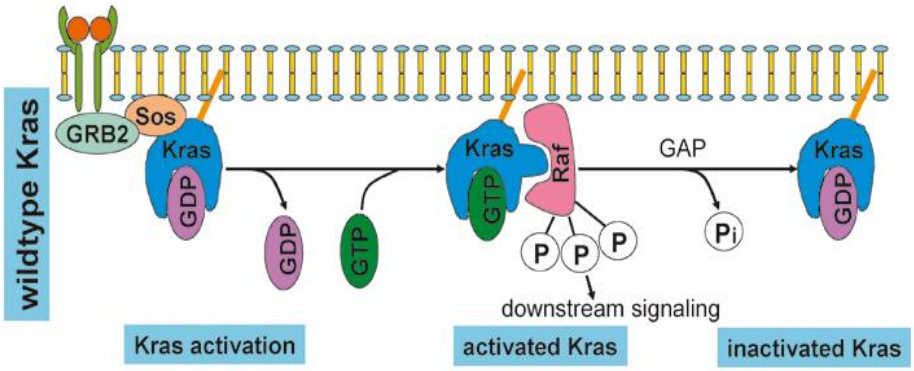

Figure 1.5: ***The activation and inactivation of KRAS*** *(Wicki et al, 2010).*

KRAS gene mutations, particularly in exon 1 (codon 12 and 13) and exon 2 (codon 61) have been evaluated for their association with colorectal cancer outcome. Many groups have linked *KRAS* mutations in these regions with advanced cancer stage (Smith *et al*, 2002) and poor prognosis (Andreyev *et al*, 1998; Andreyev *et al,* 2001; Conlin *et al*, 2005). Smith *et al* (2010) also identified a number of other *KRAS* mutations in addition to those in codons 12, 13 and 61. An alanine-to-threonine amino-acid substitution at codon 146 (A146T), in particular, was shown to occur as frequently as mutations in codon 13. In experiments using NIH3T3 mouse fibroblast cells stably transfected with various mutants of *KRAS*, cells with A146T *KRAS* mutations were found to have a similar transforming phenotype to mutations in codon 13 (Smith *et al*, 2010).

Many groups have also demonstrated that *KRAS* mutant colorectal cancer patients are less likely to respond to anti-EGFR therapy such as cetuximab and panitumumab compared to WT *KRAS* patients (Lievre *et al*, 2006; Bokemeyer *et al*, 2008; Amado *et al*, 2008). The binding of a specific ligand to EGFR activates a number of signalling cascades including the RAS/MAPK pathway (Figure 1.6).

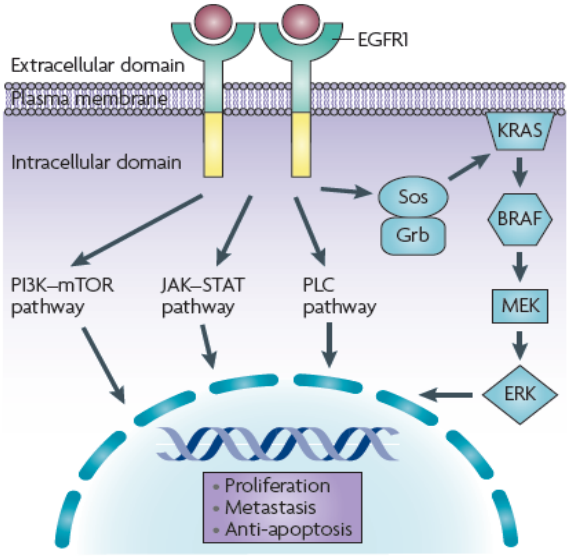

Figure 1.6: ***The downstream effects of EGFR*** *(Walther et al, 2009).*

Cetuximab and panitumumab exert their anti-cancer effects by targeting and blocking the extracellular domain of EGFR, which is up-regulated in 60-80% of colorectal cancer cases (Cunningham *et al*, 2004), and thus reducing oncogenic growth signalling. However, mutations in *KRAS* lead to the constitutive activation of downstream signalling pathways, rendering the vast majority of *KRAS* mutant patients nonresponsive to anti-EGFR therapy as EGFR no longer has regulatory control over KRAS.

DiNicolantonio *et al* (2008) showed in a cohort of 113 metastatic colorectal cancer patients that a lack of response to cetuximab in *KRAS* WT patients was very strongly associated with the presence of a *BRAF* ^{V600E} mutation. *KRAS* and *BRAF* mutations have been found to be mutually exclusive events (Rajagopalan *et al*, 2002) and both genes could be important determinates of resistance to EGFR-specific therapies.

The role of *KRAS* mutation status in response to cytotoxic drugs such as 5-FU has also been studied. *In vitro* studies from Klampfer *et al* (2005) and work later presented in this study (Chapter 3) showed that cells with mutant or increased KRAS activity were more sensitive to 5-FU. However, large scale clinical studies have not reported any conclusive associations between *KRAS* mutation status and response to 5-FU-based therapy (Markowitz *et al*, 1995; Etienne-Grimaldi *et al*, 2008).

1.1.6. Current radiotherapy approaches to rectal cancer

Radiation therapy is used for the treatment of stage III rectal cancer patients and is delivered from the outside of the body through the pelvic area. Radiotherapy is delivered as neo-adjuvant or adjuvant therapy to shrink the size of the cancer before surgery or for easier removal of the cancer after surgery. Treatment options include pre-operative short course radiotherapy where patients receive 25 Gy of radiation in 5 fractions over the course of 5 days (SIGN, 2014). Additionally, longer course pre-operative pelvic radiotherapy at doses exceeding 30 Gy (administered in a number of fractions over 5-6 weeks) is another option possibly in combination with chemotherapy, before or after surgery (SIGN, 2014).

The division of radiation doses into smaller fractions allows for a compromise between killing cancers and limiting the toxicity to normal adjacent tissue. This allows for the repair, repopulation, redistribution and reoxygenation of normal and cancer cells in what is known as the ‘4 R’s of radiotherapy’ as described by

Withers in 1975. These factors, as well as the intrinsic radio-sensitivity of cancers, dictate response to radiation therapy.

The repair and repopulation of cells between fractions allow for DNA damage repair and cell growth to occur in normal and cancer cells. This has been shown in breast cancer to be one of the possible mechanisms of radiation resistance as this has a negative effect on cancer shrinkage (Bese *et al*, 2005). Cells have been shown to be more sensitive to radiation during mitosis and the late G2 phase of the cell cycle (Pawlik & Keyomarsi, 2004). The redistribution of cells between fractions allows for the progression of cells that were originally resistant to radiation to the more radiation sensitive phases of the cell cycle (Withers, 1975). Hypoxic tissues were suggested to be more radiation resistant than normoxic tissues by Gray *et al* (1953). Reoxygenation describes the ability of hypoxic regions of cancers to become reoxygenated once the more normoxic, radiosensitive cancer cells have been killed (Semenza et al, 2004).

Intrinsic radio-sensitivity of cancers was later described as the 5^{th} 'R' of radiotherapy and is unaffected by fractionation (Steel *et al*, 1989). Although a number of factors may govern intrinsic radiation sensitivity, Chapter 5 discusses the role of the KRAS pathway in radiation resistance.

1.1.7. The nature of microRNAs

Much work has been conducted to show how molecular characteristics of cancers could act as potential markers of patient prognosis and response to chemo- and radiotherapy. However, microRNAs (miRNAs) have in the last 15 years emerged as additional regulators of gene expression. In light of this, it is necessary to gain better insights into the role of miRNAs in colorectal cancer development and regulating chemotherapy and radiotherapy response in patients.

MiRNAs are small non-coding RNAs (18-25 nucleotides) which function by repressing protein translation by binding to target messenger RNAs (mRNAs; Bartel, 2004). MiRNAs were initially discovered when the *lin-4* gene, which codes for a small non-coding RNA molecule, was found to regulate development in *Caenorhabditis elegans* (Lee *et al*, 1993). MiRNAs have since been identified in a number of species, including humans. It is suggested that miRNAs regulate up to 30% of all human genes and that each miRNA has control over hundreds of gene targets (Lewis *et al*, 2005). MiRNAs therefore play an important regulatory role in processes such as development, cellular differentiation, proliferation and apoptosis and thus have wider roles in diseases such as cancer (Esquela-Kerscher & Slack, 2006).

MiRNA genes are present throughout the genome and are transcribed from their own promoters by the action of RNA polymerase II or III to generate primary microRNA (pri-miRNA; Bartel, 2004). As shown in Figure 1.7, pri-miRNAs

are cleaved to precursor miRNA (pre-miRNA), a 70-nucleotide stem loop structure, by a microprocessor comprising Drosha (a ribonuclease) and DGCR8 (a double stranded RNA binding protein). Pre-miRNA is then transported from the nucleus to the cytoplasm by Exportin-5. In the cytoplasm, pre-miRNA is cleaved by a complex formed of the endonuclease enzyme Dicer and the double-stranded RNA binding protein TRBP to form a double-stranded miRNA duplex. One of the strands, together with argonauate (Ago2) then incorporates into the RNA-induced silencing complex (RISC). The passenger miRNA star (*) strand (e.g. miRNA-18*) is usually degraded although it can also be incorporated into RISC.

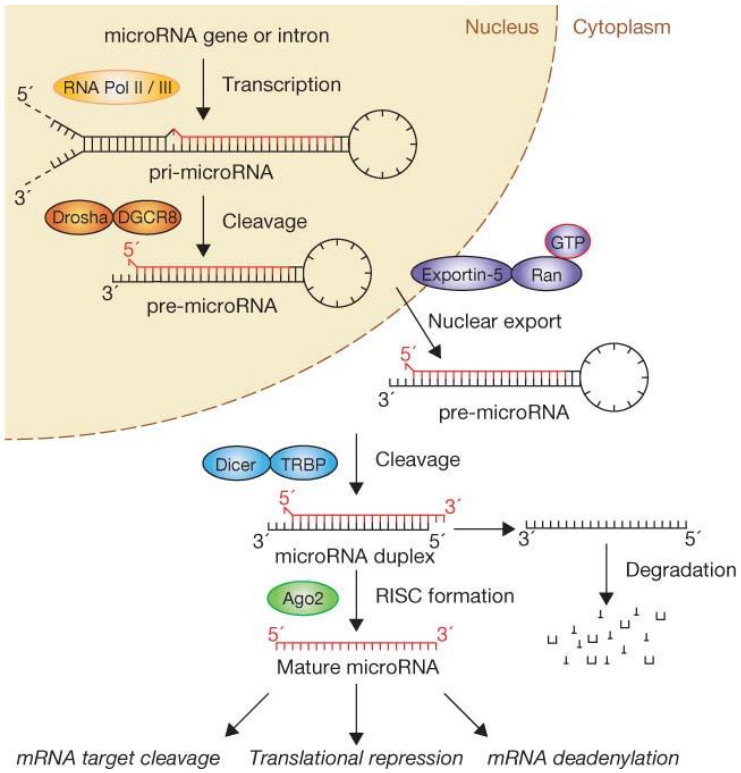

Figure 1.7: ***The classical pathway of microRNA processing*** *(Winter et al, 2009).*

Mature miRNAs are guided towards the 3'-untranslated region (3'-UTR) of an mRNA target and bind to imperfect complementary sites. This interaction leads to suppressed gene expression through mRNA cleavage, translational repression or mRNA de-adenylation (Winter *et al*, 2009). Imperfect complementarity results in one miRNA having the ability to repress the protein expression of hundreds of mRNA targets (Winter *et al*, 2009).

Studies have shown that the 'classical' miRNA maturation steps described above are not universal to all miRNAs as once believed. For example, Drosha complexes containing multiple proteins including the RNA helicases p72 and p68 have been suggested to process a subset of miRNAs, as evidenced by the reduced expression of certain miRNAs in homozygous p71 $^{(-/-)}$ and p68 $^{(-/-)}$ null mice, whilst the expression of other miRNAs remained unchanged (Fukuda *et al*, 2007). Viswanathan *et al* (2008) have also shown that LIN28 regulates the processing of let-7.

1.1.8. Role of miRNAs in carcinogenesis

The differential expression of miRNAs has been implicated in a number of cancers and their precise role in carcinogenesis is influenced by whether they target key tumour suppressor or oncogenic genes (Esquela-Kerscher & Slack, 2006; Volinia *et al*, 2006). The miRNAs differentially expressed in colorectal cancer are discussed further in Chapter 3. MiRNAs are reported to be differentially expressed due to chromosomal abnormalities, epigenetic changes,

the action of transcription factors, genetic mutations and abnormalities in miRNA biogenesis (Deng *et al*, 2008).

Calin *et al* (2002) were the first to report the down-regulation of miRNA-15 (miR-15) and miR-16 in over 70% of chronic lymphatic leukaemia (CLL) cases, suggesting their role as tumour suppressor genes in CLL. Further studies mapping the chromosomal locations of all known miRNAs revealed that many miRNA genes are located in fragile chromosomal sites frequently deleted or amplified in many human cancers (Calin *et al*, 2004*b*). In colorectal cancer, Bandres *et al* (2006) observed a differential down-regulation of chromosome 14q31 which contained a cluster of miRNAs, which were differentially decreased in colorectal cancer cell lines.

Expression of miRNAs can additionally be affected by epigenetic changes, such as the methylation of the CpG islands of their promoters. CpG islands, which consist of a sequence of cytosine-guanine dinucleotides, are located in the 5' region of many genes and are normally transcribed in the presence of the appropriate transcription factors (Croce, 2009). However, methylation of CpG islands by DNA methyltransferases (DNMTs) results in silencing of the gene and possible histone modifications (Croce, 2009). Thus, the methylation and silencing of miRNAs that normally have cancer suppressive functions, may contribute to its decreased expression and oncogenic cellular characteristics.

Toyota *et al* (2008) identified 37 miRNAs that were significantly up-regulated by DMNT inhibition in HCT116 cell lines. The study focused on the miR-34b/c genes, due to their association with p53, and found that the CpG islands in these genes

were frequently methylated and under-expressed in colorectal cell lines and cancer samples compared to normal colorectal mucosa. This effect was reversed following the treatment with 5-aza-2'-deoxycytidine (DAC), a DNA methylation inhibitor. Additional studies (Brueckner *et al*, 2007; Bandres *et al*, 2009; Balaguer *et al*, 2010) identified different miRNAs to be methylated in colorectal cancer. It is likely that those differences were due to the inter-individual variability between the colorectal cancer genotypes.

The expression of most miRNAs is controlled by transcription factors, and abnormalities in transcriptional regulation have been shown to contribute to differential miRNA expression in cancer. For example, the oncogenic miR-17-92 cluster (which comprises miR-17, miR-20a, miR-18a, miR-19a, miR-19b, miR-92) is regulated by c-Myc. c-Myc is over-expressed in several human cancers and may be one of the mechanisms by which the miR-17-92 cluster is over-expressed in cancer (Chang *et al*, 2008).

A study by Landi *et al* (2008) also revealed that single nucleotide polymorphisms (SNPs) exist within the 3'-UTR of the mRNA and thus affect miRNA-mRNA interaction. The study identified 2 polymorphisms, from 104 candidate colorectal cancer genes, that affected miRNA binding sites and increased risk of colorectal cancer. Similarly, SNPs affecting the proteins involved in miRNA biogenesis pathways have been associated with an increased risk of renal cell carcinoma (Horikawa *et al*, 2008; Lin *et al*, 2010) and lung cancer (Kim *et al*, 2010).

Since their discovery miRNAs have been described to have roles in the development of cancer through the negative regulation of key oncogenes and tumour suppressor genes (Esquela-Kerscher & Slack, 2006) and to predict patient prognosis (Calin *et al*, 2004*a*). MiRNAs have also been reported to be differentially expressed in response to chemo- and radiotherapy and may play a key role in regulating and predicting cellular response to treatment and in drug and/or radiation resistance (Hummel *et al*, 2010).

1.1.9. Aims and objectives

The aims of the present study were therefore to explore the potential of miRNAs as markers and modulators of disease progression and treatment response in colorectal cancer by undertaking 3 separate approaches:

Firstly, the present study aimed to explore how the inter-individual expression of miRNAs that regulate KRAS and its downstream pathways contributed to colorectal cancer progression and whether they could further sub-classify colorectal cancers at a molecular level (Chapter 3).

Secondly, the study aimed to identify a miRNA and mRNA signature of drug resistance in colorectal cancer by profiling 5-FU and oxaliplatin resistant colorectal cancer cells that were created by incremental drug selection, to gain a better understanding into the mechanisms of acquired drug resistance (Chapter 4).

Finally, the present study also aimed to use an *in vitro* model of radiation therapy to identify a miRNA radiation response signature that would help in the understanding of the cellular response to radiation and mechanisms by which KRAS signalling affects radiation sensitivity (Chapter 5).

Chapter 2

Materials and Methods

2.1. Materials

2.1.1. Chemicals and reagents

Mammalian cell culture

The following were purchased from Life Technologies: McCoy's 5A medium, Dulbecco's Modified Eagle's Medium (DMEM; no phenol red), 0.25% Trypsin/EDTA with phenol red, foetal bovine serum (FBS), penicillin/streptomycin solution, mirVana™ microRNA inhibitors (miR-224 and negative control), mirVana™ microRNA mimics (miR-224 and negative control) and Lipofectamine 2000. MTT reagent and dimethyl sulfoxide (DMSO) were purchased from Sigma-Aldrich. The Calbiochem InnoCyte invasion assay was purchased from Merck Millipore.

Drugs

5-Flurouracil and oxaliplatin were purchased from Sigma-Aldrich. Sorafenib-Tosylate was purchased from Selleckchem.

Molecular biology

The following were purchased from Life Technologies: pre-developed TaqMan® Small RNA Assays, pre-developed TaqMan® Gene Expression Assays, TaqMan® Reverse Transcription Reagents, TaqMan® Universal PCR Master Mix No AmpErase® UNG, TaqMan® Low Density Array microRNA cards (Card A), Megaplex™ Reverse Transcription Primers Human Pool A v2.1, Illumina® TotalPrep™ RNA Amplification Kit and RecoverAll™ Total Nucleic Acid Isolation

Kit for FFPE. The RNeasy Mini Kit and RNase free DNase Kit were purchased from Qiagen.

Protein analysis

The Bradford protein assay was purchased from Bio-Rad. The protease inhibitor phenylmethylsulfonyl fluoride (PMSF) was purchased from Sigma-Aldrich. The rainbow marker was purchased from Life Technologies. The Ras GTPase Chemi ELISA was purchased from Active motif. The PathScan Intracellular Signalling Array kit and 1X cell lysis buffer were purchased from Cell Signalling Technology. The ECL-chemiluminescence kit was purchased from GE Healthcare Life Sciences.

Antibodies

The anti-γ-H_2AX (anti-mouse) was purchased from Cell Signalling Technology and β-actin antibody (anti-mouse) was purchased from Millipore. All secondary antibodies were purchased from Dako.

Flow cytometry

Propidium iodide and ribonuclease (RNase A) were purchased from Sigma-Aldrich. The CellTrace Violet Cell Proliferation and SYTOX AADvanced Dead Cell Stain Kits were purchased from Life Technologies.

Seahorse

All reagents used in Seahorse glycolysis experiments were purchased from Seahorse Bioscience.

Chemicals

All other chemicals were purchased from Sigma Aldrich unless otherwise stated.

2.2. Methods

2.2.1. Ethical approval

All studies involving human tissue were approved by the Tayside Tissue Bank Research Ethics Committee, a devolved sub-committee of the Tayside Committee on Medical Research Ethics.

2.2.2. Mammalian cell culture

Six colorectal cancer cell lines were used for the present study. HCT116 and DLD-1 cell lines were obtained from Cancer Research UK Cell Services (London Research Institute). HCT116 is one of 3 subpopulations of malignant cells that were isolated from a primary culture of a human colorectal carcinoma obtained during surgery (Brattain *et al*, 1981). Similarly, the DLD-1 cell line was derived from specimens of colon adenocarcinomas removed during normal surgery (Dexter *et al*, 1979).

Additionally, isogenic HCT116 and DLD-1 lines specifically engineered to express the wild type (WT) or mutant form of *KRAS* were kindly donated by the laboratory of Dr Bert Vogelstein (John Hopkins University, Baltimore, MD). The parental HCT116 and DLD-1 lines have a WT *KRAS* allele and an allele with a G13D *KRAS* mutation (Jiang *et al*, 1989; Shirasawa *et al*, 1993). Isogenic cell lines

were created by deleting an allele by targeted homologous recombination to create *KRAS* mutant ($^{(KRAS\ G13D/-)}$) and WT ($^{(KRASWT/-)}$) HCT116 or DLD-1 colorectal cancer cell lines (Shirasawa *et al*, 1993; Torrance *et al*, 2001).

Cells were cultured in McCoy's 5A medium with 10% foetal bovine serum (FBS) and 1% antibiotics (penicillin and streptomycin). To ensure optimum growth, cells were routinely passaged or sub-cultured once they had reached approximately 70% confluence. Growth media was aspirated from the flask and the cells were washed once with phosphate buffered saline (PBS). The cells were then detached from the bottom of the flask by adding 2 ml 0.25% trypsin/EDTA and incubating at 37°C for 3-5 minutes. Growth media was then added to the flask to inhibit the effect of trypsin (media to trypsin ratio of 5:1) and cells were re-seeded in a fresh flask at a typical dilution factor of 1:10.

Frozen cell stocks were created by trypsinising cells and centrifuging the cell suspension for 3 minutes at 1200 rpm. The cell pellet was then re-suspended in 4 ml of freezing mixture (FBS and 10% (v/v) DMSO) and 1 ml of the cell suspension was transferred into cryovials. The cryovials were placed in a Nalgene Cryo freezing container containing isopropanol which freezes cells at a controlled rate of 1°C per minute. The container was initially stored at -80°C before the cryovials were transferred into liquid nitrogen for long term storage.

2.2.3. Growth assays

Growth assays were conducted to monitor the relative growth levels of different cell lines over a 48 hour time period. In order to calculate the number of cells in

a cell suspension a haemocytometer was used for cell counting. A cover slip was placed onto the haemocytometer ensuring that the gridlines used to count the cells were covered. A small volume of cell suspension (10 µl) was then pipetted between the cover slip and haemocytometer. Observing under a microscope, the total number of cells in the four outer boxes was counted. The number of cells per ml of cell suspension was then calculated by determining the mean number of cells per box (dividing the total cell count by 4) and multiplying by the correction factor, 10^4.

For growth assays, cells were seeded in 6 well plates (well diameter: 3.5 cm) at a density of 1 x 10^5 cells per well and incubated at 37°C and 5% CO_2 for 24 hours to allow for attachment and growth. Cells were then detached from the plate using trypsin at alternate 16 and 8 hour intervals (16 h, 24 h, 32 h, and 48 h). The cell suspension was added to a universal tube containing growth media to make a cell suspension with a total volume of 3 ml. The total number of cells were then counted and plotted against the number of hours since seeding. The doubling time of cells was also calculated as shown in Box 2.1 using an exponential trend line and equation.

Exponential equation: $y = ae^{bx}$

Where a = number of cells at 0 hours, b = growth rate and x = doubling time

Doubling time (x) = ln (2)/b

Box 2.1: ***Method for calculating cell doubling time*.**

2.2.4. MTT assay

The MTT assay is a colorimetric assay for determining cell viability (Mosmann, 1983). It can therefore be used as a measure of relative cytotoxicity caused by drug treatment in different cell lines. MTT is a yellow tetrazolium salt which is reduced to purple formazan crystals by the mitochondrial enzyme succinate dehydrogenase in active and living cells. The amount of formazan crystals is therefore proportional to the number of viable cells present in a given sample and can be estimated using a spectrophotometer.

Assays were conducted in sterile 96 clear flat-bottomed well plates. Cells were seeded at a density of 3000 cells per well, in a total volume of 100 µl growth media, and incubated at 37°C and 5% CO_2 for 24 hours to allow for attachment and growth. Following incubation, growth media was removed from each well and replaced with media containing drug. For chemosensitivity studies, each cell line was plated in triplicate per drug concentration (Table 2.1).

Table 2.1: MTT drug concentrations

5-FU concentration (µM)	Oxaliplatin concentration (µM)	Irinotecan concentration (µg/ml)	Sorafenib concentration (µM)
Vehicle control (DMSO)	Vehicle control (DMSO)	Vehicle control (DMSO)	Vehicle control (Water)
1.25	1.25	0.625	0.94
2.5	2.5	1.25	1.88
5	5	2.5	3.75
10	10	5	7.5
20	20	10	15
40	40	20	30
80	80	40	60

Drug concentrations were previously determined in preliminary experiments to find an optimum drug concentration range for drug response. A vehicle control containing the agent that each drug was solubilised in was also included in triplicate. Cells were then incubated with drug (or vehicle control) for 72 hours. Growth media containing drug or vehicle control was then removed from each well and 100 µl of 5 mg/ml MTT dissolved in phenol red deficient DMEM growth media was added to each well and incubated for 3 hours. After removal of the MTT solution, 100 µl DMSO was added to each well to solubilise the formazan crystals which are insoluble in aqueous solutions. The absorbance was then read using a ThermoScan microplate reader at a wavelength of 570 nm.

The mean absorbance for each drug concentration was calculated and represented as a percentage of the mean absorbance of the vehicle controls (designated 100%). The percentages were then plotted against the $\log_{[10]}$ of the drug concentrations on GraphPad Prism version 6. The graphs were fitted with a best fit sigmoid curve and the IC_{50}, the drug concentration at which 50% of cells are viable, was calculated.

2.2.5. Transfection

The function of miR-224 was investigated by the transient transfection of cells with a specific miRNA inhibitor or mimic. MiRNA inhibitors or antagomirs are chemically modified, single-stranded oligonucleotides which specifically bind to complementary endogenous mature miRNAs, thus competitively inhibiting the ability of miRNAs to bind to the 3'UTR of their target gene. MiRNA inhibitors are

designed to be more resistant to degradation than endogenous miRNAs within the cell. MiRNA mimics are modified double-stranded RNAs that mimic, or increase the effects of, endogenous miRNAs. The mature strand of the double stranded molecule is, like endogenous miRNAs, incorporated into the RNA induced silencing complex (RISC) by the Argonuate protein. The miRNA star (*) passenger strand is subsequently cleaved and expelled. In the present study, miRNA inhibitors and mimics were introduced into cells using Lipofectamine 2000 (Life Technologies). This allows the formation of liposomes around the inhibitors or mimics, which binds to the plasma membrane and export their contents into the cytoplasm of a cell.

Cells (1×10^5 per well) were seeded in six well plates and incubated for 24 hours to allow for attachment. For miR-224 knockdown experiments, HCT116 *KRAS* WT cells were transfected with a final concentration of 30 nM miR-224 inhibitor or miRNA inhibitor negative control (Life Technologies) in a total volume of 3 ml of growth media per well. A concentration-response optimisation experiment assessing the degree of knockdown caused by transfection with 10 nM, 15 nM, 20 nM, 25 nM and 30 nM of miR-224 inhibitor or negative control was conducted to ascertain that 30 nM was the optimum concentration, giving a knockdown of 98% as later discussed in Section 3.3.4.

To achieve this concentration for each well, 1.8 µl of 50 µM miR-224 inhibitor or negative control solutions (diluted in nuclease-free water) was diluted in PBS to make a total volume of 10 µl and was then added to 90 µl of serum-free media in an eppendorf tube. In a separate tube, 5 µl of lipofectamine was added to 95

µl of serum-free media. The contents of both tubes were combined and left to incubate at room temperature for 45 minutes. Growth media was aspirated from each well and replaced with 2.8 ml of serum-free media. The 200 µl mix was then added dropwise to each well. The cells were incubated at 37°C for 5 hours before the transfection media was removed and replaced with fresh growth media containing FBS. The cells were left for 24 hours before further experiments were conducted. The success of knockdown was assessed using miRNA quantitative RT-PCR Taqman analysis (Sections 2.2.9.1 and 2.2.9.2).

For miR-224 mimic experiments, HCT116 *KRAS* mutant cell lines were transiently transfected with final concentrations of 0.3 nM, 1 nM, 5 nM, 10 nM and 20 nM of miR-224 mimic or miRNA mimic negative control (Life Technologies) solution. To achieve these final concentrations, the miR-224 mimic or negative control solution was serially diluted in PBS according to Table 2.2 to make a total volume of 20 µl. In each well, 10 µl of the mimic or negative control and PBS mix was added to 90 µl of serum-free media in an eppendorf tube. The remainder of the procedure was then unchanged from transfection with miRNA inhibitors.

Table 2.2: MiRNA mimic dilutions in PBS

Desired final miR-224 mimic concentration per well (nM)	Volume of 50 µM miR-224 mimic stock solution (µl)	Volume of 5 µM miR-224 mimic stock solution (µl)	Volume of 0.5 µM miR-224 mimic stock solution (µl)	Volume of PBS (µl)
20	2.4	-	-	17.6
10	1.2	-	-	18.8
5	-	6	-	14
1	-	1.2	-	18.8
0.3	-	-	3.6	16.4

2.2.6. Generation of drug resistant cell lines

Two colorectal cancer cell lines, HCT116 and DLD-1, were each made resistant to either 5-fluorouracil (5-FU) or oxaliplatin over the course of a year by continuous selection. This generated four novel drug resistant cell lines which, for further analysis, were then compared to their respective non drug resistant parental lines.

Cells (2.5×10^5) were initially cultured in 5 ml McCoy's 5A medium with 10% FBS, with a final 5-FU or oxaliplatin concentration of 0.1 µM, in a 25 cm^2 flask. A concentration of 0.1 µM was selected as it was approximately 10% of the lowest concentration of drug used for MTT assays (Table 2.1). Starting at this very low concentration ensured that cells were not immediately killed and allowed the cells to gradually acquire resistance with incremental concentration increases. The cells were cultured at each concentration for 4 passages before the drug concentration was increased. During the initial months of selection, the media drug concentration was increased from 0.1 µM to 0.2 µM, 0.5 µM and 1 µM of either 5-FU or oxaliplatin. During the following months the drug concentration was increased as indicated in Table 2.3. The drug concentrations were increased until the cells reached the highest concentration at which they still remained viable and were able to grow in culture. During the first passage of each concentration period a MTT cytotoxicity assay (Section 2.2.4) was performed to determine how resistant the cells had become to the selection drug.

Table 2.3: Final concentrations of 5-FU and oxaliplatin

Drug concentration (μM)	Number of passages	Viable cell lines after 4 passages
1.5	4	HF2, HO10, DF10, DO24
2	4	**HF2**, HO10, DF10, DO24
5	4	HO10, DF10, DO24
10	4	**HO10, DF10**, DO24
12	4	DO24
24	4	**DO24**
30	-	-

Final concentrations are in bold. HF2 – HCT116 5-FU resistant cells; HO10 HCT116 oxaliplatin resistant cells; DF10 – DLD-1 5-FU resistant cells; DO24 – DLD-1 oxaliplatin resistant cells.

Once cells had reached their final drug concentration, single clone populations were isolated. Cells (5×10^4) were seeded onto 10 cm diameter plates in 5 ml McCoy's 5A media, with the final 5-FU or oxaliplatin concentration. The plates were incubated at 37°C for two to three weeks to allow for single cell colonies (visible to the eye) to grow. Clones were isolated by placing cloning cylinders around individual colonies of cells. The cells were then trypsinised by adding 100 μl of trypsin into the middle of the cylinder, incubating the plate at 37°C for 3 minutes and then pipetting the trypsin up and down within the cylinder. Trypsinised colonies were then individually transferred into 24 well plates (1.56 cm diameter per well). Once the cells had become confluent in 1.56 cm diameter wells they were gradually expanded by transferring them to 6 well plates (3.5 cm diameter per well) and then eventually into 25 cm^2 flasks.

2.2.7. Invasion assay

The Calbiochem InnoCyte invasion assay was used to model and quantify cancer cell invasion *in vitro*. The assay uses an invasion chamber consisting of a 24 well tissue culture plate and 12 cell culture inserts with an 8 µm pore sized polycarbonate membrane (Figure 2.1). The upper surface of the insert membrane is coated with a layer of dried basement membrane matrix (BMM) solution forming an extracellular matrix which prevents non-invasive cells from passing through the 8 µm pores. Invasive cells are able to degrade the matrix, pass through the pores and stick to the bottom of the polycarbonate membrane. The invasive cells can then be dissociated from the bottom of the polycarbonate membrane and fluorescently labelled to allow for quantification.

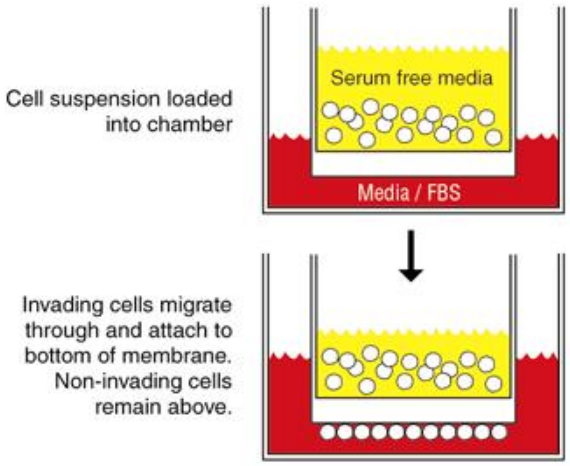

Figure 2.1: ***Diagrammatic representation of cell invasion assay.***

The cell invasion chamber (stored at 4°C) was initially left to warm to room temperature. The dried BMM in the cell culture inserts were then rehydrated by adding 400 µl of serum-free media and leaving for 30 minutes at room

temperature before it was discarded. Media (500 µl) containing 10% FBS was added to the lower chamber. Cells (1×10^6) were then added to the top chamber in a total volume of 350 µl of serum-free media. A negative control with no cells was also included. The cell invasion chamber was then incubated at 37°C and 5% CO_2 for 24 hours. Following incubation, a cell staining solution was prepared by diluting the fluorescent dye Calcein-AM in cell detachment buffer by a factor of 1:300. The upper chamber inserts were then placed into wells that had not yet been used, containing 500 µl containing cell staining solution and invasive cells were dislodged by gently tapping the inserts against the bottom of the lower chamber. The cell invasion chamber was incubated for 30 minutes at 37°C and then again after the removal of the inserts. The fluorescently labelled dislodged cell solution was then split into triplicate aliquots and transferred to a white, opaque 96 well plate (150 µl per well), and the fluorescence measured at an excitation wavelength of 485 nm and an emission wavelength of 530 nm. Invasion was therefore represented as relative fluorescence units (RFU) with a higher measurement representing increased invasion. The negative control reading was subtracted from the reading taken for cell samples.

2.2.8. RNA extraction

2.2.8.1. RNA extraction from cell lines

Once cells were 70% confluent in 75 cm^2 flasks they were trypsinised, collected in a 15 ml falcon tube and centrifuged for 3 minutes at 1200 rpm to form cell pellets. Alternatively, for RNA extraction following transfection, drug treatment or single clone expansion of drug resistant cell lines, cells were seeded on, and trypsinised from, 6 well plates. Cell pellets could then be stored at -80°C for future RNA extraction.

RNA was extracted from cell lines using a Qiagen RNeasy mini kit using spin technology by following the manufacturer's protocol for mammalian cells. Briefly, cell pellets were disrupted using a denaturing buffer containing guanidine thiocyanate, thus ensuring the inactivation of RNases, and lysed using a QIAshredder spin column. Ethanol (70% v/v) was added to the cell lysate to precipitate RNA. The sample was then transferred to an RNeasy Mini spin column where RNA was able to selectively bind to a membrane. A number of subsequent wash steps ensured removal of contaminants and RNA was finally eluted in 50 µl RNase-free water. On column DNase digestion was performed using a Qiagen RNase free DNase kit to minimise genomic DNA contamination.

2.2.8.2. RNA extraction from fresh frozen tissue

RNA was extracted from fresh frozen tissue using a Qiagen RNeasy mini kit using spin technology by following the manufacturer's protocol for animal tissue.

Fresh frozen samples of colorectal tissue were disrupted by placing the whole tissue sample (approximately 20 mg) in a small sterile tube and adding 1 ml lysis buffer containing guanidine thiocyanate. The tissue was then homogenised using a rotor – stator homogeniser (Polytron) until the sample was uniformly homogenised. Ethanol (70% w/v) was added to the homogenate to precipitate RNA. The remaining procedures following RNA precipitation was performed as detailed in Section 2.2.8.1. On column DNase digestion was also performed using a Qiagen RNase free DNase kit to minimise genomic DNA contamination.

2.2.8.3. RNA extraction from formalin-fixed, paraffin-embedded (FFPE) tissue sections

RNA was extracted from FFPE tissue sections using a RecoverAll Total Nucleic Acid isolation kit (Life Technologies) following the manufacturer's protocol. Three 20 µm FFPE sections were placed into an eppendorf tube and deparaffinised by the addition of 1 ml xylene and heating at 50°C for 3 minutes. 1 ml of 100% ethanol was then added to remove the xylene and accelerate the drying of tissue. The deparaffinised tissue was then subjected to protease digestion by the addition of 200 µl of digestion buffer with protease. RNA was precipitated by the addition of 790 µl of an ethanol/isolation buffer mix and the sample was transferred to a filter cartridge placed in a collection tube where RNA was able to selectively bind to a membrane. Following a series of wash steps, RNA was eluted in 60 µl of nuclease free water. On column DNase digestion was performed to minimise genomic DNA contamination.

2.2.8.4. Determination of RNA yield and integrity

RNA yield and integrity was determined on a Nanodrop 1000 spectrophotometer (Thermo Scientific). 2 µl of RNA sample was loaded onto the pedestal and absorbance readings were taken at 260 nm (A_{260}) and 280 nm (A_{280}). RNA concentration was represented in ng/µl and purity was estimated from the A_{260}:A_{280} ratio. An A_{260}:A_{280} ratio between 1.7 and 2.0 indicates high quality RNA.

For human tissue samples and cells used for microarray analysis, RNA integrity was further assessed using an Agilent Bioanalyser 2100 and by using a RNA 6000 Nano LabChip Kit (Agilent) following the manufacturer's protocol. Briefly, 1 µl of RNA sample was loaded into a well on the LabChip. The chip was loaded onto the Bioanalyser which separated RNA by electrophoresis and detected the separated sample via laser-induced fluorescence. The Bioanalyzer 2100 software generates an electropherogram and a gel like image and displays the sample concentration, the 18s and 28s ribosomal subunit ratios, and RNA integrity number (RIN; Figure 2.2). The RIN, a uniform measure of RNA integrity, ranges from 0-10. RNA samples with a RIN value of over 7 are deemed high enough quality to be used for microarray and Taqman analysis. A RIN value of 10 indicated that RNA was 100% intact whereas a lower RIN value indicated RNA degradation. The 18s and 28s ribosomal subunit ratios indicated the fragment length of RNA. The ideal ratio is approximately 2:1 indicating full length RNA.

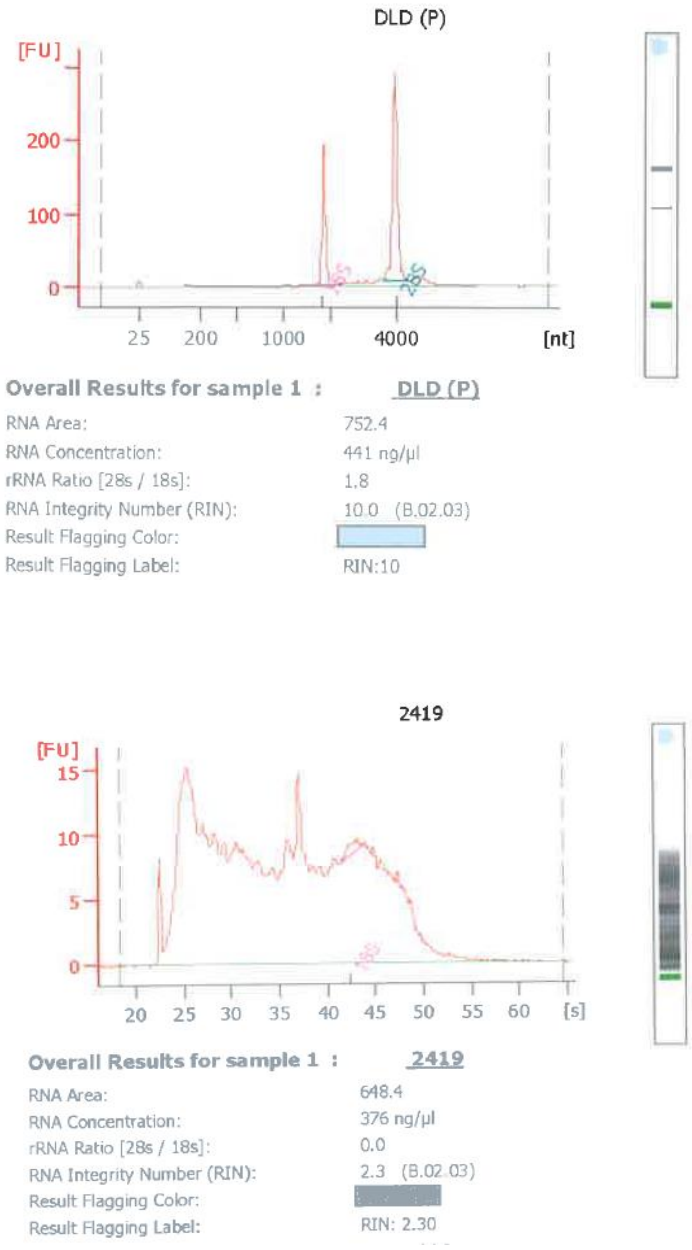

Figure 2.2: ***An electropherogram generated by the Bioanalyzer 2100 software.*** *A representation of the electropherogram generated by the Bioanalyzer 2100 software, indicating RNA concentration, 18s and 28s ribosomal subunit ratios (rRNA Ratio [28s/18s]), and RNA integrity number (RIN). The RIN in* ***A)*** *is 10 indicating high quality RNA whereas the RIN in* ***B)*** *is 2.3 indicating degraded RNA.*

2.2.9. Taqman quantitative real time PCR Analysis

Relative miRNA and mRNA expression was assessed by Taqman quantitative real time PCR analysis. Taqman quantitative real time PCR analysis is performed in two steps. In miRNA analysis, the initial reverse transcription (RT) reaction produces cDNA from total RNA using a small miRNA-specific, stem-loop RT primer (Figure 2.3). The PCR step amplifies products from cDNA samples using Taqman Universal PCR master mix and Taqman Small RNA Assays. In mRNA expression analysis, cDNA is reverse transcribed from total RNA using random primers. During PCR, products are then amplified from cDNA again using Taqman Universal PCR master mix and Taqman Gene Expression assays.

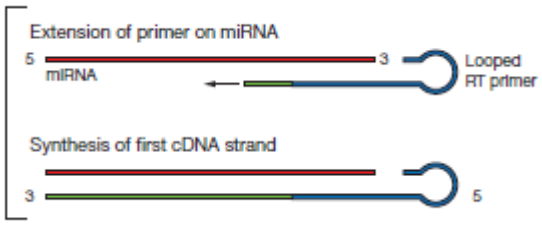

Figure 2.3: ***Reverse transcription from a stem-loop miRNA primer*** *(Life Technologies Taqman Small RNA Assays protocol).*

Taqman systems use fluorescent probe-based chemistry to allow quantification of the amplified PCR product. Taqman probes have a fluorescent reporter dye linked to the 5' end and a non-fluorescent quencher (NFQ) dye linked to the 3'end (Figure 2.4). The NFQ reduces the fluorescence emitted by the reporter dye by Fluorescence Resonance Energy Transfer (FRET) due to their proximity to each other. During PCR, the Taqman probe anneals specifically to a complementary sequence between the forward and reverse primer sites. DNA

polymerase degrades the probe that has annealed to the template leading to the separation of the reporter dye from the quencher dye and causing an increase in the fluorescent signal of the reporter dye. Therefore, with each PCR cycle, additional reporter dye molecules are cleaved resulting in an exponential increase in the fluorescent signal, which in turn is directly proportional to the amount of the amplified PCR product produced.

The degradation and removal of the probe from the target strand also allows primer extension to continue to the end of template strand, thereby not interfering with the exponential accumulation of PCR product.

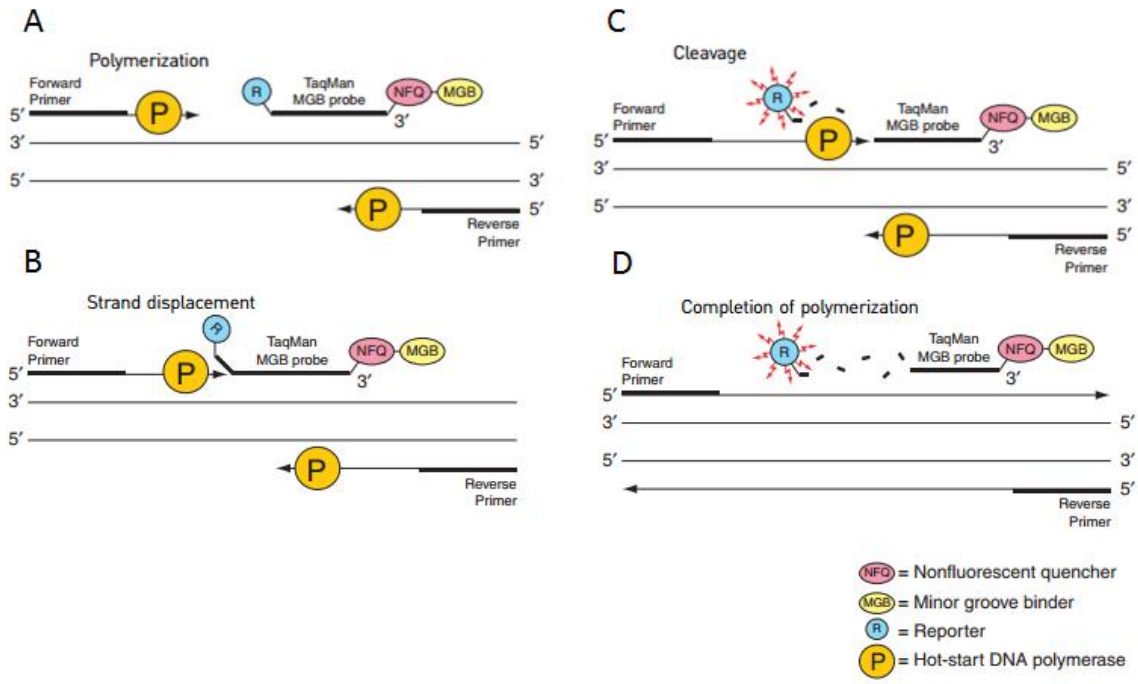

Figure 2.4: ***Schematic diagram of Taqman chemistry and the process of gene amplification*** *(Life Technologies Taqman Gene Expression Assays protocol).*

2.2.9.1. Taqman Small RNA Assays - reverse transcription

The initial RT step for miRNA expression analysis was performed using a specific miRNA stem-loop RT primer and reagents from the Taqman MicroRNA Reverse Transcription Kit in accordance with the manufacturer's protocol. For each sample, 10 ng of RNA, diluted in a total of 5 µl of nuclease-free water, was added to 10 µl of reaction mix to make a RT reaction volume of 15 µl. The reaction mix consisted of 0.15 µl dNTPs, 1 µl reverse transcriptase, 1.5 µl reverse transcriptase buffer, 0.19 µl of RNase inhibiter, 4.16 µl nuclease-free water and 3 µl of a miRNA specific primer.

The RT reaction was then performed on a thermal cycler (MJ Research PTC-225 Peltier) under the following conditions: 16°C for 30 minutes, 42°C for 30 minutes and 85°C for 4 minutes.

2.2.9.2. Taqman Small RNA Assays – quantitative PCR analysis

The PCR step amplified PCR products from cDNA samples using Taqman Small RNA Assays, containing a miRNA specific probe and primer mix and Taqman Universal PCR Master Mix II in a 96 well plate format. In each well, 1.33 µl of cDNA was added to 1 µl of a miRNA-specific probe mix, 10 µl of Taqman Universal PCR Master Mix II and 7.67 µl of nuclease-free water. Each cDNA sample was added to the plate in triplicate. The 96 well plates were sealed using a heated plate sealer and centrifuged at 1200 rpm for 10 seconds. The PCR reaction was then run on the standard Real Time PCR program on the 7900 Taqman real-time system under the following conditions: 50°C for 2 minutes and

95°C for 10 minutes, followed by 40 cycles of 95°C for 15 seconds and 60°C for 1 minute.

The endogenous control used for all single Taqman Small RNA Expression Assays was U6 snRNA, one of the most common normalising genes in miRNA quantification (Peltier & Latham, 2008).

2.2.9.3. Taqman mRNA Expression assays - reverse transcription

The RT step for mRNA expression analysis was performed using a Taqman reverse transcription reagents kit. For each sample 200 ng of RNA, diluted in a total of 20 µl of nuclease-free water was added to 30 µl of reaction mix to make a RT reaction volume of 50 µl. The reaction mix consisted of 5 µl RT buffer, 11 µl magnesium chloride, 10 µl dNTPs, 1 µl RNase inhibitor, 1.25 µl reverse transcriptase and 2.5µl random hexamers.

The RT reaction was then performed on a thermal cycler (MJ Research PTC-225 Peltier) under the following conditions: 25°C for 10 minutes, 37°C for 60 minutes and 95°C for 5 minutes.

2.2.9.4. Taqman Gene Expression assays – quantitative PCR analysis

The PCR step amplified PCR products from cDNA samples using Taqman Gene Expression Assays, containing a specific probe and primer mix and Taqman Universal PCR Master Mix II in a 96 well plate format. In each well, 1 µl of cDNA was added to 1 µl of a gene specific Taqman probe mix, 10 µl of Taqman Universal PCR Master Mix II and 8 µl of nuclease-free water. Each cDNA sample

was added to the plate in triplicate. The 96 well plates were sealed and briefly centrifuged as previously described. The PCR reaction was then run on the standard Real Time PCR program on the 7900 Taqman real-time system (Applied Biosystems) under the following conditions: 50°C for 2 minutes and 95°C for 10 minutes, followed by 40 cycles of 95°C for 15 seconds and 60°C for 1 minute.

The endogenous control used for all single Taqman Gene Expression Assays was 18S ribosomal RNA. 18S ribosomal is universally used as a normalising gene in relative mRNA quantification.

2.2.9.5. Taqman data analysis

The data was analysed using SDS 2.3 software (Applied Biosystems) to determine a Ct (cycle threshold) value for each sample. The Ct value is described as the minimum PCR cycle at which fluorescence can be detected over background. The Ct value is therefore inversely proportional to the amount of the target gene in the PCR reaction. The relative expression of each gene and standard errors were then calculated. Firstly, the mean Ct of the endogenous control gene (i.e. U6 snRNA or 18S ribosomal RNA) was subtracted from the mean Ct of the target gene of interest to give the delta CT (δCt). Secondly, the standard deviation (sd) of δCt was calculated using the equation $(\text{sd target}^2 + \text{sd control}^2)^{1/2}$. Thirdly, the relative expression was determined by calculating the $2^{-\delta CT}$ value, converting it from a log to linear scale. Finally, the positive and negative errors of relative expression were determined by calculating $2^{(-\delta Ct + \text{sd } \delta Ct)}$ and $2^{(-\delta Ct - \text{sd } \delta Ct)}$.

2.2.9.6. Taqman Low Density Array (TLDA) microRNA Cards

Taqman human miRNA arrays are 384 well plates pre-loaded with Taqman Small RNA Assays (Figure 2.5) allowing for the simultaneous quantification of hundreds of miRNAs. The arrays are split into an 'A' and 'B' card with a combination of 667 unique human miRNA assays. The 'A' card represents the miRNAs which were considered to be most well characterised at the time of manufacture, whereas the 'B' card were loaded with the lesser known miRNAs. At the time of writing, there are now over 2000 known unique human miRNAs (http://www.mirbase.org/). For the present study, card 'A', pre-loaded with 377 unique human miRNA assays, 3 endogenous controls and one negative control, was used (Appendix A).

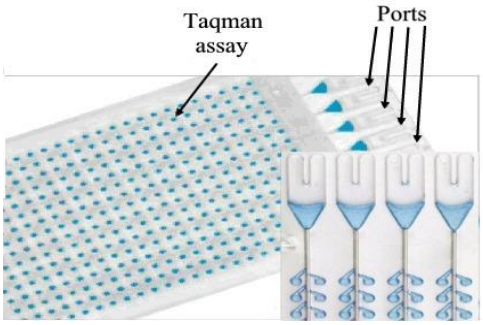

Figure 2.5: ***The 384-well format Taqman Low Density Array miRNA cards with ports for sample loading***.

2.2.9.7. Megaplex reverse transcription

The RT step was performed using Taqman reverse transcription reagents kit and Megaplex RT primers, a pool of 377 unique human miRNA RT primers. For each sample 600 ng of RNA, diluted in a total of 3 µl of nuclease-free water was

added to 4.5 µl of reaction mix to make a RT reaction volume of 7.5 µl. The reaction mix consisted of 0.8 µl Megaplex RT primers, 0.2 µl dNTPs, 1.5 µl reverse transcriptase, 0.8 µl RT buffer, 0.9 µl magnesium chloride, 0.1 µl RNase inhibitor and 0.2 µl nuclease-free water.

The RT reaction was then performed on a thermal cycler (MJ Research PTC-225 Peltier) under the following conditions: 40 cycles of 16°C for 2 minutes, 42°C for 1 minute and 50°C for 1 second followed by an additional 5 minutes at 85°C.

2.2.9.8. Taqman Low Density Array miRNA cards – quantitative PCR analysis

For each sample, 6 µl of megaplex RT product was added to 450 µl of Taqman Universal PCR Master Mix II and 444 µl of nuclease-free water to make a 900 µl PCR reaction mix. The TLDA card was then loaded by adding 100 µl of PCR reaction mix into each port. The plate was then centrifuged twice at 1200 rpm for 1 minute to evenly distribute the sample into each individual well. The card was then sealed using a TLDA card sealer (Applied Biosystems) before the sample ports were removed using scissors.

The TLDA PCR reaction was then run on the standard Real Time PCR program on the 7900 Taqman real-time system (Applied Biosystems) under the following conditions: 50°C for 2 minutes and 94.5°C for 10 minutes, followed by 40 cycles of 97°C for 30 seconds and 59.7°C for 1 minute.

Each individual sample was run in triplicate (3 different TLDA cards) and the data were analysed as detailed in Section 2.2.9.5.

2.2.10. Illumina HT-12 BeadChip mRNA expression arrays

Illumina HT-12 BeadChip mRNA expression arrays provide a genome-wide, high-throughput method of simultaneously quantifying the expression of thousands of well characterized genes, gene candidates and splice variants. The array uses a novel BeadArray technology where 3 µm silica beads self-assemble into micro-wells. Each bead is covered with thousands of gene-specific probes which capture sequence specific antisense RNA.

The RNA amplification steps (Figure 2.6) involve the generation of biotinylated, amplified antisense RNA for hybridisation with Illumina arrays. Firstly, single strand cDNA is generated from total RNA by reverse transcription using oligo (dT) primers to produce cDNA containing a T7 promoter sequence. This reaction is catalysed by ArrayScript, a reverse transcriptase enzyme engineered to produce a high yield of cDNA. Secondly, single stranded cDNA is converted to a double stranded cDNA (ds cDNA) template by the action of DNA polymerase, whilst RNA is simultaneously degraded by the action of an RNAse enzyme. The ds cDNA is then purified to remove enzymes, salts, RNAs and excess primers. Finally, T7 RNA polymerase catalyses the production of biotin labelled antisense RNA (cRNA) copies of each mRNA. In the present study, biotin labelled cRNA was generated using an Illumina TotalPrep RNA amplification kit (Life Technologies) by following the manufacturer's protocol.

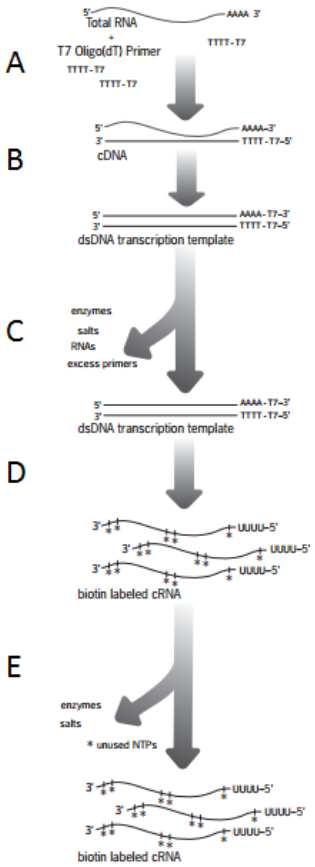

Figure 2.6: ***The process of RNA amplification***. *The synthesis of A) cDNA and B) double stranded cDNA; C) the purification of cDNA; D) the reverse transcription to biotin labelled cRNA and E) the purification of cRNA (modified from Life Technologies Illumina TotalPrep RNA amplification kit protocol).*

2.2.10.1. Reverse transcription to synthesise cDNA

The initial reverse transcription step was performed using specific oligo (dT) primers to produce single strand cDNA bearing a T7 promoter. For each sample, 500 ng of total RNA diluted in a total of 11 µl of nuclease-free water was added to 9 µl of reverse transcription master mix. The master mix consisted of 1 µl T7 oligo (dT) primer, 2 µl first strand buffer, 4 µl dNTP mix, 1 µl RNAse inhibitor and

1 µl Array Script reverse transcriptase. The samples were incubated at 16°C for 2 hours in a thermal cycler (MJ Research PTC-225 Peltier).

2.2.10.2. Second strand cDNA synthesis

Double stranded cDNA (ds cDNA) was then generated by adding 80 µl of second strand master mix to each sample to make a total reaction volume of 100 µl. The second strand master mix consisted of 63 µl nuclease-free water, 10 µl second strand buffer, 4 µl dNTP mix, 2 µl DNA polymerase and 1 µl RNAse H. The samples were then incubated at 16°C for 2 hours in a thermal cycler (MJ Research PTC-225 Peltier).

2.2.10.3. *In vitro* transcription to synthesise cRNA

To generate cRNA, 7.5 µl of *in vitro* transcription master mix was added to purified ds cDNA and eluted into 17.5 µl of nuclease-free water. The *in vitro* transcription mix consisted of 2.5 µl each of T7 reaction buffer, T7 enzyme mix and biotin-NTP mix. The samples were incubated at 37°C for 14 hours in a thermal cycler (MJ Research PTC-225 Peltier). The reaction was subsequently stopped by the addition of 75 µl nuclease free water. 350 µl of cDNA binding buffer was added to each cRNA sample. The cRNA was then precipitated by the addition of 250 µl 100% ethanol. The mixture was added to a cRNA filter cartridge placed in a collection tube. A number of subsequent wash steps using a wash buffer ensured removal of contaminants and cRNA was finally eluted in 200 µl of RNase-free water pre-heated to 55°C.

2.2.10.4. Generation of mRNA expression array data

cRNA samples were sent to the Wellcome Trust Clinical Research Facility, Western General Hospital, Edinburgh, where the gene expression array was performed according to the manufacturer's protocol. Each sample was analysed in triplicate. Expression data was analysed as described in Section 2.2.17.

2.2.11. Protein Determination and Western Blotting

To extract cellular protein, cells were seeded in 6 well plates and incubated at 37°C in McCoy's 5A growth media and 10% FBS until 70% confluent. The cells were then washed once with PBS and incubated at 37°C in FBS free media for 5 hours. Following incubation, the cells were washed again with PBS and 200 µl of 1X cell lysis buffer (Cell Signalling Technology) and 1 mM PMSF (a protease inhibitor) was added to the cells and incubated on ice for 5 minutes. The lysed cells were then scraped from the plates using a cell scraper and transferred into an eppendorf tube. The cell lysate was then centrifuged for 10 minutes at 14000 rpm at 4°C and the pellet was discarded.

The protein concentration in the cell lysate was determined by performing a Bradford assay using the Bio-Rad protein assay. The Bio-Rad assay is based on the colour change of Coomassie brilliant blue G-250 dye in response to various concentrations of protein. The dye was diluted in water by a factor of 1:5 before use. 2 µl of each cell lysate sample was added to 200 µl of dye on a 96 well plate. A standard curve was also prepared using bovine serum albumin (BSA) at concentrations ranging from 0 mg/ml to 8 mg/ml. Each sample was added to the

96 well plate in triplicate. The absorbance was then read using a ThermoScan microplate reader at a wavelength of 595 nm.

The mean absorbance of each BSA sample was plotted against the protein concentration. The protein concentration of the test samples were then calculated by using the equation of the line (y=mx + c), where m = slope of the dose response curve obtained from a BSA dilution series and c = the absorbance at 0 mg/ml.

Western Blot analysis was performed on SDS-polyacrylamide gels which were prepared prior to the procedure. 10% resolving gels were prepared by adding together 4 ml water, 3.3 ml 30% acrylamide mix, 2.5 ml 1.5M Tris buffer, 100 µl SDS, 100 µl 10% ammonium persulfate (APS) and 4 µl TEMED and casting the mixture using the Bio-Rad Mini-PROTEAN II system. A 5% stacking gel was also prepared by adding together 2.7 ml water, 670 µl 30% acrylamide mix, 400 µl 1.0 M Tris, 40 µl 10% SDS, 40 µl 10% APS and 4 µl TEMED. The stacking gel was added on top of the resolving gel once it had set. A comb was placed into the stacking gel whilst it set to produce wells for loading protein samples.

For Western blot analysis, 40 µg of protein was diluted in 5X SDS sample buffer (0.2 M Tris, 10% SDS, 0.05% bromphenol blue, 20% glycerol) to make a total volume of 20 µl. Samples were then denatured at 95°C for 5 minutes before they were loaded onto SDS-polyacrylamide gels. SDS-PAGE was run using the Bio-Rad mini-PROTEAN 3 Cell system and samples underwent electrophoresis at 100 volts in Tris-glycine running buffer (25 nM Tris, 250 nM glycine, 0.1% SDS in water). Rainbow protein molecular weight marker was also loaded onto the gels.

Proteins were then transferred from gels onto nitrocellulose membranes in Tris-glycine-methanol transfer buffer (48 mM Tris, 39 mM glycine, 0.037 (w/v) SDS, 10% (v/v) methanol). The nitrocellulose membranes were then blocked in 5% milk supplemented with 0.05% Tween-20 for 2 hours at room temperature to prevent non-specific protein binding. The membranes were then incubated at 4°C for at least 12 hours in primary antibody. In the present study γH_2AX and β-actin (loading control) anti-mouse antibodies were used as primary antibodies. In both cases the antibodies were diluted in milk by a factor of 1:1000. The membranes were washed 3 times for 5 minutes in PBS before incubation with an anti-mouse secondary antibody (diluted in milk by a factor of 1:1000) for 2 hours at room temperature. The blots were then developed using an ECL-chemiluminescence kit (Millipore) and used to expose autoradiography films for an appropriate amount of time. The same procedure was repeated to develop blots for the loading control β-actin after bands for γH_2AX had been successfully visualised.

2.2.12. Ras GTPase Chemi ELISA - Quantification of GTP-bound activated KRAS

KRAS activation or the amount of GTP bound KRAS in a cellular extract was determined using a RAS GTPase Chemi ELISA (Active Motif). The ELISA kit contains a glutathione-S-transferase (GST)-bound RAF-RBD protein that is coated on to a glutathione-coated 96 well plate by the interaction between GST and glutathione. Activated GTP-bound RAS in a cellular extract binds specifically to Raf-RBD, the Ras binding domain of RAF, whereas inactive GDP-bound RAS does not. Incubation with a primary HRAS antibody that specifically binds to KRAS in

human samples (or HRAS in mouse samples) followed by a secondary antibody conjugated to horseradish peroxidise (HRP) that binds specifically to the primary antibody allows the quantification of bound activated KRAS by luminescence. In the present study, the ELISA was used to compare the relative innate KRAS activation between cell lines or following miR-224 knockdown (Section 2.2.5).

Cellular extracts were obtained from cells 24 hours after transfection with miR-224 inhibitors and miRNA inhibitor negative controls or from cells that were seeded in six well plates and left to grow until 70% confluent. Cells were washed with ice cold PBS and lysed by adding 500 µl of complete lysis/binding buffer. The cell lysate was then incubated for 15 minutes at 4°C, centrifuged at 14000 rpm for 10 minutes also at 4°C and the supernatant was collected. Protein concentration was determined by the Bradford assay (Section 2.2.11).

The next steps were performed according the manufacturer's protocol. Briefly, 2 µg of GST-RAF-RBD protein diluted in 50 µl of complete lysis/binding buffer was added to each well and incubated for 1 hour at 4°C with mild agitation. Following wash steps, 40 µg of protein sample was diluted in 200 µl of complete lysis/binding buffer and added to each well. Each sample was added in triplicate and included a negative control (50 µl of complete lysis/binding buffer). The plate was then incubated for one hour at room temperature with mild agitation. The primary HRAS antibody (1:500 dilution in antibody buffer) was added to each well and incubated for 1 hour at room temperature. Following wash steps, the secondary antibody (1:5000 dilution in antibody buffer) was also added to each well and incubated for 1 hour at room temperature. Finally, 50 µl of

chemiluminescent working solution was added to each well, following final wash steps, and luminescence was measured using a Modulus II microplate multimode reader (Turner Biosystems). KRAS activation was therefore represented as relative luminescence units (RLU) with a higher measurement representing increased KRAS activation.

2.2.13. PathScan Intracellular Signalling Array

The PathScan intracellular signalling array is a slide based antibody array allowing for the simultaneous detection of 18 well characterised and important phosphorylated or cleaved signalling molecules (Figure 2.7). Each kit contains two slides with 16 nitrocellulose pads on which each target specific antibody has been spotted in duplicate. The array therefore allows for 32 samples to be tested. The assay was performed according to the manufacturer's protocol.

A

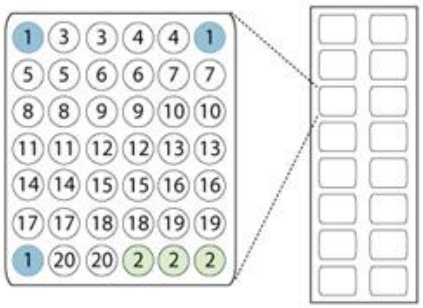

B

Intracellular Signaling

	Target	Phosphorylation Site	Modification
1	Positive Control	N/A	N/A
2	Negative Control	N/A	N/A
3	ERK1/2	Thr202/Tyr204	Phosphorylation
4	Stat1	Tyr701	Phosphorylation
5	Stat3	Tyr705	Phosphorylation
6	Akt	Thr308	Phosphorylation
7	Akt	Ser473	Phosphorylation
8	AMPKα	Thr172	Phosphorylation
9	S6 Ribosomal Protein	Ser235/236	Phosphorylation
10	mTOR	Ser2448	Phosphorylation
11	HSP27	Ser78	Phosphorylation
12	Bad	Ser112	Phosphorylation
13	p70 S6 Kinase	Thr389	Phosphorylation
14	PRAS40	Thr246	Phosphorylation
15	p53	Ser15	Phosphorylation
16	p38	Thr180/Tyr182	Phosphorylation
17	SAPK/JNK	Thr183/Tyr185	Phosphorylation
18	PARP	Asp214	Cleavage
19	Caspase-3	Asp175	Cleavage
20	GSK-3β	Ser9	Phosphorylation

Figure 2.7: ***The PathScan Intracellular Signalling Array***. ***A)*** *A representation of one of the slides and the 16 nitrocellulose pads, and* ***B)*** *the names and positions of each target antibody (modified from Cell Signalling PathScan Intracellular Signalling Array protocol).*

A protein lysate was obtained as described in Section 2.2.11 and was diluted to a total protein concentration of 1 mg/ml. A multi-well gasket was fixed onto the slide to isolate each nitrocellulose pad. Each pad was incubated at room temperature with an array blocking buffer to prevent non-specific protein binding. The pads were then incubated at room temperature with protein lysate for 1 hour with mild agitation. Subsequently, the pads were incubated with a biotin-conjugated detection antibody cocktail (containing specific antibodies to each phosphorylated or cleaved signalling molecule) followed by a fluorescently-linked antibody conjugated to streptavidin which binds biotin.

Following a series of wash steps the slide was scanned using a LiCor Odyssey (LiCor Biosciences), a fluorescent digital imaging system. An image of the slide

was captured at an excitation wavelength of 680 nm and detecting wavelength of 700 nm and the relative fluorescent intensities of the spots were quantified by using the imaging program Image Studio Software (Li-Cor Biosciences).

2.2.14. Fluorescence-activated cell sorting

Fluorescence-activated cell sorting (FACS) is a specialised form of flow cytometry used to measure a number of parameters of individual cells within a heterogeneous population based upon the specific light scattering and fluorescent characteristics of each cell. In flow cytometry thousands of cells per second are passed individually in a stream of flowing fluid through a laser beam. Each individual cell can cause the scatter or refraction of light as it passes though the laser beam. The flow cytometer is able to detect the amount of light scattered in the direction of the laser beam (forward scatter) or light scattered at 90 degrees from the path of the laser beam (side scatter) and convert this information into voltage pulses. The intensity of the forward and side scattered light detected is proportional to the size of a cell and the inner structural complexity of a cell respectively. Additionally, targeted fluorescently-tagged molecules or fluorescent dyes, which bind to specific components or receptors of a cell, may be added to a cell sample. The fluorophore can be excited by the laser beam at the appropriate wavelength thus emitting a fluorescent signal that can also be detected by the flow cytometer and provide further insight into cell phenotype. The light scattering and fluorescent characteristics of cells can therefore be analysed graphically and can be represented in single dimensional histograms of two dimensional dot plots.

2.2.14.1. DNA cell cycle analysis using Propidium Iodide

Propidium iodide (PI) is a fluorescent dye used to stain cells and quantify DNA content in cell cycle analysis. PI only permeates non-viable cells, which have been fixed in ethanol, and binds to both DNA and RNA. PI fluorescence is emitted at an excitation wavelength of 535 nm and emission wavelength of 617 nm. The fluorescence emitted once PI is bound to DNA and excited by a laser source increases and the amount of fluorescence is proportional to the amount of DNA present in a cell. As PI does not discriminate between DNA and RNA, samples are also treated with a ribonuclease (RNase A) to eliminate RNA.

DNA content is known to change during the cell cycle. As the DNA content of cells is duplicated during the synthesis or S phase of the cell cycle, the DNA content and thus the fluorescence of cells is assumed to be twice as high in cells in the G2/M phase than cells in the G0/G1 phase.

In the present study, DNA cell cycle analysis was used to assess the effect of miRNA knockdown (Section 2.2.5), acute drug treatment or acquired drug resistance (Section 2.2.6) on the cell cycle. In miRNA knockdown and acute drug treatment analysis cells (1×10^6) were seeded on 5 cm diameter plates and were fixed at alternate 16 and 8 hour intervals (16 h, 24 h, 32 h, 48 h, 64 h and 72 h) within a 72 hour period. In the acquired drug resistance analysis cells (1×10^6) were seeded on 10 cm diameter plates and were fixed every 24 hours within a 96 hour period. Each experiment was performed 3 times.

Each sample was fixed by adding 1 x 10^6 cells drop-wise into 2 ml of ice cold 70% (w/v) ethanol and was stored at -20°C for a minimum of 12 hours but for no longer than 7 days before analysis on the flow cytometer. On the day of flow cytometry analysis the fixed cell samples were left to warm to room temperature and then centrifuged at 1200 rpm. The pelleted cells were then washed with PBS and then resuspended in 950 µl PBS, 40 µl propidium iodide solution (1 mg/ml) and 10 µl RNase A (10 mg/ml). The samples were then incubated at 37°C for 30 minutes in darkness.

Samples were analysed on a BD FACScan system (BD Biosciences) and the cell events were visualised using CellQuest Pro (BD Biosciences) software. The data was firstly represented in the form of a dot plot where the area (FL2-A) of the fluorescent light pulse, representing the total fluorescence of a cell, was plotted against the width (FL2-W), representing the time it takes for the cell to pass through the laser beam. This plot was used to distinguish between single cells and doublets, cells that have aggregated and have passed through the laser beam together and thus have larger FL2-A or FL2-W values than single cells (Figure 2.8 A). Single cells were therefore gated and an FL2-area histogram was generated to only show the events inside of the gated region (Figure 2.8 B). 10,000 events were collected within defined gates during data acquisition. The histogram was used to assess the percentage of gated single cells in each defined phase of the cell cycle.

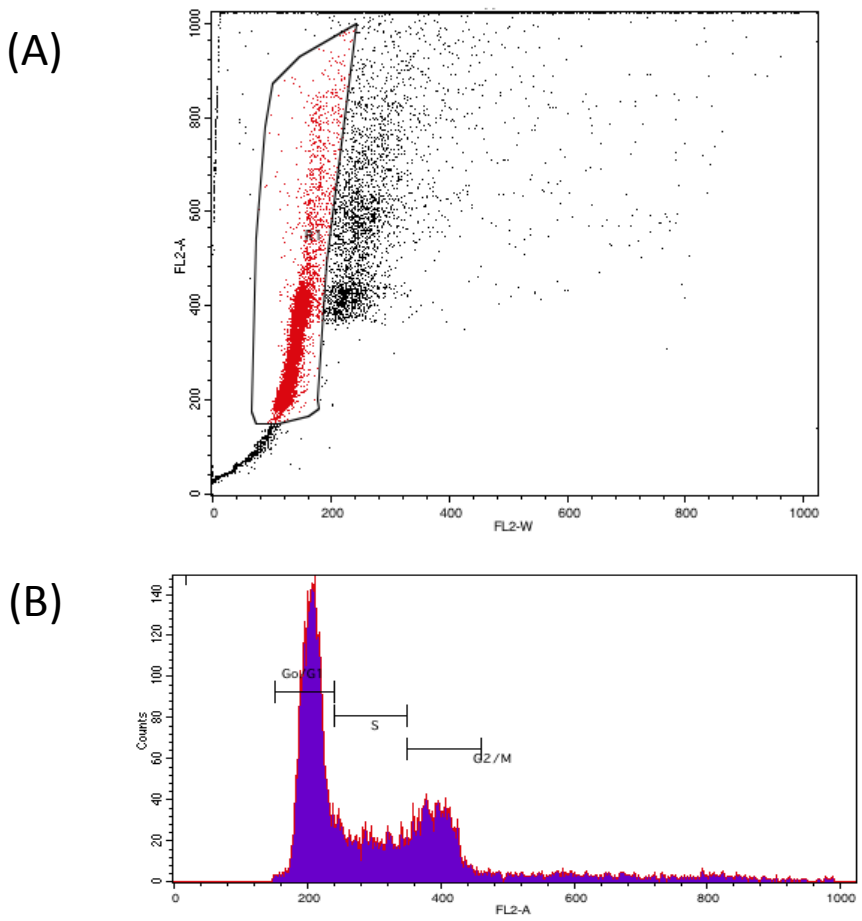

Figure 2.8: ***Analysis of DNA content using Propidium iodide analysis****. **A)** A representation of a dot plot where FL2-A is plotted against FL2-W. The red dots represent the events that have been gated. **B)** A representation of an FL2-area histogram generated to assess the percentage of cells in the G0/G1, S and G2/M phases of the cell cycle.*

2.2.14.2. SYTOX AADvanced Dead Cell Stain Kit

SYTOX AADvanced dead cell stain (Life Technologies) is a fluorescent stain that distinguishes live and dead cells by binding to nucleic acid after penetrating non-viable cells with compromised plasma membranes. The dye emits fluorescence at an excitation wavelength of 488 nm, which is enhanced 500 fold upon binding to nucleic acid. In the present study, the SYTOX AADvanced Dead Cell Stain Kit

was used to assess changes in cell viability following treatment with ionising radiation (Section 2.2.16.3). Following treatment and 72 hours incubation (see Section 2.2.16.3), cells were trypsinised, collected in a 15 ml falcon tube and centrifuged for 3 minutes at 1200 rpm to form cell pellets. The cells were resuspended in 1 ml of PBS with a final stain concentration of 0.5 µM. The samples were incubated on ice for 5 minutes to allow for the stain to bind nucleic acid. The samples were then analysed on an Attune Flow cytometer (Life Technologies) and the cell events were analysed using Attune Cytometric software (Life Technologies).

The data was represented by plotting the total fluorescence of a cell detected to be side scattered (SSC-A) with cells detected to be forward scattered (FSC-A). This dot plot identified a population of cells emitting fluorescence at a wavelength of 625 nm (Figure 2.9 A). A BL3-area plot was also generated to calculate the percentage of gated cells that contained the dead cell stain dye and were therefore considered non-viable (Figure 2.9 B). BL3 represents the filter used to detect cells with the SYTOX AADvanced Dead Cell Stain (those emitting fluorescence at wavelength 625 nm). A negative control where cells were resuspended in 1 ml of PBS without the stain helped to identify the population of cells where the stain had permeated the membrane.

(A)

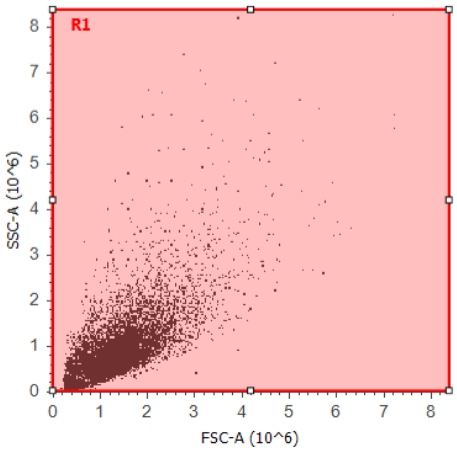

(B)

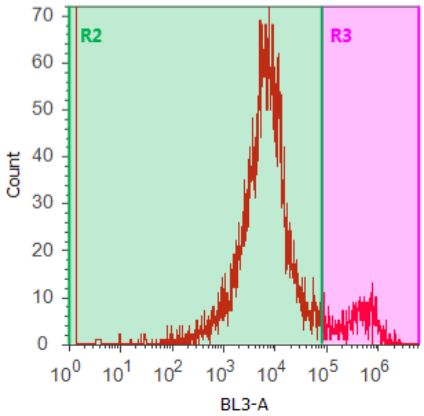

Figure 2.9: ***Analysis of viable cell number using the SYTOX AADvanced Dead Cell Stain kit. A)*** *A representation of a dot plot where SSC-A has been plotted against FSC-A. R1 represents the total area that has been gated.* ***B)*** *A representation of the proportion of gated cells emitting fluorescence at a wavelength of 625 nm. R2 represents the proportion of cells that do not emit fluorescence whereas R3 represents the cells that do emit fluorescence at a wavelength of 625 nm and are thus non-viable.*

2.2.14.3. CellTrace Violet Cell Proliferation Kit

CellTrace Violet is a dye that diffuses into cells where it is cleaved by intracellular esterases to yield a highly fluorescent compound. This compound covalently binds to intracellular amines, resulting in stable, well-retained fluorescent staining. The fluorescent signal emitted by this dye is halved at every cell division and is still detected after up to 10 generations or cell divisions.

In the present study, the CellTrace Violet Cell Proliferation Kit was used to assess the effect of miRNA knockdown (Section 2.2.5) or acquired drug resistance (Section 2.2.6) on cell proliferation and doubling time. In miRNA knockdown analysis cells (1×10^6) were seeded on 5 cm diameter plates and labelled with 5 µM CellTrace dye diluted in PBS (loading solution) as detailed in the manufacturer's protocol according to the alternative method for labelling adherent cells. Cells were harvested at alternate 16 and 8 hour time points (16 h, 24 h, 32 h, 48 h, 64 h and 72 h) within a 72 hour period. In the acquired drug resistance analysis cells (1×10^6) were seeded on 10 cm diameter plates and also labelled with 5 µM CellTrace loading solution as described above. Cells were harvested every 24 hours within a 96 hour period. Each experiment was performed in triplicate. The samples were then analysed on an Attune Flow cytometer (Life Technologies) and the cell events were analysed using Attune Cytometric software (Life Technologies).

The data was represented by plotting the total fluorescence of a cell detected to be side scattered (SSC-A) with cells detected to be forward scattered (FSC-A; Figure 2.10 A). This dot plot identified a population of live cells. Further analysis

involved using ModFit LT (Version 4; Verity Software House) to create a proliferation model generating a visual representation in the changes in the proportion of cells within a particular generation at each time point (Figure 2.10 B). The software calculated the proliferation index, the total number of divisions divided by the number of cells that went into division, which was plotted against time. The doubling time of cells was calculated as shown in Box 2.1 (Section 2.2.3) using an exponential trend line and equation.

(A)

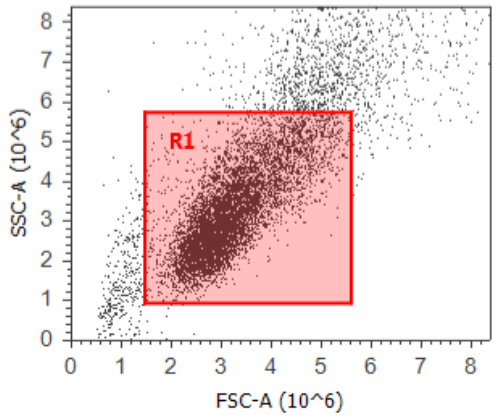

(B)

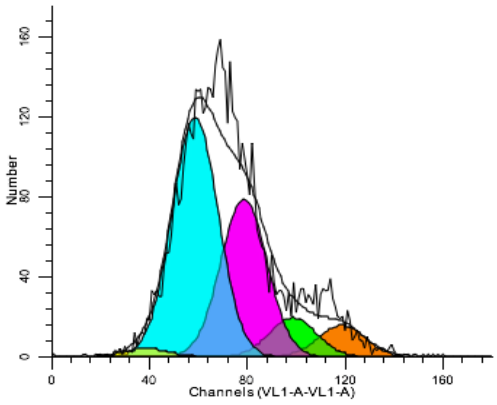

Figure 2.10

Figure 2.10: ***Analysis of cell proliferation using the CellTrace Violet Cell Proliferation kit. A)*** *A representation of a dot plot where SSC-A has been plotted against FSC-A. R1 represents the total area that has been gated.* ***B)*** *A representation of the proliferation model created using ModFit LH where the changes in the proportion of cells within a particular generation (indicated by different colours) at each time point can be visualised. ModFit LH then calculates the proliferation index.*

2.2.15. Measurement of glycolytic activity – Seahorse Bioanalyser

The Seahorse Bioanalyser presents a way of investigating the metabolic behaviour of cells in real time *in vitro.* The set up consists of a sensor cartridge that can simultaneously measure changes in oxygen and proton (H^+) concentration in a transient micro-chamber, with 24 solid state sensors that reside 200 µm above cells that are seeded in a 24 well plate. Each sensor is surrounded by four drug injection ports which allow for the injection of up to four drugs into each well. The rate of oxygen consumption (OCR) is proportional to mitochondrial respiration whereas the extracellular acidification rate (ECAR) is proportional to glycolysis.

The XF glycolysis stress test kit is set up to assess three key parameters of glycolytic function: glycolysis, glycolytic capacity and glycolytic reserve (Figure 2.11). These parameters are calculated by analysing the changes in ECAR following consecutive injection of glucose, oligomycin (an ATP synthase inhibitor) and 2-deoxy-D-glucose (2-DG; a glucose analogue). In the present study, due to time constraints, the effect of glucose on ECAR in parental and drug resistant cell lines was restricted to DLD-1 based cell lines.

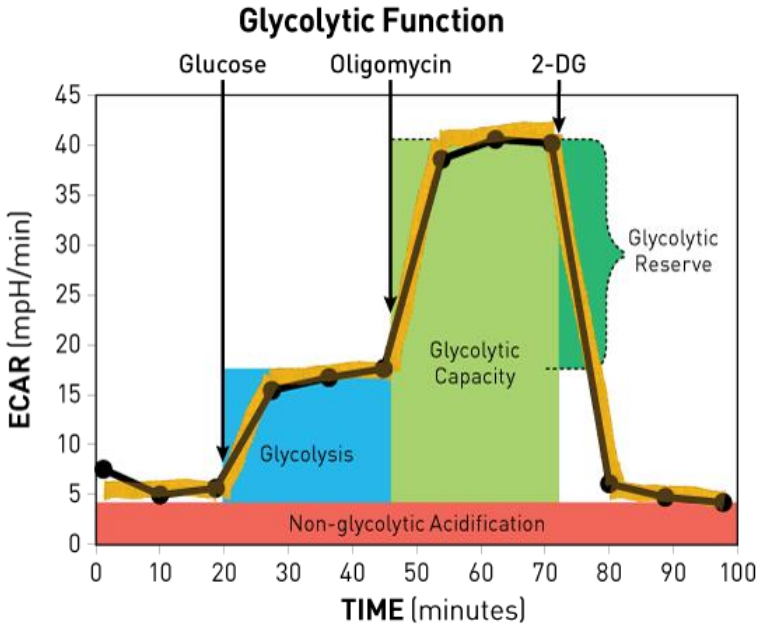

Figure 2.11: ***The three parameters used to assess glycolytic function****. The injection of glucose, oligomycin and 2-DG allows for the assessment of glycolysis, glycolytic capacity and glycolytic reserve respectively (XF glycolysis stress test protocol).*

DLD-1 parental, DLD-1 oxaliplatin resistant and DLD-1 5-FU resistant cells were seeded in a total of 100 µl of McCoy's 5A medium at densities of 4 x 10^4, 4.23 x 10^4 and 4.99 x 10^4 cells per well respectively in a XF24 24 well V7 cell culture plate (Seahorse Bioscience). The different densities were based on relative doubling times so that each cell line reached a similar level of confluence within the wells. Each cell line was seeded in 6 wells. Four control wells were left empty for background measurements. The XF24 plate was left at room temperature for one hour before it was incubated at 37°C for 24 hours.

A cell number titration was performed to determine the optimal seeding density for the DLD-1 parental line. Cells were seeded at densities ranging from 1 x 10^4 to 1 x 10^5 cells per well, left at room temperature for one hour and incubated at 37°C for 24 hours, to determine the density at which there was a complete and

uniform monolayer of cells. The relative densities for the 5-FU and oxaliplatin resistant cell lines were determined based on their doubling times (Section 2.2.14.3).

The XF24 sensor cartridge (Seahorse Bioscience) was also hydrated prior to the assay by adding 1 ml of Seahorse Bioscience calibrant (pH 7.4) into each well of a utility plate and placing the sensor cartridge on top. The sensor cartridge and utility plate were then incubated at 37°C without CO_2 for 24 hours.

On the day of analysis, the McCoy's 5A medium was removed from the adherent cells and the wells were washed with 1 ml of pre-warmed Seahorse DMEM (pH 7.4; assay medium) containing no glucose or pyruvate. A final volume of 500 µl of assay medium was added to each well and the plate was then incubated at 37°C without CO_2 for 1 hour.

A volume of 50 µl glucose (20 mM final concentration in well; pH 7.4) or assay media was added to injection port A of the XF24 sensor cartridge in triplicate resulting in triplicate glucose and control readings for each cell line. The sensor cartridge and cell culture plate were them equilibrated by incubating them for at least 15 minutes prior to analysis at 37°C without CO_2.

The Seahorse software was then used to calibrate the XF24 sensor cartridge in the Seahorse XF24 analyzer (Seahorse Bioscience), which was pre-warmed to 37°C. Following calibration, the cell culture plate containing the adherent DLD-1 cell lines was placed into the analyzer and the extracellular acidification rate (ECAR) was measured by the following protocol: five cycles of mix (3 minutes),

delay (2 minutes), measure (3 minutes); port A injection; five cycles of mix (3 minutes), delay (2 min) and measure (3 minutes).

Upon completion of the protocol, assay medium was removed from each well and 100 µl of 1X cell lysis buffer (Cell Signalling Technology) was added to each well and left on ice for 5 minutes. The cell lysis buffer was pipetted up and down in the well to dislodge the attached cells. The protein content of each sample was determined by the Bradford assay (Section 2.2.11), and the ECAR rates were normalised to protein content (mpH/min/µg protein).

2.2.16. *In vitro* cell irradiation

The laboratory irradiator was designed and constructed at the University of Dundee for studies led by Dr Ian Sanders and Professor Alastair Munro. The irradiator was originally used as an *in vitro* simulation of rectal intraoperative radiotherapy (IORT) to identify biological markers of IORT response. In the present study the laboratory irradiator was used to investigate the role of miRNAs in modulating response to radiotherapy in colorectal cancer cell lines.

The laboratory irradiator was constructed using a photon radio-surgery system (PRS) x-ray source (Figure 2.12). The PRS x-ray source is attached to a stainless steel safe box lined with 3 mm of lead, with the x-ray probe pointing downwards into the box. An external response monitor (ERM) is also attached to the top of the safe box with its sensor inside the box which must measure radiation for the x-ray source to operate. Below the x-ray probe is a sample tray with an ionisation chamber and a shelving system which allows the distance between

the tip of the x-ray probe and the sample tray and ionisation chamber to be adjusted. The location of the ionisation chamber directly below the sample tray allows for a real time feedback of absorbed dose by a sample. The irradiator is made with a number safety interlocks to ensure the x-ray source is switched off if the safe box is opened or the x-ray source is lifted from the box during treatment.

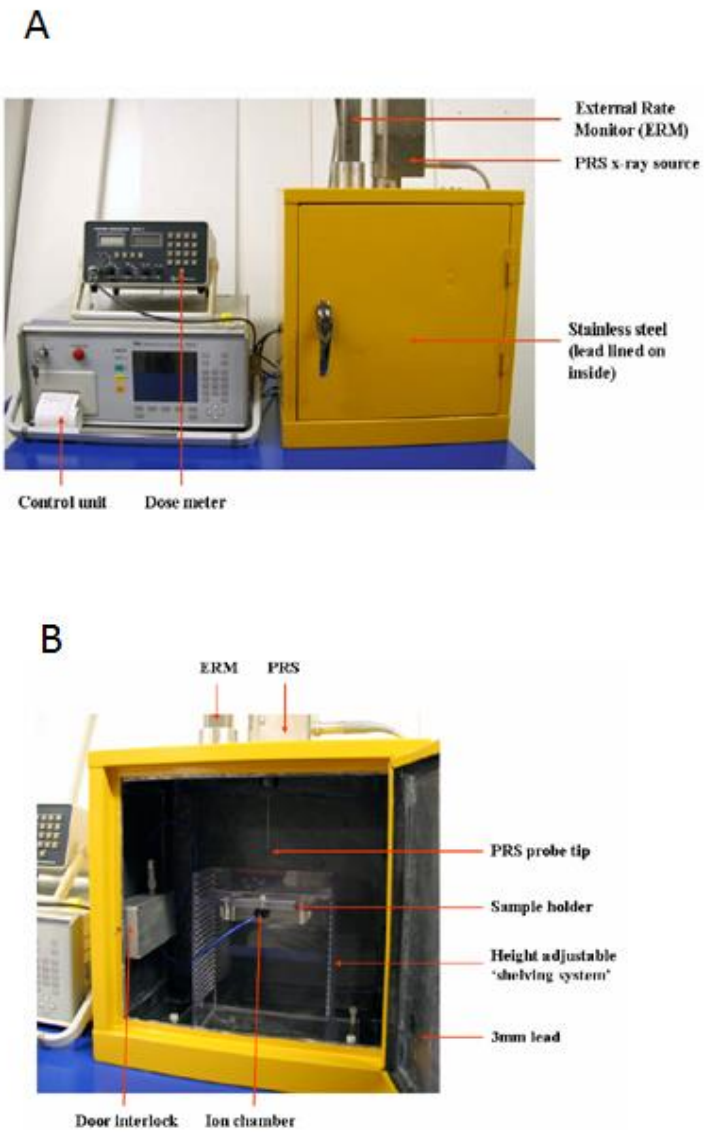

Figure 2.12: ***The laboratory irradiator****. The photographs show* ***A)*** *the outside and* ***B)*** *inside of the laboratory irradiator (Sanders, 2011).*

To deliver a target dose in Gray (Gy) to a sample, a dose in nano-Coulombs (nC) was calculated as shown in Box 2.2 for input into the dosemeter. The calculation was based on a number of preliminary experiments by the manufacturer to determine the PRS dose rate in air at each tray level and the attenuation factors of the culture dishes (Sanders, 2011). The calculation also involves correcting for changes in atmospheric pressure and temperature.

$$\text{Dose Limit (nC)} = \frac{\text{Target Dose (Gy)} \times \text{Attenuation Factor}}{\text{Ion Chamber Conversion factor}} \div \text{f.T.P}$$

For example, for a 5 Gy irradiation at tray level 4 using a plastic circular 3.5 cm diameter dish (Temperature 21°C, Pressure 1000 mb):

$$\text{Dose Limit (nC)} = \frac{5 \times 0.720}{1.279} \div \left(\frac{273.15 + 21}{293.13} \times \frac{1013.25}{1000}\right)$$

$$\text{Dose Limit (nC)} = 2.812 \div 1.017$$

$$\text{Dose Limit (nC)} = 2.765$$

Box 2.2: ***Equation for dose limit calculations.*** *f.T.P – factor for temperature and pressure*

In the present study, cells were seeded onto 3.5 cm diameter plates for irradiation and placed 8.5 cm from the x-ray probe (tray level 4). Sanders (2011) report that this would ensure the homogenous delivery of x-radiation to the whole sample within an acceptable time frame, given the rapid attenuation of

PRS x-rays. Three different types of experiments with different endpoints were performed following irradiation to investigate the effect of ionising radiation on global miRNA expression, protein expression and cell viability.

2.2.16.1. Taqman Low Density Array analysis

Cells were seeded on 3.5 cm diameter plates at density of 2.5 x 10^5 cells per plate and incubated at 37°C for 24 hours. The cells were then irradiated in triplicate at 5 Gy and incubated at 37°C for 1 hour. The 1 hour incubation period was determined by performing an optimisation experiment whereby the expression of 3 miRNAs previously reported to be induced or inhibited by ionising radiation (miR-24, miR-100, miR-125b) was measured 10, 30, 60 and 180 minutes after radiation. Following incubation, cells were harvested for RNA extraction (Section 2.2.8.1) for TLDA card analysis (Section 2.2.9.8).

2.2.16.2. Western blot analysis

Cells were seeded on 3.5 cm diameter plates at a density of 2.5 x 10^5 cells per plate and incubated at 37°C for 24 hours. The cells were then irradiated in duplicate at 5 Gy and incubated at room temperature for 5 minutes before protein samples were obtained as detailed in Section 2.2.11. Western blot analysis was then performed to blot for γH_2AX.

2.2.16.3. Flow cytometry

Cells were seeded on 3.5 cm diameter plates at a density of 2.5 x 10^4 cells per plate and incubated at 37°C for 24 hours. The cells were then irradiated in triplicate at 5 Gy. Changes in cell viability were then assessed using SYTOX AADvanced Dead Cell Stain on a flow cytometer (Section 2.2.14.2).

2.2.17. Bioinformatics and statistics

MicroRNA and mRNA expression data from TLDA miRNA cards and Illumina HT-12 BeadChip mRNA expression arrays, in collaboration with Probir Chakravarty (CRUK Bioinformatics and Biostatistics Service, London), was analysed using Bioconductor 1.9 (Gentleman *et al*, 2004) running on R 2.6.0 (R Development Core Team, 2008).

MiRNA expression data was normalised to MammU6 (the TLDA card equivalent of the single Taqman probe U6 snRNA). Statistically significant differentially expressed miRNAs were determined by using eBayes t-test from the limma package. P values were adjusted for multiple testing correction using the Benjamini-Hochberg method (Benjamini & Hochberg, 1995). MiRNAs that exhibited adjusted p values of less than 0.05 were then used to predict target genes that were predicted by at least 2 out of 5 of the following miRNA target prediction databases: mirDB (www.mirdb.org), miRANDA (www.microrna.org), miRBase (www.mirbase.org), TargetMiner (www.isical.ac.in) and TargetScan (www.targetscan.org). For each differentially expressed miRNA, a list of genes

was extracted, whereby a target gene was called if it was identified in at least 2 of the 5 databases.

Messenger RNA expression data was normalised using the Robust Multi-array Average (RMA) algorithm. Differentially expressed genes were then determined using eBayes t-test as described above. P values were also adjusted for multiple testing correction using the Benjamini-Hochberg method (Benjamini & Hochberg, 1995). Genes that exhibited adjusted p values of less than 0.05 and were differentially expressed by more than two-fold were then selected for further analysis.

Pathway and biological processes enrichment analyses were performed using Metacore (http://thomsonreuters.com/metacore/). The analysis employs a hyper-geometric distribution to determine enriched gene sets.

Independent T-tests were used to assess statistically significant ($p \leq 0.05$) differences in the means of continuous variables in cell lines (e.g. relative gene expression). Mann Whitney tests were used to compare the median and distribution of continuous variables in patient groups. In all Figures, * denotes $p \leq 0.05$, ** denotes $p \leq 0.01$, *** denotes $p \leq 0.001$ and **** denotes $p \leq 0.0001$.

Chapter 3

The role of microRNAs in colorectal cancer progression

3.1. Introduction

3.1.1. Colorectal cancer

Sporadic colorectal cancer development, as discussed in Chapter 1, was initially proposed to be driven by the progressive acquisition of genetic mutations in key oncogenes and tumour suppressor genes (Vogelstein *et al*, 1988). However, subsequent studies have suggested that the original model may not represent the vast majority of sporadic colorectal cancers (Smith *et al*, 2002; Frattini *et al*, 2004; Samowitz *et al*, 2007). For example, Smith *et al* (2002) reported that only 6% of the cancers profiled from 106 colorectal cancer patients had simultaneous mutations in the *KRAS*, *TP53* and *APC* genes, suggesting inter-patient variation in the mechanisms of development of colorectal cancer. Additionally, chromosomal instability, characterised by allelic losses, chromosomal amplification and translocation, and microsatellite instability, characterised by the epigenetic inactivation of DNA mismatch repair mechanisms, are proposed alternative mechanisms of colorectal carcinogenesis (Söreide *et al*, 2006). MicroRNAs are described as additional regulators of gene expression and have been presented as an additional level of complexity in the development of colorectal cancer (Bartel, 2004). As discussed previously, miRNAs may act as oncogenes or tumour suppressor genes through the negative regulation of key target genes involved in the development of colorectal cancer and metastatic disease.

3.1.2. Colorectal cancer miRNAs

Calin *et al* (2002) first linked the differential expression of miRNAs with cancer by reporting the decreased expression of miR-15 and miR-16 in 70% of chronic lymphatic leukaemia (CLL) cases. Following this, Michael *et al* (2003) were the first to report that mature miR-143 and miR-145 expression levels were reduced in colorectal cancers compared to patient-matched normal mucosa, and speculated that they may play an important role in colorectal carcinogenesis.

To date, a large number of studies have identified miRNAs differentially expressed in colorectal cancer. Table 3.1 summarises 20 studies in which miRNAs have been profiled in colorectal cancers and normal mucosa samples.

One difficulty with attempting to collectively analyse the studies listed in Table 3.1 is the inevitable variability between the patient samples and the profiling and statistical methodologies employed. For example, the number of miRNAs profiled ranged from 156 (Bandres *et al*, 2006) to 904 (Li *et al*, 2012). Additionally, some studies used RT-PCR technology whereas others used miRNA microarrays, while Schepeler *et al* (2008) used LNA-based oligonucleotide arrays and Li *et al* (2012) used miRCURY LNA Arrays. Furthermore, each study determined its own criteria for defining whether a particular miRNA was significantly differentially expressed meaning that they differed in the algorithms, statistical tests and cut offs employed.

Table 3.1: Studies assessing differential miRNA expression in colorectal cancers and normal colorectal tissue

Study	**Tissue samples**	**Technology**	**Number of miRNAs profiled**	**Number of differentially expressed miRNAs**
Bandres *et al* (2006)	12 matched cases	qRT-PCR	156	30 up, 23 down
Volinia *et al* (2006)	46 cancers, 8 normal tissue	miRNA microarray	228	21 up, 1 down
Monzo *et al* (2008)	22 matched cases	qRT-PCR	156	21 up, 7 down
Schepeler *et al* (2008)	49 cancers, 10 normal colon tissue	LNA-based oligonucleotide arrays + qRT-PCR	315	13 up, 6 down
Schetter *et al* (2008)	84 matched cases (test) 113 matched cases (validation)	miRNA microarray + qRT-PCR	389	26 up, 11 down
Arndt *et al* (2009)	45 cancers, 4 normal tissue	qRT-PCR	169	21 up, 16 down
Chen *et al* (2009)	13 matched cases	qRT-PCR	200	8 up, 7 down
Motoyama *et al* (2009)	69 matched cases	miRNA microarray – 4/69 cases qRT-PCR validation in all 69 cases	455	21 up*
Sarver *et al* (2009)	80 cancers, 29 normal colon tissue	qRT-PCR	735	19 up, 20 down
Earle *et al* (2010)	55 matched cases	qRT-PCR	20	12 up, 9 down
Wang *et al* (2010*c*)	3 matched cases	miRNA microarray + qRT-PCR	723	12 up, 2 down
Chang *et al* (2011)	20 matched cases	qRT-PCR	380	20 up, 13 down

Table 3.1 continued

Study	Tissue samples	Technology	Number of miRNAs profiled	Number of differentially expressed miRNAs
Slattery *et al* (2011)	30 matched cases 70 additional colorectal cancers	miRNA microarray	866	19 up, 16 down
Faltejskova *et al* (2012)	8 matched cases	qRT-PCR	667	4 up, 38 down
Fu *et al* (2012)	40 matched cases	miRNA microarray + qRT-PCR	-	16 up, 16 down
Hamfjord *et al* (2012)	8 matched cases	Illumina digital sequencing + qRT-PCR	-	18 up, 19 down
Li *et al* (2012)	6 matched cases (rectal)	miRCURY LNA Array	904	65 up, 25 down
Mosokhani *et al* (2012)	60 matched cases	miRNA microarray + qRT-PCR	723	7 up, 39 down
Nishida *et al* (2012)	13 cancers, 4 normal tissue	miRNA microarray + qRT-PCR	-	127 up, 29 down
Reid *et al* (2012)	40 matched cases	qRT-PCR	621	43 up, 27 down

* *Indicates that decreased miRNAs were not mentioned in this study,*

- Indicates that the number of miRNAs profiled not reported

However, despite the aforementioned biological and methodology differences, a group of miRNAs were identified to be consistently differentially expressed in colorectal cancer (Table 3.2), among which miR-21, miR-135b, miR-183, miR-31, and miR-20a were increased, and miR-145 and miR-378 were decreased in 9 or more studies.

Table 3.2: The most consistently differentially expressed miRNAs in colorectal cancer as determined from the studies listed in Table 3.1.

Increased in CRC		Decreased in CRC	
miRNA	Number of studies	miRNA	Number of studies
miR-21	10	miR-145	13
miR-135b	9	miR-378	10
miR-183	9	miR-143	6
miR-31	9	miR-1	6
miR-20a	9	miR-195	6
miR-19a	8	miR-139-5p	6
miR-93	7	miR-133a	5
miR-96	7	miR-422a	5
miR-17	7	miR-133b	5
miR-203	7	miR-375	5
miR-182	6	miR-10b	5
miR-18a	6	miR-192	4
miR-224	**6**	miR-215	4
miR-25	6	miR-30a-3p	4
miR-106a	6	miR-497	4
miR-29b	6	miR-26b	3
miR-106b	5	miR-30b	3
miR-19b	5	miR-30c	3
miR-424	5	miR-139	3
miR-92	5	miR-363	3
miR-223	5	miR-378*	3
miR-130b	4	miR-551b	3
miR-142-3p	4	miR-9	3
miR-148a	4	miR-30e	3
miR-29a	4	miR-125b	3
miR-221	4	miR-137	3
miR-15a	3	miR-204	3
miR-17-5p	3	miR-30a	3
miR-20	3	miR-150	3
miR-200a*	3		
miR-27a	3		
miR-552	3		
miR-98	3		
miR-7	3		
miR-191	3		

MiR-224 has been highlighted as it was the focus of the present study, as discussed later. MiR-224 expression was reported in six studies to be increased in colorectal cancers.

When the present study was established in October 2010, few studies had explored the expression of miRNAs in colorectal adenomas in an attempt to elucidate the role of colorectal miRNAs in the development of colorectal adenomas and progression of some of those adenomas to adenocarcinomas.

Schetter *et al* (2008) showed that miR-21 expression was increased in colorectal adenomas compared to patient-matched adjacent normal mucosa and also in colorectal cancers compared to colorectal adenomas. This suggested that the aberrant expression of miR-21 was an early and persistent event in colorectal tumorigenesis. Schmitz *et al* (2009) also reported that the expression of miR-21, as well as miR-181b, was significantly higher in serrated adenomas than in normal mucosa.

The six members of the miR-17-92 cluster (miR-17, miR-20a, miR-18a, miR-19a, miR-19b, miR-92) located on chromosome 13q31 had also been reported to be increased in colorectal cancers relative to both colorectal adenomas and normal mucosa (Disodado *et al*, 2009). The gain of chromosome 13q has also previously been characterised in colorectal cancers (Reid *et al*, 2009) and adenomas (Leslie *et al*, 2006).

Furthermore, miRNAs are detectable in patient serum and plasma samples at stable and reproducible levels (Chen *et al*, 2008; Mitchell *et al*, 2008). Huang *et al* (2010) reported that the increased expression of miR-29a and miR-92a could distinguish between the 37 advanced adenoma and 59 healthy patients recruited to the study. Despite these advances, there was a need for more comprehensive miRNA profiling in colorectal adenomas.

3.1.3. The role of miRNAs in colorectal tumorigenesis

The differential expression of miRNAs in colorectal cancer, as discussed in Chapter 1, is proposed to be caused by a number of factors including chromosomal abnormalities, epigenetic changes, the action of transcription factors and SNPs affecting miRNA biogenesis.

Prominent tumour suppressor miRNAs in colorectal cancer such as miR-143, which has decreased expression in cancers compared to normal mucosa, have been shown to promote colorectal carcinogenesis by direct targeting of the oncogene *KRAS*. Chen *et al* (2009) showed in Lovo colon cancer cell lines that a specific miR-143 inhibitor increased cell proliferation, an effect that was reverted when miR-143 was overexpressed. The inhibition of *KRAS* by miR-143 also inhibited the constitutive phosphorylation of ERK 1/2, an important intracellular protein kinase in the RAS/MAPK pathway.

The oncogenic miR-21 has also been reported to drive colorectal carcinogenesis through the repression of the tumour suppressors *PTEN*, which regulates cell proliferation and the cell cycle (Xiong *et al*, 2013), and *PDCD4* which plays a key role in apoptosis (Asangani *et al*, 2008). Furthermore, Asangani *et al* (2008) first reported that miR-21 drives colorectal cell invasion *in vitro* and that miR-21 and *PDCD4* expression was inversely related in colorectal cancer specimens.

Epithelial to mesenchymal transition (EMT) has also been implicated as a mechanism for the development of cancer metastasis, and miRNAs have since been shown to promote cancer metastasis through the regulation of EMT. EMT

is the conversion of immotile epithelial cells into mobile mesenchymal cells. This process was first described for the remodelling of tissues during embryonic development. However it has since been described as a way by which cancers can detach, migrate and disseminate through blood and lymphatic vessels during cancer metastasis (Thiery, 2002; Acloque *et al,* 2008).

Examples of miRNAs that have been established as regulators of EMT include the miR-200 family. The loss or down-regulation of epithelial (E-) cadherin, an adhesion molecule that forms adherin junctions and contribute to tissue structure and integrity, is a characteristic of EMT (Thiery, 2002). E-cadherin expression is repressed by the action of, amongst others, transcription factors known as zinc finger E-box binding homeobox (ZEB-) 1 and ZEB 2. Members of the miR-200 family, which include miR-200a, miR-200b, miR-200c, miR-141 and miR-429, directly target and negatively regulate the expression of ZEB 1/2 and thus induce EMT (Christoffersen *et al*, 2007; Hurteau *et al*, 2007). ZEB 1/2 however, has been shown to directly repress the transcription of the miR-200 family (Burk *et al*, 2008). ZEB 1/2 also promotes the transcription of vimentin, a type III intermediate filament protein expressed in mesenchymal cells that forms part of the cell cytoskeleton (Thiery & Sleeman, 2006).

The down-regulation of the miR-200 family, therefore, leads to the up-regulation of ZEB 1/2 which consequently leads to a decrease of E-cadherin and increase in vimentin and thus promotes EMT. As ZEB 1/2 also represses the transcription of the miR-200 family, a feed-forward loop is created (Burk *et al*, 2008). This relationship between the miR-200 family, ZEB 1/2 and EMT has been reported in

colorectal cancer (Chen *et al*, 2012; Bojmar *et al*, 2013) and a decrease in their expression is associated with lower survival in colorectal cancer patients.

MiRNAs may also contribute to colorectal progression and metastatic disease by regulation of angiogenesis. Cancers adapt to hypoxic conditions by increasing the induction of angiogenesis allowing for the exchange of oxygen and respiratory waste products and also providing a network by which cancer cells can disseminate and form metastases at secondary sites (Harris, 2002). One of the many transcription factors implicated in angiogenesis is vascular endothelial growth factor (VEGF; Harris, 2002). A recent study, in colorectal cancer, reported that epigenetic silencing of miR-126, which is under-expressed in colorectal cancer, contributed to cancer invasion and angiogenesis *in vivo* (Zhang *et al*, 2013*c*). Restoration of miR-126, by 5-aza-CdR, inhibited cell growth, migration and invasion, an effect that was shown to occur through the miR-126 targeting and repression of VEGF.

3.1.4. MiRNAs as biomarkers of disease progression

There are now many examples where miRNAs that are commonly differentially expressed in colorectal cancer have been shown to be differentially expressed in different stages of colorectal cancer and to correlate with cancer staging and survival in colorectal cancer patients. Increased expression of miR-21, for example, is associated with advanced TNM staging and poor survival (Schetter *et al*, 2008; Liu *et al*, 2011).

Furthermore, miRNA expression profiles have been shown to discriminate between cancers on the basis of molecular characteristics such as microsatellite status or the mutation status of important oncogenes and tumour suppressors known to drive colorectal tumorigenesis. Given the multiple functions of miRNAs due to their imperfect complementarity with gene targets, the activation or repression of different cancer-related pathways may be caused or affected by miRNAs, thus leading to unique miRNA signatures and the mediation of variable phenotypes.

Lanza *et al* (2007) were the first group to investigate the differences in miRNA expression between microsatellite stable (MSS) and microsatellite unstable (MSI) cancers where 14 miRNAs were identified as differentially expressed. Among the differentially expressed miRNA were members of the miR-17-92 family that were significantly over-expressed in MSS cancers. In a similar study, Schepeler *et al* (2008) highlighted miR-142-3p, miR-212, miR-151 and miR-144 as miRNAs that could predict the microsatellite status of colon cancers with relatively high accuracy. MSI cancers have been suggested to have favourable clinical outcome compared to non-MSI cancers (Popat *et al*, 2005), and adds to the importance of identifying miRNA biomarkers to aid diagnosis.

A series of studies led by Ju and colleagues identified 54 miRNAs that were differentially expressed in HCT116 p53-WT and null cell lines (Xi *et al*, 2006*b*). When a subset of these miRNAs was tested in a cohort of 24 colorectal cancer patients, the increased expression of miR-181b and miR-200c was strongly associated with a mutant p53 status in colorectal cancers, with high expression

of miR-200c also having a negative impact on patient survival (Xi *et al*, 2006*a*). This indicated that miRNAs that regulated, or were regulated by, p53 could discriminate between mutant and WT p53 cancers and also predict patient prognosis.

Our research group has a particular interest in *KRAS* as a previous study published from within the group showed that colorectal cancer patients with *KRAS* mutations had a significantly lower survival than patients with WT *KRAS*, an effect that was not observed with APC and p53 (Conlin *et al*, 2005). The miRNAs that are able to discriminate between *KRAS* mutant and WT cancers and regulate the RAS/MAPK pathway may therefore be important in further classifying colorectal cancers based on patient prognosis.

Ragusa *et al* (2010) reported that miR-146b-3p and miR-486-5p, miRNAs that were differentially increased following cetuximab treatment in HCT116 cells, were also increased in *KRAS* mutant cancers compared to *KRAS* WT cancers in colorectal cancer patients. However, the genetic background of the cancers apart from their *KRAS* mutation status was not considered. It is therefore necessary to identify novel regulators of *KRAS* and the RAS/MAPK pathway in a controlled, isogenic cell line background and test their potential in assisting with *KRAS*-based diagnosis in predicting patient prognosis.

3.2. Aims and objectives

The aim of this study was therefore to extend the molecular sub-classification of colorectal cancers by investigating the extent to which individuality in miRNA expression influences oncogene expression. In particular, I sought to explore how the inter-individual expression of miRNAs that regulate KRAS and its downstream pathways may sub-classify colorectal cancers at a molecular level in terms of disease progression.

To achieve this, my aim was firstly to analyse miRNAs that were differentially expressed in colorectal adenomas and cancers compared to normal mucosa. Secondly I sought to discover novel miRNA regulators of KRAS and the RAS/MAPK pathway by identifying differentially expressed miRNAs in isogenic *KRAS* mutant and WT cell lines.

3.3. Results

3.3.1. MicroRNA profiling in human colorectal tissue

Twelve colorectal cancer samples, previously profiled (Affymetrix mRNA gene expression profiles and mutation status) within our research group, were profiled for miRNA expression using TLDA cards, as described in Section 2.2.9.8. Figure 3.1 shows, using the first 55 miRNAs on the TLDA cards as an example, that inter-patient differences in miRNA expression were observed across the cancer cohort (full data set for all 377 miRNAs in Appendix B). This is of particular interest in the present study as the differences existing between the expression of certain miRNAs may have important phenotypic or clinical characteristics in a patient. The expression of miR-17, for example, (highlighted by red circles in Figure 3.1) is shown to be variable across the cohort of 12 cancers. Heightened expression of miR-17, which is part of the miR-17-92 cluster, has previously been shown to be associated with poor survival in colon cancer patients (Yu *et al*, 2012).

The profiling data from the present study shows that of the 377 miRNAs profiled, 153 were not expressed in any of the cancers. The data also show that 199 miRNAs (52.7%) were expressed in at least 2 of the 12 cancers and 108 miRNAs (28.6%) were expressed in all 12 cancers (Appendix E, Table E1). The most abundantly expressed miRNAs were miR-200c, miR-222 and miR-24 whereas miR-331-5p, miR-481 and miR-98 were the least abundantly expressed. The mean expression of miR-200c, relative to the control miRNA let-7a (using the method detailed in Section 2.2.9.5), was the arbitrary value of 60.5 whereas

the mean expression of miR-98 was 0.042, showing that there was a 1440-fold difference between the highest and lowest expressed miRNA.

Furthermore, eighteen miRNAs (miR-193b, miR-323-3p, miR-324-3p, miR-331-5p, miR-339-3p, miR-362-5p, miR-365, miR-374, miR-449b, miR-487a, miR-491-5p, miR-494, miR-501, miR-532-5p, miR-574-3p, miR-671-3p, miR-744, miR-99b) not previously described in colorectal cancer were expressed in all 12 cancers.

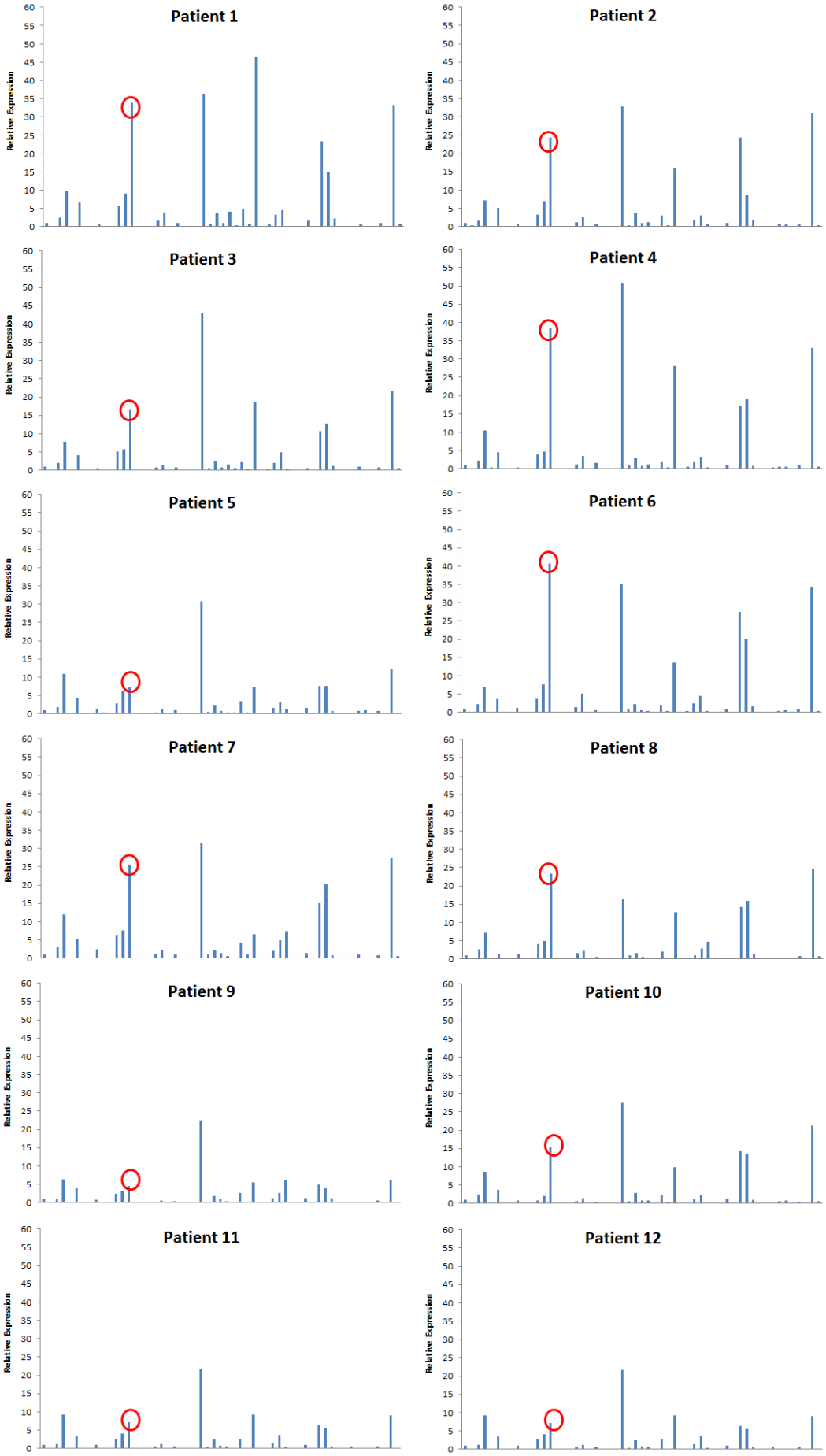
Patient 1
Patient 2
Patient 3
Patient 4
Patient 5
Patient 6
Patient 7
Patient 8
Patient 9
Patient 10
Patient 11
Patient 12
Relative Expression
0
5
10
15
20
25
30
35
40
45
50
55
60

Figure 3.1: ***Inter-patient variability in the expression of individual miRNAs.*** *TLDA miRNA 'A' cards (Life Technologies) were used to profile the expression of 377 miRNAs in 12 colorectal cancers, as detailed in Section 2.2.9.8. The expression of the first 55 miRNAs on the TLDA card, relative to the control gene let-7a, is shown and the full data set is presented in Appendix B. Each bar represents a single point determinant of relative expression. Red circles indicate the variability of expression of miR-17 across the 12 cancers.*

To investigate which miRNAs may drive the progression of colorectal cancer, 12 normal colorectal mucosa samples, patient-matched to the colorectal cancers mentioned above, as well as 12 samples of mainly tubulovillous adenomas were obtained from Tayside Tissue Bank. The adenomas were split equally into those defined as displaying high grade or low grade dysplasia.

To minimise the number of TLDA cards used in my initial screen, only 3 of the 12 patient-matched normal mucosa samples and 6 of the 12 adenoma samples (3 high grade, 3 low grade) were profiled for miRNA expression and compared to the profiling data from 3 of the 12 cancers that had already been profiled. The colorectal cancer and normal mucosa samples were matched from the same patient. The normal mucosa and adenoma samples used for TLDA miRNA profiling were chosen based on their high RNA yield and integrity (RIN) relative to other samples following RNA extraction, as assessed by the methods detailed in Section 2.2.8.4 (Appendix C and Appendix D).

TLDA miRNA profiling identified that 111 miRNAs out of 377 (29.4%) were expressed in all of the normal, adenoma and cancer samples profiled (Appendix E, Table E2). The expression of seven miRNAs was significantly increased in low grade adenomas, high grade adenomas and colorectal cancers compared to

normal mucosa. Additionally, 6 miRNAs were identified to have a significantly decreased level of expression in all stages of colorectal cancer progression compared to normal mucosa (Table 3.3).

All 13 miRNAs have subsequently been shown to be differentially expressed in colorectal cancers compared to normal mucosa. The data in the present study is consistent with Bartley *et al* (2011) who at the same time identified that the expression of miR-15b, miR-29c, miR-27a, and miR-500 was increased in colorectal adenomas and cancers compared to normal mucosa. Oberg *et al* (2011) found that miR-139-5p expression was decreased in colorectal adenomas and cancers compared to normal mucosa. Moreover, both Bartley *et al* (2011) and Oberg *et al* (2011) reported that miR-224 and miR-133a expression was increased and decreased respectively in colorectal adenomas and cancers compared to normal mucosa, consistent with the data in the present study.

Table 3.3: MicroRNAs differentially expressed in colorectal adenomas and cancers relative to colorectal normal mucosa

	Normal vs LGA	**Normal vs HGA**	**Normal vs cancer**
	Fold change	**Fold change**	**Fold change**
miR-15b	3.32	2.83	1.86
miR-27a	5.45	8.35	6.83
miR-29c	9.17	15.29	5.87
miR-92a	3.72	4.66	4.01
miR-93	3.15	3.46	4.25
miR-224	**7.41**	**5.86**	**5.15**
miR-500	2.22	7.29	3.13

	Normal vs LGA	**Normal vs HGA**	**Normal vs cancer**
	Fold change	**Fold change**	**Fold change**
miR-125b	-7.28	-7.04	-2.12
miR-127-3p	-3.38	-2.85	-1.76
miR-133a	-3.75	-4.29	-27.26
miR-139-5p	-3.01	-3.19	-13.35
miR-145	-3.32	-3.47	-9.42
miR-149	-3.49	-2.16	-3.32

The fold change in mean miRNA expression, calculated relative to the control miRNA let-7a, in low grade adenomas (LGA), high grade adenomas (HGA) and colorectal cancers compared to normal mucosa. All miRNAs listed are statistically significantly differentially expressed ($p \leq 0.05$) as determined using Mann Whitney tests. MiR-224, the later focus of the present study is highlighted.

3.3.2. MicroRNA profiling in colorectal cancer cell lines

TLDA miRNA profiling was also used to identify miRNAs that were differentially expressed in HCT116 colorectal cancer cell lines, engineered to express either the WT or mutant form of *KRAS*, as described in Section 2.2.9.8. As the two cell lines are isogenic apart from their *KRAS* mutation status, the present study investigated whether differentially expressed miRNAs would have an influence on KRAS signalling or its downstream pathways. Twelve miRNAs were differentially expressed in *KRAS* WT cell lines compared to mutant cell lines (Table 3.4). Of the 12 miRNAs, 5 miRNAs were significantly decreased in *KRAS* WT cells relative to mutant cells whereas 7 miRNAs were significantly increased in *KRAS* WT cells compared to mutant cells. Interestingly, miR-193b has recently been experimentally validated to directly target *KRAS* (Gastaldi *et al*, 2014).

Table 3.4: MicroRNAs differentially expressed in HCT116 *KRAS* WT and mutant cell lines

microRNA	Fold Change	Adjusted p value
miR-224	**5.13**	**0.008**
miR-636	3.02	0.004
miR-34a	2.57	0.011
miR-193b	1.92	0.021
miR-125a-5p	1.85	0.018
miR-28-3p	1.83	0.022
miR-139-5p	1.65	0.043
miR-29a	-1.89	0.021
miR-494	-2.15	0.002
miR-886-3p	-2.34	0.013
miR-29c	-2.35	0.002
miR-18a	-2.47	0.003

Three miRNAs (miR-224, miR-29c and miR-miR-139-5p) were differentially expressed in HCT116 *KRAS* WT and mutant cells (Table 3.4) and additionally differentially expressed in colorectal adenomas and cancers (Table 3.3). The expression of miR-29c was increased in colorectal adenomas and cancers compared to normal mucosa and significantly decreased in *KRAS* WT cells compared to *KRAS* mutant cells. On the other hand, miR-139-5p was significantly increased in *KRAS* WT cells compared to *KRAS* mutant cells but was significantly decreased in colorectal adenomas and cancers compared to normal colorectal mucosa.

The expression of miR-224, like miR-29c, was increased in colorectal adenomas and cancers relative to normal colorectal mucosa but, like miR-139-5p, was increased in *KRAS* WT cell lines. As miR-224 was also the most abundantly differentially expressed miRNA in the comparison between the *KRAS* WT and mutant HCT116 cells, this chapter investigates the association between miR-224, KRAS and its downstream pathways and also the potential role of miR-224 in colorectal cancer progression.

To validate the results from the TLDA analysis described above, a single probe Taqman small RNA assay specific to miR-224 was used to confirm that miR-224 expression was significantly increased (3.3-fold; p=0.0002) in HCT116 *KRAS* WT cells compared to *KRAS* mutant cells (Figure 3.2).

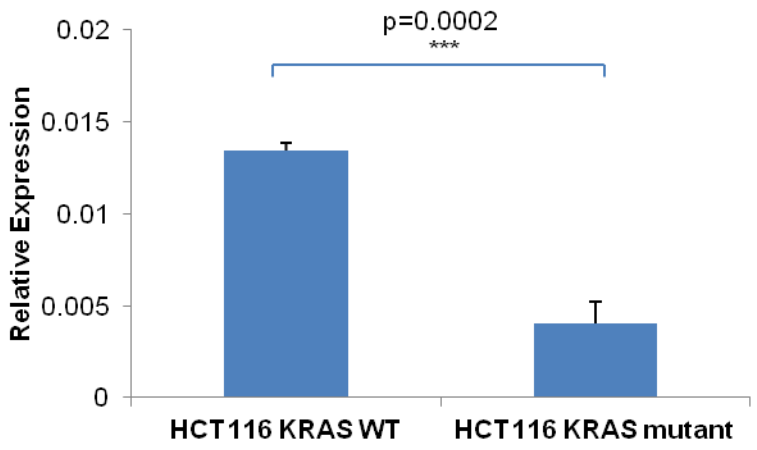

Figure 3.2: ***The validation of miR-224 expression in HCT116 KRAS WT and mutant cell lines***. *A miR-224 specific Taqman small RNA assay was used to assess the expression of miR-224 in HCT116 KRAS WT and mutant cell lines, relative to the expression of the control miRNA let-7a, as described in Section 2.2.9.2. MiR-224 expression was assessed in both cell lines in triplicate and errors were determined by calculating* $2^{(-\delta Ct + sd\ \delta Ct)}$ *and* $2^{(-\delta Ct - sd\ \delta Ct)}$*, as detailed in Section 2.2.9.5. Statistical significance (p≤0.05) was determined by performing independent T-tests.*

3.3.3. MiR-224 expression in human cancers

I next sought to confirm that miR-224 expression was increased in colorectal cancers relative to normal mucosa, and to investigate whether miR-224 expression was influenced by *KRAS* or *BRAF* mutation status. Twelve colorectal cancers and their patient-matched normal mucosa samples were selected on the basis of cancer *KRAS* and *BRAF* mutation status (4 G13D *KRAS* mutant, 4 $BRAF^{V600E}$ mutant and 4 *KRAS* and *BRAF* WT). G13D *KRAS* mutant cancers were chosen as the HCT116 *KRAS* mutant cell line harbours the same type of *KRAS* mutation. The cancers were otherwise variable for other factors such as the mutation status of other genes and cancer stage (Appendix F, Table F1). A marked inter-patient difference in miR-224 expression was observed across the

cohort of cancers and normal mucosa (Figure 3.3 A). The expression of miR-224 was significantly increased in cancers compared to normal mucosa in 10 of the 12 patients (Figure 3.3 B). Overall, across the cohort of 12 patients, the expression of miR-224 was significantly increased ($p=0.005$; Mann Whitney test) in colorectal cancers compared to normal mucosa, consistent with the initial screen in Table 3.3.

(A)

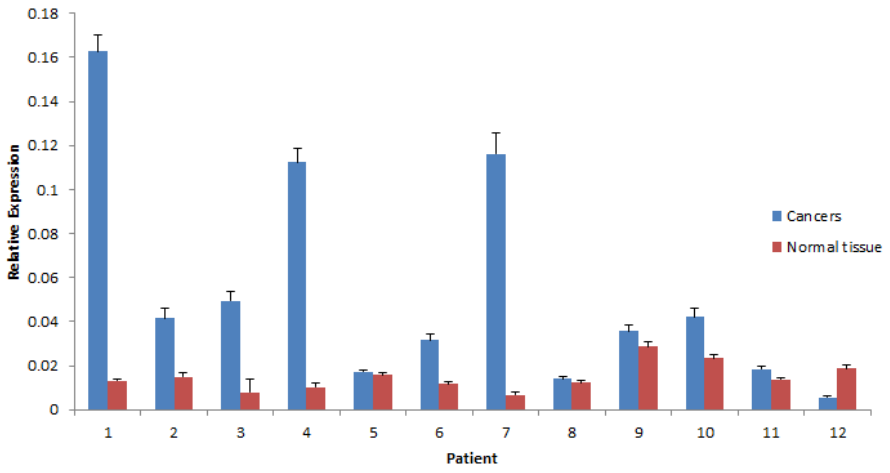

(B)

Patient	Fold change	p value
1	12.25	p<0.0001
2	2.79	0.002
3	6.13	0.002
4	10.75	p<0.0001
5	1.10	0.042
6	2.70	0.001
7	16.78	0.002
8	1.12	0.079
9	1.25	0.025
10	1.79	p<0.0001
11	1.34	0.007
12	-3.35	0.002

Figure 3.3: ***MiR-224 expression in colorectal cancers and patient-matched normal mucosa. A)*** *The expression of miR-224, relative to the control miRNA let-7a, was assessed in 12 colorectal cancers and patient-matched normal mucosa samples using a miR-224 specific Taqman small RNA assay, as detailed in Section 2.2.9.2. MiR-224 expression was assessed in all patient samples in triplicate and errors were determined by calculating* $2^{(-\delta Ct + sd\ \delta Ct)}$ *and* $2^{(-\delta Ct - sd\ \delta Ct)}$*, as detailed in Section 2.2.9.5;* ***B)*** *Fold change of relative miR-224 expression in colorectal cancers compared to matched normal mucosa was calculated and statistical significance (p≤0.05) of miR-224 expression in colorectal cancers compared to normal mucosa was determined by performing independent T-tests.*

Furthermore, to explore whether miR-224 could stratify colorectal cancers based on their *KRAS* or *BRAF* mutation status, the cancer series was extended to a cohort of 41 cancers including 14 *KRAS* and *BRAF* WT cancers, 9 *BRAF* mutant and 18 *KRAS* mutant cancers (Appendix F, Table F2). Compared to the *KRAS* and *BRAF* WT cancers, miR-224 expression was significantly decreased (p=0.012) in *BRAF* mutant cancers (Figure 3.4). In contrast, the expression of miR-224 was not significantly changed in *KRAS* mutant cancers compared to *KRAS* and *BRAF* WT cancers. An explanation for this could be that all 9 *BRAF* mutant cancers harboured a common $BRAF^{V600E}$ mutation. However, within the *KRAS* mutant cancers were a number of different *KRAS* mutations. Previous data within our group have shown using a NIH3T3 mouse fibroblast cell line model that other types of *KRAS* mutations cause varying cell phenotypes such as different sensitivities to 5-FU (see Section 3.3.6) and colony formation potential. This raises the question of whether miR-224 would be significantly differentially expressed in cell lines or cancers with only a G13D mutation, but we unfortunately did not have sufficient power to formally test this hypothesis.

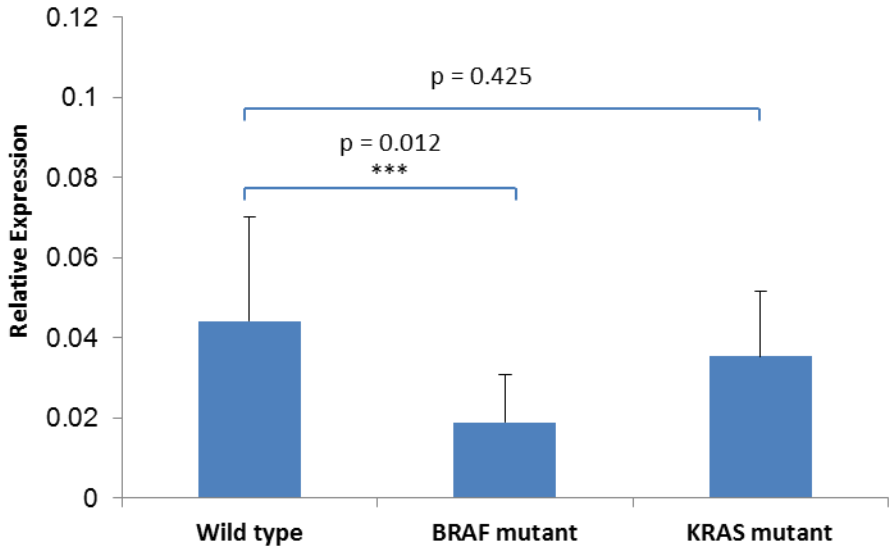

Figure 3.4: ***MiR-224 expression in KRAS/BRAF WT colorectal cancers compared to BRAF mutant and KRAS mutant cancers:*** *The expression of miR-224, relative to the control miRNA let-7a, was assessed in 41 colorectal cancers, including 14 KRAS and BRAF WT cancers, 9 BRAF mutant and 18 KRAS mutant cancers. MiR-224 expression was assessed in all patient samples in triplicate and errors were calculated by using* $2^{(-\delta Ct + sd\ \delta Ct)}$ *and* $2^{(-\delta Ct - sd\ \delta Ct)}$*, as detailed in Section 2.2.9.5; statistical significance (p≤0.05) of miR-224 expression in BRAF mutant cancers compared to KRAS/BRAF WT cancers and KRAS mutant cancers compared to KRAS/BRAF WT cancers was determined by performing Mann Whitney tests.*

I also investigated whether miR-224 expression could stratify the 41 colorectal cancers based on correlations with gene expression data generated using Affymetrix profiling in previous studies within our laboratory. Spearman rank correlation was used to correlate the relative expression of miR-224 across the cohort of 41 colorectal cancers and each of the 3566 probes from the Affymetrix data targeted to the 1305 predicted gene targets of miR-224 (Appendix I) as determined by bioinformatics analysis described later in Section 3.3.8. The strongest positive correlation was seen with *YIP1* (Yip1 domain family, member

6; correlation value: +0.629) whereas the strongest negative correlation was with *TLR1* (Toll-like receptor 1; correlation value: -0.626; Appendix G). Neither *YIP1* nor *TLR1* have been previously associated with miR-224. The inverse correlation between miR-224 and TLR1 suggests that TLR1 could be a potential novel target of miR-224. No strong correlations however were seen with between miR-224 expression and the expression of the genes that have been experimentally validated to be direct targets of miR-224 such as *SMAD4* (Wang et al, 2013; Zhang *et al*, 2013*a*) or *API5* (Wang *et al*, 2008). This may indicate the limitations of correlating miRNA expression with mRNA expression as, in some cases, mRNA levels are unchanged following the binding of miRNAs to the 3'UTR of mRNA whereas protein translation is blocked. This highlights the importance of correlating miR-224 expression with protein expression, a priority for future studies. Furthermore, this approach may have been further limited by the fact that the cohort of 41 colorectal cancers may have been too small, also highlighting the need to perform this type of analysis in a larger cohort.

Pre-mir-224 is located on, and transcribed from, the q arm of the X chromosome to form the mature miR-224. It was therefore hypothesised that there could be a difference in the expression of miR-224 expression between male and female patients. The expression of miR-224 was not, however, significantly different between the 18 male and 23 female colorectal cancer patients (p=0.331; Mann Witney test)

I also investigated whether miR-224 expression was higher in later staged cancers. Within the 41 cancers investigated, 4 were identified to be Dukes' stage

A (T1/T2 N0 MX – by TNM staging), 20 as Dukes' stage B (T3/T4 N0 MX) and 17 as Dukes' stage C (T3/T4 N1/N2 MX). There was no significant difference in miR-224 expression between Dukes' stage A and B (p=0.64), Dukes' stage A and C (p=0.65) or between Dukes' stage B and C cancers (p=0.48; Mann Whitney test).

3.3.4. MiR-224 knockdown in HCT116 *KRAS* WT cells

To investigate the functional role of miR-224, a specific miR-224 inhibitor was transiently transfected into HCT116 *KRAS* WT cell lines, as described in Section 2.2.5. As miR-224 expression is higher in *KRAS* WT cells it was speculated that lowering the expression of miR-224 may show a *KRAS* mutant-like phenotype in *KRAS* WT cells by increasing KRAS activity. An initial optimisation experiment where final concentrations of 10 nM, 15 nM, 20 nM, 25 nM and 30 nM of miR-224 inhibitor or a negative control was transfected into HCT116 *KRAS* WT cells showed that the degree of miR-224 knockdown ranged from 91% at 10 nM ($p=1.5x10^{-8}$) to 98% at 30 nM after 24 hours ($p=1.1x10^{-6}$; Figure 3.5). In contrast, the expression of miR-224 following transfection with negative control was not significantly changed between the lowest and highest concentration (p=0.12; ANOVA; Figure 3.5). A final concentration of 30 nM miR-224 inhibitor or negative control was therefore used for subsequent experiments.

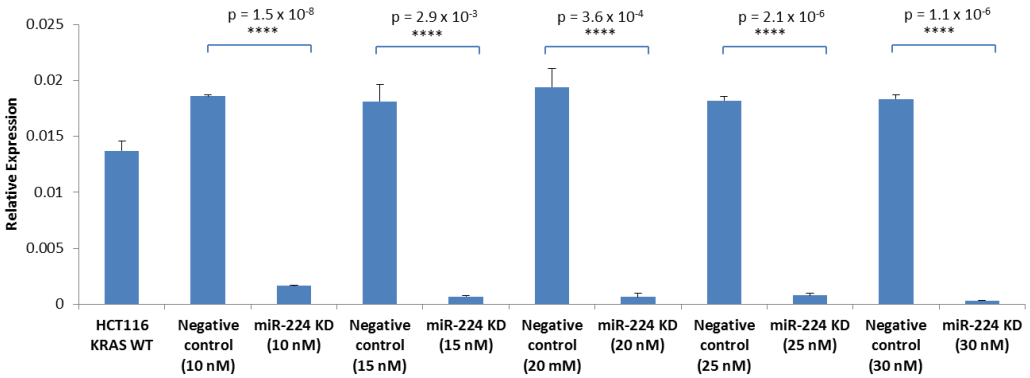

Figure 3.5: ***MiR-224 inhibitor and miRNA inhibitor negative control optimisation.*** *HCT116 KRAS WT cells were transiently transfected with 10 nM, 15 nM, 20 nM, 25 nM and 30 nM of miR-224 specific miRNA inhibitor and a miRNA inhibitor negative control, as described in Section 2.2.5. The expression of miR-224, relative to the control let-7a, was assessed as described in Section 2.2.9.2. MiR-224 expression was assessed in each sample in triplicate and errors were calculated by using* $2^{(-\delta Ct + sd\ \delta Ct)}$ *and* $2^{(-\delta Ct - sd\ \delta Ct)}$*, as detailed in Section 2.2.9.5; statistical significance (p≤0.05) of miR-224 expression in negative control transfected HCT116 KRAS WT cells compared to miR-224 inhibitor transfected cells was determined by performing independent T-tests.*

The knockdown of miR-224 ranged from 96% ± 0.3% ($p=1.1x10^{-5}$) 24 hours after transfection to 89% ± 0.8% ($p=9.1x10^{-5}$) 96 hours after transfection (Figure 3.6). By 168 hours the knockdown of miR-224 had reduced to 51% ± 4.8% ($p=8.6x10^{-3}$). This demonstrated that there was a window of at most 96 hours post-transfection where miR-224 expression was sufficiently diminished to allow for investigating the phenotypic consequences of its absence.

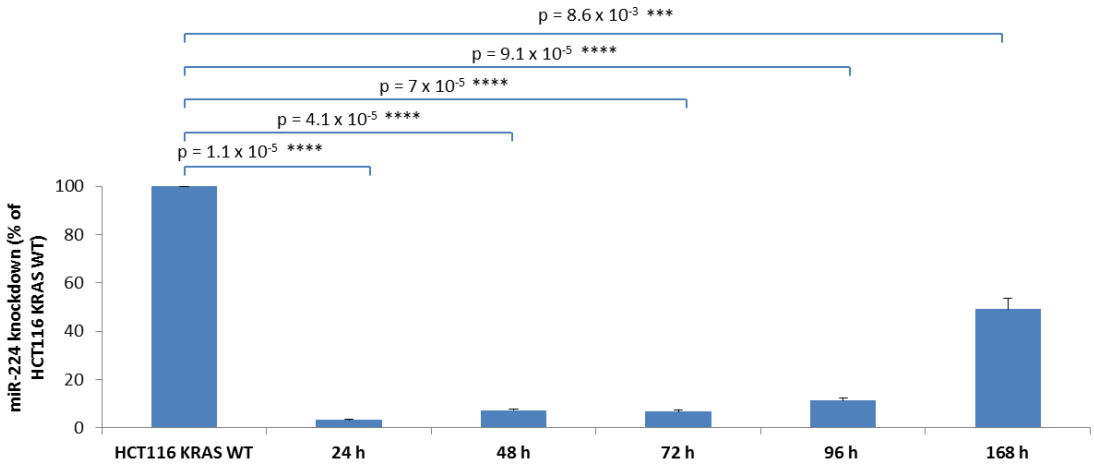

Figure 3.6: ***The knockdown of miR-224 over 168 hours.*** *HCT116 KRAS WT cells were transiently transfected with a final concentration of 30 nM miR-224 inhibitor, as described in Section 2.2.5. MiR-224 expression was assessed, relative to the control miRNA let-7a, 24, 48, 72, 96 and 168 hours after transfection in miR-224 knockdown cells and the untransfected HCT116 KRAS WT cells, as described in Section 2.2.9.2. The experiment was performed 3 times and the error bars represent the SEM. Statistical significance (p≤0.05) of miR-224 expression in untransfected HCT116 KRAS WT cells compared to miR-224 knockdown cells at each time point was determined by performing independent T-tests.*

3.3.5. The effects of miR-224 knockdown on KRAS activation

As miR-224 was significantly differentially expressed in HCT116 *KRAS* WT and mutant cells, the effect of miR-224 knockdown on the amount of GTP-bound activated KRAS was next investigated using a RAS ELISA, as described in Section 2.2.12. KRAS activation, as expected, was inherently higher (2.5 fold, p=0.0017) in *KRAS* mutant cells compared to *KRAS* WT cells (Figure 3.7). The knockdown of miR-224 in HCT116 *KRAS* WT cells significantly increased KRAS activation (1.9 fold, p=0.0012) compared to the untransfected *KRAS* WT cells. Consistent with

my hypothesis, this suggests that the knockdown of miR-224 may convert the *KRAS* WT phenotype to a more active or *KRAS* mutant-like phenotype.

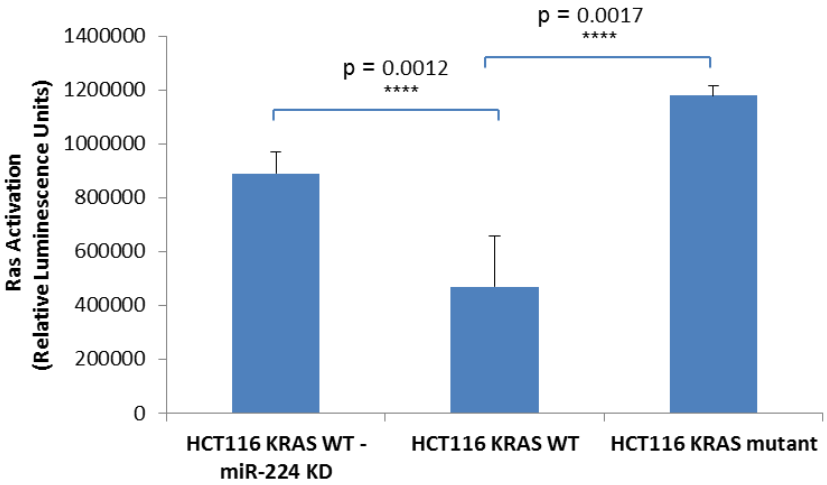

Figure 3.7: The effect of miR-224 knockdown in HCT116 KRAS WT cells on KRAS activation. A *Ras ELISA was used to assess the effect of miR-224 knockdown in HCT116 KRAS WT cells on the amount of GTP-bound activated KRAS (measured in relative luminescence units) in a cellular extract compared to untransfected HCT116 KRAS WT and mutant cells, as described in Section 2.2.12. Each sample was assessed in triplicate and the errors represent the SEM of relative luminescence units. Statistical significance ($p \leq 0.05$) of KRAS activation in miR-224 knockdown HCT116 KRAS WT cells compared to untransfected HCT116 KRAS WT and mutant cells was determined by performing independent T-tests.*

To investigate the effect of miR-224 knockdown in HCT116 *KRAS* WT cells on downstream signalling pathways, a PathScan intracellular signalling array which detects the phosphorylation or cleavage of 18 well characterised signalling molecules was used as described in Section 2.2.13. The array firstly suggested that, consistent with KRAS activation, the phosphorylation of ERK, an important downstream intracellular protein kinase in the RAS/MAPK pathway, was increased (1.6 fold) in HCT116 *KRAS* WT cells after miR-224 knockdown and thus also exhibited a *KRAS* mutant-like phenotype (Figure 3.8).

(A)

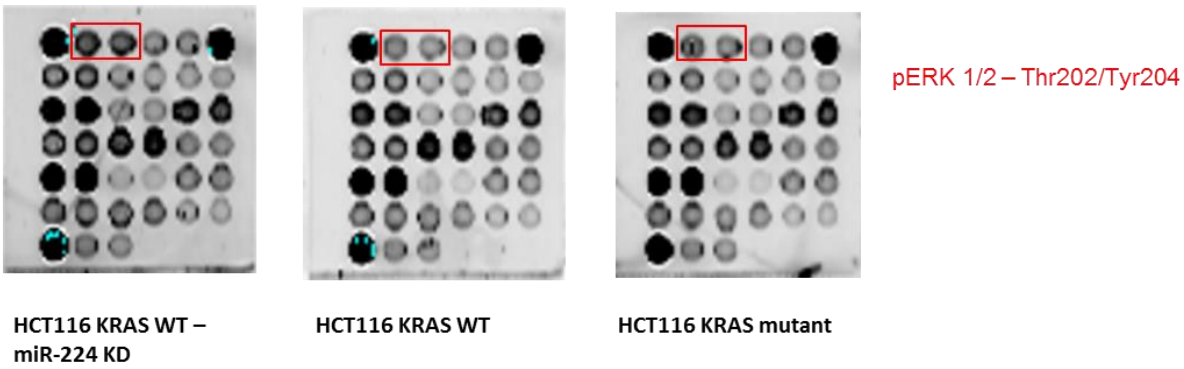

(B)

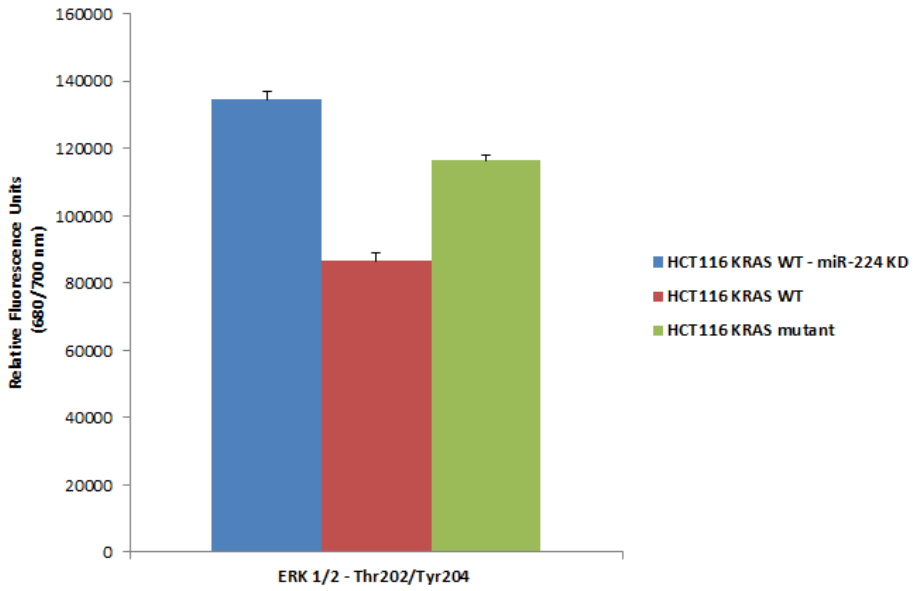

Figure 3.8: ***The effect of miR-224 knockdown on ERK 1/2 phosphorylation. A)*** *The PathScan intracellular signalling array and LiCor Odyssey fluorescence imaging system was used to assess the effect of miR-224 knockdown in HCT116 KRAS WT cells on the phosphorylation or cleavage of 18 signalling molecules compared to untransfected HCT116 KRAS WT and mutant cells, as detailed in Section 2.2.13; highlighted in red is pERK 1/2. Each signalling molecule is represented in duplicate.* ***B)*** *The fluorescent signals at wavelength 680/700 nm as determined by LiCor Image Studio are represented graphically. Experiment was performed once and error bars represent the technical replicates.*

Secondly, the array suggested that the phosphorylation of AKT at tyrosine 308 and serine 473 was significantly higher (1.4 and 1.3 fold respectively) in HCT116 *KRAS* WT cells after miR-224 knockdown compared to untransfected *KRAS* WT cells and *KRAS* mutant cells suggesting that miR-224 knockdown may also affect the pro-survival Ras-Akt-PI3K pathway. Surprisingly, there was no difference between the *KRAS* WT and mutant cells (Figure 3.9).

(A)

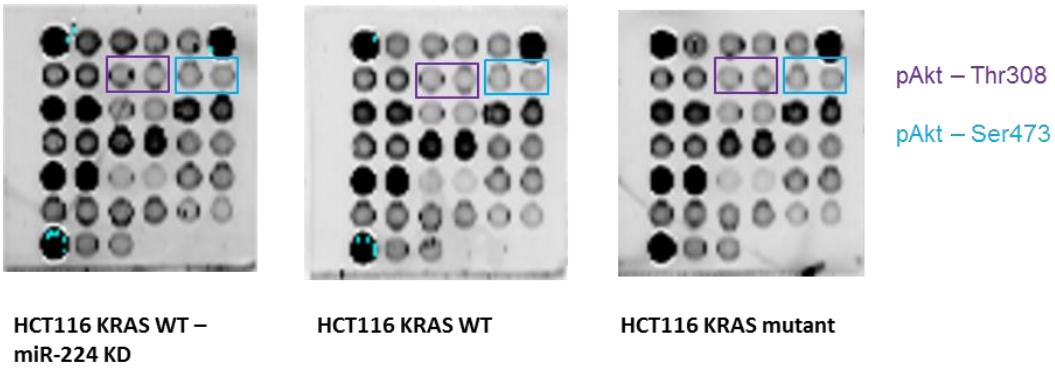

(B)

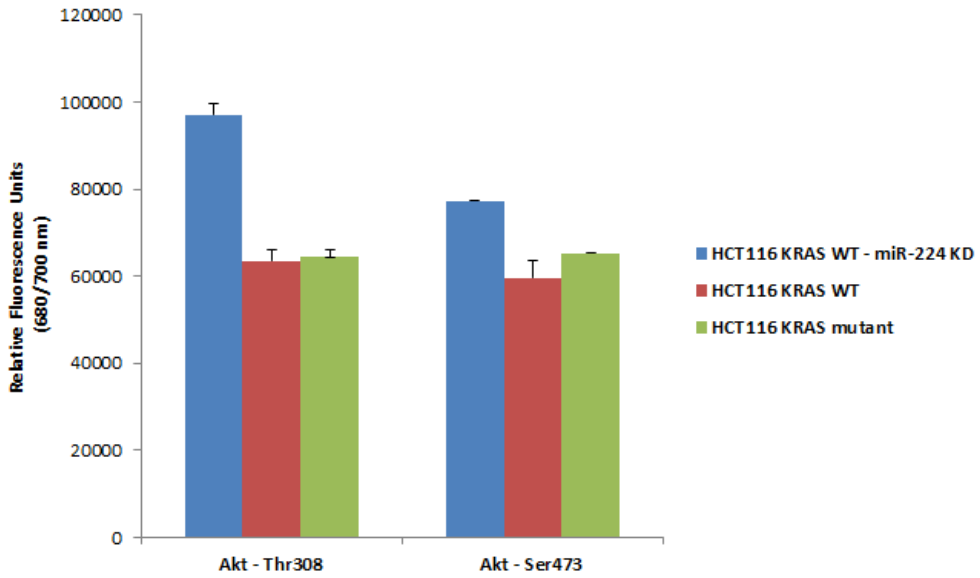

Figure 3.9

Figure 3.9: ***The effect of miR-224 knockdown on AKT phosphorylation. A)*** *The PathScan intracellular signalling array and LiCor Odyssey fluorescence imaging system was used to assess the effect of miR-224 knockdown in HCT116 KRAS WT cells on the phosphorylation or cleavage of 18 signalling molecules compared to untransfected HCT116 KRAS WT and mutant cells, as detailed in section 2.2.13; highlighted in purple is AKT Thr 308 and highlighted in blue is AKT Ser473. Each signalling molecule is represented in duplicate.* ***B)*** *The fluorescent signals at wavelength 680/700 nm as determined by LiCor Image Studio are represented graphically. Experiment was performed once and error bars represent the technical replicates.*

Thirdly, the PathScan array identified a number of signalling molecules that were significantly increased in HCT116 *KRAS* WT cells post-miR-224 knockdown compared to untransfected *KRAS* WT cells indicating the variety of pathways that may also be affected by miR-224. These included Stat1, Stat3, AMPK, HSP27, PRAS40 and p38 (Figure 3.10). A specific association with miR-224 and the activation of these pathways have not been previously reported. However, these results would need to be validated by performing Western blots for native and phosphorylated forms of each protein.

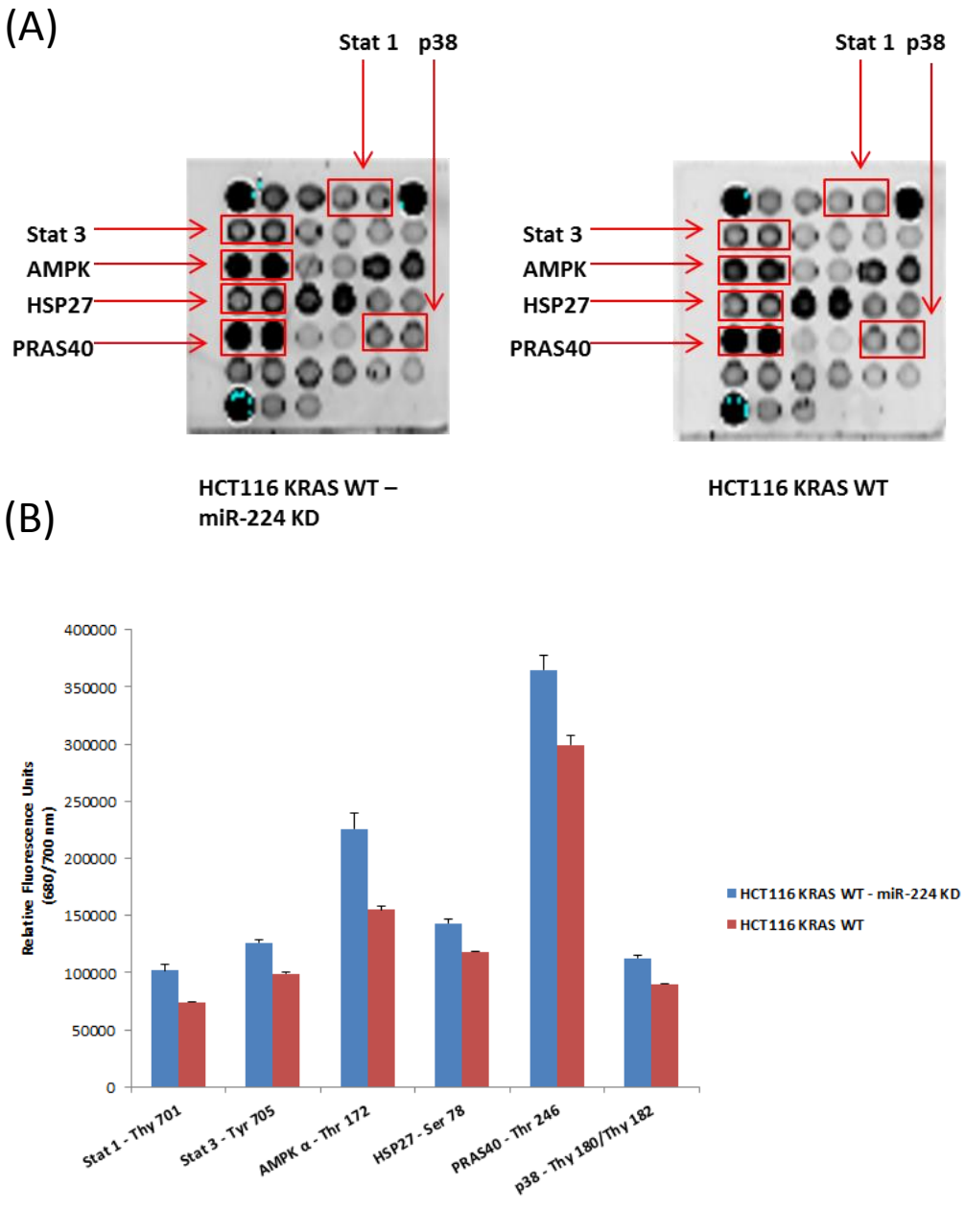

Figure 3.10: ***The effect of miR-224 knockdown on the phosphorylation of other signalling molecules. A)*** *The PathScan intracellular signalling array and LiCor Odyssey fluorescence imaging system was used to assess the effect of miR-224 knockdown in HCT116 KRAS WT cells on the phosphorylation or cleavage of 18 signalling molecules compared to untransfected HCT116 KRAS WT, as detailed in Section 2.2.13. Each signalling molecule is represented in duplicate.* ***B)*** *The fluorescent signals at wavelength 680/700 nm as determined by LiCor Image Studio are represented graphically. Experiment was performed once and error bars represent the technical replicates.*

To further investigate why miR-224 knockdown increased KRAS activity, other than through GTP-bound activation, the expression of *KRAS* and two other human Ras genes, *NRAS* and *HRAS* was compared in HCT116 *KRAS* WT miR-224 knockdown cells and untransfected *KRAS* WT and mutant cells by Taqman RT-PCR as detailed in Section 2.2.9.4. There was no significant change in *KRAS* gene mRNA expression between the *KRAS* WT and mutant cells. However, consistent with the KRAS activation data presented above, miR-224 knockdown significantly increased (1.7-fold, p=0.007) *KRAS* expression in *KRAS* WT cells (Figure 3.11 A). This suggests that an increase in *KRAS* expression may contribute to the mutant-line phenotype in *KRAS* WT cells following miR-224 knockdown. This appears to be a *KRAS* specific rather than a general Ras effect as there was no significant change in *NRAS* (p=0.12) or *HRAS* (p=0.09) expression due to miR-224 knockdown (Figure 3.11 B, C), although NRAS and HRAS expression was significantly increased in *KRAS* mutant cells (NRAS: 1.3 fold, p=0.04; HRAS: 1.7-fold, p=0.007). Future studies would be directed towards confirming these results using Western blots.

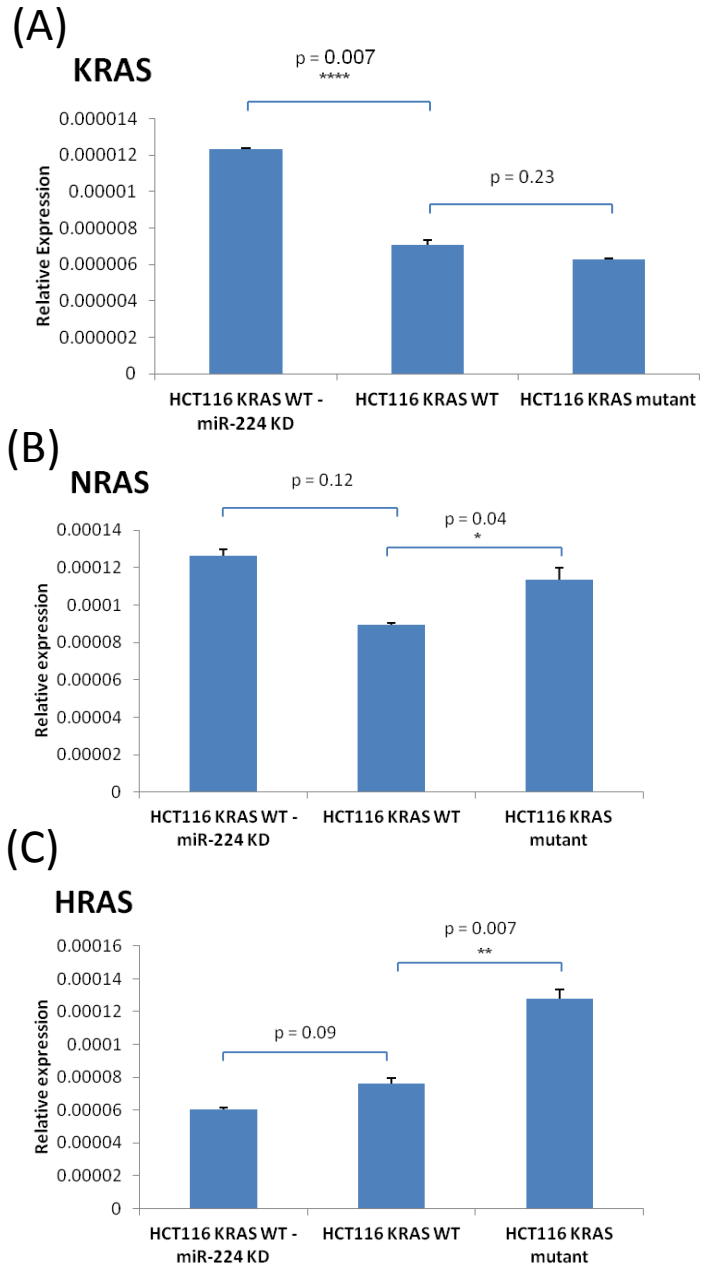

Figure 3.11: ***The impact of miR-224 knockdown on KRAS, NRAS and HRAS mRNA expression.***

A*) KRAS mRNA expression was assessed, relative to the control gene 18S ribosomal RNA , in miR-224 knockdown HCT116 KRAS WT cells and untransfected KRAS WT and mutant cells as detailed in Section 2.2.9.4.* ***B)*** *NRAS and* ***C)*** *HRAS mRNA expression was also assessed in miR-224 knockdown HCT116 KRAS WT cells and untransfected KRAS WT cells. Each sample was assessed in triplicate and the errors were determined by calculating* $2^{(-\delta Ct + sd\ \delta Ct)}$ *and* $2^{(-\delta Ct - sd\ \delta Ct)}$*, as detailed in Section 2.2.9.5. Statistical significance (p≤0.05) was determined by performing independent T-tests.*

3.3.6. The effect of miR-224 knockdown on drug sensitivity

The MTT cytotoxicity assay was used to investigate the effect of miR-224 knockdown on drug sensitivity, as detailed in Section 2.2.4. Cell sensitivity to 5-FU and oxaliplatin was investigated as these are drugs commonly used in colorectal cancer treatment. I also intended to investigate cetuximab, the EGFR inhibitor which has been approved for the treatment of *KRAS* WT colorectal cancer and which has little or no effect in *KRAS* mutant colorectal cancer. However, in contrast to antimetabolites or DNA damaging drugs, it is difficult to study the *in vitro* effects of cetuximab as its efficacy depends on the presence of EGFR on the cell surface and the presence of a receptor ligand, and is therefore difficult to evaluate in cell line models. Sorafenib is a small molecule BRAF inhibitor that inhibits the RAS/MAPK pathway downstream of KRAS and was therefore used as an alternative to cetuximab.

The knockdown of miR-224 increased the sensitivity of HCT116 *KRAS* WT cells to 5-FU. The IC_{50}, the concentration of drug where 50% of cells are no longer viable, was significantly decreased 1.9-fold ($p=0.04$) in miR-224 knockdown *KRAS* WT cells compared to untransfected *KRAS* WT cells (Figure 3.12). In contrast, miR-224 knockdown had no significant effect on the sensitivity of HCT116 *KRAS* WT cells to sorafenib (Figure 3.13) or oxaliplatin (Figure 3.14).

(A)

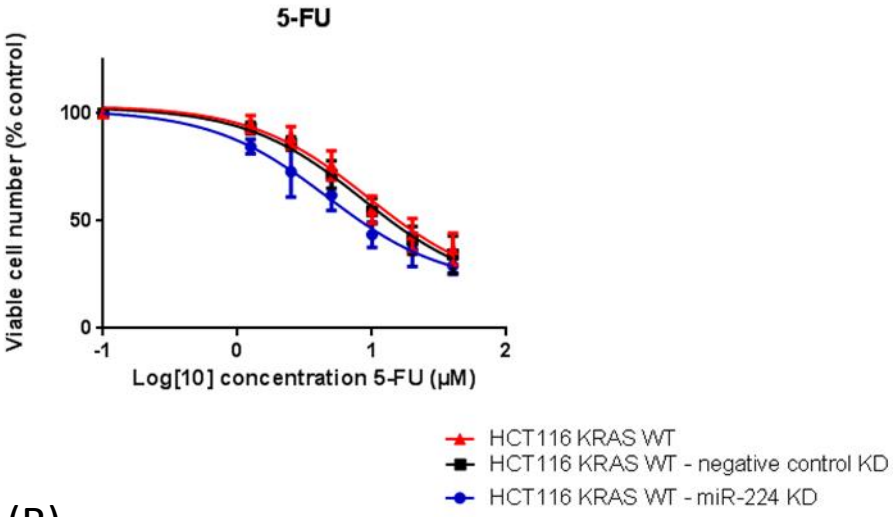

(B)

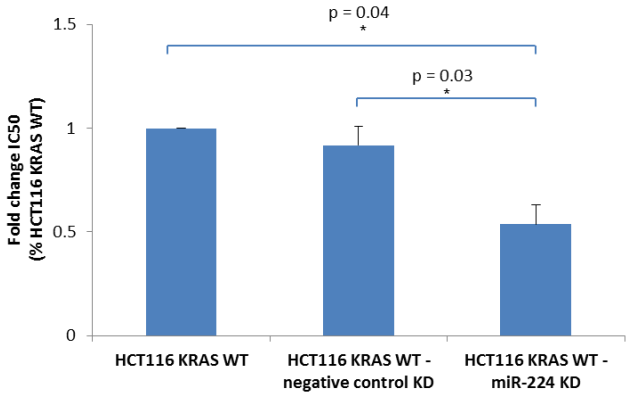

Figure 3.12: ***The effect of miR-224 knockdown on HCT116 KRAS WT cell sensitivity to 5-FU. A)*** *MTT cytotoxicity assays were used to compare 5-FU sensitivities of miR-224 knockdown HCT116 KRAS WT, negative control transfected and untransfected HCT116 KRAS WT cells, as detailed in Section 2.2.4.* ***B)*** *The IC_{50} for each cell line was calculated on GraphPad Prism version 6 and presented graphically as a fold change from the IC_{50} of the untransfected HCT116 KRAS WT cell line. The errors represent the SEM of three separate experiments. Statistical significance ($p \leq 0.05$) was determined by performing independent T-tests.*

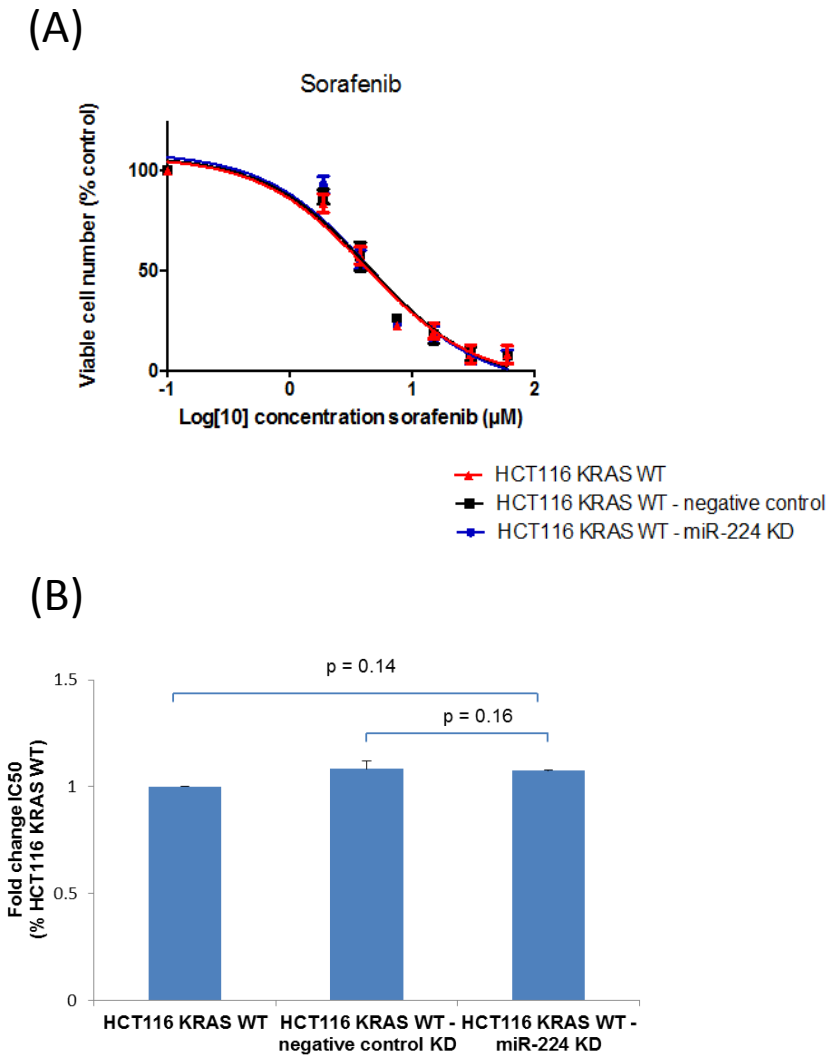

Figure 3.13: ***The effect of miR-224 knockdown on HCT116 KRAS WT cell sensitivity to sorafenib. A)*** *MTT cytotoxicity assays were used to compare sorafenib sensitivities of miR-224 knockdown HCT116 KRAS WT, negative control transfected and untransfected HCT116 KRAS WT cells, as detailed in Section 2.2.4.* ***B)*** *The IC_{50} for each cell line was calculated on GraphPad Prism version 6 and presented graphically as a fold change from the IC_{50} of the untransfected HCT116 KRAS WT cell line. The errors represent the SEM of three separate experiments. Statistical significance ($p \leq 0.05$) was determined by performing independent T-tests.*

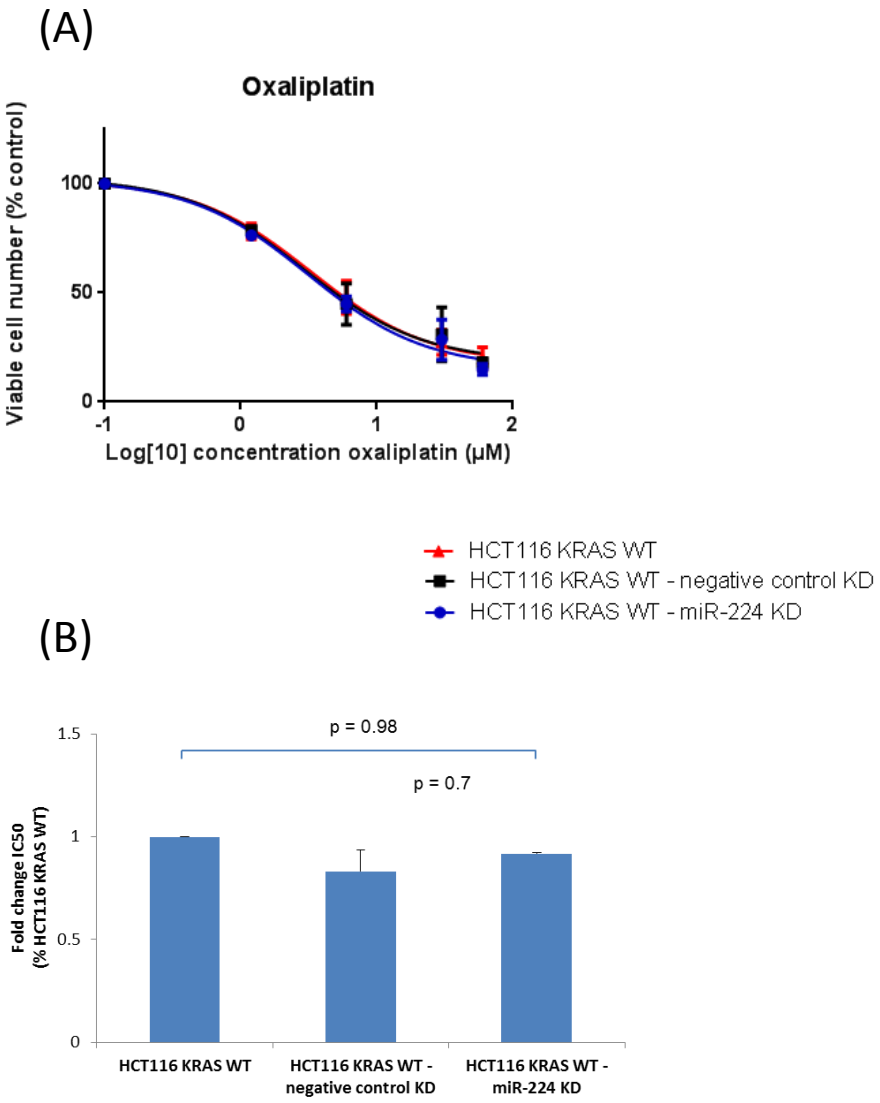

Figure 3.14: ***The effect of miR-224 knockdown on HCT116 KRAS WT cell sensitivity to oxaliplatin. A)*** *MTT cytotoxicity assays were used to compare oxaliplatin sensitivities of miR-224 knockdown HCT116 KRAS WT, negative control transfected and untransfected HCT116 KRAS WT cells, as detailed in Section 2.2.4.* ***B)*** *The IC_{50} for each cell line was calculated on GraphPad Prism version 6 and presented graphically as a fold change from the IC_{50} of the untransfected HCT116 KRAS WT cell line. The errors represent the SEM of three separate experiments. Statistical significance ($p \leq 0.05$) was determined by performing independent T-tests.*

The observation that a *KRAS* mutant-like increase in KRAS activity or activation caused by miR-224 knockdown is associated with increased sensitivity to 5-FU is consistent with previous data generated by Dr. Simone Weidlich in our research group using a NIH3T3 mouse fibroblast cell line model. NIH3T3 cells were stably transfected with WT *KRAS*, 17 mutants of *KRAS*, WT *BRAF* or the V600E mutant of *BRAF* to generate 20 novel cell lines (Figure 3.15).

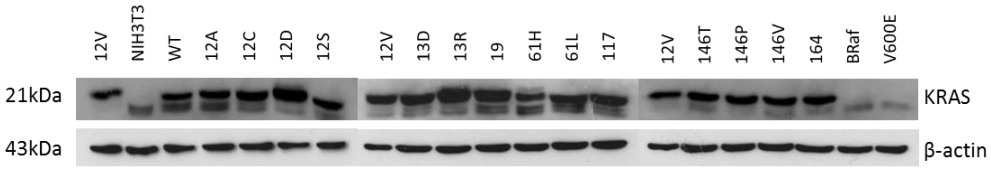

Figure 3.15: ***The stable transfection of WT and various mutants of KRAS and BRAF in NIH3T3 cells.*** *NIH3T3 cells were previously stably transfected with WT KRAS, 17 mutant KRAS, WT BRAF and mutant (V600E) BRAF constructs. A Western blot was performed to confirm the protein expression of WT and the various mutants of KRAS and BRAF, relative to the expression of β-actin.*

Consistent with my miR-224 knockdown data, the mutant *KRAS* (G12V and G13D mutants used as examples) and *BRAF* (V600E) NIH3T3 cells were more sensitive (lower IC_{50}) to 5-FU (Figure 3.16 A). Conversely, the mutant *KRAS* and *BRAF* cells were more resistant to sorafenib (Figure 3.16 B), an effect that what not observed following miR-224 knockdown in HCT116 *KRAS* WT cells. Consistent with the miR-224 data presented above, the *KRAS* or *BRAF* mutation status of the cells had no effect on their sensitivity to oxaliplatin (Figure 3.16 C).

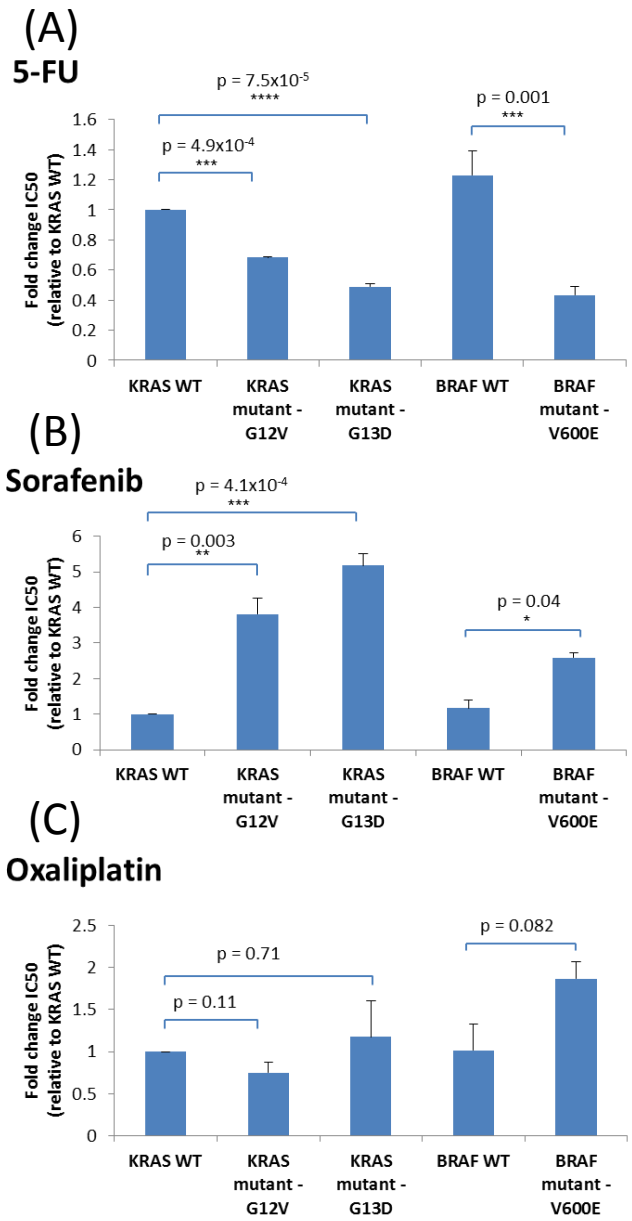

Figure 3.16: ***KRAS and BRAF mutation status and drug sensitivity in stably transfected NIH3T3 cells.*** *MTT cytotoxicity assays were used, previous to the present study, to compare the sensitivities of* ***A)*** *5-FU* ***B)*** *sorafenib and* ***C)*** *oxaliplatin in KRAS WT and KRAS mutant (G12V and G13D) and BRAF WT and BRAF mutant (V600E) NIH3T3 mouse fibroblast cells. G12V and G13D KRAS mutants are presented here as representative examples. The* IC_{50} *for each cell line was calculated on GraphPad Prism version 6 and presented graphically as a fold change from the* IC_{50} *of the KRAS WT cell line. The errors represent the SEM of three separate experiments. Statistical significance (p≤0.05) was determined by performing independent T-tests.*

3.3.7. The effect of miR-224 expression on drug metabolism genes

Differences in chemosensitivity could relate to differences in cell proliferation or differences in drug metabolism. Given the effect of miR-224 on the sensitivity of 5-FU, we sought to investigate whether the knockdown of miR-224 affected the expression of a number of enzymes that have been extensively investigated for their ability to predict response to 5-FU - Thymidylate synthase (TYMS), thymidine phosphorylase (TYMP) and dihydropyrimidine dehydrogenase (DPYD).

As discussed in Chapter 1, TYMP is involved in the conversion of 5-FU to one of its active metabolite, fluorodeoxyuridine monophosphate (FdUMP). FdUMP inhibits TYMS, an enzyme involved in the synthesis of thymidine triphosphate (TTP), one of the four nucleotide triphosphates used in the *in vivo* synthesis of DNA. DPYD inactivates 5-FU to FDHU for excretion.

Although contentious in the literature, a 5-FU sensitive phenotype has been associated with low expression of *DPYD* as this increases the amount of available and active drug available for the target cancers (Goto *et al*, 2012). Similarly, a low expression of *TYMS* is associated with 5-FU sensitivity as the resulting lower levels of TTPs negatively affect DNA synthesis. Elevated expression levels of *TYMP* have also been associated with 5-FU sensitivity as more FdUMP is produced leading to greater inhibition of *TYMS* (Goto *et al*, 2012).

The expression of *TYMS*, *TYMP* and *DPYD* was assessed by Taqman qRT-PCR analysis in HCT116 *KRAS* WT miR-224 knockdown and untransfected cells, as described in Section 2.2.9.4. The knockdown of miR-224 in *KRAS* WT cells

significantly increased the expression of TYMS (1.96-fold; $p=7.65x10^{-6}$), TYMP (1.48-fold; p=0.007) and DPYD (1.53-fold; p=0.045) compared to untransfected *KRAS* WT cells (Figure 3.17 A, B, C). If however, miR-224 induced changes in drug metabolism and sensitised HCT116 *KRAS* WT cells to 5-FU, it would be expected that the expression of TYMS and DPYD would be decreased.

Additionally, miR-224 knockdown significantly increased the expression of ERCC1 (1.52-fold; p=0.01), which codes for a protein involved in DNA damage repair (Figure 3.17 D). The increased expression of ERCC1 is associated with resistance to oxaliplatin (Seetharam *et al*, 2010). However, ERCC1 induction caused by miR-224 knockdown had no effect on oxaliplatin resistance.

The aforementioned effects on gene expression would need to be validated at a protein level using Western blots. However, the effect of miR-224 knockdown on the regulation of drug response enzymes is of interest given the aforementioned marked inter-patient differences in miR-224 expression in colorectal cancers (Figure 3.3).

(A)

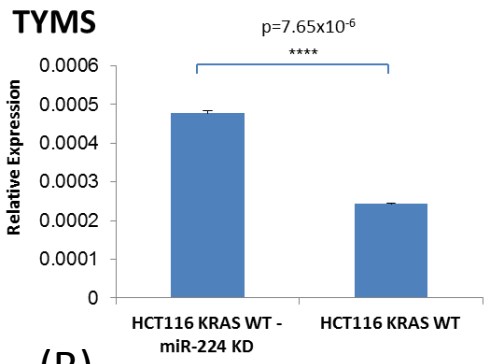

(B)

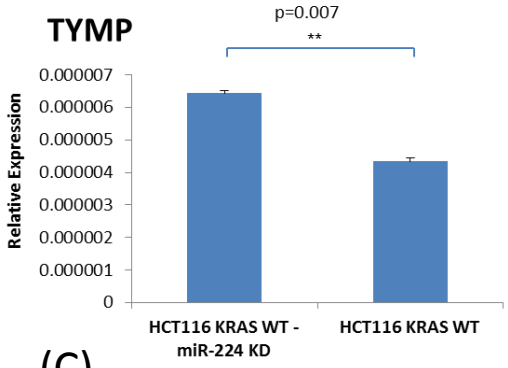

(C)

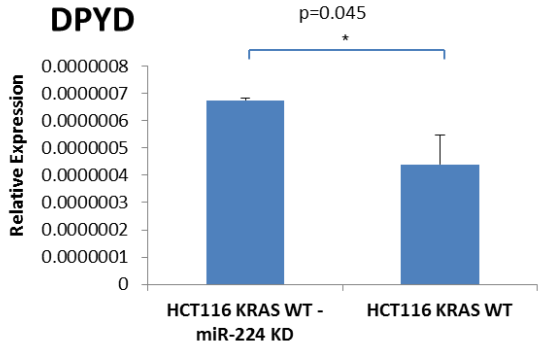

(D)

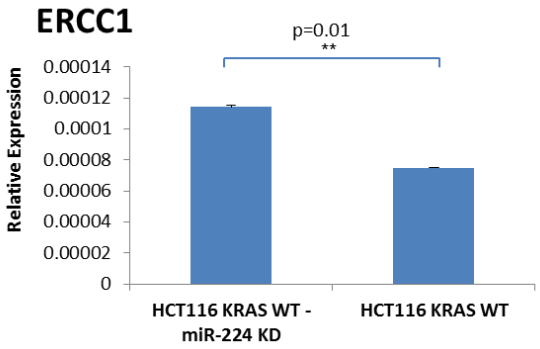

Figure 3.17

Figure 3.17: ***The effect of miR-224 knockdown on the expression of drug response enzymes.*** ***A****) TYMS,* ***B)*** *TYMP,* ***C)*** *DPYD and* ***D)*** *ERCC1 mRNA expression was assessed, relative to the control gene 18S ribosomal RNA, in miR-224 knockdown HCT116 KRAS WT cells and untransfected KRAS WT cells as detailed in Section 2.2.9.4. Each sample was assessed in triplicate and the errors were determined by calculating* $2^{(-\delta Ct + sd\ \delta Ct)}$ *and* $2^{(-\delta Ct - sd\ \delta Ct)}$*, as detailed in Section 2.2.9.5. Statistical significance* ($p \leq 0.05$) *was determined by performing independent T-tests.*

3.3.8. MiRNA target prediction databases

A single miRNA is known to regulate a large number of genes due to the imperfect complementarity between the miRNA sequence and the seed sequence of the 3' UTR of target genes. There are now many readily available online miRNA target prediction databases which use unique algorithms to predict targets. The targets are ranked within each database based on the predicted affinity of the miRNA to the target gene, although it is important to note that the majority of predicted targets have not been experimentally verified.

In the present study, in collaboration with Probir Chakravarty (CRUK Bioinformatics and Biostatistics Service, London), five well characterised miRNA target prediction databases, mirDB (www.mirdb.org), miRANDA (www.microrna.org), miRBase (www.mirbase.org), TargetMiner (www.isical.ac.in) and TargetScan (www.targetscan.org) were used to predict the targets of the 12 miRNAs (Table 3.2) differentially expressed in HCT116 *KRAS* WT and mutant cells, as described in Section 2.2.17. A total of 4083 and 3612 predicted targets were identified for the over and under-expressed miRNAs

respectively. In order to limit the number of false positives, the predicted targets that were common to at least two of the five databases were selected for further analysis. Therefore, 2305 unique predicted targets for the 7 up-regulated miRNAs and 1859 for the 5 down-regulated miRNAs were selected (Appendix H).

The bioinformatics tool, Metacore was then used to identify pathways and processes that were enriched and significantly associated with the predicted targets of the over and under-expressed miRNAs, as described in Section 2.2.17. As shown in Tables 3.5 and 3.6, several common cancer-related processes and pathways involved in development of epithelial to mesenchymal transition (EMT), cell adhesion, cytoskeleton remodelling and cell proliferation were prominent. However, processes and pathways associated with cardiac development or neurogenesis, for example, were also identified further demonstrating the wide ranging effects of differential miRNA expression.

Within the Tables, the ratio indicates the number of genes found to be in our target list compared to the number of genes identified by the program to be involved in a particular process or pathway. In this initial analysis, although significant associations were identified, less than 50% of the genes in our target list appeared in the genes involved in the vast majority of the processes and pathways identified (Tables 3.5 and 3.6).

Table 3.5: Pathways and processes associated with 7 miRNAs differentially increased in HCT116 *KRAS* WT cells relative to HCT116 *KRAS* mutant cells

	Pathway name	p value	Ratio
1	Cytoskeleton remodeling_TGF, WNT and cytoskeletal remodelling	5.84E-19	54/111
2	Cytoskeleton remodeling_Cytoskeleton remodelling	7.98E-18	50/102
3	Development_Thrombopoietin-regulated cell processes	3.96E-16	30/45
4	Cell adhesion_Chemokines and adhesion	2.02E-14	45/100
5	Development_HGF signaling pathway	2.58E-14	29/47
6	Development_Regulation of epithelial-to-mesenchymal transition (EMT)	7.41E-14	34/64
7	Transcription_CREB pathway	2.56E-13	28/47
8	Cardiac Hypertrophy_NF-AT signaling in Cardiac Hypertrophy	9.36E-13	33/65
9	Reproduction_GnRH signalling	9.93E-13	35/72
10	Development_TGF-beta-dependent induction of EMT via MAPK	2.33E-12	27/47

	Process name	p value	Ratio
1	Signal transduction_WNT signalling	5.26E-12	85/177
2	Development_Neurogenesis_Axonal guidance	2.73E-10	99/230
3	Proliferation_Positive regulation cell proliferation	6.91E-10	95/221
4	Development_EMT_Regulation of epithelial-to-mesenchymal transition	2.73E-09	97/232
5	Signal Transduction_Cholecystokinin signalling	2.95E-09	54/106
6	Signal transduction_NOTCH signalling	3.48E-09	98/236
7	Development_Blood vessel morphogenesis	1.13E-08	94/228
8	Development_Neurogenesis_Synaptogenesis	1.55E-08	78/180
9	Cell adhesion_Cadherins	1.55E-08	78/180
10	Reproduction_Feeding and Neurohormone signaling	1.74E-08	88/211

Table 3.6: Pathways and processes associated with 5 miRNAs differentially decreased in HCT116 *KRAS* WT cells relative to HCT116 *KRAS* mutant cells

	Pathway name	p value	Ratio
1	Development_Regulation of epithelial-to-mesenchymal transition (EMT)	4.07E-13	31/64
2	Development_WNT signaling pathway. Part 2	2.26E-11	26/53
3	Signal transduction_PKA signaling	5.62E-11	25/51
4	Cytoskeleton remodeling_Role of PKA in cytoskeleton reorganisation	3.82E-10	21/40
5	Cytoskeleton remodeling_TGF, WNT and cytoskeletal remodeling	3.98E-10	38/111
6	Transport_Clathrin-coated vesicle cycle	4.13E-10	29/71
7	Development_TGF-beta-dependent induction of EMT via SMADs	1.08E-08	18/35
8	Cell adhesion_Chemokines and adhesion	1.62E-08	33/100
9	Cytoskeleton remodeling_Cytoskeleton remodeling	2.81E-08	33/102
10	Proteolysis_Role of Parkin in the Ubiquitin-Proteasomal Pathway	5.82E-08	14/24

	Process name	p value	Ratio
1	Development_EMT_Regulation of epithelial-to-mesenchymal transition	8.67E-11	92/232
2	Development_Hedgehog signaling	1.74E-09	95/254
3	Development_Neurogenesis_Synaptogenesis	1.68E-08	71/180
4	Cell adhesion_Synaptic contact	1.97E-08	72/184
5	Cytoskeleton_Regulation of cytoskeleton rearrangement	9.03E-08	70/183
6	Signal transduction_WNT signaling	1.14E-07	68/177
7	Development_Neurogenesis_Axonal guidance	1.21E-07	83/230
8	Cytoskeleton_Actin filaments	2.11E-07	67/176
9	Cardiac development_FGF_ErbB signaling	3.87E-07	51/124
10	Signal transduction_NOTCH signaling	4.31E-07	83/236

To further investigate the phenotypic consequences of miR-224 knockdown, a similar bioinformatics approach was used to analyse HCT116 cells before and after miR-224 knockdown. TLDA miRNA profiling of HCT116 *KRAS* WT cells after miR-224 knockdown identified that, compared to untransfected HCT116 *KRAS* WT cells, 35 miRNAs (3 up, 32 down) were differentially expressed (Table 3.7)

Table 3.7: MicroRNAs differentially expressed in HCT116 *KRAS* WT and miR-224 knockdown HCT116 *KRAS* WT cells

microRNA	Fold Change	Adjusted p value	microRNA	Fold Change	Adjusted p value
miR-532-5p	3.53	0.0044	miR-636	-3.04	0.0097
miR-34a	2.54	0.0250	miR-744	-3.27	0.0086
miR-342-3p	1.98	0.0469	miR-375	-3.52	0.0076
miR-19a	-1.71	0.0475	miR-642	-3.63	0.0076
miR-31	-1.81	0.0475	miR-532-3p	-3.79	0.0038
miR-222	-1.91	0.0387	miR-197	-4.17	0.0029
miR-140-5p	-1.92	0.0469	miR-331-3p	-4.17	0.0095
miR-103	-2.00	0.0338	miR-125b	-4.21	0.0057
miR-132	-2.01	0.0296	miR-193b	-4.75	0.0029
miR-93	-2.13	0.0271	miR-320	-5.18	0.0044
miR-29c	-2.23	0.0469	miR-671-3p	-5.63	0.0469
let-7d	-2.23	0.0275	miR-574-3p	-5.98	0.0076
let-7e	-2.37	0.0340	miR-92a	-6.09	0.0044
miR-149	-2.58	0.0076	miR-181a	-6.86	0.0029
miR-345	-2.68	0.0126	let-7b	-10.20	0.0102
miR-324-3p	-2.72	0.0336	miR-210	-15.00	0.0003
miR-183	-2.84	0.0436	miR-328	-22.98	0.0029
miR-99b	-2.92	0.0336			

The same five miRNA target prediction databases were also used to identify predicted targets for these over and under-expressed miRNAs. Metacore bioinformatics analysis showed that cytoskeleton remodelling, cell adhesion, development of EMT, cell cycle regulation and cell proliferation again were prominent processes and pathways (Tables 3.8 and 3.9). In this analysis there was a marked enrichment of the genes involved in the processes and pathways identified, with the majority now within the 95% to 100% range. This is likely to be because our target lists for this analysis was a lot larger; therefore they were more likely to contain target genes identified by the program to be involved in a particular pathway. I next went on to experimentally validate the phenotypes identified by bioinformatics analysis.

Table 3.8: Pathways and processes associated with 3 miRNAs differentially increased in HCT116 *KRAS* WT miR-224 knockdown cells relative to untransfected HCT116 *KRAS* WT cells

	Pathway name	p value	Ratio
1	Cytoskeleton remodeling_TGF, WNT and cytoskeletal remodeling	3.10E-21	82/111
2	Cell adhesion_Chemokines and adhesion	1.16E-17	72/100
3	Cytoskeleton remodeling_Cytoskeleton remodeling	4.89E-17	72/102
4	Immune response_IL-15 signaling	8.38E-13	48/64
5	Development_EGFR signaling pathway	1.18E-11	50/71
6	Development_Regulation of epithelial-to-mesenchymal transition (EMT)	2.60E-11	46/64
7	Development_Gastrin in cell growth and proliferation	2.60E-11	45/62
8	Immune response_Gastrin in inflammatory response	2.85E-10	47/69
9	Chemotaxis_CXCR4 signaling pathway	3.09E-10	29/34
10	Development_TGF-beta-dependent induction of EMT via MAPK	3.19E-10	36/47

	Process name	p value	Ratio
1	Cytoskeleton_Regulation of cytoskeleton rearrangement	7.33E-08	128/183
2	Signal transduction_NOTCH signaling	7.33E-08	158/236
3	Development_Neurogenesis_Synaptogenesis	2.33E-07	124/180
4	Cell adhesion_Synaptic contact	2.34E-07	126/184
5	Development_EMT_Regulation of epithelial-to-mesenchymal transition	4.39E-07	149/226
6	Reproduction_FSH-beta signaling pathway	1.43E-05	107/160
7	Cell cycle_G1-S Growth factor regulation	2.21E-05	126/195
8	Development_Neurogenesis_Axonal guidance	2.57E-05	145/230
9	Development_Skeletal muscle development	4.26E-05	96/144
10	Cytoskeleton_Actin filaments	4.26E-05	114/176

Table 3.9: Pathways and processes associated with 32 miRNAs differentially decreased in HCT116 *KRAS* WT miR-224 knockdown cells relative to untransfected HCT116 *KRAS* WT cells

	Pathway name	p value	Ratio
1	Cytoskeleton remodeling_TGF, WNT and cytoskeletal remodeling	1.74E-24	107/111
2	Cytoskeleton remodeling_Cytoskeleton remodeling	1.10E-19	96/102
3	Cell adhesion_Chemokines and adhesion	3.59E-18	93/100
4	Development_Regulation of epithelial-to-mesenchymal transition (EMT)	7.42E-16	63/64
5	Transport_Clathrin-coated vesicle cycle	4.24E-15	68/71
6	Immune response_HSP60 and HSP70/ TLR signaling pathway	7.84E-15	54/54
7	Development_TGF-beta receptor signaling	1.08E-13	50/50
8	Development_WNT signaling pathway. Part 2	6.36E-13	52/53
9	Cell adhesion_ECM remodeling	1.11E-12	51/52
10	Immune response_IL-18 signalling	2.65E-12	57/60

	Process name	p value	Ratio
1	Development_Neurogenesis_Synaptogenesis	2.04E-11	180/180
2	Cytoskeleton_Actin filaments	6.58E-10	175/176
3	Transcription_mRNA processing	5.77E-09	159/160
4	Cell cycle_G2-M	5.92E-09	202/206
5	Cytoskeleton_Regulation of cytoskeleton rearrangement	1.64E-08	180/183
6	Cytoskeleton_Cytoplasmic microtubules	1.70E-07	115/115
7	Cell adhesion_Integrin-mediated cell-matrix adhesion	2.96E-07	207/214
8	Signal transduction_NOTCH signaling	3.27E-07	227/236
9	Development_Skeletal muscle development	3.35E-07	142/144
10	Proliferation_Positive regulation cell proliferation	4.03E-07	213/221

3.3.9. The effect of miR-224 on cell proliferation and the cell cycle

The impact of miR-224 knockdown in HCT116 *KRAS* WT cells on cell proliferation was investigated, firstly, by flow cytometry using the CellTrace Violet Cell Proliferation Kit as detailed in Section 2.2.14.3, and secondly by a growth assay, as described in Section 2.2.3.

The knockdown of miR-224 in HCT116 *KRAS* WT cells significantly increased their doubling time (from 19.8 hours to 27.5 hours, p=0.01) over a 48 hour period as determined by the CellTrace Violet Cell Proliferation Kit (Table 3.10).

Table 3.10: Doubling time of HCT116 *KRAS* WT miR-224 knockdown cells compared to negative control and untransfected *KRAS* WT and mutant cells as determined by the CellTrace Violet Cell Proliferation Kit

Cell line	Doubling time (hours)	p value (compared to HCT116 *KRAS* WT – miR-224 KD)
HCT116 *KRAS* WT – miR-224 KD	27.5 ± 1.39	-
HCT116 *KRAS* WT – negative control KD	21.5 ± 2.60	0.113
HCT116 *KRAS* WT	19.8 ± 0.93	**0.010**
HCT116 *KRAS* mutant	19.1 ± 0.31	0.471

This result was confirmed by an independent cell growth assay where the knockdown of miR-224 in HCT116 *KRAS* WT cells significantly increased their doubling time from 23.5 hours to 26.1 hours ($p=8.7x10^{-4}$) over a 48 hour period (Figure 3.18). Surprisingly, in contrast, there was no significant difference in doubling time between the *KRAS* WT and *KRAS* mutant cells in both experiments (CellTrace Violet Cell Proliferation Kit, p=0.51; growth assay, p=0.07; independent T test). This may be an effect of using immortalised cell lines which have been in culture for long periods and where the biology has been altered in the process. It was expected that the *KRAS* mutant cells, which have a constitutively activated RAS/MAPK pathway, would proliferate at a faster rate and have a lower doubling time than the *KRAS* WT cells.

(A)

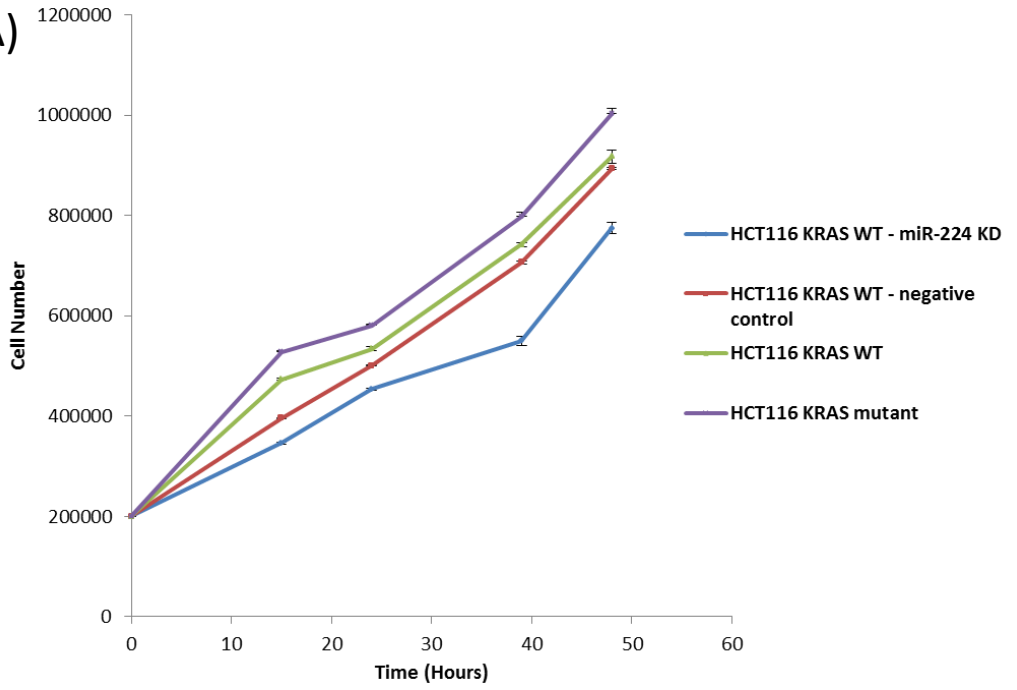

(B)

Cell line	Doubling time (hours)	p value (compared to HCT116 *KRAS* WT – miR-224 KD)
HCT116 *KRAS* WT – miR-224 KD	26.1 ± 0.14	-
HCT116 *KRAS* WT – negative control KD	23.1 ± 0.17	$1.8x10^{-4}$
HCT116 *KRAS* WT	23.5 ± 0.26	**$8.7x10^{-4}$**
HCT116 *KRAS* mutant	22.5 ± 0.31	0.06

Figure 3.18: ***Cell growth after miR-224 knockdown in HCT116 KRAS WT cells. A)*** *Cells were seeded at a density of $1x10^5$ cells per 3.5 cm diameter well and counted at 5 different time points over a 48 hour period as detailed in Section 2.2.3. Errors bars represent the SEM of cell number over 3 separate experiments.* ***B)*** *The doubling times were then calculated as detailed in Section 2.2.3 (Box 2.1). Statistical significance ($p \leq 0.05$) was determined by performing independent T-tests.*

The effect of miR-224 knockdown on cell cycle kinetics was then investigated by staining cells with propidium iodide and analysing DNA content using a flow cytometer, as described in Section 2.2.14.1.

Figure 3.19 shows progression through the different stages of the cell cycle and suggests that *KRAS* mutant cells inherently remained in the G0/G1 phase for longer at 36 and 48 hours after seeding compared to *KRAS* WT cells. This was a surprising result as this suggests that the *KRAS* mutant cells did not progress through the cell cycle at the same rate as the *KRAS* WT cells. As mentioned previously Table 3.10 and Figure 3.18 suggest that the *KRAS* mutant and WT cells did not have significantly different doubling times. Due to time constraints this experiment could only be performed once and further analysis will shed better light on this observation. The knockdown of miR-224 or transfection with a miRNA inhibitor negative control, however, had no effect on the cell cycle kinetics of *KRAS* WT cells, an effect that has also been shown in HepG2 human liver carcinoma cells (Li *et al*, 2010), suggesting that there is not a direct association between doubling time and cell cycle progression.

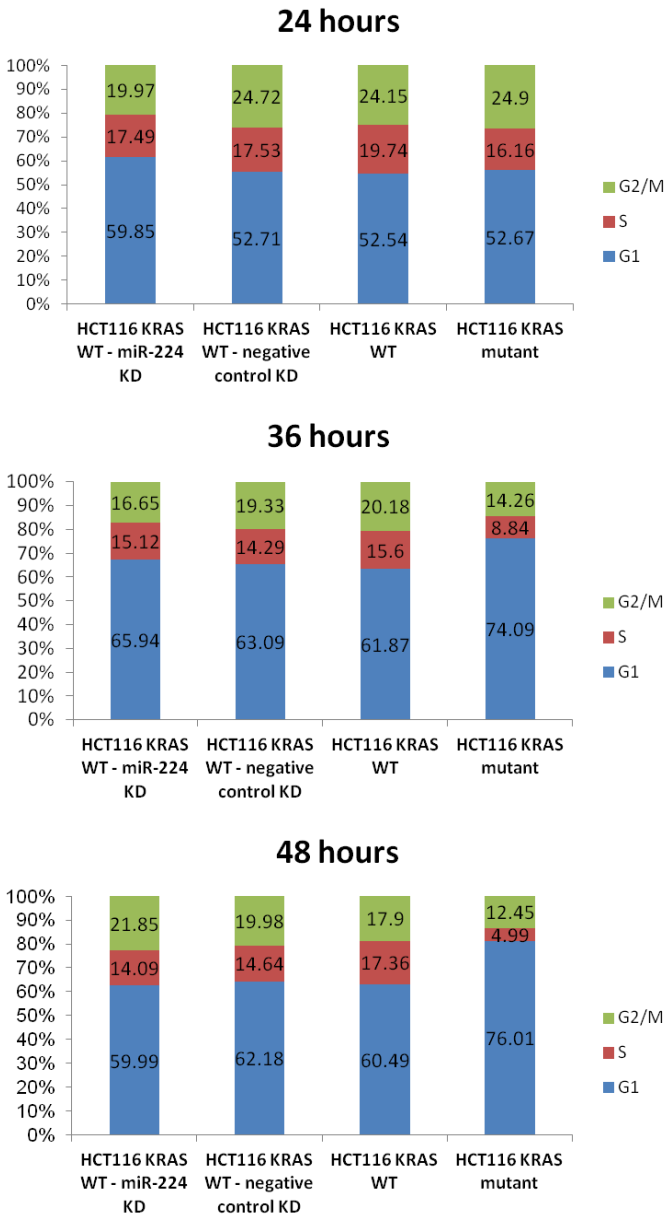

Figure 3.19: ***The effect of miR-224 knockdown in HCT116 KRAS WT cells on cell cycle kinetics.***

Cells were seeded at a density of 1x10^6 cells per 5 cm diameter plate, harvested at 3 time points over 48 hours and labelled with Propidium iodide. DNA content was then analysed by flow cytometry to determine the percentage of cells in the defined phases of the cell cycle, as described in Section 2.2.14.1. Experiment was performed once.

To investigate whether the above result would be different in response to cellular stress, the cells were treated with 10 µM 5-FU for 12, 24 and 48 hours. 5-FU caused an S-phase arrest particularly from 24 hours post drug exposure (Figure 3.20), an effect that commonly occurs in response to drugs to halt the cell cycle and repair damaged DNA. In response to drug, *KRAS* mutant cells once again remained in G1 phase for longer than *KRAS* WT cells. However, the knockdown of miR-224 in *KRAS* WT cells did not affect the cell cycle kinetics compared to untransfected *KRAS* WT cells.

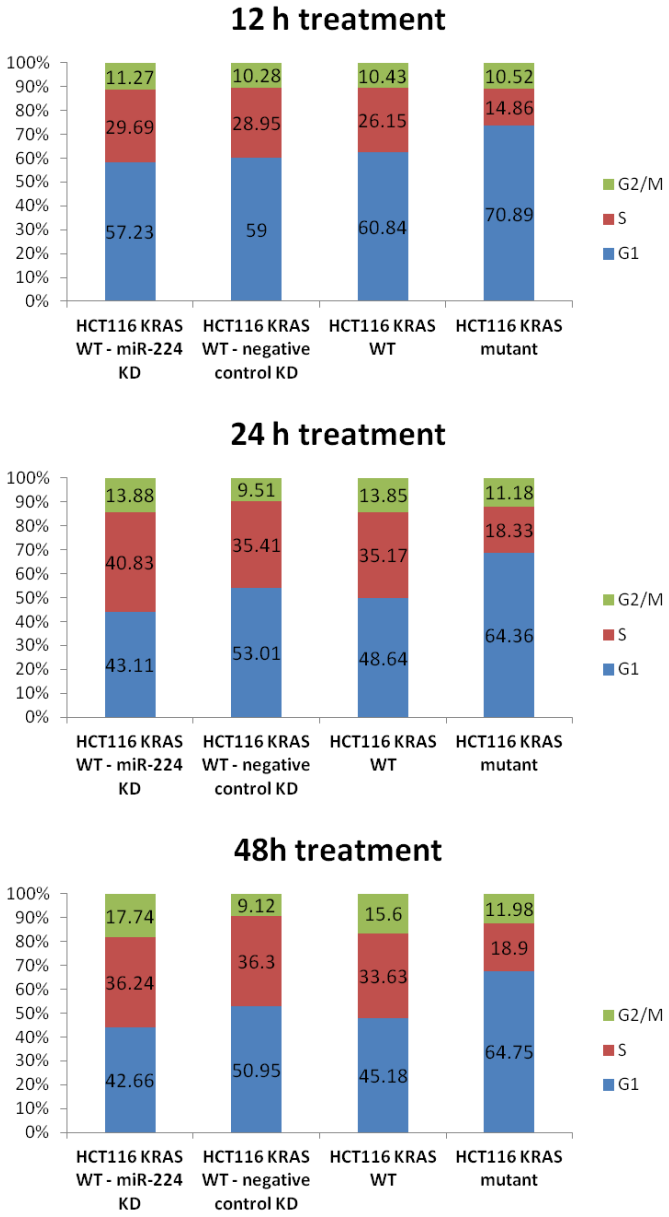

Figure 3.20: ***The effect of miR-224 knockdown in HCT116 KRAS WT cells on cell cycle kinetics in response to cellular stress.*** *Cells were seeded at a density of 1x10^6 cells per 5 cm diameter plate and treated with 10 µM 5-FU for 12, 24 and 48 hours. Cells were harvested at these 3 time points over 48 hours and labelled with Propidium iodide. DNA content was then analysed by flow cytometry to determine the percentage of cells in the defined phases of the cell cycle, as described in Section 2.2.14.1. Experiment was performed once.*

3.3.10. The effect of miR-224 on the development of EMT and cell invasion

To explore the predicted association between miR-224 and EMT, the expression of a panel of well-known EMT genes, *CDH1* (E-cadherin), *CDH2* (N-cadherin), *TWIST1* (Twist-related protein 1) and *VIM* (Vimentin) was compared in untransfected *KRAS* WT cells and miR-224 knockdown *KRAS* WT cells, by Taqman qRT-PCR analysis as described in Section 2.2.9.4. E-cadherin has previously been shown to be down-regulated during EMT whereas N-cadherin is known to be up-regulated.

CDH1 expression was significantly increased (1.12 fold; p=0.005) in miR-224 knockdown *KRAS* WT cells compared to the untransfected *KRAS* WT cells (Figure 3.21 A). Vimentin was also decreased (1.7 fold; p=0.04) in miR-224 knockdown *KRAS* WT cells compared to untransfected WT cells (Figure 3.21 B), while *CDH2* was not expressed in HCT116 *KRAS* WT and mutant cells (data not shown).

TWIST1, when activated, causes the indirect down-regulation of E-cadherin or up-regulation of vimentin and is associated with up-regulation of matrix mellatoproteases (MMPs; Zhao *et al*, 2011). The knockdown of miR-224 significantly increased (2.3 fold; p=0.008) the expression of *TWIST1* (3.21 C). An important extension of this work would therefore be to confirm the above gene expression changes using Western blots and immunohistochemical analysis and to explore the effect of miR-224 knockdown on both MMP mRNA and protein expression.

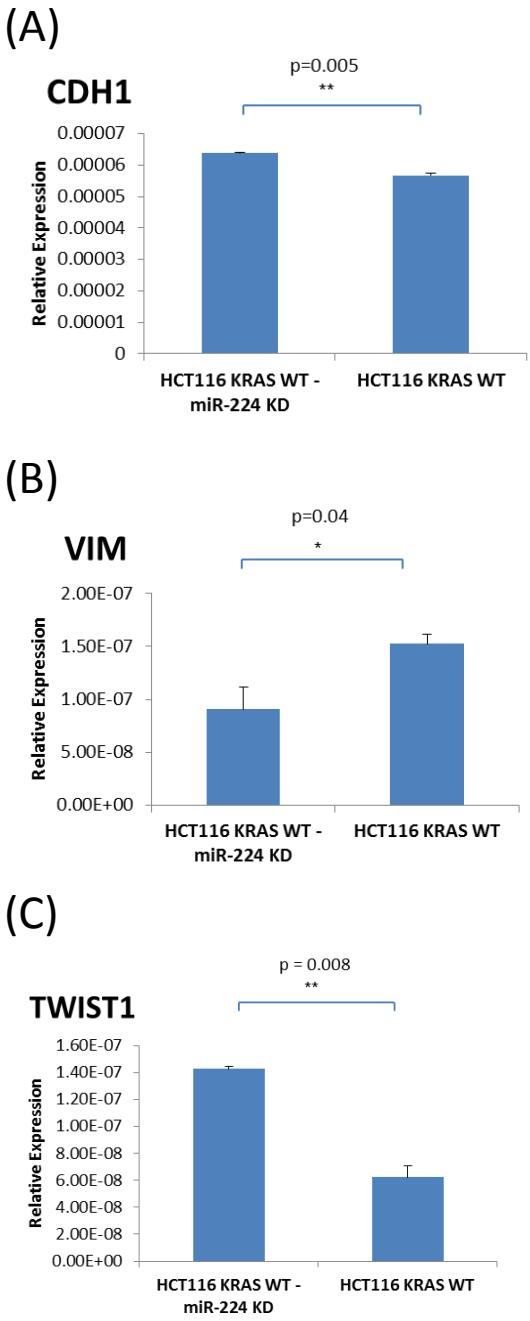

Figure 3.21: The effect of miR-224 knockdown on the expression of EMT genes. *The mRNA expression of **A)** CDH1, **B)** VIM and **C)** TWIST1 was assessed, relative to the control gene 18S ribosomal RNA, in miR-224 knockdown HCT116 KRAS WT cells and untransfected KRAS WT cells as detailed in Section 2.2.9.4. Each sample was assessed in triplicate and the errors were determined by calculating* $2^{(-\delta Ct + sd\ \delta Ct)}$ *and* $2^{(-\delta Ct - sd\ \delta Ct)}$*, as detailed in Section 2.2.9.5. Statistical significance ($p \leq 0.05$) was determined by performing independent T-tests.*

To investigate possible changes in cell invasion caused by miR-224 knockdown, a Calbiochem InnoCyte invasion assay was used to model and quantify cancer cell invasion *in vitro*, as detailed in Section 2.2.7. The invasion assay showed that miR-224 knockdown in *KRA*S WT cells significantly reduced (1.75 fold; p=0.009) its invasive capabilities (Figure 3.22 A). HCT116 *KRAS* mutant cells were significantly less invasive (1.2 fold; p=0.04) than HCT116 *KRAS* WT cells, suggesting that again miR-224 knockdown in *KRAS* WT cells exhibited a mutant *KRAS*-like phenotype.

However, in the NIH3T3 model, previously discussed in Section 3.3.6, where WT or mutant *KRAS* was stably transfected into mouse fibroblast cells, NIH3T3 G13D *KRAS* mutant cells were significantly more invasive (4.6 fold; p=0.002) compared to NIH3T3 *KRAS* WT cells (Figure 3.22 B). This suggests that in this case the input of a dominant oncogenic mutant *KRAS* drives an invasive phenotype and further highlights the limitations of using immortalised cell lines as previously discussed.

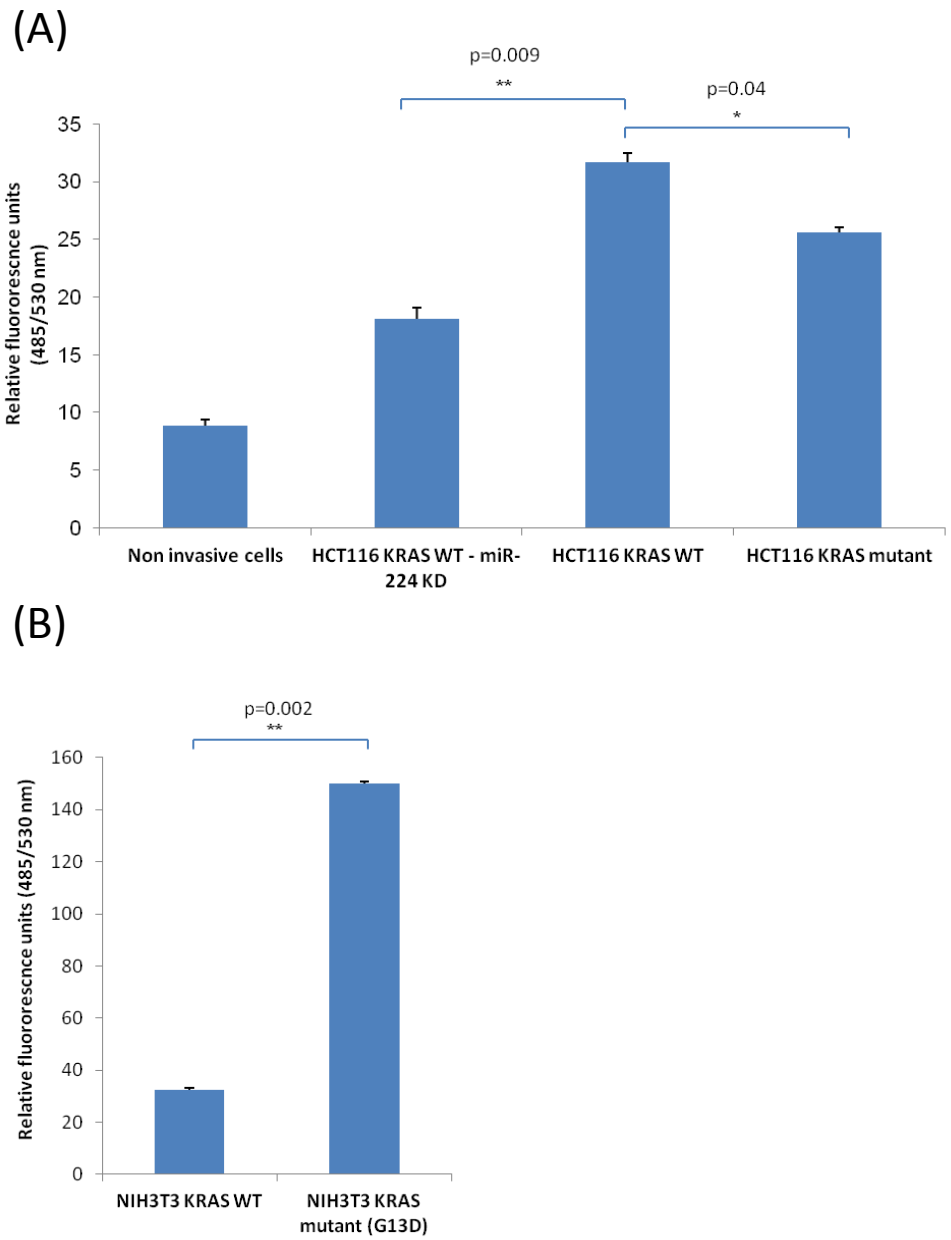

Figure 3.22: The impact of miR-224 knockdown and KRAS mutation status on cell invasion.

The *Calbiochem InnoCyte invasion assay was used to model and quantify cancer cell invasion in vitro, as detailed in Section 2.2.7.* ***A)*** *The effect of miR-224 knockdown in HCT116 KRAS WT cells was compared to untransfected HCT116 KRAS WT and mutant cells.* ***B)*** *The effect of stable transfection of KRAS WT and G13D mutant KRAS constructs into NIH3T3 cells was also compared. Each sample was analysed in triplicate and errors represent the SEM of three separate experiments. Statistical significance ($p \leq 0.05$) was determined by performing independent T-tests.*

3.3.11. The expression of miR-224 in cancer metastases

As the present study shows that miR-224 affects cell invasion, *in vitro*, I next investigated whether miR-224 was also differentially increased in cancer metastases compared to patient-matched primary colorectal cancers. In the present study, 15 matched lymph node metastases and primary colorectal cancer samples and 20 matched liver metastases and primary colorectal cancer samples from 24 patients were selected for analysis by Professor Frank Carey (Consultant pathologist, Ninewells Hospital, Dundee). The expression of miR-224 was compared within each matched pair by Taqman qRT-PCR analysis as described in Section 2.2.9.2.

MiR-224 expression was significantly decreased in lymph node metastasis samples compared to primary colorectal cancers in 11 patients and significantly increased in 1 patient (Figure 3.23). There was no significant change in 4 patients.

(A)

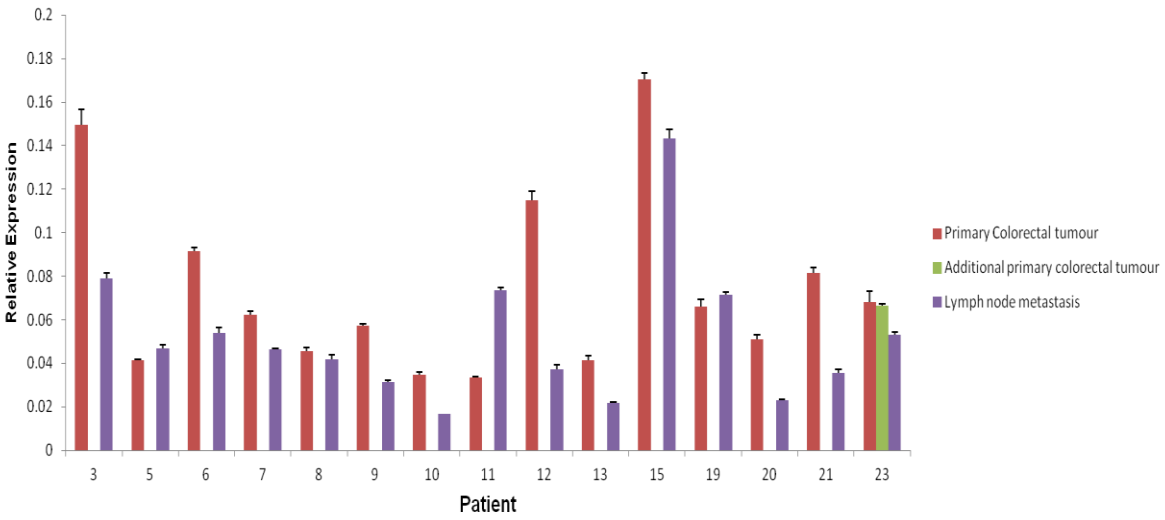

(B)

Patient	Fold Change	p value
3	-1.89	0.005
6	-1.69	0.0004
7	-1.35	0.004
9	-1.83	3.1E-05
10	-2.10	0.003
11	2.21	2.9E-05
12	-3.11	0.0004
13	-1.92	0.005
15	-1.19	0.01
20	-2.23	0.003
21	-2.29	0.0001
23*	-1.28	0.0004

Figure 3.23: ***Differential miR-224 expression in primary colorectal cancers and patient-matched lymph node metastases****. **A)** The expression of miR-224, relative to the control miRNA let-7a, was compared in 15 primary colorectal cancers and patient-matched lymph node metastases as detailed in Section 2.2.9.2. Each sample was assessed in triplicate and the errors were determined by calculating* $2^{(-\delta Ct + sd\ \delta Ct)}$ *and* $2^{(-\delta Ct - sd\ \delta Ct)}$*, as detailed in Section 2.2.9.5* ***B)*** *Fold change represents the change of relative miR-224 expression from colorectal cancers to lymph node metastases. Statistical significance ($p \leq 0.05$) was determined by performing independent T-tests.*

The expression of miR-224 was significantly increased in liver metastases samples compared to primary colorectal cancers in 13 patients and significantly decreased in 8 patients. There was no significant difference in 2 patients (Figure 3.24). However, miR-224 expression was increased in 9 of the 13 patients where there was a differential expression greater than 1.5-fold.

In collaboration with Professor Frank Carey, we assessed whether there was any association between increased, decreased or unchanged miR-224 expression in each matched case with patient gender, cancer differentiation (e.g. aggressive and poorly differentiated compared to less aggressive and well differentiated) and cancer origin (i.e. left colon and rectum versus right colon), but found no significant association. The patient cohort size in the present study was perhaps too small to look for these types of associations and therefore a larger patient cohort may allow for better interpretation.

In the present study I hypothesised that miR-224 expression may be increased in lymph node or liver metastases compared to primary colorectal cancers. A recent study reports that high miR-224 expression drives colorectal cancer cell invasion *in vitro* and is associated with lower survival and greater risk of relapse in colorectal cancer patients (Zhang *et al*, 2013*a*). In contrast, Yuan *et al* (2013) showed that miR-224 inhibited colorectal cancer cell invasion *in vitro* and was under-expressed in colorectal lung metastases compared to primary cancers and inversely correlated with patient survival. This highlights the dual role miR-224 may have in the development of cancer metastasis in different organs and

tissues by affecting different pathways and its possible role of reflecting the aggressiveness of the disease.

In the present study, there was insufficient information available on patient survival to determine any correlation with increased or decreased miR-224 expression, particularly in patients with liver metastases.

(A)

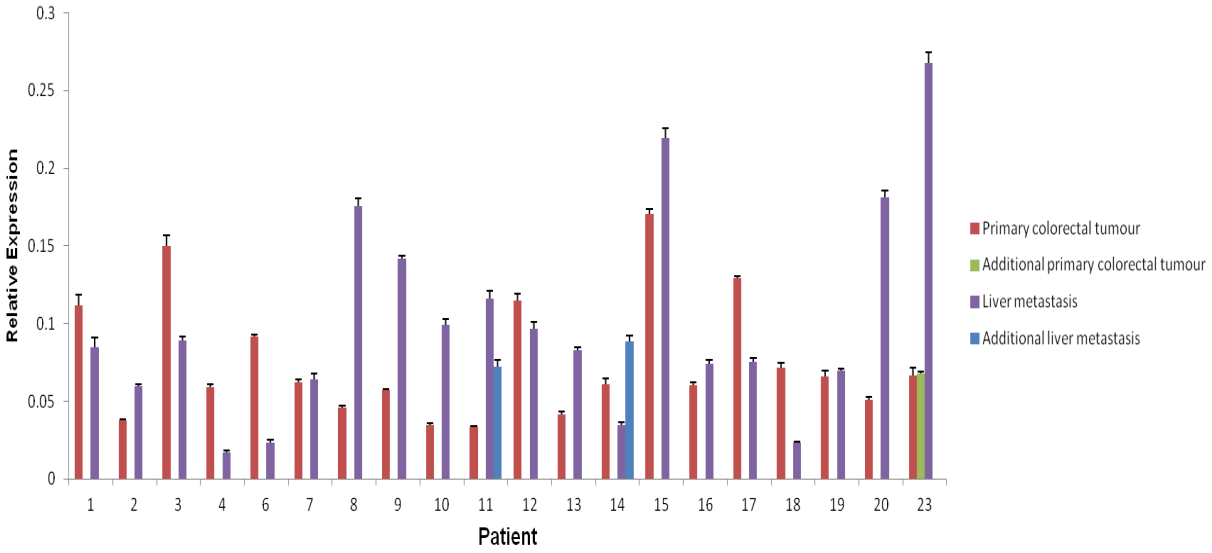

(B)

Patient	Fold change	p value
1	-1.32	0.04
2	1.57	0.0007
3	-1.68	0.008
4	-3.48	0.0003
6	-3.92	1E-05
8	3.84	0.0008
9	2.48	3.7E-05
10	2.86	0.001
11 (i)	3.48	0.003
11 (ii)	2.16	0.01
12	-1.19	0.04
13	1.99	0.0003
14 (i)	-1.77	0.009
14 (ii)	1.46	0.006
15	1.29	0.007
16	1.23	0.01
17	-1.72	0.0007
18	-3.07	0.003
20	3.55	0.0002
23 (i)	4.04	3.4E-05
23 (ii)	3.93	0.001

Figure 3.24

Figure 3.24: ***Differential miR-224 expression in primary colorectal cancers and patient-matched liver metastases****. **A)** The expression of miR-224, relative to the control let-7a, was compared in 20 primary colorectal cancers and patient matched liver metastases as detailed in Section 2.2.9.2. Each sample was assessed in triplicate and the errors were determined by calculating* $2^{(-\delta Ct + sd\ \delta Ct)}$ *and* $2^{(-\delta Ct - sd\ \delta Ct)}$*, as detailed in Section 2.2.9.5* ***B)*** *Fold change represents the change of relative miR-224 expression from colorectal cancers to liver metastases. Statistical significance ($p \leq 0.05$) was determined by performing independent T-tests.*

3.4. Discussion

A great wealth of research has described the many molecular events that occur during colorectal cancer progression. However we are still some way from identifying exactly how individuality in these molecular events leads to different clinical outcomes in colorectal cancer patients. The increasing understanding of the role of miRNAs in cancer progression may aid in this objective.

The present study aimed to explore how individuality in miRNAs that regulate KRAS and its downstream pathways may mediate different clinical outcomes and further sub-classify colorectal cancers at a molecular level or serve as markers of disease progression.

MiRNA profiling of colorectal cancers, normal mucosa and adenomas and HCT116 *KRAS* WT and mutant cell lines identified miR-224 as being overexpressed in colorectal cancer progression and potentially having an important role in the regulation of KRAS and its downstream pathways.

The present study shows that miR-224 expression was increased in colorectal cancers compared to normal mucosa, an observation that is supported by a number of other studies (Monzo *et al*, 2008; Arndt *et al*, 2009; Sarver *et al*, 2009; Wang *et al*, 2010*c*; Fu *et al*, 2012; Liao *et al*, 2012; Yuan *et al*, 2013; Zhang *et al*, 2014). Furthermore, our data is also supported by Bartley *et al* (2011) and Oberg *et al* (2011) who also reported that miR-224 expression was increased in both colorectal adenomas and cancers compared to normal mucosa. This suggests that the increased expression of miR-224 is an early and persistent

event in colorectal cancer development and progression. In addition to miR-224, miR-29c and miR-139-5p were found to be differentially expressed in HCT116 *KRAS* WT and mutant cells and additionally differentially expressed in colorectal adenomas and cancers compared to normal mucosa.

Given the increase in miR-29c in *KRAS* mutant cell lines compared to *KRAS* WT cells, one could speculate that the constitutive activation of the RAS/MAPK pathway activates the expression of miR-29c. Similar to miR-21 (Hatley *et al*, 2010), miR-29c may possibly itself also potentiate the activation of the pathway, if there was no activating mutation present, through the silencing of negative regulators of the RAS/MAPK pathway. Considering that miR-29c is increased in colorectal cancer in the present study, miR-29c may have a role in KRAS-mediated tumorigenesis through this proposed regulation of the RAS/MAPK pathway.

On the other hand, as low expression of miR-139-5p is associated with a constitutively active RAS/MAPK pathway and is also decreased in colorectal cancer, it may suggest that miR-139-5p may influence KRAS-mediated tumorigenesis through the targeting and repression of a driver of the pathway, including KRAS itself.

MiR-224 expression was increased in colorectal adenomas and cancers but also decreased in *KRAS* mutant cell lines. Interestingly, miR-224 has been experimentally validated to directly target and repress RAF kinase inhibitory protein (RKIP; Huang *et al*, 2012*a*).

RKIP has been shown to be cancer suppressive and protect against metastasis in a number of cancers by dissociating the interaction between RAF-1 and MEK and thus inhibiting the RAF/MAPK pathway. Al-Mulla *et al* (2006) were first to demonstrate that RKIP expression was directly correlated with patient survival in colorectal cancer and that it was an indicator of metastatic recurrence. Whilst low miR-224 expression is associated with a constitutively active RAS/MAPK pathway in *KRAS* mutant cell lines, the interaction between miR-224 and RKIP shows that increasing the expression of miR-224 could also, under the right selective pressures, increase the activity of the RAS/MAPK pathway downstream of RAF-1. This highlights the complexities of miRNA and target mRNA networks and show that miRNAs may have, in theory, opposing effects on a pathway. The eventual dominant phenotype may depend on outward selective pressures.

Previous studies have investigated why and how miR-224 is up-regulated in hepatocellular carcinoma (HCC), which may shed light on how it is overexpressed in colorectal cancer. The miR-224 gene is located at chromosome Xq28, a chromosomal region (Xq) which has been reported to be duplicated in colorectal cancer (Reid *et al*, 2009). The Xq28 region consists of the pre-miR-224 and pre-miR-452 genes which reside in intron 6 of *GABRE*, the gene that codes for the GABA-A receptor, and the testis antigen genes *MAGEA4* and *MAGEA5* that reside either side of *GABRE*.

Wang *et al* (2012) showed that the expression of miR-224 and other Xq28 genes were increased in HCC patients through epigenetic mechanisms. They showed *in vitro* that the Xq28 locus was regulated by the histone deacetylases HDAC1 and

HDAC3, which render the locus transcriptionally inactive and also by the histone acetylase protein, EP300 which allows for transcription. Cancer progression was therefore linked with an increase in EP300 and thus an increase in miR-224 expression. Moreover, the pre-miR-224 gene has its own promoter which is predicted *in silico* to contain NF-kB sites (Scisciani *et al*, 2012). The increased transcription of miR-224 and cancer cell invasion was subsequently shown to be induced by inflammatory pathways in HCC (Scisciani *et al*, 2012). To date no work has explored in colorectal cancer whether the increase in miR-224 expression could be due to the increased copy number of the Xq28 locus, to altered epigenetic mechanisms at the Xq28 locus or through inflammatory activation.

An additional important finding in the present study was that the expression of miR-224 was 3.3-fold higher in *KRAS* WT HCT116 cells compared to *KRAS* mutant cells. We also demonstrated that the transient knockdown of miR-224 in *KRAS* WT cells by a specific miR-224 inhibitor increased the activation (and thus GTP binding) of KRAS. This was confirmed by showing that the phosphorylation of ERK and AKT in *KRAS* WT cells was increased following miR-224 knockdown, mimicking a *KRAS*-mutant like phenotype.

The inherent low expression of miR-224 in HCT116 *KRAS* mutant cells could suggest a downstream repression of miR-224 transcription and thus expression by one of the many effectors that are activated. Using the 5 miRNA target prediction databases described earlier in the chapter, we produced a list of 1305 predicted miR-224 targets that were common to at least two of the databases

(Appendix I). Although the overwhelming majority of the predicted targets have not been experimentally validated, the size of the list shows the many downstream effects miR-224 could potentially have. Noteworthy was the inclusion of the sons of sevenless (SOS-) 2 gene, which was predicted by 3 of the 5 databases to be potentially targeted by miR-224.

As discussed in Chapter 1, KRAS in its inactive form is bound to guanosine disphosphate (GDP) and is activated when bound to guanosine trisphosphate (GTP). The SOS genes code for guanine nucleotide exchange factors (GEFs) that function by binding to KRAS and causing the dissociation of KRAS and GDP. As cytosol contains much higher levels of GTP than GDP, KRAS is more likely to bind to GTP and thus become activated (illustrated in Figure 3.25).

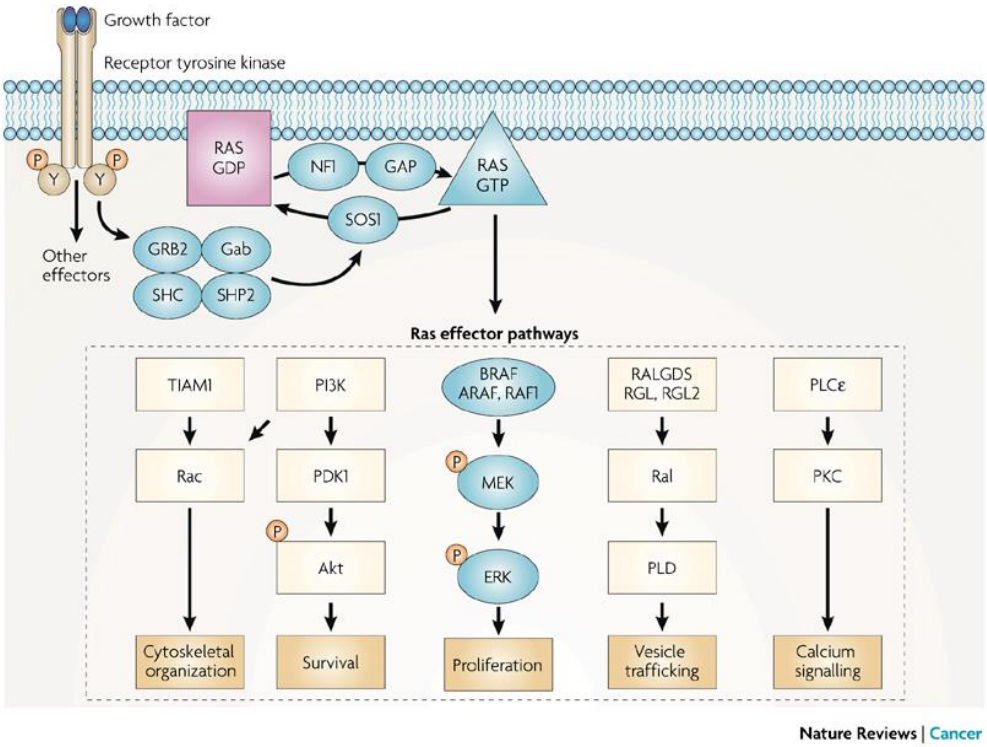

Figure 3.25: ***A schematic diagram of the downstream pathways affected by RAS*** *(Schubbert et al, 2007).*

The increase in SOS2 levels by the knockdown of miR-224 in HCT116 *KRAS* WT cells could cause KRAS activation by increased GTP binding. The subsequent repression of miR-224 as a result of the activation of the RAS/MAPK pathway (as seen in HCT116 *KRAS* mutant cells) could create a feed forward loop of KRAS activation. A priority experiment in future studies would therefore be to determine experimentally whether *SOS2* is targeted by miR-224 and to determine exactly what causes a repression in miR-224 expression in HCT116 cells when the RAS/MAPK pathway is activated.

The human cancer data shows that there was no statistically significant difference in miR-224 expression in *KRAS* and *BRAF* WT cancers and *KRAS* mutant cancers. However, the significant decrease in *BRAF* mutant cancers compared to WT cancers suggest that a factor downstream of the RAF-1, MEK or ERK could play a role in repressing miR-224 expression in cancers.

To date, miR-146b-3p and miR-486-5p (Ragusa *et al*, 2010; discussed above) and miR-92a, miR-127-3p and miR-378 (Mosakhani *et al*, 2012) are miRNAs that have been shown to differentiate between *KRAS* mutant and WT cancers. Mosakhani *et al* (2012) profiled the expression of 723 miRNAs in 15 *KRAS* mutant cancers, 45 *KRAS* WT cancers as well as their patient-matched normal mucosa samples. They reported that miR-92a and miR-127-3p were increased and miR-378 was decreased in *KRAS* mutant cancers compared to WT cancers, suggesting that the RAS/MAPK pathway may control the expression of these miRNAs. Mosakhani *et al* (2012) did not look at how the three aforementioned miRNAs affected clinical outcomes. However, miR-92a, a member of the miR-17-92 cluster, has been

consistently reported to be increased in colorectal cancer (Table 3.1) and has been shown to predict lower patient survival (Tsuchida *et al*, 2011; Zhou *et al*, 2013). The poor patient survival seen in *KRAS* mutant colorectal patients (Conlin *et al*, 2005) may therefore be, in part, attributed to the effects of miR-92 in colorectal cancer progression.

Further investigation of the phenotypic effects of miR-224 in cell lines showed that the knockdown of miR-224 in HCT116 *KRAS* WT cells increased cell doubling time. This suggests that the net phenotypic function of miR-224 under normal physiological conditions is to favour proliferation and survival by inhibiting apoptosis. MiR-224 has been shown to increase proliferation in colorectal and liver cancers through the repression of the tumour suppressor gene *SMAD4* (Wang *et al*, 2013; Zhang *et al*, 2013*b*). In contrast, miR-224 has also been shown to be pro-apoptotic. In hepatocellular carcinoma (HCC), miR-224 was shown to directly target apoptosis inhibitor protein-5 (API-5), and thus promote apoptotic cell death (Wang *et al*, 2008).

In the present study, based on the measured phosphorylation of key signalling molecules as determined by the PathScan signalling array, the knockdown of miR-224 could in theory have opposing phenotypic effects on cells if selective conditions were set in the favour of one pathway. The increased phosphorylation of ERK and AKT in *KRAS* WT cells, following miR-224 knockdown, suggests an increase in pro-proliferation and pro-survival pathways. This is also reflected in the increased phosphorylation of Stat3, which has been shown to be constitutively active and overexpressed in colorectal cancers and

reported to induce angiogenesis (Kasuba *et al*, 2006). The knockdown of miR-224, in contrast, also suggested the phosphorylation of Stat1 which is reported to affect cancer suppressive and anti-angiogenesis pathways (Battle *et al*, 2006). The chaperone protein HSP27, which has pro-apoptotic functions, was also activated. Interestingly, the phosphorylation of p38 MAPK which induces apoptosis following genotoxic stress was also increased. The α-isoform of p38 is coded by the *MAPK14* gene, a predicted target of miR-224 (Appendix I). However, the nature of the PathScan signalling array as a screening method means that further validation work using Western blots is required to better understand the effect of miR-224 knockdown on a number of signalling pathways.

Our data also shows that the knockdown of miR-224 did not have any marked effect on cell cycle kinetics in HCT116 *KRAS* WT cells, even in the presence of 5-FU. The percentage of cells that were in either G1 or S phase of the cell cycle as determined by flow cytometry suggests that miR-224 knockdown in HCT116 *KRAS* WT cells had no impact on cell cycle regulation, even in response to 5-FU (Figure 3.19 and Figure 3.20). As mentioned previously, the higher proportion of cells in the G1 phase in *KRAS* mutant cells compared to *KRAS* WT cells is inconsistent with the cell proliferation data that shows that the two cell lines did not have significantly different doubling times.

MiR-224 has been shown to directly target *CDKN1A* which codes for $p21^{cip1}$ (Olaru *et al*, 2013). Our bioinformatics data also suggests that miR-224 is

predicted to target CDKN1B, which codes for $p27^{kip1}$, in 2 of the 5 databases used (Appendix I).

Both p21 and p27 are cyclin dependent kinase (CDK) inhibitors which function as cell cycle regulators particularly in the transition from early to mid-phase G1 to late G1/S phase. They are able to cause cell cycle arrest in response to DNA damage or other types of stress if their levels are increased.

A recent study by Liao *et al* (2013) reports that miR-224 increased the G1/S transition by down-regulating $p21^{cip1}$ and $p27^{kip1}$ and up-regulating cyclin-D. It also shows that miR-224 increased proliferation through AKT signalling and by the direct suppression of the tumour suppressor genes PHLPP1 and PHLPP2. The interaction between miR-224 and $p21^{cip1}$ and $p27^{kip1}$ may therefore contribute to why miR-224 knockdown slows cell proliferation in HCT116 *KRAS* WT cells.

Another key and novel finding in the present study was that miR-224 knockdown could sensitise *KRAS* WT cells to 5-FU, possibly in part by increasing KRAS activation. The increased sensitivity of HCT116 *KRAS* WT cells to 5-FU could be due to a number of reasons. One theory proposed was that the increase in KRAS activation by miR-224 knockdown to resemble a mutant-*KRAS*-like phenotype increased cell proliferation. The cells would therefore be more sensitive to 5-FU as the active metabolite F-UTP would incorporate into the RNA, replacing uracil, at a higher rate. However, the present study shows that miR-224 knockdown in fact decreased cell proliferation. There was also no significant difference in the proliferation of the *KRAS* WT and mutant cells, which could be a limitation of the use of immortalised cell lines.

The present study did not explore whether miR-224 knockdown could have potentiated 5-FU induced apoptosis. Data from the PathScan signalling array suggests that miR-224 knockdown could potentially have pro-apoptotic effects. Therefore, in further work it would be important to determine what pro-apoptotic pathways, if any, miR-224 may affect in response to 5-FU treatment.

Consistent with the findings of the present study, Klampfer *et al* (2005) suggests a link between *KRAS* mutation status and 5-FU chemosensitivity. They found that HCT116 colorectal cells were protected from 5-FU induced apoptosis after targeted deletion of a mutant *KRAS* allele. Additionally, they showed that intestinal epithelial cells with inducible mutant *KRAS* (V12) promoted cell death upon 5-FU treatment and that KRAS promoted the accumulation of p53 in response to 5-FU in colorectal cancer cells.

Many studies including work from our own research group (Conlin *et al*, 2005) have published data on the lower survival of colorectal patients with *KRAS* mutant cancers. This therefore raises questions on whether we would want to hypothetically modulate *KRAS* WT cancers to phenotypically resemble those of *KRAS* mutants. Large scale clinical studies, however, have not seen any conclusive association between *KRAS* mutation status and response to 5-FU based therapy (Markowitz *et al*, 1995; Etienne-Grimaldi *et al*, 2008).

The present study also shows that miR-224 knockdown in HCT116 *KRAS* WT cells increase the expression *TYMP*, *TYMS* and *DPYD*. In clinical studies however, the decreased expression of *TYMS* and *DPYD* and the increased expression of *TYMP* in colorectal cancers have been associated with better response to 5-FU based

therapy (Goto *et al*, 2012). *TYMP*, *TYMS* or *DPYD* have not been reported to have any association with miR-224 nor do they appear to be predicted targets of miR-224 (Appendix I). However, our data suggests that miR-224 may have an impact on 5-FU response in patients through the indirect regulation of 5-FU drug metabolising enzymes. A large-scale study based on whether miR-224 can stratify patients based on *KRAS* mutation status and response to 5-FU-based therapy would be of interest, and we have begun to identify appropriate patient cohorts.

With regards to oxaliplatin, our data suggests that there is no association with *KRAS* mutation status and oxaliplatin sensitivity. This is perhaps unsurprising given the nature of the drug in forming cross-links in DNA and having less involvement in the proliferative or apoptotic nature of KRAS in its active or inactive state. The data does show, however, that the expression of ERCC1 was significantly increased following miR-224 knockdown in *KRAS* WT cells. The increase of this DNA damage repair pathway is associated with resistance to oxaliplatin (Seetharam *et al*, 2010). Time constraints prevented an investigation into the effects of miR-224 on irinotecan sensitivity, which could be an interesting future direction.

The drugs sorafenib and cetuximab both function, all be it at different targets, to block KRAS mediated cancer growth in *KRA*S and *BRAF* WT patients. The present study shows that various *KRAS* mutations and V600E *BRAF* mutation confer resistance to sorafenib by increasing KRAS activity in NIH3T3 cells, however this was not observed following miR-224 knockdown. This may suggest that miR-224

knockdown does not sufficiently activate KRAS to the level of when *KRAS* mutants have been stably transfected into NIH3T3 cells, where heterozygous *KRAS* expression is able to counteract the effects of sorafenib. However at higher concentrations sorafenib successfully kills cells regardless of miRNA modulation and KRAS activity.

The present study has shown through bioinformatics analysis that miRNAs that are differentially expressed in *KRAS* WT and mutant cells, and thus may represent a miRNA signature of KRAS activation, are predicted to mediate a large number of cancer related pathways such as cell proliferation, cell cycle regulation, cytoskeleton remodelling and EMT. This is perhaps not surprising given the known variety of pathways affected by KRAS. This also shows that the phenotypic consequences of oncogenic changes can be regulated or mediated through miRNAs.

The bioinformatics analysis showed a predicted link with miR-224 and EMT. Testing this association experimentally, it was shown that cell invasion was inherently decreased in HCT116 *KRAS* mutant cells compared to *KRAS* WT cells. We also showed that miR-224 knockdown cells were less invasive than untransfected *KRAS* WT cells. Therefore, miR-224 knockdown in WT cells again reflects a *KRAS* mutant-like phenotype. In contrast, stably transfecting a dominant mutant *KRAS* construct into NIH3T3 cells had a very marked effect on cell invasion.

This suggests that in the HCT116 model the effect of miR-224 on cell invasion may not be directly due to activation of KRAS and the RAS/MAPK pathway. This

may be supported by the fact that, as discussed previously, miR-224 knockdown decreases cell proliferation in HCT116 *KRAS* WT cells.

MiR-224 knockdown in *KRAS* WT cells was causal in the increased expression of E-cadherin and decrease in vimentin suggesting that miR-224 knockdown may have some impact on mediating a less mesenchymal cell phenotype. However, more detailed protein analysis is needed to fully elucidate if miR-224 drives cell invasion through EMT. Our bioinformatics data (Appendix I) suggests that miR-224 is predicted to target claudins (*CLDN11* and *CLDN14*) and desmogleins (*DGS2*) groups of proteins involved in cell adhesion and reported to be down-regulated during EMT (Lamouille *et al*, 2014).

Previous studies in hepatocellular carcinoma support the data in the present study that miR-224 promotes cell migration and invasion in colorectal cancer. Ma *et al* (2012) showed in HEPG2 cells that miR-224 promoted cell invasion and migration by activating the AKT signalling pathway and by directly targeting the tumour suppressor gene, PPP2R1B.

Rho GTPases such as CDC42 are activated when they dissociate from GDP and bind to GTP, and contribute to migration and invasion by affecting a number of downstream pathways including cytoskeleton remodelling. MiR-224 was suggested to target the Rho GTPase-activating proteins ARHGAP9 and ARHGAP21 which deactivates CDC42 (Scisciani *et al*, 2012). Thus through the repression of ARHGAP9 and ARHGAP21, miR-224 was suggested to increased cell migration and invasion in HEPG2 cells.

MiR-224 may also play a role in invasion and metastasis through the indirect regulation of matrix metalloproteinases, enzymes that are usually secreted by cancer cells to degrade the extracellular matrix and aid cancer dissemination. Li *et al* (2010) showed that increased miR-224 expression correlated with increased expression of *PAK4*, an effector of CDC42 that plays a role in cytoskeleton remodelling, and one of the matrix metalloproteinases *MMP9*. A later study by the same group confirmed that miR-224 regulated *PAK4* and *MMP9* expression, and thus cell invasion, though directly targeting the transcription factor *HOXD10* (Li *et al*, 2014). An earlier study by Illemann *et al* (2006) reports that *MMP9* was differentially expressed in primary colorectal cancers and their matched liver and lymph node metastases. Further studies could explore the relationship with miR-224 and the aforementioned targets in colorectal cancer cells.

To support my *in vitro* data linking miR-224 with cell invasion, the expression of miR-224 was assessed in metastasis samples and patient-matched primary colorectal cancers. My data shows that miR-224 expression was decreased in lymph node metastases compared to primary colorectal cancers in the majority of patients studied. It also shows that the majority of matched liver metastases-primary colorectal cancers in which miR-224 was differentially expressed by more than 1.5-fold were over-expressed in liver metastases.

Recent studies that explore the role of miR-224 in cell invasion and metastasis specifically in colorectal cancer contradict each other. Whilst Zhang *et al* (2013*a*) report miR-224 as pro-metastatic; Yuan *et al* (2013) suggest that miR-224

suppresses metastasis. This may suggest that miR-224 expression in metastases is affected by the anatomical site of metastases or that miR-224 has a dual role in promoting and suppressing cancer metastasis by affecting different pathways and thus impact patient survival. This may also suggest inter-patient differences in the mechanisms by which metastatic disease develops in colorectal cancer patients. There could be patients, for example, in which miR-224 is one of the dominant drivers of metastasis whereas in other patients miR-224 expression is suppressed in favour of other more dominant drivers.

To date, only a small number of studies have investigated the differential expression of a small number of miRNAs in primary colorectal cancers and patient-matched metastases samples. Global miRNA profiling in primary colorectal cancers and patient-matched metastases samples could identify what miRNAs, and therefore the pathways they mediate, collectively drive metastasis in colorectal cancer patients.

3.5. Conclusions and future work

3.5.1. Conclusions

The present study has shown that increased expression of miR-224 is an early and persistent feature of colorectal cancer development. The study also shows for the first time that miR-224 regulates KRAS activation in colorectal cancer. However, miR-224 affects a large variety of pathways and for this reason the regulation of KRAS-mediated tumorigenesis may not necessarily be the

dominant way by which miR-224 exerts its oncogenic effects as summarised in Figure 3.26.

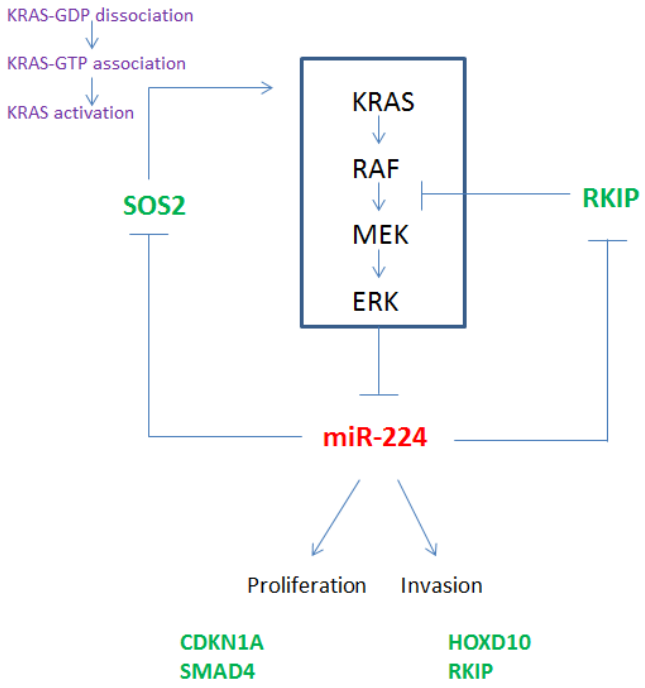

Figure 3.26: A schematic diagram showing the effect of miR-224 on the RAS/MAPK pathway and its wider implications. *The data in the present study suggests that miR-224 promotes cell proliferation and invasion as the transient knockdown of miR-224 reduces proliferation and invasion. These phenotypes could be mediated, in part, through the repression of previously validated targets of miR-224 such as CDKN1A, SMAD4, HOXD10 and RKIP. The reduced expression of miR-224 in KRAS mutant cells and BRAF mutant colorectal cancers suggest that the RAS/MAPK pathway represses the transcription and expression of miR-224. The knockdown of miR-224 may also cause KRAS activation through the repression of the predicted miR-224 target, SOS2. The subsequent activation of the RAS/MAPK pathway leads to a repression of miR-224 expression, creating a feed forward loop. The reduced expression of miR-224 may also, in theory, de-repress the RAS/MAPK pathway downstream of RAF-1 through its repression of RKIP. This highlights the many opposing roles of a single miRNA in one pathway.*

Furthermore, miR-224 has been shown *in vitro* to modulate 5-FU chemosensitivity perhaps, in part, through the regulation of KRAS pathways and by indirectly affecting the expression of 5-FU metabolising enzymes.

Finally, miR-224 has been shown to promote cell invasion in HCT116 *KRAS* WT cells. The variability of differential miR-224 expression in lymph node or liver metastases and primary colorectal cancers may reflect the variability in the mechanisms by which metastatic disease may develop.

3.5.2. Future work

Future cell line studies would be directed towards trying to establish exactly why and how miR-224 regulates KRAS activation. A possible link with *SOS2* has been suggested above and therefore there is a need to validate whether miR-224 directly targets the 3'UTR of *SOS2*. Furthermore, to support the data linking miR-224 with KRAS activation, it would be of interest to use miR-224 mimics to increase miR-224 expression in *KRAS* mutant cells (low miR-224 expression) and repeat the above experiments to establish whether we see a reversal of the effects that have been described above in relation to KRAS activation, cell cycle and proliferation, cell invasion and 5-FU sensitivity. I did attempt to perform these experiments but had difficulty in restoring miR-224 expression at physiological levels. As shown in Figure 3.27, miR-224 expression in HCT116 *KRAS* mutant cells was 414-fold higher following transfection with miR-224 mimic at the very lowest concentration suggested by the manufacturer. The

expression of miR-224 was, in contrast, 3.3-fold higher in HCT116 *KRAS* WT cells compared to HCT116 *KRAS* mutant cells (Figure 3.2)

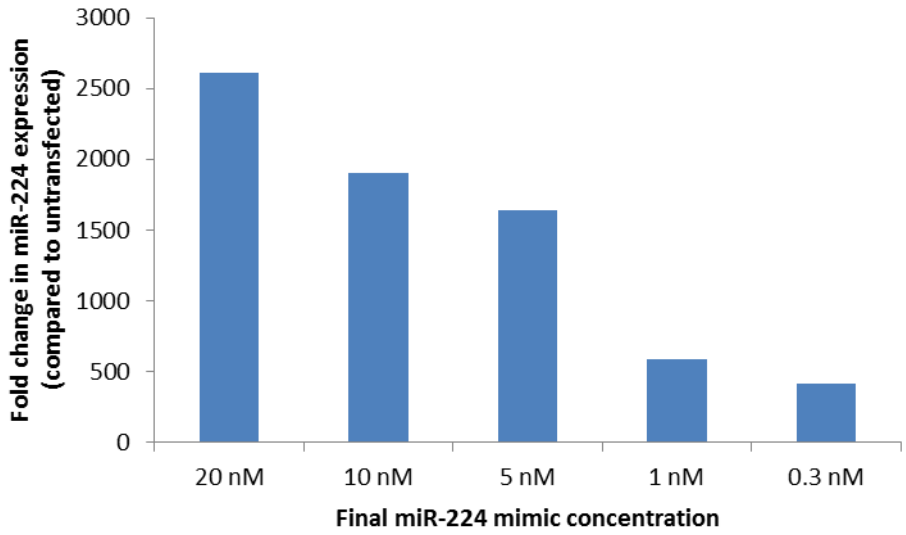

Figure 3.27: ***MiR-224 mimic optimisation.*** *HCT116 KRAS mutant cells were transiently transfected with 0.3 nM, 1 nM, 5 nM, 10 nM and 20 nM of miR-224 specific miRNA mimic and a negative control, as described in Section 2.2.5. The expression of miR-224, relative to the control miRNA let-7a, was assessed as described in Section 2.2.9.2. The fold change in miR-224 expression in transfected KRAS mutant cells compared to untransfected KRAS mutant cells is represented. Experiment was performed once.*

Future human tissue based studies would be directed towards correlating miR-224 expression with colorectal cancer patient survival and response to 5-FU based therapy. Furthermore, it would be important to relate the variability in differential miR-224 expression in lymph node or liver metastasis compared to primary colorectal cancers to patient relapse.

Chapter 4

4. Identification of novel candidate 5-FU and oxaliplatin drug resistance mechanisms

4.1. Introduction

4.1.1. Mechanisms of 5-FU and oxaliplatin resistance in colorectal cancer

Colorectal cancer treatment, as discussed in Chapter 1, involves the administration of 5-FU based chemotherapy regimens with folinic acid. However, response to treatment is very poor in colorectal cancer patients, with only 10-15% of patients responding (Johnston & Kaye, 2001). Second line treatment may include the addition of oxaliplatin (FOLFOX) or irinotecan (FOLFIRI) which have been shown in clinical trials to improve response rate to up to 50% (de Gramont *et al*, 2000; Douillard *et al*, 2000) in advanced colorectal cancer. However, a large proportion of patients see little, if any, benefit from standard chemotherapeutic treatment. The limitations to drug treatment are due to the development of resistance to drugs such as 5-FU, oxaliplatin and irinotecan and inherent drug resistance.

As discussed below, many studies have proposed and demonstrated that mechanisms of resistance to 5-FU may include the aberrant expression of 5-FU metabolising enzymes and alterations to drug efflux via drug transporters. Additionally, common mechanisms of resistance to 5-FU and oxaliplatin are reported to involve alterations to DNA damage repair mechanisms and the evasion of apoptosis (Longley *et al*, 2006). Most previous studies have also taken a candidate gene approach to investigating the mechanisms of drug resistance.

Dihydropyrimidine dehydrogenase (DPD), which is coded by the gene *DPYD*, is the rate-limiting enzyme in the catabolism of 5-FU (Figure 4.1). DPD

overexpression has been shown to be associated with 5-FU resistance, as 5-FU resistant cells adapt by increasing the removal of 5-FU (Soong *et al*, 2008). Increased expression of *TYMS* and under-expression of *TYMP* have been associated with 5-FU resistance in colorectal cancer patients (Goto *et al*, 2012).

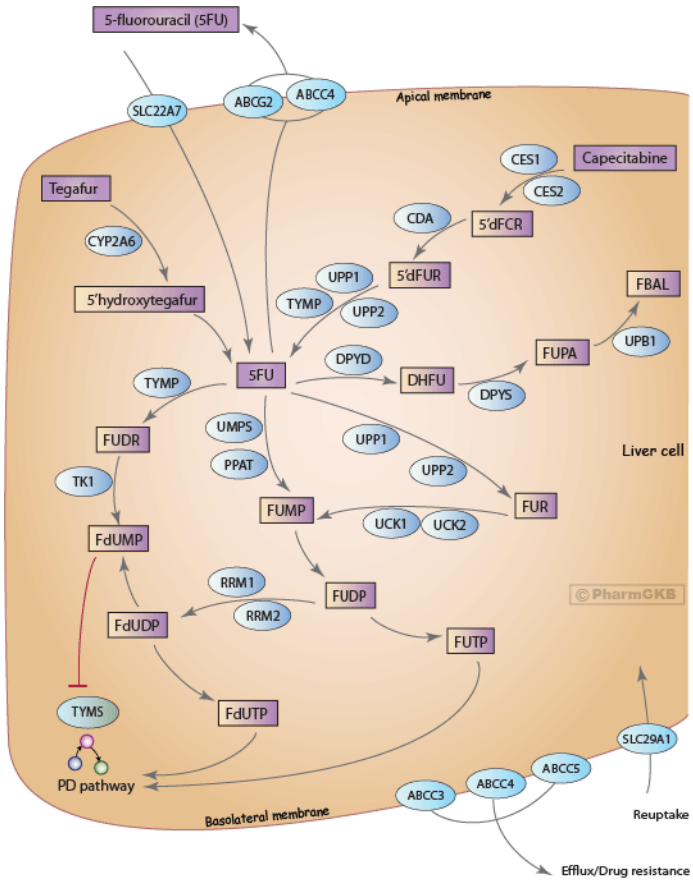

Figure 4.1: ***5-FU metabolism pathways****. Many factors are involved in the cellular response, metabolism and efflux/reuptake of 5-FU. Abnormal changes in the expression of genes such as DPYD, TYMP, TYMS and ABCC5 are reported to have an impact on 5-FU resistance (https://www.pharmgkb.org/pathway/PA150653776).*

ATP-binding cassette transporter (ABC transporter) proteins are a family of transmembrane proteins that transport various substances across the cell membrane. The multi-drug resistance P-glycoprotein (coded by the *ABCB1* gene) is reported to be involved in the efflux of a number of chemotherapeutic drugs

thus reducing the accumulation of drug within the cancer cell excluding 5-FU. Pratt *et al* (2005) showed that human kidney embryo (HEK-293) cells transfected with, and therefore expressing a higher protein level of, MRP5 (coded by *ABCC5* gene) were more resistant to 5-FU and oxaliplatin. They showed that there was a lower intracellular accumulation of 5-FU and that its metabolites were transported out of the cell via MRP5, as shown in Figure 4.1. A more recent study showed that MRP5-positive circulating cancer cells (CTCs) isolated from colorectal cancer patients correlated with a shorter progression-free survival in patients (Gazzaniga *et al*, 2010).

An increase in repair mechanisms to the drugs that cause DNA damage is another way by which cancer cells resist the cytotoxic effects of 5-FU and oxaliplatin. Nuclear excision repair (NER) is one of the major DNA repair mechanisms (Shuck *et al*, 2008). Among the many protein involved in NER is the excision repair cross-complementing 1 (ERCC1) protein. The aim of NER is to target and remove damage such as DNA adducts, created by drugs like oxaliplatin, allowing for the normal replication of DNA (Shuck *et al*, 2008). *ERCC1* expression has been shown to be increased in oxaliplatin resistant cells compared to drug sensitive cells (Arnould *et al*, 2003; Boyer *et al*, 2004) and was shown to be increased in colorectal cancer patients with lower survival (Shirota *et al*, 2001).

The DNA mismatch repair (MMR) system is another mechanism of DNA damage repair. This system recognises and repairs the misincorporation of bases during DNA replication and the repair of double stranded breaks. One of the main

proteins involved in MMR is human MutL homolog 1 (hMLH1). Defects in hMLH1 are associated with the microsatellite instability (MSI) phenotype and studies suggest that MSI correlates with adaptive resistance to 5-FU in colorectal cancer patients (Meyers *et al*, 2001; Arnold *et al*, 2003; Ribic *et al*, 2003).

Studies have also shown that cells may develop resistance to 5-FU or oxaliplatin through a p53 dependent arrest of the cell cycle. This decrease in cell cycle progression with respect to 5-FU, may reduce the rate of the incorporation of 5-FU metabolites into DNA and allow for more time for DNA repair to occur. Furthermore, Nita *et al* (1998) demonstrated that 5-FU was an apoptosis-inducing agent which modulated members of the BCL-2 family of apoptosis-related protein such as the pro-apoptotic factor Bax. Violette *et al* (2002) also suggest that the anti-apoptotic protein BCL-2 is increased in 5-FU resistant cells. Oxaliplatin resistance cells have also been shown to be associated with a loss of the pro-apoptotic factor, Bax (Gourdier *et al*, 2002).

There is now evidence emerging that cells can evade the effect of chemotherapeutic drugs by undergoing an epithelial-to-mesenchymal transition (EMT) and as a consequence becoming more invasive. The exact reasons for why undergoing EMT may provide a survival advantage in the long term presence of a drug are poorly understood. Yang *et al* (2006) were the first to describe the concept of chemotherapy-induced EMT in oxaliplatin resistant colorectal cell lines. They speculated that oxaliplatin resistant cells may switch from a proliferative, epithelial phenotype to one of a more invasive and migratory but

less proliferative phenotype. This would in turn allow the resistant cells to escape the effects of oxaliplatin due to the decrease in proliferation.

We are clearly a long way from knowing the full extent by which colorectal cancer cells develop resistance to 5-FU and oxaliplatin. However, the emergence of miRNAs as regulators of gene expression with key roles in many biological processes means that it is logical to investigate the role miRNAs may have in the development of drug resistance.

4.1.2. The role of miRNAs in 5-FU and oxaliplatin resistance

Blower *et al* (2007) introduces a panel of cell lines, NCI-60, which were used by the National Institute of Cancer (NCI) to screen thousands of chemical compounds and natural product extracts (including known chemotherapeutic drugs) for their pharmacological activities. The panel comprises a large variety of different human cell lines derived from cancers of the breast, central nervous system, colon and rectum, lungs, ovaries, prostate and renal tissue, as well as from leukaemia and melanomas. Prior to the study, the cell lines had been extensively profiled for their mRNA and protein expression, as well as for mutation status, chromosomal aberration and DNA copy number (http://discover.nci.nih.gov/cellminer/).

Due to the emerging knowledge at the time of the role of miRNAs as additional regulators of gene expression and their role in cancer progression, the authors used microarray technology to profile for miRNA expression in the NCI-60 panel. The study used a number of algorithms and computational tools to ascertain

that miRNAs cluster based on tissue type, reaffirming the notion that miRNA expression profiles can classify cancers. Furthermore, Blower *et al* (2007) demonstrated significant correlations between miRNA expression profiles and compound potency (measured by growth inhibition), suggesting a role for miRNAs in chemoresistance, although paired drug sensitive and drug resistant cell lines were not directly compared. A later study predicted that miR-224 and miR-24-1* (the passenger strand of miR-24-1) were negatively correlated with, amongst others drugs, 5-FU and irinotecan sensitivity (Gmeiner *et al*, 2010).

Climent *et al* (2007) initially implied a link between miRNA deregulation and chemoresistance by suggesting that the increased sensitivity of breast cancer patients to anthracycline-based chemotherapy may be related to the deletion of chromosome 11q, which contains the miR-125b gene. Prior to the beginning of the present study in October 2010, only a small number of studies had investigated the relationship between miRNAs and the drugs 5-FU and oxaliplatin. In colorectal cancer, Nakajima *et al* (2006) investigated the clinical significance of let-7g, miR-143, miR-145, miR-181b and miR-200c in cancer samples from a cohort of colon cancer patients (responders and non-responders) treated with the 5-FU based antimetabolite, S-1. The study found that let-7g and miR-181b were strongly associated with patient response to S-1, although they were not significant prognostic factors for predicting survival.

In colorectal cancer cell line studies, Rossi *et al* (2007) were the first to report that acute 5-FU treatment in colorectal cancer cell lines modulated miRNA expression. The study reported that clones of the colorectal cancer cell lines

HT29 and HCT116 were treated with 10 µM 5-FU for 6 days. MiRNA expression profiling showed that, compared to their respective non-drug treated parental cells, 18 miRNAs were differentially over-expressed in both cell lines whereas 3 miRNAs were differentially under-expressed. Amongst the miRNAs that were overexpressed in response to 5-FU were miR-20a, miR-21 and miR-135b whereas miR-224 was amongst the miRNAs under-expressed in response to 5-FU treatment. These miRNAs have been shown to be some of the most consistently differentially expressed miRNAs in colorectal cancer (Section 3.1.2, Table 3.2). As previously discussed in Chapter 3, these miRNAs may have important impacts on colorectal cancer progression by affecting multiple pathways. This suggests that the pharmacodynamic action of 5-FU could partly be due to the alteration of miRNA expression leading to changes in apoptosis, cell cycle and cell proliferation.

In a similar study, Zhou *et al* (2010) treated HCT-8 and HCT116 colorectal cancer cells with either 5-FU or oxaliplatin for 24 hours. They report that 56 and 50 miRNAs were differentially over and under-expressed respectively in treated cells compared to untreated cells.

Other studies reported on miRNAs that could modulate 5-FU sensitivity and resistance in colorectal cancer. The studies that were conducted prior to the beginning of the present study are listed in Table 4.1.

Table 4.1: Studies in colorectal cancer cell lines that report miRNA modulation of 5-FU sensitivity

Study	Cell line	Number of microRNAs examined	miRNAs (↑or ↓expression associated with 5-FU resistance)	mRNA targets
Song *et al*, 2009	HCT116	1	miR-140 ↑	HDAC4
Borralho *et al*, 2009	HCT116	1	miR-143 ↓	ERK5, NF-kB, BCL-2*
Boni et al, 2010	RKO, LoVo, DLD1, SW620	2	miR-192 ↑ miR-215 ↑	TYMS**
Wang *et al*, 2010*a*	HCT116	1	miR-31 ↑	None
Valeri *et al* (2010)	Colo-320 DM, SW620, HCT116, SW480, RKO	1	miR-21 ↑	hMSH2

*Determined by inverse protein expression

** Direct target but phenotype but effect on 5-FU resistance through independent mechanism

Borralho *et al* (2009) showed that miR-143 expression was inversely correlated with the expression of *BCL2* and that miR-143 contributed to increased sensitivity to 5-FU by potentiating 5-FU-induced apoptosis. Boni *et al* (2010) show that miR-192/215 directly target *TYMS*. However, the miRNA mediated down regulation of *TYMS* did not sensitise cells to 5-FU. It was in fact due to the induction of $p21^{cip1}$ and $p27^{kip1}$ which slows down cell cycle progression by causing arrest in G1. This therefore showed that miR-192 and miR-215 mediated another mechanism of 5-FU resistance other than through *TYMS* overexpression. Furthermore, Valeri *et al* (2010) reported that miR-21 conferred resistance to 5-FU by directly targeting and down-regulating the mismatch repair

enzyme, hMSH2 thus promoting a MSI phenotype. This shows that miRNAs are able to affect adaptive resistance to 5-FU through regulating genes involved in apoptosis, DNA repair and cell cycle regulation.

The above studies show what happens to miRNA expression in the immediate aftermath of acute 5-FU challenge. However, there were no studies looking at the role of miRNA in acquired 5-FU or oxaliplatin resistance in colorectal cancer. Although many groups had successfully generated 5-FU and oxaliplatin resistant colorectal cancer cell lines, none at the time had profiled for differential miRNA expression.

4.2. Aims and objectives

The aims of the present study were therefore twofold. Firstly to generate 5-FU and oxaliplatin resistant cell lines in two different colorectal cancer cell line backgrounds (HCT116 and DLD-1). Secondly, we aimed to use mRNA and miRNA expression profiling to predict novel mechanisms of acquired 5-FU and oxaliplatin resistance.

4.3. Results

4.3.1. Generation of drug resistant cell lines

To identify and investigate novel mechanisms of acquired drug resistance in colorectal cancer, two colorectal cancer cell lines, HCT116 and DLD-1, were each made resistant to either 5-FU or oxaliplatin by continuous selection, as described in Section 2.2.6, generating four novel drug resistant cell lines.

The concentration of 5-FU or oxaliplatin in which HCT116 or DLD-1 cells were cultured was incrementally increased from 0.1 μM to the highest concentration at which the cells remained viable and able to grow in culture. As shown in Section 2.2.6 (Table 2.3), the highest 5-FU concentration at which HCT116 and DLD-1 cells were still viable was 2 μM and 10 μM respectively, and at oxaliplatin concentrations of 10 μM and 24 μM respectively. This suggests that HCT116 cells were inherently more sensitive to both drugs compared to DLD-1 cells.

MTT cytotoxicity assays were performed to confirm that the drug resistant cells, compared to their respective drug-sensitive parental cells, were resistant to their selection drug, as described in Section 2.2.4. Cytotoxicity assays were also used to determine whether HCT116 and DLD-1 5-FU resistant cells were also cross-resistant to oxaliplatin and *vice versa*. Additionally, MTT cytotoxicity assays were used to ascertain whether 5-FU and oxaliplatin resistant DLD-1 cells were cross-resistant to irinotecan.

HCT116 5-FU resistant cells were significantly more resistant to 5-FU (higher IC_{50}) than the HCT116 parental cells (4.65-fold, p=0.01; Figure 4.2) but were not

cross-resistant to oxaliplatin (1.42-fold; p=0.75; Figure 4.2). In contrast, HCT116 oxaliplatin resistant cells were 28.22-fold more resistant to oxaliplatin than HCT116 parental cells (p=0.01; Figure 4.3) and also cross-resistant to 5-FU (2.1-fold; p=0.04; Figure 4.3).

(A)

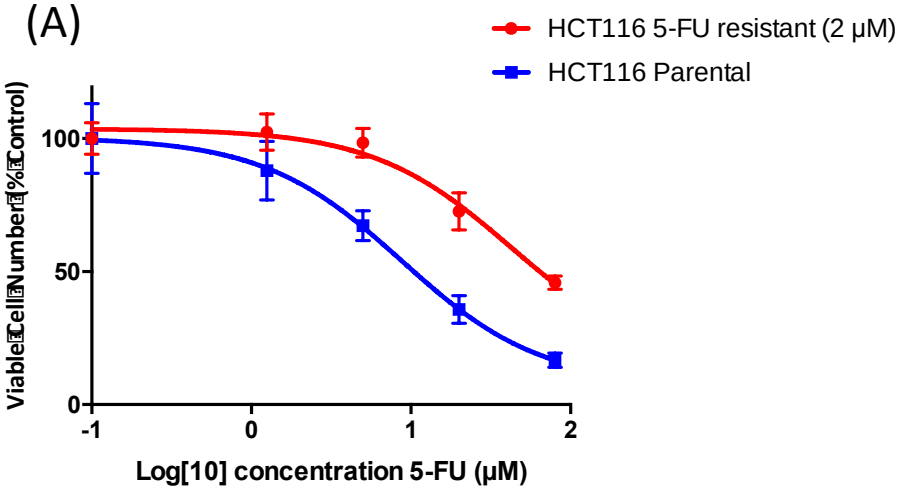

(B)

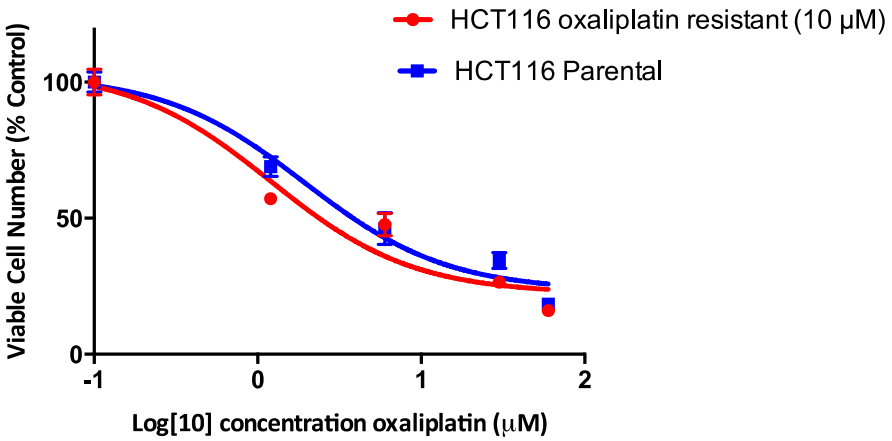

(C)

Cell line	5-FU		Oxaliplatin	
	IC_{50} fold change	p value	IC_{50} fold change	p value
HCT116 5-FU (2 µM)	**4.65 ± 0.58**	**0.01**	1.42 ± 0.66	0.75

Figure 4.2

Figure 4.2: ***5-FU and oxaliplatin sensitivity in HCT116 5-FU resistant cells.*** *MTT assays were used to compare the sensitivities of* ***A)*** *5-FU and* ***B)*** *oxaliplatin in HCT116 5-FU resistant cells compared to HCT116 parental cells as described in Section 2.2.4. MTT assays were performed 3 times and a representative graph is presented here.* ***C)*** *The IC_{50} for each cell line was calculated on GraphPad Prism version 6 and presented as a fold change relative to the IC_{50} of the HCT116 parental cell line. The errors represent the SEM of 3 separate experiments. Statistical significance ($p \leq 0.05$) was determined by performing independent T-tests.*

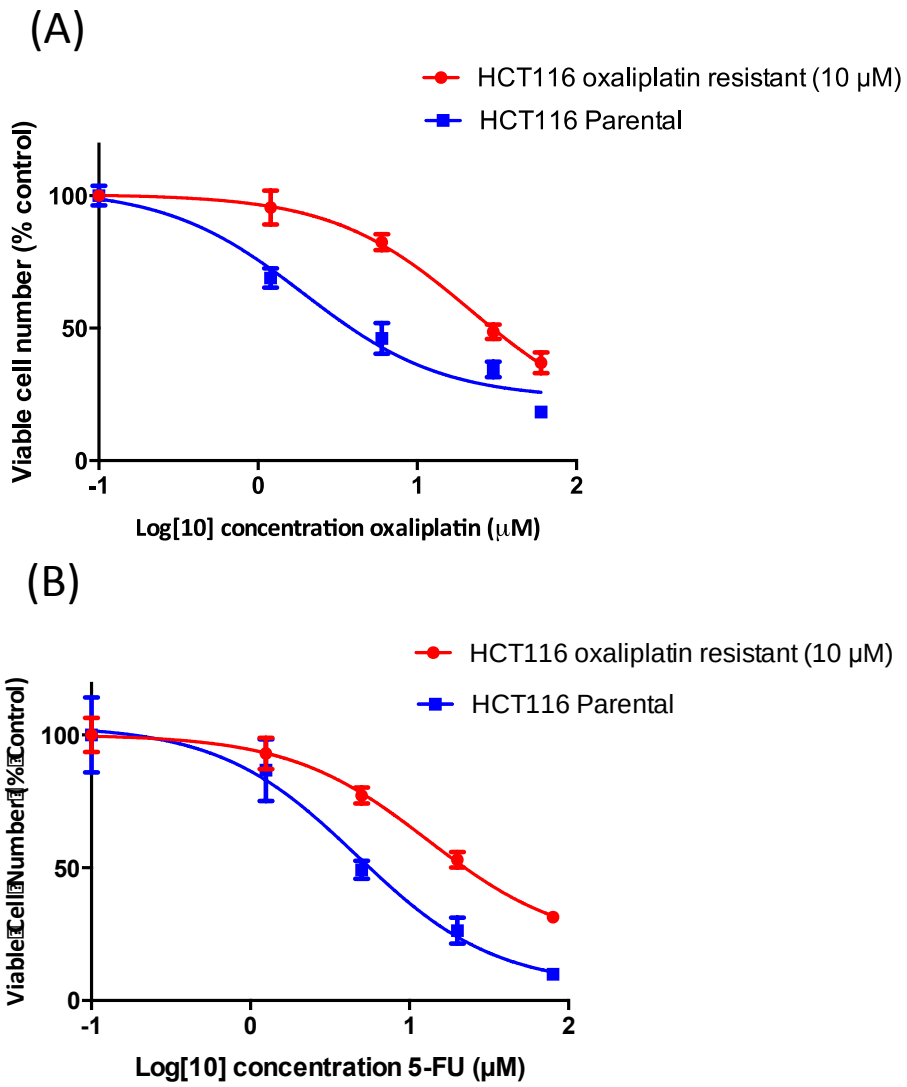

Figure 4.3

(C)

Cell lines	5-FU		Oxaliplatin	
	IC_{50} fold change	p value	IC_{50} fold change	p value
HCT116 oxaliplatin (10 µM)	**2.1 ± 0.43**	**0.04**	**28.22 ± 16.67**	**0.01**

Figure 4.3: ***5-FU and oxaliplatin sensitivity in HCT116 oxaliplatin resistant cells.*** *MTT assays were used to compare the sensitivities of* ***A)*** *oxaliplatin and* ***B)*** *5-FU in HCT116 oxaliplatin resistant cells compared to HCT116 parental cells as described in Section 2.2.4. MTT assays were performed 3 times and a representative graph is presented here.* ***C)*** *The IC_{50} for each cell line was calculated on GraphPad Prism version 6 and presented as a fold change relative to the IC_{50} of the HCT116 parental cell line. The errors represent the SEM of 3 separate experiments. Statistical significance ($p \leq 0.05$) was determined by performing independent T-tests.*

DLD-1 5-FU resistant cells were significantly more resistant to their selection drug 5-FU (21.49-fold; p=0.016) compared to DLD-1 parental cells. However, DLD-1 5-FU resistant cells did not confer cross resistance to oxaliplatin (1.39-fold; p=0.12; Figure 4.4).

Similarly, DLD-1 oxaliplatin resistance cells were significantly more resistant to oxaliplatin (8.87-fold; p=0.03). However, in contrast to HCT116 oxaliplatin resistant cells, they were not cross-resistant to 5-FU (1.13-fold; p=0.49; Figure 4.5).

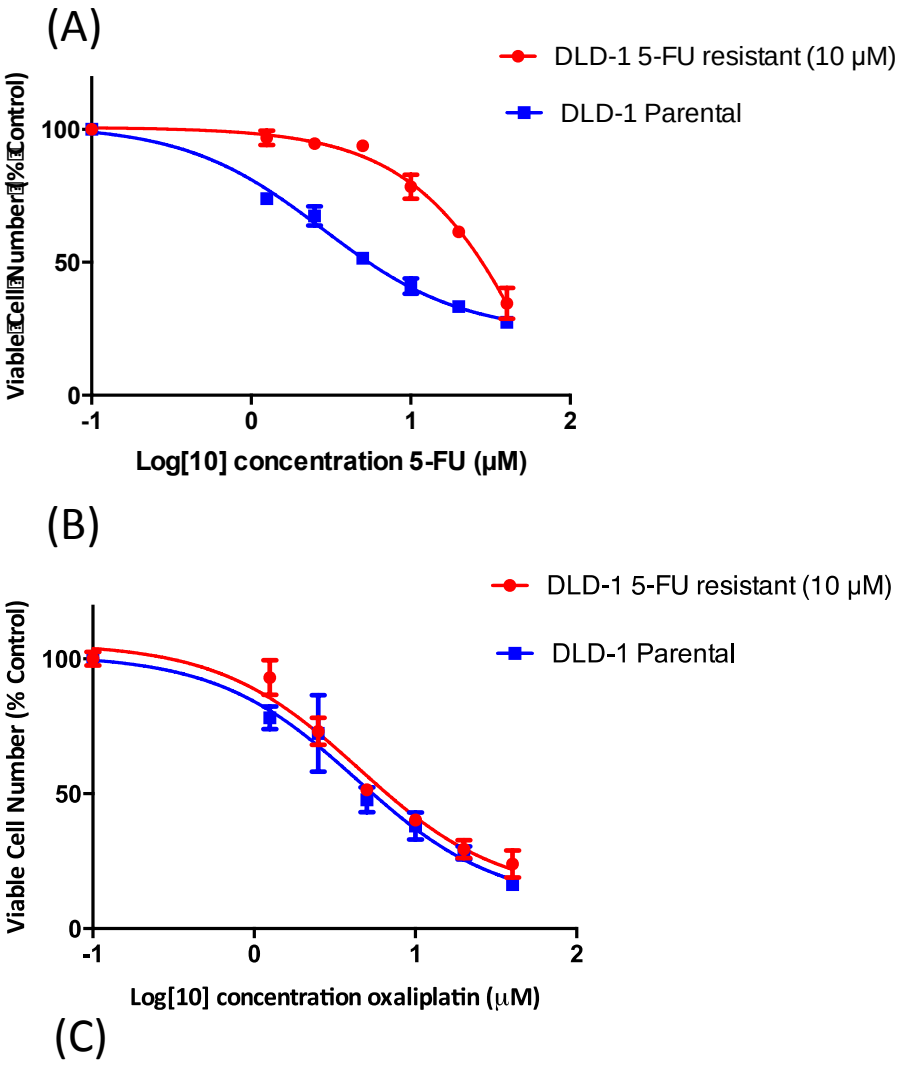

Cell lines	5-FU		Oxaliplatin	
	IC_{50} fold change	p value	IC_{50} fold change	p value
DLD-1 5-FU (10 µM)	**21.49 ± 2.45**	**0.016**	1.39 ± 0.5	0.12

Figure 4.4: ***5-FU and oxaliplatin sensitivity in DLD-1 5-FU resistant cells.*** *MTT assays were used to compare the sensitivities of* ***A)*** *5-FU and* ***B)*** *oxaliplatin in DLD-1 5-FU resistant cells compared to DLD-1 parental cells as described in Section 2.2.4. MTT assays were performed 3 times and a representative graph is presented here.* ***C)*** *The IC_{50} for each cell line was calculated on GraphPad Prism version 6 and presented as a fold change relative to the IC_{50} of the DLD-1 parental cell line. The errors represent the SEM of 3 separate experiments. Statistical significance ($p \leq 0.05$) was determined by performing independent T-tests.*

(A)

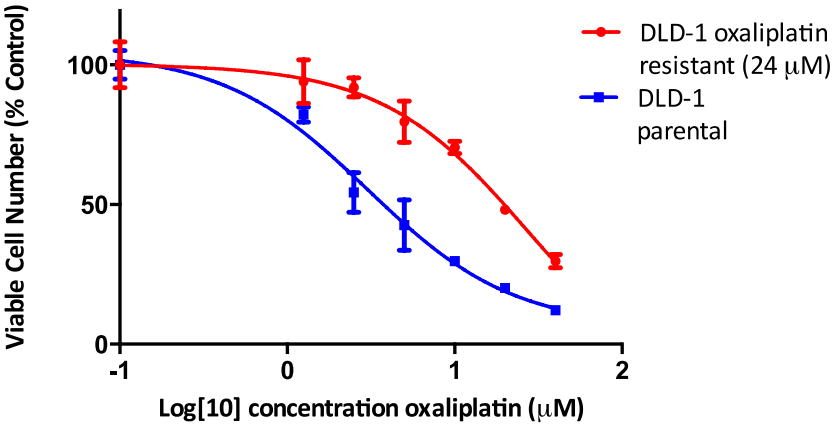

(B)

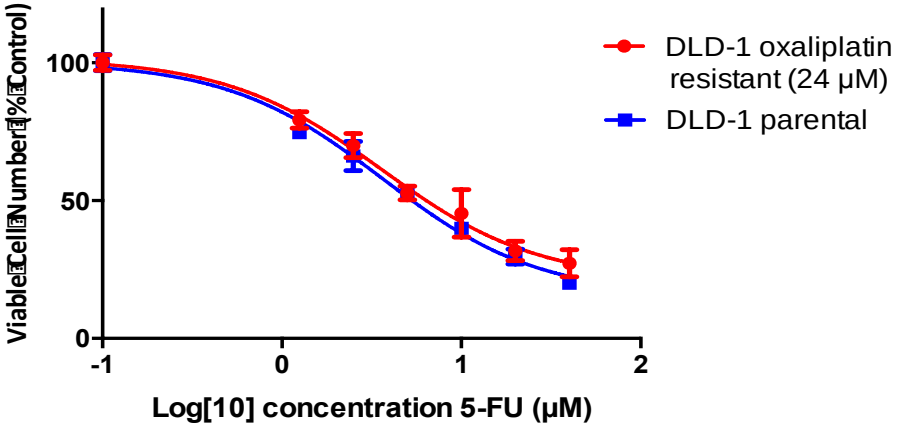

(C)

Cell lines	5-FU		Oxaliplatin	
	IC_{50} fold change	p value	IC_{50} fold change	p value
DLD-1 oxaliplatin (24 μM)	1.13 ± 0.31	0.49	**8.87 ± 1.55**	**0.03**

Figure 4.5: ***5-FU and oxaliplatin sensitivity in DLD-1 oxaliplatin resistant cells.*** *MTT assays were used to compare the sensitivities of* ***A)*** *oxaliplatin and* ***B)*** *5-FU in DLD-1 oxaliplatin resistant cells compared to DLD-1 parental cells as described in Section 2.2.4. MTT assays were performed 3 times and a representative graph is presented here.* ***C)*** *The IC_{50} for each cell line was calculated on GraphPad Prism version 6 and presented as a fold change relative to the IC_{50} of the DLD-1 parental cell line. The errors represent the SEM of 3 separate experiments. Statistical significance ($p \leq 0.05$) was determined by performing independent T-tests.*

Additionally, MTT cytotoxicity assays showed that neither DLD-1 5-FU resistant cells nor DLD-1 oxaliplatin resistant cells were cross resistant to irinotecan (DLD-1 5-FU resistant: 0.67 fold; p=0.27; DLD-1 oxaliplatin resistant: 1.19 fold; p=0.63; Figure 4.6). Therefore, if this represented a patient, it also suggests that irinotecan would be an effective course of treatment if the patient was resistant to 5-FU and/or oxaliplatin. Time constraints, however, meant that the effect of 5-FU or oxaliplatin resistance on sensitivity to irinotecan could not be investigated in HCT116 cells. This would therefore be a priority future experiment.

Previous studies show that 5-FU and oxaliplatin cross-resistance was observed in 5-FU and oxaliplatin resistant HT-29 cells (Dallas *et al*, 2009) and cross-resistance to 5-FU in SW620 oxaliplatin resistant cells (Liu *et al*, 2010). Cross-resistance to irinotecan has also been observed in HCT116 oxaliplatin resistant cells (Gourdier *et al*, 2002) and 5-FU resistant HCT116 cells (Boyer *et al*, 2004).

(A)

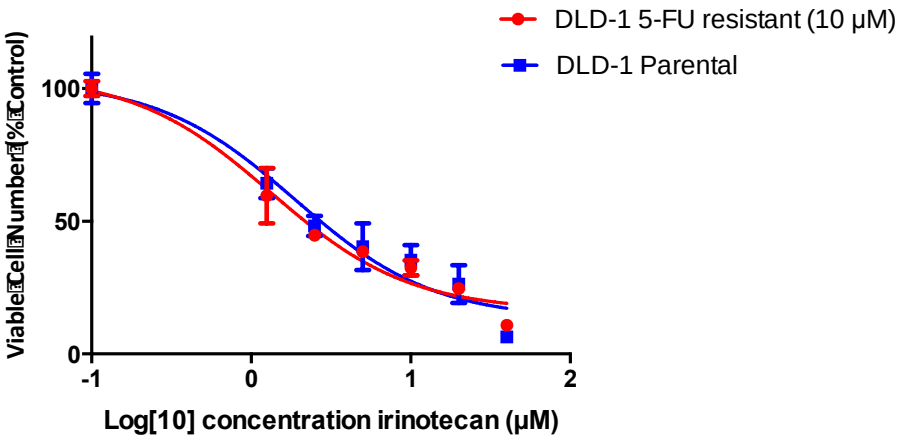

(B)

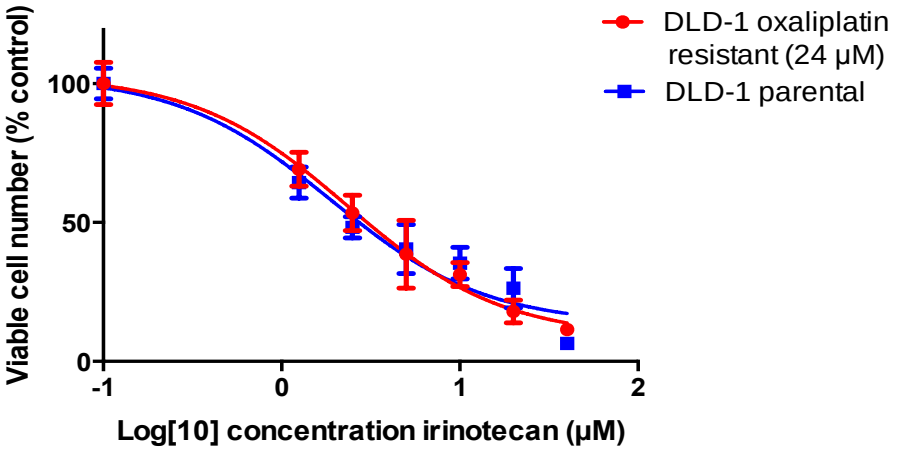

(C)

Cell Lines	Irinotecan	
	IC_{50} fold change	p value
DLD-1 5-FU (10 µM)	0.64 ± 0.08	0.27
DLD-1 oxaliplatin (24 µM)	1.19 ± 0.07	0.63

Figure 4.6: ***Irinotecan sensitivity in DLD-1 5-FU and oxaliplatin resistant cells.*** *MTT assays were used to compare the sensitivity of irinotecan in A**)** DLD-1 5-FU resistant and B**)** DLD-1 oxaliplatin resistant cells compared to DLD-1 parental cells as described in Section 2.2.4. MTT assays were performed 3 times and a representative graph is presented here.* ***C)*** *The IC_{50} for each cell line was calculated on GraphPad Prism version 6 and presented as a fold change relative to the IC_{50} of the DLD-1 parental cell line. The errors represent the SEM of 3 separate experiments. Statistical significance ($p \leq 0.05$) was determined by performing independent T-tests.*

4.3.2. Messenger RNA profiling and predicted drug resistance mechanisms

The present study then took a bioinformatics approach in an attempt to identify, firstly, the common mechanisms by which cells may develop drug resistance to both 5-FU and oxaliplatin and, secondly, the unique mechanisms by which cells may develop resistance to either 5-FU or oxaliplatin. These objectives were addressed by using Illumina HT-12 BeadChip mRNA expression arrays, as described in Section 2.2.10, to identify differentially expressed genes in HCT116 or DLD-1 drug resistant cells compared to their respective drug sensitive parental cells.

In our analysis, only known genes that were differentially increased or decreased in 5-FU or oxaliplatin resistant cells by more than 2-fold (following correction for multiple testing) compared to their respective parental cells were included in further analysis. Therefore, 1998 and 392 genes were differentially expressed in HCT116 5-FU resistant and HCT116 oxaliplatin resistant cells respectively compared to HCT116 parental cells. In DLD-1 cells, 3617 and 4982 genes were differentially expressed in 5-FU and oxaliplatin resistant cells respectively (Appendix J).

Tables 4.2 – 4.5 show the top 20 over and under-expressed genes in each drug resistant cell line compared to their respective drug sensitive parental cells. Among the most prominently differentially expressed genes in 5-FU or oxaliplatin resistance were genes coding for actin filaments. *ACTG1* (actin, gamma 1) was the most differentially under-expressed gene in HCT116 5-FU

resistant cells and the 7th and 11th most decreased in DLD-1 5-FU and oxaliplatin resistant cells respectively. Additionally *ACTB* (actin, beta) expression was the 1st and 2nd most differentially decreased gene in DLD-1 5-FU and oxaliplatin resistant cells respectively.

Similarly, genes coding for various tubulin proteins were also prominently represented within the top 20 under-expressed genes in 5-FU or oxaliplatin resistant cells. *TUBA1C* (tubulin, alpha 1C) was the 1st and 2nd most under-expressed gene in DLD-1 oxaliplatin and 5-FU resistant cells respectively whereas *TUBA1A* (tubulin, alpha 1A) was the 4th and 9th most abundantly decreased gene in DLD-1 5-FU and oxaliplatin resistant cells respectively. Additionally, *TUBB* (tubulin, beta) was the 10th and 13th most under-expressed gene in DLD-1 oxaliplatin and 5-FU resistant cells respectively. Actin and tubulin proteins are components of the cell cytoskeleton which aid in cell motility. The prominence of these genes in Tables 4.2 – 4.5 suggests that 5-FU and oxaliplatin resistance mechanisms involve cytoskeleton remodelling.

Other gene families that were among the top 20 differentially increased or decreased in 5-FU and oxaliplatin resistant cells included the ATP-binding cassette transporter genes involved in multi-drug resistance (*ABCC3*) or cholesterol and lipid transport and homeostasis (*ABCA1*, *ABCG1*), aldo-ketose reductases (*AKR1C3*, *AKR1B10*) which are involved in Phase II detoxification of a large number of drugs and xenobiotics (Barski *et al*, 2008) and some poorly characterised cytochrome P450 enzymes (*CYP4X1*, *CYP4F11*, *CYP4F12*).

Table 4.2: Top 20 over and under-expressed genes in HCT116 5-FU resistant cells

Gene	Fold change	Adjusted p value	Gene	Fold Change	Adjusted p value
SUSD2	19.22	9.81E-32	ACTG1	-25.66	3.44E-32
APOBEC3G	16.86	2.45E-30	ALDOA	-21.25	1.83E-28
TGM2	15.56	1.94E-32	THOC4	-15.88	1.46E-30
BMP4	11.29	4.26E-30	PSMC4	-11.94	2.90E-32
APOBEC3G	11.07	2.10E-28	CLEC2D	-11.61	2.65E-28
ABCC3	10.34	7.27E-27	PGAM1	-11.08	4.06E-29
ABCA1	10.34	1.38E-26	CCT7	-9.69	3.11E-28
IDUA	9.93	6.07E-29	RPL8	-9.03	2.75E-29
GNE	9.57	1.50E-27	MKX	-8.24	3.32E-27
GDF15	9.32	8.31E-29	C20orf127	-7.78	4.06E-26
TACSTD2	8.86	4.27E-26	ID2	-7.70	4.89E-27
ITGB4	8.84	6.18E-29	CD151	-7.38	6.71E-27
LAMB2	8.38	1.73E-23	MAEA	-7.25	2.26E-28
PLAU	8.21	1.49E-20	PSMC4	-7.17	5.63E-24
FGF19	8.15	1.28E-26	ID2	-7.16	1.48E-24
KRT80	7.88	1.90E-24	MT1E	-7.14	1.12E-27
GSN	7.86	3.44E-26	RGS2	-7.01	4.75E-27
GRB7	7.83	2.20E-27	MAGEB6B	-6.93	1.16E-23
MEGF6	7.70	2.10E-26	MCM4	-6.85	8.39E-26
LCN2	7.31	6.27E-25	RPL13	-6.53	1.34E-25

Full gene names and full list of genes presented in Appendix J

Table 4.3: Top 20 over and under-expressed genes in HCT116 oxaliplatin resistant cells

Gene	Fold change	Adjusted p value	Gene	Fold Change	Adjusted p value
HIST1H2BD	7.15	2.70E-26	PDE4B	-8.93	2.35E-26
KLK6	7.11	3.37E-23	MKX	-6.14	2.41E-24
TP53I3	6.48	2.50E-26	IRS1	-5.30	3.40E-24
GDF15	6.10	3.23E-25	FBLN1	-5.08	9.38E-23
BST2	6.09	2.52E-23	PRKACB	-4.36	1.65E-22
KLK5	5.82	3.23E-25	RGS2	-4.10	3.89E-22
VCAN	5.70	2.74E-24	IFIT1	-4.07	8.50E-22
HINT3	5.64	3.76E-24	TMEM16A	-3.57	1.35E-19
HIST1H2BD	4.94	3.40E-24	PCDH7	-3.48	1.61E-17
HAS3	4.90	1.31E-21	ARMC4	-3.44	1.49E-22
ABCC3	4.89	4.12E-21	PDE4B	-3.44	4.34E-21
AKAP12	4.51	3.62E-18	IFI27	-3.43	1.11E-21
CPA4	4.42	4.29E-20	GPR126	-3.35	6.52E-22
KLK8	4.36	3.53E-23	INSIG1	-3.34	3.43E-18
JUN	4.35	6.24E-23	CAV1	-3.30	1.18E-15
ANGPTL4	4.27	1.47E-21	CAV1	-3.22	2.66E-20
FERMT1	4.18	2.90E-20	NMB	-3.21	4.08E-19
AKR1C3	4.08	1.71E-19	SREBF1	-3.14	6.68E-20
KRT15	4.07	3.40E-24	EMP1	-3.14	5.49E-20
EIF3CL	3.90	1.89E-21	ANXA10	-3.04	7.88E-20

Full gene names and full list of genes presented in Appendix J

Table 4.4: Top 20 over and under-expressed genes in DLD-1 5-FU resistant cells

Gene	Fold change	Adjusted p value	Gene	Fold Change	Adjusted p value
ANGPTL4	31.46	2.38E-34	ACTB	-99.09	4.45E-37
FBXO32	26.74	4.59E-34	TUBA1C	-71.37	1.19E-34
ALDH1A3	18.58	1.34E-34	RPLP0	-52.57	5.94E-38
C15orf48	17.86	3.05E-35	TUBA1A	-43.65	4.54E-35
TRIM31	16.65	1.65E-33	EEF1G	-39.80	5.35E-34
LAMB2	12.45	2.29E-26	FKSG30	-37.48	3.27E-34
TPM2	12.37	4.62E-31	ACTG1	-36.32	2.02E-34
YPEL3	12.02	2.58E-29	RPS2	-33.07	4.59E-34
CYP4F12	11.92	2.88E-32	PGAM1	-31.64	3.05E-35
GCNT3	11.53	5.09E-31	ALDOA	-31.60	4.80E-31
AKR1C3	11.50	3.31E-28	CYBA	-30.96	4.05E-34
TPM2	11.48	5.34E-31	HNRNPK	-30.37	8.25E-36
RARRES3	11.32	3.57E-31	TUBB	-30.07	4.13E-33
CYBRD1	11.31	8.54E-28	PRDX2	-29.31	3.05E-35
HIST1H2BD	11.09	9.49E-31	AP1S1	-28.64	6.18E-35
C20orf54	10.79	6.86E-32	RPLP0	-28.35	1.24E-32
LCN2	10.64	6.18E-28	CCT7	-28.13	3.85E-34
CLIP2	10.60	1.32E-31	CXCL5	-24.67	9.41E-34
LINCR	10.59	2.88E-32	TPI1	-23.99	3.30E-31
ARL14	10.38	2.22E-31	AP1S1	-23.33	6.10E-35

Full gene names and full list of genes presented in Appendix J

Table 4.5: Top 20 over and under-expressed genes in DLD-1 oxaliplatin resistant cells

Gene	Fold change	Adjusted p value	Gene	Fold Change	Adjusted p value
AKR1C3	20.04	3.50E-31	TUBA1C	-128.21	1.42E-36
M160	17.28	4.08E-35	ACTB	-101.62	2.10E-37
AKR1B10	17.09	1.50E-35	RPLP0	-60.78	4.26E-38
CYP4X1	14.17	4.57E-33	EEF1G	-53.54	2.85E-35
SCG5	13.18	6.14E-33	RPS2	-51.34	7.79E-36
LAMB2	12.50	1.31E-26	FTL	-47.07	7.99E-37
ABCG1	12.06	2.73E-31	FTL	-44.34	3.22E-36
CD163L1	11.36	3.50E-31	HNRNPK	-41.01	3.02E-37
CYP4F11	10.45	5.38E-31	TUBA1A	-39.84	3.52E-35
CYP4F12	10.32	9.27E-32	TUBB	-39.67	1.89E-34
EPOR	10.05	2.09E-32	ACTG1	-38.42	4.90E-35
PVRL3	9.81	1.12E-29	PGAM1	-37.84	3.13E-36
SERPINA1	9.57	2.64E-29	FKSG30	-36.94	1.51E-34
ACOX2	9.17	2.01E-29	CYBA	-35.73	5.62E-35
CYTH2	9.00	3.34E-29	RPS3	-35.68	5.71E-37
KLHL24	8.88	1.95E-25	RPLP0	-33.54	1.44E-33
LCN2	8.60	6.93E-27	RPL10A	-33.48	1.41E-35
WDR72	8.41	1.31E-27	AP1S1	-33.13	7.80E-36
CD44	8.20	1.18E-24	PRDX2	-32.52	5.11E-36
DHRS3	8.19	4.19E-29	AHCY	-31.98	1.60E-31

Full gene names and full list of genes presented in Appendix J

Using the bioinformatics tool Metacore, as described in Section 2.2.17, we identified pathways and processes that were enriched and significantly associated with the differentially increased and decreased genes in each drug resistant cell line compared to their respective parental cells.

Tables 4.6 – 4.9 show the top ten most enriched pathways and processes associated with all significantly under-expressed genes in HCT116 5-FU resistant, HCT116 oxaliplatin resistant, DLD-1-5-FU resistant and DLD-1 oxaliplatin resistant cells compared to their respective parental cells. The tables show that there was an overwhelming enrichment of cell cycle regulation and progression. This suggests that decreased cell cycle progression is a major mechanism of drug resistance irrespective of the cell line or selection drug. There was also enrichment in ATP and ITP metabolism in both HCT116 and DLD-1 5-FU resistant cells (Tables 4.6 and 4.8).

Table 4.6: Pathways and processes associated with the genes differentially under-expressed in HCT116 5-FU resistant cells compared to HCT116 parental cells

	Pathway name	p value	Ratio
1	Cell cycle_The metaphase checkpoint	2.29E-11	29/36
2	Cell cycle_Start of DNA replication in early S phase	4.58E-11	26/31
3	dATP/dITP metabolism	1.55E-10	37/54
4	Cell cycle_Role of APC in cell cycle regulation	1.92E-09	25/32
5	Oxidative phosphorylation	2.37E-09	42/69
6	Cell cycle_Chromosome condensation in prometaphase	5.12E-09	18/20
7	ATP/ITP metabolism	1.26E-08	47/84
8	dCTP/dUTP metabolism	5.10E-08	30/46
9	GTP-XTP metabolism	7.20E-08	35/58
10	Cell cycle_Transition and termination of DNA replication	1.37E-07	20/26

	Process name	p value	Ratio
1	Cell cycle_Mitosis	1.30E-29	118/177
2	Translation_Translation in mitochondria	1.39E-29	82/103
3	Cell cycle_G2-M	7.67E-21	117/205
4	Cell cycle_S phase	1.11E-20	92/146
5	Transcription_mRNA processing	5.51E-19	95/159
6	Cell cycle_Core	1.16E-18	75/114
7	Translation_Translation initiation	1.91E-13	87/163
8	Cell cycle_G1-S	1.99E-12	85/163
9	DNA damage_DBS repair	2.47E-12	63/108
10	DNA damage_Checkpoint	4.86E-12	69/124

Table 4.7: Pathways and processes associated with the genes differentially under-expressed in HCT116 oxaliplatin resistant cells compared to HCT116 parental cells

	Pathway name	p value	Ratio
1	Cell cycle_The metaphase checkpoint	1.17E-15	32/36
2	Cell cycle_Role of APC in cell cycle regulation	4.42E-11	26/32
3	Cell cycle_Start of DNA replication in early S phase	1.45E-10	25/31
4	Cell cycle_Spindle assembly and chromosome separation	5.03E-10	25/32
5	Cell cycle_Chromosome condensation in prometaphase	3.39E-08	17/20
6	Cell cycle_Transition and termination of DNA replication	3.01E-06	18/26
7	dCTP/dUTP metabolism	6.00E-06	26/46
8	Development_MAG-dependent inhibition of neurite outgrowth	9.15E-06	20/32
9	Cholesterol Biosynthesis	1.16E-05	15/21
10	Cell cycle_Sister chromatid cohesion	1.16E-05	15/21

	Process name	p value	Ratio
1	Cell cycle_Mitosis	3.00E-29	114/177
2	Cell cycle_S phase	2.23E-27	98/146
3	Cell cycle_Core	1.68E-24	80/114
4	Cytoskeleton_Spindle microtubules	2.59E-14	64/108
5	Cell cycle_G2-M	1.99E-13	99/205
6	DNA damage_DBS repair	1.40E-09	56/108
7	Transcription_mRNA processing	2.00E-09	74/159
8	Proteolysis_Ubiquitin-proteasomal proteolysis	4.13E-09	75/164
9	Transcription_Chromatin modification	5.66E-09	61/125
10	DNA damage_Checkpoint	2.48E-07	57/124

Table 4.8: Pathways and processes associated with the genes differentially under-expressed in DLD-1 5-FU resistant cells compared to DLD-1 parental cells

	Pathway name	p value	Ratio
1	Cell cycle_The metaphase checkpoint	4.54E-12	32/36
2	Cell cycle_Role of APC in cell cycle regulation	2.87E-09	27/32
3	Cell cycle_Start of DNA replication in early S phase	6.74E-08	25/31
4	Cholesterol Biosynthesis	7.05E-08	19/21
5	Cell cycle_Chromosome condensation in prometaphase	1.94E-07	18/20
6	Cell cycle_Spindle assembly and chromosome separation	2.12E-07	25/32
7	Cell cycle_Transition and termination of DNA replication	7.71E-07	21/26
8	Apoptosis and survival_BAD phosphorylation	1.68E-06	26/36
9	dATP/dITP metabolism	6.05E-06	34/54
10	Cell cycle_Role of Nek in cell cycle regulation	6.57E-06	21/28

	Process name	p value	Ratio
1	Cell cycle_Mitosis	9.25E-29	127/177
2	Cytoskeleton_Spindle microtubules	6.67E-20	80/108
3	Cell cycle_S phase	4.63E-19	98/146
4	Cell cycle_Core	4.96E-19	82/114
5	Translation_Translation in mitochondria	8.50E-19	76/103
6	Transcription_mRNA processing	4.76E-17	101/159
7	Cell cycle_G2-M	1.55E-16	121/205
8	DNA damage_DBS repair	8.13E-13	70/108
9	Translation_Translation initiation	2.84E-12	94/163
10	DNA damage_Checkpoint	6.72E-11	74/124

Table 4.9: Pathways and processes associated with the genes differentially under-expressed in DLD-1 oxaliplatin resistant cells compared to DLD-1 parental cells

	Pathway name	p value	Ratio
1	Cell cycle_The metaphase checkpoint	7.77E-09	30/36
2	Cell cycle_Role of APC in cell cycle regulation	2.68E-08	27/32
3	Apoptosis and survival_Granzyme B signalling	3.45E-07	24/29
4	Apoptosis and survival_BAD phosphorylation	4.05E-07	28/36
5	Cell cycle_Chromosome condensation in prometaphase	9.15E-07	18/20
6	DNA damage_ATM/ATR regulation of G1/S checkpoint	1.51E-06	25/32
7	Cell cycle_Spindle assembly and chromosome separation	1.51E-06	25/32
8	Apoptosis and survival_FAS signaling cascades	1.51E-06	30/41
9	Development_IGF-1 receptor signalling	1.90E-06	32/45
10	DNA damage_ATM / ATR regulation of G2 / M checkpoint	4.17E-06	21/26

	Process name	p value	Ratio
1	Cell cycle_Mitosis	2.92E-21	122/177
2	Cell cycle_S phase	5.77E-20	104/146
3	Cell cycle_G2-M	2.51E-18	131/205
4	Cytoskeleton_Spindle microtubules	1.92E-14	76/108
5	Cell cycle_Core	2.26E-14	79/114
6	DNA damage_Checkpoint	2.01E-11	79/124
7	Cell cycle_G1-S	3.45E-11	97/163
8	Translation_Translation in mitochondria	1.82E-10	67/103
9	DNA damage_DBS repair	3.21E-10	69/108
10	Transcription_mRNA processing	9.05E-10	92/159

In contrast, Tables 4.10 – 4.13 show that the pathways and processes enriched by genes over-expressed in 5-FU or oxaliplatin resistant cells were less definitive than those enriched by under-expressed genes. In general, pathways and processes involved in inflammatory or immune responses, cytoskeleton remodelling and cell adhesion were enriched, consistent with work published by de Angelis *et al* (2006). Cytoskeleton remodelling, in particular, has been suggested to occur in EMT and cancer invasion (Yilmaz & Christofori, 2009). In DLD-1 oxaliplatin cells (Table 4.13) there was also a strong predicted association with lipid metabolism.

Table 4.10: Pathways and processes associated with the genes differentially over-expressed in HCT116 5-FU resistant cells compared to HCT116 parental cells

	Pathway name	p value	Ratio
1	Cytoskeleton remodeling_TGF, WNT and cytoskeletal remodelling	3.27E-07	61/107
2	G-protein signaling_Proinsulin C-peptide signalling	8.92E-07	27/37
3	Development_A3 receptor signalling	9.78E-06	25/36
4	Immune response _IFN gamma signaling pathway	1.81E-05	29/45
5	Immune response_Neurotensin-induced activation of IL-8 in colonocytes	2.07E-05	24/35
6	Development_c-Kit ligand signaling pathway during hemopoiesis	2.69E-05	32/52
7	Immune response_IL-15 signaling	3.85E-05	34/57
8	Apoptosis and survival_NGF activation of NF-kB	3.88E-05	19/26
9	Cell adhesion_Histamine H1 receptor signaling in the interruption of cell barrier integrity	4.26E-05	24/36
10	G-protein signaling_RhoA regulation pathway	4.34E-05	23/34

	Process name	p value	Ratio
1	Cell adhesion_Integrin-mediated cell-matrix adhesion	2.77E-10	110/210
2	Development_Neurogenesis_Axonal guidance	2.35E-08	108/218
3	Cell adhesion_Attractive and repulsive receptors	6.12E-08	87/169
4	Inflammation_Neutrophil activation	1.52E-07	92/184
5	Signal transduction_NOTCH signalling	5.84E-07	108/229
6	Development_Regulation of angiogenesis	5.84E-07	99/206
7	Cytoskeleton_Regulation of cytoskeleton rearrangement	1.34E-06	88/181
8	Reproduction_Feeding and Neurohormone signaling	4.27E-06	95/203
9	Development_Blood vessel morphogenesis	5.86E-06	98/212
10	Cell adhesion_Integrin priming	6.25E-06	52/97

Table 4.11: Pathways and processes associated with the genes differentially over-expressed in HCT116 oxaliplatin resistant cells compared to HCT116 parental cells

	Pathway name	p value	Ratio
1	Immune response_HSP60 and HSP70/ TLR signaling pathway	8.55E-05	24/54
2	Cytoskeleton remodeling_Cytoskeleton remodeling	1.36E-04	36/96
3	Development_GDNF signaling	1.63E-04	12/20
4	Cytoskeleton remodeling_TGF, WNT and cytoskeletal remodelling	3.31E-04	38/107
5	Glutathione metabolism / Rodent version	5.75E-04	17/37
6	Immune response_HMGB1/RAGE signaling pathway	6.03E-04	21/50
7	Apoptosis and survival_Role of IAP-proteins in apoptosis	6.13E-04	14/28
8	Development_VEGF signaling via VEGFR2 - generic cascades	6.21E-04	26/67
9	Glutathione metabolism	1.30E-03	16/36
10	Reproduction_GnRH signaling	1.53E-03	23/60

	Process name	p value	Ratio
1	Response to hypoxia and oxidative stress	2.73E-05	41/109
2	Cell adhesion_Integrin-mediated cell-matrix adhesion	3.02E-05	68/210
3	Inflammation_Amphoterin signaling	4.94E-05	42/115
4	Cell adhesion_Attractive and repulsive receptors	7.44E-05	56/169
5	Cytoskeleton_Actin filaments	9.20E-05	57/174
6	Cytoskeleton_Regulation of cytoskeleton rearrangement	3.00E-04	57/181
7	Inflammation_TREM1 signaling	4.13E-04	42/125
8	Inflammation_Neutrophil activation	4.79E-04	57/184
9	Inflammation_Protein C signaling	5.66E-04	33/93
10	Cell adhesion_Cell junctions	8.07E-04	47/148

Table 4.12: Pathways and processes associated with the genes differentially over-expressed in DLD-1 5-FU resistant cells compared to DLD-1 parental cells

	Pathway name	p value	Ratio
1	Development_VEGF signaling via VEGFR2 - generic cascades	2.20E-06	45/67
2	Immune response _IFN gamma signaling pathway	1.07E-05	32/45
3	Development_c-Kit ligand signaling pathway during hemopoiesis	2.81E-05	35/52
4	Cytoskeleton remodeling_TGF, WNT and cytoskeletal remodeling	4.12E-05	62/107
5	Regulation of CFTR activity (norm and CF)	6.13E-05	28/40
6	PGE2 pathways in cancer	1.22E-04	28/41
7	ENaC regulation in airways (normal and CF)	1.50E-04	23/32
8	Translation _Regulation of EIF4F activity	1.50E-04	32/49
9	Immune response_Gastrin in inflammatory response	1.64E-04	37/59
10	Cell adhesion_Cadherin-mediated cell adhesion	1.74E-04	19/25

	Process name	p value	Ratio
1	Inflammation_Interferon signaling	5.03E-06	64/109
2	Inflammation_IFN-gamma signaling	1.46E-05	59/101
3	Cell adhesion_Amyloid proteins	3.69E-05	93/178
4	Signal transduction_NOTCH signaling	4.71E-05	115/229
5	Cell adhesion_Cell junctions	5.41E-05	79/148
6	Autophagy_Autophagy	1.27E-04	32/50
7	Cytoskeleton_Actin filaments	1.47E-04	89/174
8	Reproduction_FSH-beta signaling pathway	2.31E-04	79/153
9	Immune response_Innate immune response to RNA viral infection	2.80E-04	40/68
10	Apoptosis_Anti-Apoptosis mediated by external signals via MAPK and JAK/STAT	3.66E-04	80/157

Table 4.13: Pathways and processes associated with the genes differentially over-expressed in DLD-1 oxaliplatin resistant cells compared to DLD-1 parental cells

	Pathway name	p value	Ratio
1	Immune response_Antiviral actions of Interferons	8.37E-04	23/33
2	Immune response _IFN gamma signaling pathway	1.31E-03	29/45
3	Regulation of lipid metabolism_Regulation of acetyl-CoA carboxylase 1 activity in lipogenic tissue	2.00E-03	7/7
4	Regulation of lipid metabolism_Regulation of acetyl-CoA carboxylase 1 activity in keratinocytes	2.00E-03	7/7
5	Immune response_CD40 signaling	2.33E-03	33/54
6	PGE2 pathways in cancer	3.23E-03	26/41
7	Cortisone biosynthesis and metabolism	3.59E-03	10/12
8	Phosphatidylinositol metabolism	3.85E-03	19/28
9	Development_WNT signaling pathway. Part 1. Degradation of beta-catenin in the absence WNT signaling	4.15E-03	14/19
10	Development_Role of IL-8 in angiogenesis	5.34E-03	31/52

	Process name	p value	Ratio
1	Signal transduction_NOTCH signaling	1.83E-04	119/229
2	Development_Regulation of angiogenesis	6.46E-04	106/206
3	Immune response_Innate immune response to RNA viral infection	1.47E-03	40/68
4	Apoptosis_Apoptotic nucleus	2.12E-03	79/152
5	Inflammation_Interferon signaling	2.24E-03	59/109
6	Reproduction_FSH-beta signaling pathway	2.68E-03	79/153
7	Apoptosis_Death Domain receptors & caspases in apoptosis	4.06E-03	64/122
8	Cell adhesion_Leucocyte chemotaxis	6.08E-03	93/188
9	Development_ERK5 in cell proliferation and neuronal survival	8.07E-03	16/24
10	Inflammation_TREM1 signaling	8.26E-03	64/125

To support the predicted pathways and processes analysis generated in Tables 4.6 - 4.13 and to further investigate mechanisms of resistance common to both 5-FU and oxaliplatin, we identified genes that were common to both HCT116 5-FU and oxaliplatin resistant cell lines and both DLD-1 5-FU and oxaliplatin resistant cell lines compared to their respective parental cell lines. We identified that 135 genes were differentially expressed (90 up, 45 down) in both 5-FU and oxaliplatin resistant HCT116 cells (Appendix K, Table K1). In addition, 2357 genes were differentially expressed (980 up, 1377 down) in both 5-FU and oxaliplatin resistant DLD-1 cells (Appendix K, Table K2). Ultimately, we identified 48 genes that were differentially expressed (31 up, 17 down) in all four drug resistant cells compared to their respective parental cells, representing a possible general drug resistance mRNA signature (Appendix K, Table K3).

Consistent with the bioinformatics data presented above, the 1377 genes under-expressed in DLD-1 drug resistant cells were associated with pathways and processes involving cell cycle regulation and ATP/ITP metabolism when analysed using Metacore (Appendix L, Table L1). This approach, however, yielded few cancer-related processes and pathways significantly associated with genes over-expressed in DLD-1 drug resistant cells or genes over or under-expressed in HCT116 drug resistant cells due to the small number of genes in each group (Appendix L, Tables L2 – L4).

Metacore was further used to identify pathways and processes associated with genes (213 in total; Appendix K, Table K4) that were uniquely differentially expressed in 5-FU resistant HCT116 and DLD-1 cells but not in oxaliplatin

resistant cells in an attempt to identify the unique mechanisms by which cells may develop resistance to 5-FU. Table 4.14 shows that pathways involved in glucocorticoid receptor signalling, ERBB family signalling, evasion of apoptosis and immune responses were prominent. Additionally, enriched processes involved in regulation of the cytoskeleton were also identified.

Conversely, genes (21 in total, Appendix K, Table K5) that were uniquely differentially expressed in oxaliplatin resistant HCT116 and DLD-1 cells but not 5-FU resistant cells were not significantly associated with any enriched pathways or processes, most likely because of the very small number of genes (data not shown). However, genes differentially expressed in oxaliplatin resistant DLD-1 cells but not HCT116 (5-FU or oxaliplatin resistant) or DLD-1 5-FU resistant cells were significantly associated with pathways and processes involved in cell cycle regulation, cell adhesion and cytoskeleton remodelling (Table 4.15).

Table 4.14: Pathways and processes associated with the 5-FU resistance specific genes common to HCT116 and DLD-1 cells

	Pathway name	p value	Ratio
1	Development_Glucocorticoid receptor signaling	1.35E-02	4/24
2	Development_ERBB-family signaling	3.18E-02	4/39
3	Apoptosis and survival_Anti-apoptotic TNFs/NF-kB/Bcl-2 pathway	3.18E-02	4/42
4	Apoptosis and survival_Lymphotoxin-beta receptor signaling	3.18E-02	4/42
5	Immune response_TNF-R2 signaling pathways	3.32E-02	4/45
6	Immune response_MIF-mediated glucocorticoid regulation	3.83E-02	3/22
7	Transcription_NF-kB activation pathways	3.83E-02	4/51
8	Apoptosis and survival_Role of PKR in stress-induced apoptosis	3.88E-02	4/53
9	Immune response_Role of PKR in stress-induced antiviral cell response	4.22E-02	4/57
10	HCV-dependent regulation of membrane receptors signaling in HCC	4.22E-02	3/27
11	Neurophysiological process_Constitutive and activity-dependent synaptic AMPA receptor delivery	4.222E-02	4/59
12	Immune response_Innate immune response to RNA viral infection	4.24E-02	3/28
13	Immune response_CD137 signaling in immune cell	4.34E-02	3/29
14	Immune response_IL-4 - antiapoptotic action	4.45E-02	3/30

	Process name	p value	Ratio
1	Cytoskeleton_Actin filaments	4.34E-03	11/176
2	Cytoskeleton_Regulation of cytoskeleton rearrangement	4.34E-03	11/183
3	Cytoskeleton_Intermediate filaments	7.07E-03	7/81
4	Immune response_Phagocytosis	1.19E-02	11/222
5	Inflammation_Protein C signaling	2.46E-02	7/108
6	Cell cycle_G1-S Growth factor regulation	4.13E-02	9/195
7	Reproduction_FSH-beta signaling pathway	4.13E-02	8/160

Table 4.15: Pathways and processes associated with the oxaliplatin resistance specific genes in DLD-1 cells

	Pathway name	p value	Ratio
1	Cell cycle_Role of Nek in cell cycle regulation	3.82E-03	10/32
2	Transport_Clathrin-coated vesicle cycle	3.82E-03	15/71
3	G-protein signaling_RhoA regulation pathway	3.82E-03	10/34
4	Colorectal cancer (general schema)	6.47E-03	9/30
5	Cell cycle_Role of APC in cell cycle regulation	9.14E-03	9/32
6	Cell cycle_Spindle assembly and chromosome separation	9.94E-03	9/33
7	Immune response_Function of MEF2 in T lymphocytes	1.30E-02	11/51
8	Development_Notch Signaling Pathway	1.30E-02	10/43
9	Cell adhesion_Ephrin signalling	1.74E-02	10/45
10	Transcription_Transcription factor Tubby signaling pathways	1.88E-02	6/17
11	Glutathione metabolism / Human version	2.00E-02	12/65
12	Cell cycle_Initiation of mitosis	2.44E-02	7/25
13	Signal transduction_Calcium signaling	4.89E-02	9/45

	Process name	p value	Ratio
1	Cytoskeleton_Spindle microtubules	7.94E-04	26/109
2	Cell cycle_Mitosis	3.08E-02	31/179
3	Cardiac development_Wnt_beta-catenin, Notch, VEGF, IP3 and integrin signalling	3.08E-02	27/150

4.3.3. MicroRNA profiling and predicted drug resistance mechanisms

Section 4.3.2 used mRNA profiling and bioinformatics analysis to predict mechanisms by which HCT116 and DLD-1 cells may develop 5-FU and oxaliplatin resistance, some of which have been previously reported. We show that hundreds of genes are differentially expressed in 5-FU or oxaliplatin resistant cells and contribute to a complex network of pathways involved in acquired resistance.

To support the above data, TLDA miRNA cards were used to profile each drug resistant cell line compared to their respective parental cell line, as detailed in Section 2.2.9.8. Due to the nature of miRNAs as key regulators of gene expression, we aimed to identify differentially expressed miRNA 5-FU and/or oxaliplatin resistance signatures and determine whether they predicted mechanisms of resistance.

In HCT116 5-FU resistant cells, 19 miRNAs were differentially expressed (5 up, 14 down) compared to HCT116 parental cells, with miR-99a and miR-483-5p the most abundantly over and under-expressed miRNAs respectively (Table 4.16). Only 5 miRNAs were differentially expressed (2 up, 3 down) in HCT116 oxaliplatin resistant cells compared to HCT116 parental cells with miR-19b and miR-328 the most abundantly over and under-expressed miRNAs respectively (Table 4.17).

Table 4.16: miRNAs differentially expressed in HCT116 5-FU resistant cells compared to HCT116 parental cells

microRNA	Fold change	Adjusted p value
miR-99a	6.26	0.025
miR-19b	5.18	0.010
miR-15b	3.94	0.015
miR-17	3.24	0.024
miR-494	3.04	0.048
let-7c	-3.75	0.040
miR-886-5p	-3.89	0.014
miR-223	-4.04	0.015
miR-193b	-4.63	0.003
miR-196b	-4.81	0.015
miR-197	-4.86	0.014
miR-181a	-5.16	0.036
miR-574-3p	-8.66	0.011
miR-210	-9.28	0.036
miR-320	-9.41	0.003
let-7b	-10.96	0.001
miR-328	-16.59	0.003
miR-886-3p	-26.13	0.003
miR-483-5p	-40.97	0.001

Table 4.17: miRNAs differentially expressed in HCT116 oxaliplatin resistant cells compared to HCT116 parental cells

microRNA	Fold change	Adjusted p value
miR-19b	7.21	0.027
miR-25	3.46	0.033
let-7b	-3.46	0.034
miR-320	-6.85	0.033
miR-328	-6.96	0.033

In DLD-1 5-FU resistant cells, 36 miRNAs were differentially expressed (29 up, 7 down) when compared to DLD-1 parental cells with miR-20a the most abundantly and miR-146a the least abundantly expressed miRNAs (Table 4.18). In addition, 27 miRNAs were differentially expressed (23 up, 4 down) in DLD-1 oxaliplatin resistant cells relative to DLD-1 parental cells with miR-17 and miR-886-3p the most abundantly over and under-expressed miRNAs respectively (Table 4.19).

Table 4.18: Differentially expressed miRNAs in DLD-1 5-FU resistant cells

microRNA	Fold Change	Adjusted p value
miR-20a	16.84	0.005
miR-10a	13.82	0.007
miR-186	11.21	0.006
let-7a	10.70	0.013
miR-19b	9.07	0.008
miR-200a	8.72	0.003
miR-200b	8.56	0.003
miR-106a	7.74	0.006
miR-494	7.38	0.031
miR-16	7.15	0.003
miR-17	7.10	0.003
miR-221	5.83	0.016
miR-26b	5.15	0.015
miR-203	5.12	0.015
let-7e	4.56	0.013
miR-29a	4.52	0.006
miR-93	4.48	0.003
miR-30c	4.45	0.015
miR-149	4.39	0.010
miR-26a	4.20	0.003
miR-375	3.90	0.015
let-7d	3.79	0.009
miR-744	3.76	0.021
miR-15b	3.38	0.037
miR-532-3p	3.25	0.006
miR-92a	2.98	0.015
miR-484	2.89	0.003
miR-24	2.53	0.023
miR-196b	1.95	0.034
miR-320	-1.70	0.042
miR-574-3p	-2.64	0.015
miR-192	-2.68	0.015
miR-328	-2.77	0.023
miR-483-5p	-2.83	0.013
miR-886-3p	-7.17	0.006
miR-146a	-9.96	0.015

Table 4.19: Differentially expressed miRNAs in DLD-1 oxaliplatin resistant cells

microRNA	Fold change	Adjusted p value
miR-17	21.97	0.001
miR-16	18.02	0.002
miR-106a	18.01	0.002
let-7a	16.78	0.014
miR-93	14.10	0.003
let-7e	10.45	0.002
miR-200b	8.95	0.002
miR-149	8.44	0.006
miR-186	7.40	0.006
miR-29a	7.09	0.002
miR-200a	5.69	0.005
miR-92a	4.56	0.005
miR-24	4.40	0.002
miR-331-3p	4.08	0.014
miR-345	3.81	0.004
miR-222	3.49	0.002
miR-26a	3.45	0.005
miR-196b	3.20	0.002
miR-223	2.70	0.017
miR-31	2.39	0.019
miR-200c	2.07	0.017
miR-191	2.00	0.002
miR-484	1.45	0.026
miR-320	-2.02	0.004
miR-574-3p	-3.37	0.002
miR-146a	-6.71	0.015
miR-886-3p	-16.35	0.002

During the development of the drug resistant cell lines in the present study, two studies were published reporting the generation of DLD-1 5-FU resistant cells and describing miRNAs differentially expressed in resistant cells relative to DLD-1 parental cells (Akao *et al*, 2011; Kurokawa *et al*, 2012). Akao *et al* (2011) and Kurokawa *et al* (2012) used miRNA microarray to profile 180 and 723 miRNAs respectively.

Consistent with the present study, microarray data from Akao *et al* (2011) suggests that miR-92 was differentially over-expressed in 5-FU resistant cells. Our TLDA data show that miR-92 was overexpressed in both 5-FU and oxaliplatin resistant cells compared to parental cells. Moreover, Kurokawa *et al* (2012) showed that miR-19b was overexpressed in DLD-1 5-FU resistant cells, which we also show to be overexpressed in our DLD-1 5-FU resistant cells and HCT116 5-FU and oxaliplatin resistant cells. In a recent study, Zhou *et al* (2014) generated HT29, RKO and HCT116 oxaliplatin resistant cell lines. The study also used miRNA microarrays to profile 389 miRNAs in paired drug resistant and sensitive cells. There were no similarities, however, in differentially expressed miRNAs in the HCT116 oxaliplatin resistant cells generated in the present study and those generated in the study by Zhou *et al* (2014).

In the present study, we identified miRNAs that were, for example, differentially expressed in both HCT116 5-FU and oxaliplatin resistant cells (e.g. let-7b) or in both DLD-1 5-FU and oxaliplatin resistant cells (e.g. 200a, miR-200b) compared to their respective parental cells. Additionally, miRNAs that were commonly differentially expressed in both HCT116 and DLD-1 5-FU resistant cells compared to their parental cells (miR-15b, miR-494, miR-483-5p) or uniquely differentially expressed in only DLD-1 5-FU resistant cells (e.g. miR-20a) or DLD-1 oxaliplatin resistant cells (e.g. miR-31) compared to DLD-1 parental cells were identified (Figure 4.7). Our analysis therefore identified potential miRNA signatures of 5-FU or oxaliplatin resistance in colorectal cancer.

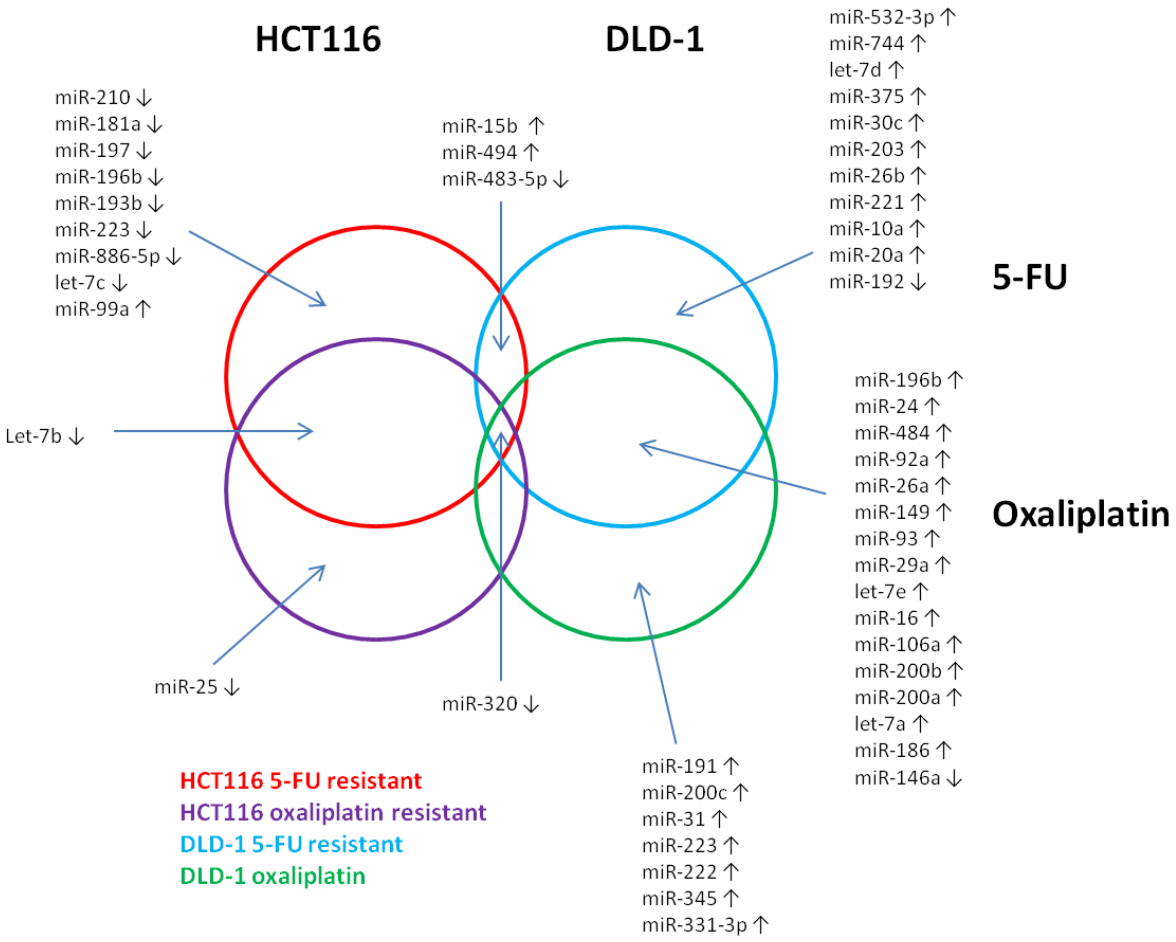

Figure 4.7: ***MiRNAs uniquely or commonly differentially expressed in 5-FU and oxaliplatin resistant cells.*** *TLDA miRNA cards were used, as described in Section 2.2.9.8, to identify miRNAs that were differentially expressed in HCT116 5-FU and oxaliplatin resistant cells compared to HCT116 parental cells and in DLD-1 5-FU and oxaliplatin resistant cells compared to DLD-1 parental cells. The Venn diagram shows miRNAs that were uniquely differentially expressed in one particular cell line or that were commonly differentially expressed in at least 2 of the drug resistant cell lines. ↑ and ↓represent over and under-expressed miRNAs respectively.*

The bioinformatics tool Metacore, as previously described, was used to identify pathways and processes that were enriched and associated with the predicted targets (identified from 5 miRNA target prediction databases, Section 2.2.17) of differentially expressed miRNAs in each drug resistant cell line compared to their

respective parental cells. In this analysis, the most prominently represented cancer-related pathways and processes that were enriched were those involved in cytoskeleton remodelling and cell adhesion (Tables 4.20 – 4.23), consistent with the pathways and processes analysis generated from the differentially expressed mRNA data. The next step was therefore to experimentally validate the phenotypes predicted by bioinformatics analysis.

Table 4.20: Pathways and processes associated with the predicted targets of miRNAs differentially expressed in HCT116 5-FU resistant cells compared to HCT116 parental cells

	Pathway name	Adjusted p value	Ratio
1	Cytoskeleton remodeling_TGF, WNT and cytoskeletal remodeling	1.93E-26	94/111
2	Cytoskeleton remodeling_Cytoskeleton remodeling	2.62E-20	82/102
3	Development_Regulation of epithelial-to-mesenchymal transition (EMT)	9.81E-19	57/64
4	Cell adhesion_Chemokines and adhesion	2.32E-16	76/100
5	Development_WNT signaling pathway. Part 2	2.16E-14	46/53
6	Cell adhesion_ECM remodeling	5.44E-13	44/52
7	Cell adhesion_Ephrin signaling	2.44E-12	39/45
8	Development_GM-CSF signaling	3.08E-12	42/50
9	Normal and pathological TGF-beta-mediated regulation of cell proliferation	3.34E-12	31/33
10	Development_TGF-beta-dependent induction of EMT via SMADs	9.67E-12	32/35

	Process name	Adjusted p value	Ratio
1	Cytoskeleton_Regulation of cytoskeleton rearrangement	5.45E-12	155/183
2	Signal transduction_WNT signaling	1.11E-11	150/177
3	Signal transduction_NOTCH signaling	1.17E-11	193/236
4	Development_Neurogenesis_Synaptogenesis	1.59E-10	150/180
5	Cytoskeleton_Actin filaments	1.73E-10	147/176
6	Development_EMT_Regulation of epithelial-to-mesenchymal transition	9.23E-09	179/226
7	Development_Hedgehog signaling	3.67E-08	197/254
8	Reproduction_FSH-beta signaling pathway	6.28E-08	130/160
9	Development_Neurogenesis_Axonal guidance	1.01E-07	179/230
10	Reproduction_Feeding and Neurohormone signaling	4.07E-07	164/211

Table 4.21: Pathways and processes associated with the predicted targets of miRNAs differentially expressed in HCT116 oxaliplatin resistant cells compared to HCT116 parental cells

	Pathway name	Adjusted p value	Ratio
1	Cytoskeleton remodeling_TGF, WNT and cytoskeletal remodeling	3.36E-25	73/111
2	Cytoskeleton remodeling_Cytoskeleton remodeling	8.68E-20	63/102
3	Cell adhesion_Chemokines and adhesion	9.12E-16	57/100
4	Cardiac Hypertrophy_NF-AT signaling in Cardiac Hypertrophy	3.58E-12	39/65
5	Development_WNT signaling pathway. Part 2	4.01E-11	33/53
6	Development_VEGF signaling via VEGFR2 - generic cascades	8.39E-11	44/84
7	Transport_Macropinocytosis regulation by growth factors	1.72E-10	36/63
8	Cell adhesion_Ephrin signaling	1.85E-10	29/45
9	Cell adhesion_Histamine H1 receptor signaling in the interruption of cell barrier integrity	1.85E-10	29/45
10	Cytoskeleton remodeling_Fibronectin-binding integrins in cell motility	1.87E-10	23/31

	Process name	Adjusted p value	Ratio
1	Development_Neurogenesis_Synaptogenesis	3.66E-11	107/180
2	Cytoskeleton_Regulation of cytoskeleton rearrangement	1.47E-10	107/183
3	Cytoskeleton_Actin filaments	3.04E-10	103/176
4	Signal transduction_WNT signaling	1.23E-09	102/177
5	Cardiac development_BMP_TGF_beta_signaling	7.74E-09	72/117
6	Reproduction_FSH-beta signaling pathway	9.38E-09	92/160
7	Cell adhesion_Synaptic contact	2.12E-08	102/184
8	Cardiac development_Wnt_beta-catenin, Notch, VEGF, IP3 and integrin signaling	3.45E-08	86/150
9	Cell adhesion_Attractive and repulsive receptors	1.10E-07	96/175
10	Signal transduction_ESR1-nuclear pathway	2.49E-07	113/216

Table 4.22: Pathways and processes associated with the predicted targets of miRNAs differentially expressed in DLD-1 5-FU resistant cells compared to DLD-1 parental cells

	Pathway name	Adjusted p value	Ratio
1	Cytoskeleton remodeling_TGF, WNT and cytoskeletal remodeling	4.01E-26	101/111
2	Cytoskeleton remodeling_Cytoskeleton remodeling	3.66E-22	91/102
3	Development_Regulation of epithelial-to-mesenchymal transition (EMT)	2.37E-20	62/64
4	Cell adhesion_Chemokines and adhesion	1.16E-18	86/100
5	Immune response_HSP60 and HSP70/ TLR signaling pathway	2.08E-18	53/54
6	Transport_Clathrin-coated vesicle cycle	1.95E-15	63/71
7	Development_WNT signaling pathway. Part 2	3.68E-15	50/53
8	Development_TGF-beta-dependent induction of EMT via MAPK	1.94E-14	45/47
9	Neurophysiological process_Receptor-mediated axon growth repulsion	9.45E-14	43/45
10	Cell adhesion_ECM remodeling	1.31E-13	48/52

	Process name	Adjusted p value	Ratio
1	Development_Neurogenesis_Synaptogenesis	5.43E-13	170/180
2	Signal transduction_WNT signaling	3.25E-11	165/177
3	Cell adhesion_Cadherins	7.54E-11	167/180
4	Cytoskeleton_Actin filaments	1.91E-10	163/176
5	Cytoskeleton_Regulation of cytoskeleton rearrangement	6.87E-10	168/183
6	Signal transduction_NOTCH signaling	2.36E-09	211/236
7	Cell adhesion_Integrin-mediated cell-matrix adhesion	6.38E-09	192/214
8	Cell cycle_G1-S Growth factor regulation	2.92E-08	175/195
9	Proliferation_Positive regulation cell proliferation	4.30E-08	196/221
10	Cell adhesion_Attractive and repulsive receptors	5.06E-08	158/175

Table 4.23: Pathways and processes associated with the predicted targets of miRNAs differentially expressed in DLD-1 oxaliplatin resistant cells compared to DLD-1 parental cells

	Pathway name	Adjusted p value	Ratio
1	Cytoskeleton remodeling_TGF, WNT and cytoskeletal remodeling	6.43E-23	98/111
2	Immune response_HSP60 and HSP70/ TLR signaling pathway	3.17E-20	54/54
3	Cytoskeleton remodeling_Cytoskeleton remodeling	3.89E-20	89/102
4	Cell adhesion_Chemokines and adhesion	1.31E-18	86/100
5	Development_Regulation of epithelial-to-mesenchymal transition (EMT)	1.45E-17	60/64
6	Cell adhesion_ECM remodeling	3.92E-16	50/52
7	Immune response_IL-1 signaling pathway	7.80E-15	43/44
8	Transport_Clathrin-coated vesicle cycle	1.99E-14	62/71
9	Development_WNT signaling pathway. Part 2	6.60E-14	49/53
10	Immune response_HMGB1/RAGE signaling pathway	6.60E-14	49/53

	Process name	Adjusted p value	Ratio
1	Development_Neurogenesis_Synaptogenesis	4.53E-14	171/180
2	Signal transduction_WNT signaling	1.81E-11	165/177
3	Transcription_mRNA processing	1.04E-09	148/160
4	Cytoskeleton_Regulation of cytoskeleton rearrangement	1.53E-09	167/183
5	Cell adhesion_Cadherins	2.97E-09	164/180
6	Signal transduction_NOTCH signaling	1.10E-08	209/236
7	Proliferation_Positive regulation cell proliferation	6.85E-08	195/221
8	Cytoskeleton_Actin filaments	8.23E-08	158/176
9	Cell cycle_G1-S Interleukin regulation	9.45E-08	118/128
10	Cytoskeleton_Cytoplasmic microtubules	1.01E-07	107/115

4.3.4. The relationship between acquired drug resistance, EMT and cell invasion

To investigate the predicted association between acquired 5-FU or oxaliplatin resistance in HCT116 and DLD-1 cells and EMT, the expression of a panel of well-known EMT genes, *CDH1*, *CDH2*, *TWIST1* and *VIM* was compared in drug resistant cells and their respective drug sensitive parental cells, by Taqman qRT-PCR analysis as described in Section 2.2.9.4.

CDH1 (E-cadherin) expression was significantly increased in HCT116 5-FU (2.4-fold; p=0.003) and oxaliplatin resistant cells (2.1-fold, p=0.008) compared to HCT116 parental cells (Figure 4.8 A), and in DLD-1 5-FU (3.7-fold, p=0.007) and oxaliplatin resistant cells (3.9-fold, p=0.04) compared to DLD-1 parental cells (Figure 4.8 B). As a decrease in E-cadherin is a hallmark of EMT, this was a surprising result. However, pathways and processes associated with cell adhesion are significantly associated with genes over-expressed in drug resistant cell lines compared to their respective parental cells. Moreover, it was observed whilst culturing the drug resistant cell lines that the cells were more clumped together and more resistant to the effects of trypsin.

The expression of *CDH2* (N-cadherin) was not significantly changed in DLD-1 5-FU (1.4-fold; p=0.17) and oxaliplatin (0.66-fold; fold; p=0.16) resistant cells (Figure 4.8 C), and was not expressed at all in HCT116 cells (data not shown). The expression of vimentin was significantly decreased (1.4-fold; p=0.03) in oxaliplatin resistant HCT116 cells. *VIM* expression was also decreased in 5-FU resistant HCT116 cells but not to a statistically significant level (1.3-fold; p=0.08;

Figure 4.8 D). The expression of *TWIST1* was significantly increased (2.5-fold; p=0.02; Figure 4.8 E) in 5-FU resistant HCT116 cells but not in oxaliplatin resistant cells (1.6-fold; p=0.1). The data suggests that an EMT phenotype may not be consistently displayed. However, the change in expression of many other genes also defines EMT. *DSG2* (desmoglein 2), for example, is decreased in DLD-1 5-FU and oxaliplatin resistant cells (Appendix J, Table J3 and J4). Therefore further studies may be needed to assess the expression of other EMT genes and to also assess protein expression.

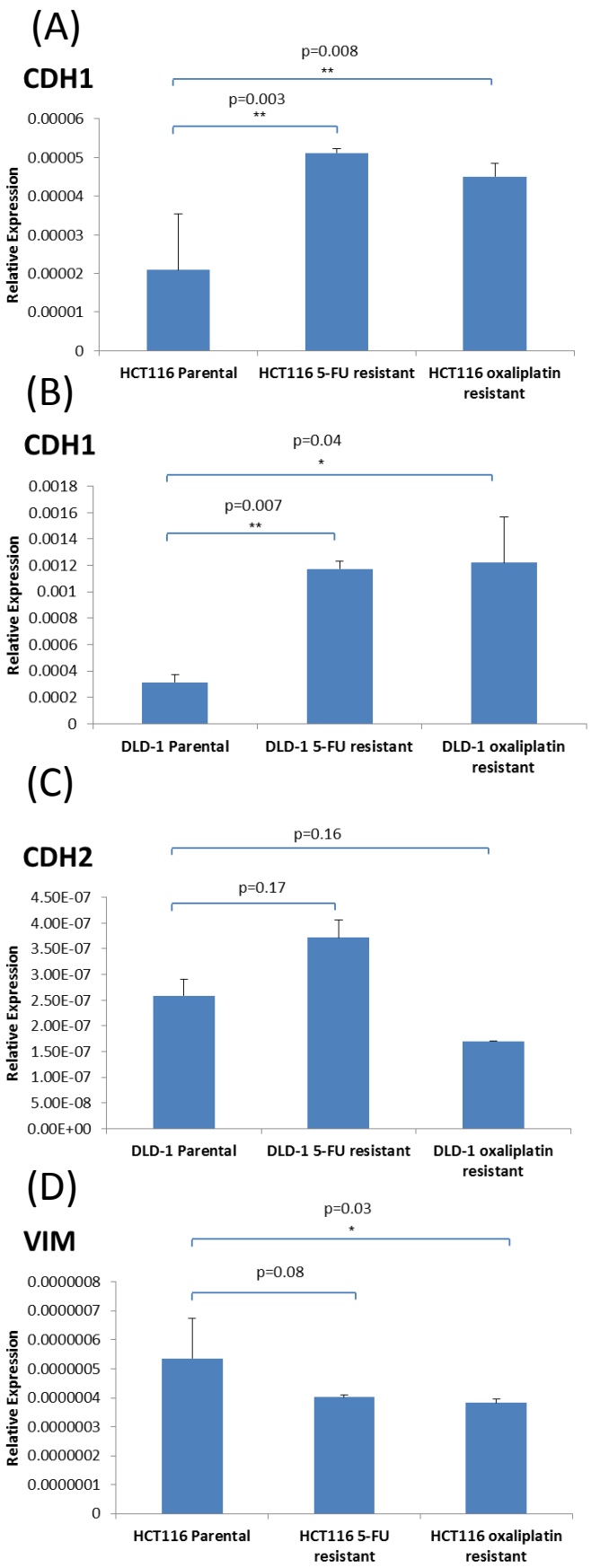
(A)
CDH1
p=0.008
**
p=0.003
**
Relative Expression
0.00006
0.00005
0.00004
0.00003
0.00002
0.00001
0
HCT116 Parental
HCT116 5-FU resistant
HCT116 oxaliplatin resistant
(B)
CDH1
p=0.04
*
p=0.007
**
Relative Expression
0.0018
0.0016
0.0014
0.0012
0.001
0.0008
0.0006
0.0004
0.0002
0
DLD-1 Parental
DLD-1 5-FU resistant
DLD-1 oxaliplatin resistant
(C)
CDH2
p=0.16
p=0.17
Relative Expression
4.50E-07
4.00E-07
3.50E-07
3.00E-07
2.50E-07
2.00E-07
1.50E-07
1.00E-07
5.00E-08
0.00E+00
DLD-1 Parental
DLD-1 5-FU resistant
DLD-1 oxaliplatin resistant
(D)
VIM
p=0.03
*
p=0.08
Relative Expression
0.0000008
0.0000007
0.0000006
0.0000005
0.0000004
0.0000003
0.0000002
0.0000001
0
HCT116 Parental
HCT116 5-FU resistant
HCT116 oxaliplatin resistant

Figure 4.8

(E)

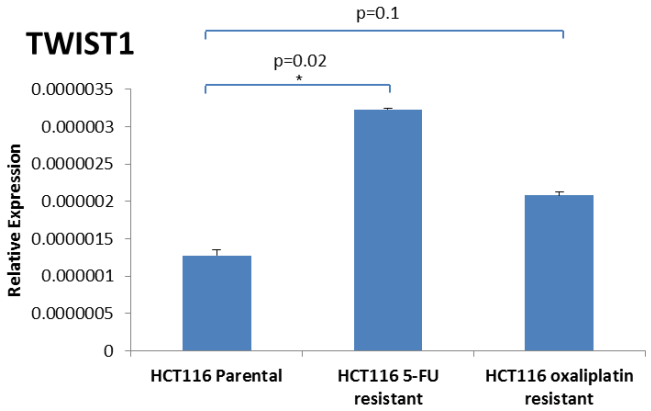

Figure 4.8: ***The expression of EMT genes in 5-FU and oxaliplatin resistant cells.*** *The mRNA expression of* ***A)*** *CDH1 in HCT116 5-FU resistant, oxaliplatin resistant and parental cells,* ***B)*** *CDH1 in DLD-1 5-FU resistant, oxaliplatin resistant and parental cells,* ***C)*** *CDH2 in DLD-1 5-FU resistant, oxaliplatin resistant and parental cells,* ***D)*** *VIM in HCT116 5-FU resistant, oxaliplatin resistant and parental cells and* ***E)*** *TWIST1 in HCT116 5-FU resistant, oxaliplatin resistant and parental cells. Gene expression was relative to the control gene 18S ribosomal RNA and assessed as detailed in Section 2.2.9.4. Each sample was assessed in triplicate and the errors were determined by calculating* $2^{(-\delta Ct + sd\ \delta Ct)}$ *and* $2^{(-\delta Ct - sd\ \delta Ct)}$*, as detailed in section 2.2.9.5. Statistical significance (p≤0.05) was determined by performing independent T-tests.*

To investigate possible changes in cell invasion as a result of acquired drug resistance, a Calbiochem InnoCyte invasion assay was used to model and quantify cancer cell invasion *in vitro*, as described in Section 2.2.7. In both HCT116 and DLD-1 cell line backgrounds, oxaliplatin resistant cells were more invasive than their respective parental cells (HCT116: 2.5-fold; p=0.008; DLD-1: 7.5-fold; p=0.01; Figure 4.9). This is consistent with a study by Yang *et al* (2006) which showed that in oxaliplatin resistant KM12L4 and HT29 colorectal cancer cells showed more migration and invasion compared to their respective parental cells. Surprisingly, however, there were no significant differences in cell invasion

in both 5-FU resistant cells compared to their respective parental cells (HCT116: 0.9-fold; p=0.45; DLD-1: 1.5-fold; p=0.07) , in spite of the predicted phenotypes (Figure 4.9).

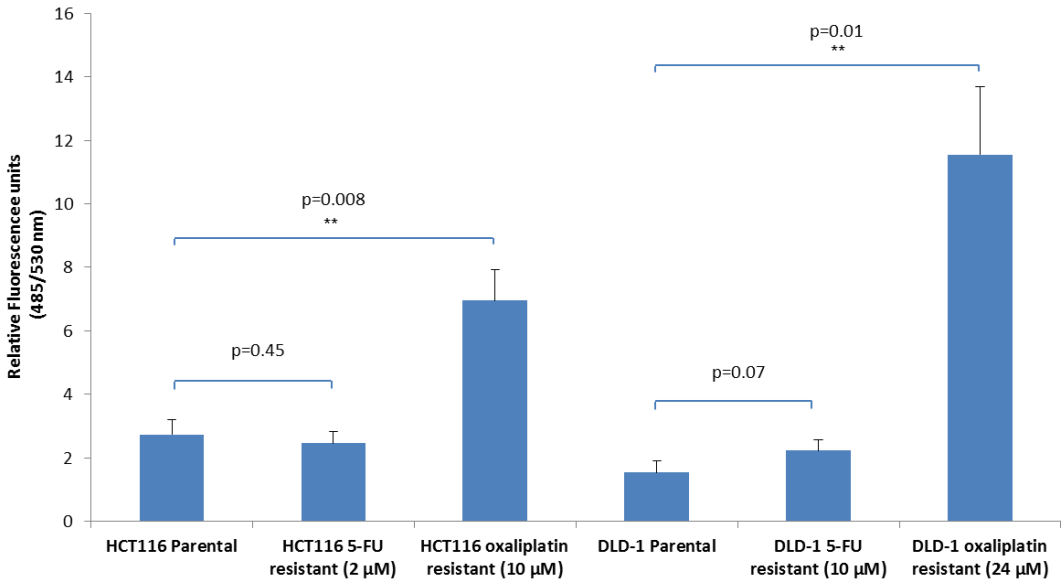

Figure 4.9: The invasiveness of 5-FU and oxaliplatin resistant cells. The *Calbiochem InnoCyte invasion assay was used to model and quantify cancer cell invasion in vitro, as detailed in Section 2.2.7. The invasiveness of 5-FU and oxaliplatin resistant HCT116 and DLD-1 cells was compared to the parental cells. Each sample was analysed in triplicate and errors represent the SEM of three separate experiments. Statistical significance (p≤0.05) was determined by performing independent T-tests.*

4.3.5. The effect of drug resistance on cell proliferation and the cell cycle

We next investigated the effect of 5-FU and oxaliplatin resistance on cell proliferation by flow cytometry using the CellTrace Violet Cell Proliferation Kit as detailed in Section 2.2.14.3. In HCT116 cells, cell doubling time was significantly increased in oxaliplatin resistant cells compared to parental cells (from 25.2

hours to 26.3 hours, p=0.04) over a 96 hour period (Table 4.24). In contrast, the doubling time of 5-FU resistant cells was significantly decreased (from 25.2 hours to 20.9 hours, p=0.0007). Similarly, DLD-1 oxaliplatin resistant cells did not have a significantly different doubling time compared to their parental line (24.2 hours to 25.6 hours, p=0.12; Table 4.24). DLD-1 5-FU resistant cells however doubled at a slower rate compared to parental cells (24.2 hours to 29.8 hours, p=0.008).

Table 4.24: Doubling times of HCT116 and DLD-1 parental cells compared to their respective 5-FU and oxaliplatin resistant cells as determined by the CellTrace Violet Cell Proliferation Kit

Cell line	Doubling time (hours)	p value (compared to respective parental)
HCT116 Parental	25.2 ± 0.11	-
HCT116 oxaliplatin resistant	26.3 ± 0.15	0.004
HCT116 5-FU resistant	20.9 ± 0.44	0.0007
DLD-1 Parental	24.2 ± 0.13	-
DLD-1 oxaliplatin resistant	25.6 ± 0.54	0.12
DLD-1 5-FU resistant	29.8 ± 0.48	0.008

The effect of drug resistance on cell cycle kinetics was then investigated by staining cells with Propidium iodide and analysing DNA content using a flow cytometer, as described in Section 2.2.14.1. Figure 4.10 shows that over 96 hours the HCT116 5-FU resistant cells were arrested in the G0/G1 phase compared to HCT116 parental cells. HCT116 oxaliplatin resistant cells spent less time in the G0/G1 phase compared to parental cells (with the exception of the 72 hour time point) and also compared to the 5-FU resistant cells. These results

suggest, firstly, that HCT116 5-FU resistant cells progress through the cell cycle slower than its drug sensitive parental cells. Secondly, the data presented in Figure 4.10 suggests that oxaliplatin resistant HCT116 cells proliferate at similar or slightly faster rate to HCT116 parental cells and also at a faster rate than 5-FU resistant cells. These observations were not reflected by the proliferation data presented in Table 4.24 and suggest that there is not a direct association between doubling time and cell cycle progression. However, due to time constraints this analysis was only performed once and further studies may shed better light on this relationship.

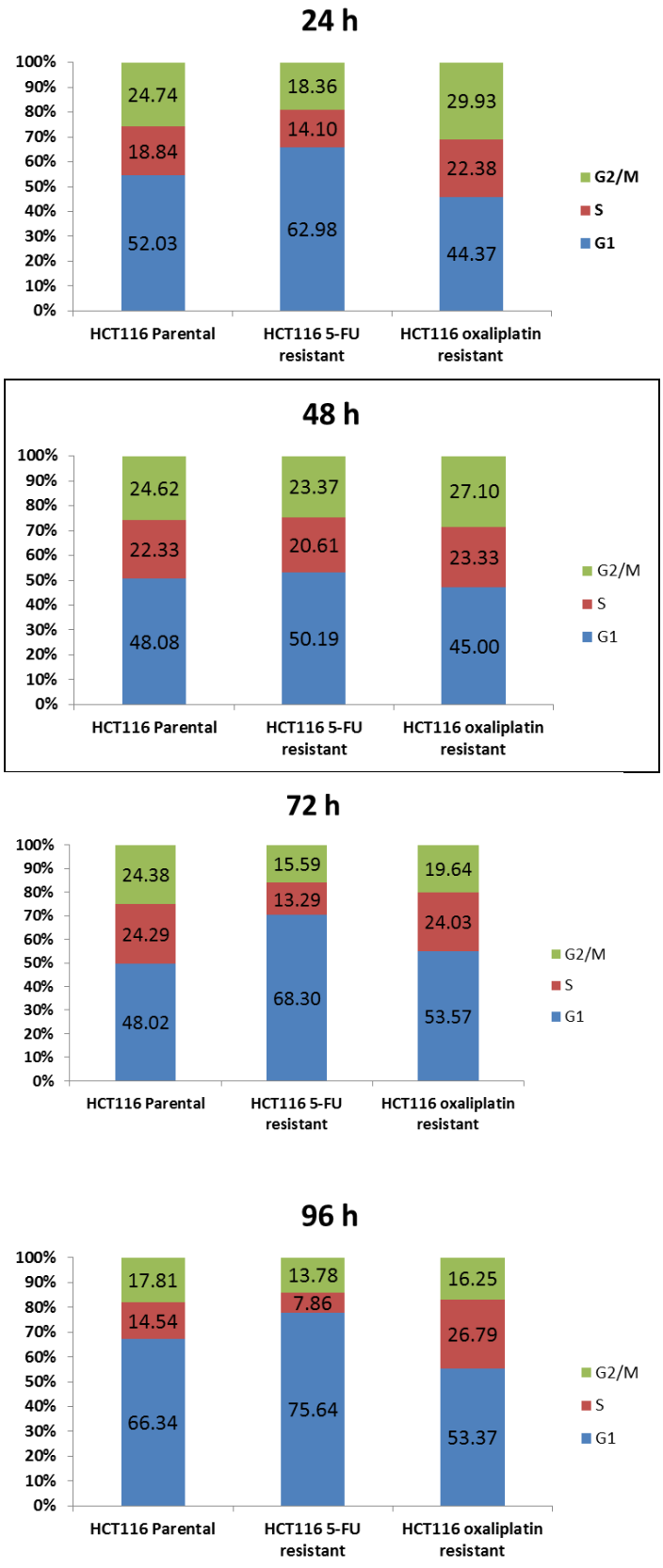
24 h
100%
90%
80%
70%
60%
50%
40%
30%
20%
10%
0%
24.74
18.84
52.03
18.36
14.10
62.98
29.93
22.38
44.37
HCT116 Parental
HCT116 5-FU resistant
HCT116 oxaliplatin resistant
G2/M
S
G1
48 h
24.62
22.33
48.08
23.37
20.61
50.19
27.10
23.33
45.00
72 h
24.38
24.29
48.02
15.59
13.29
68.30
19.64
24.03
53.57
96 h
17.81
14.54
66.34
13.78
7.86
75.64
16.25
26.79
53.37

Figure 4.10

Figure 4.10: ***The cell cycle kinetics of 5-FU and oxaliplatin resistant HCT116 cells.*** *Cells were seeded at a density of 1x10^6 cells per 10 cm diameter plate, harvested at 4 time points over 96 hours and labelled with Propidium iodide. DNA content was then analysed by flow cytometry to determine the percentage of cells in the defined phases of the cell cycle, as described in Section 2.2.14.1. Experiment was performed once.*

Similarly, Figure 4.11 shows that in DLD-1 cells there was an evident arrest in G0/G1 phase in 5-FU resistant cells at 48 and 72 hours. This is reflected in the much slower proliferation of DLD-1 5-FU resistant cells (Table 4.24). There was also a slight arrest at G1 in oxaliplatin resistant cells.

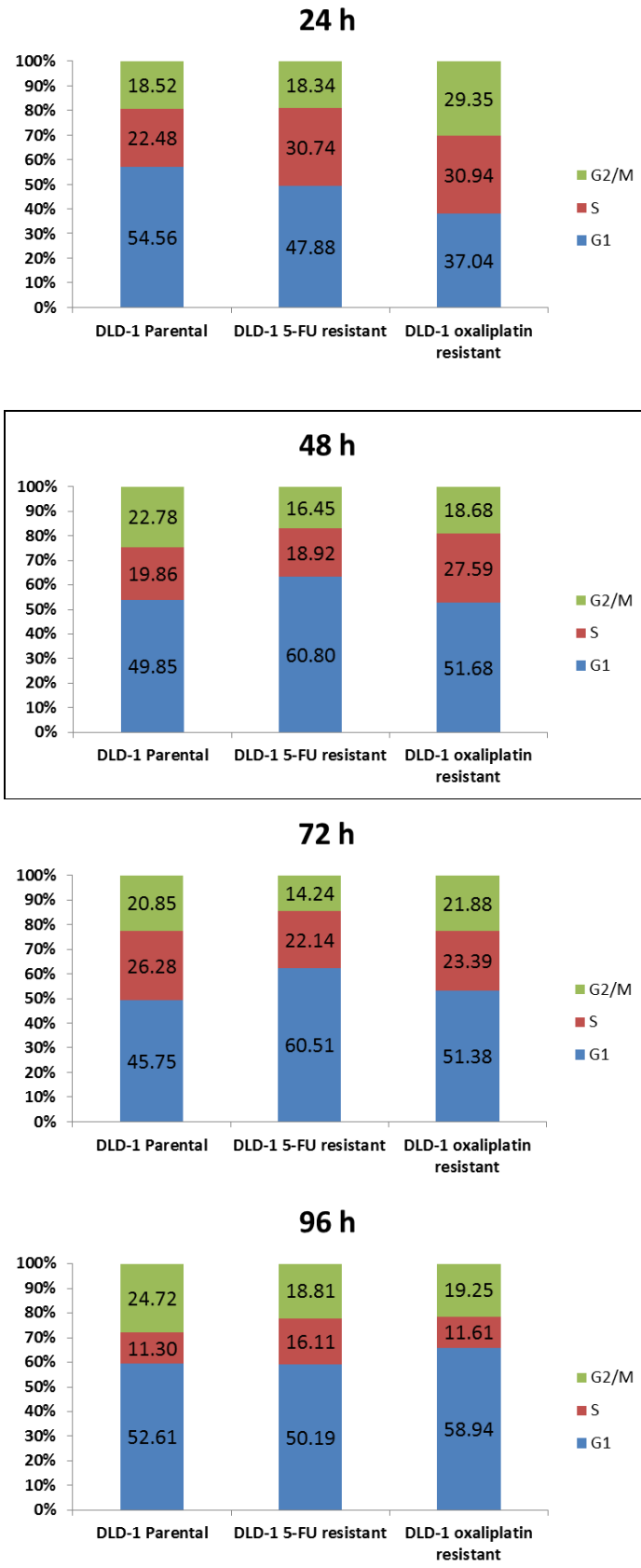
24 h
100%
90%
80%
70%
60%
50%
40%
30%
20%
10%
0%
18.52
22.48
54.56
18.34
30.74
47.88
29.35
30.94
37.04
G2/M
S
G1
DLD-1 Parental
DLD-1 5-FU resistant
DLD-1 oxaliplatin resistant
48 h
22.78
19.86
49.85
16.45
18.92
60.80
18.68
27.59
51.68
72 h
20.85
26.28
45.75
14.24
22.14
60.51
21.88
23.39
51.38
96 h
24.72
11.30
52.61
18.81
16.11
50.19
19.25
11.61
58.94

Figure 4.11

Figure 4.11: ***The cell cycle kinetics of 5-FU and oxaliplatin resistant DLD-1 cells.*** *Cells were seeded at a density of 1x10^6 cells per 10 cm diameter plate, harvested at 4 time points over 96 hours and labelled with Propidium iodide. DNA content was then analysed by flow cytometry to determine the percentage of cells in the defined phases of the cell cycle, as described in Section 2.2.14.1. Experiment was performed once.*

In collaboration with Professor Julian Blow and colleagues (University of Dundee), we next sought to distinguish between cells that were in G0 and therefore quiescent and cells that were in G1. This was determined by using flow cytometry to determine DNA content and plotting these results against levels of chromatin-bound MCM2. MCM2 is a minichromosome maintenance protein which plays an essential role in the initiation of eukaryotic DNA replication and binds with chromatin (Kearsey & Labib, 1998). MCM proteins are licensing factors that allows for DNA replication to be initiated and ensures that DNA is replicated only once during the cell cycle (Kearsey & Labib, 1998). Therefore in this assay, cells that were in the G1 phase, as determined by analysing DNA content, and also had low levels of chromatin-bound MCM2 were considered to be in G0 whereas cells showing intermediate or high levels of MCM2 where considered to be in G1.

Figure 4.12 independently suggested that there was a greater proportion of HCT116 5-FU resistant cells in G1 (51.3%) compared to HCT116 parental cells (48.5%) and HCT116 oxaliplatin resistant cells (47.7%; Figure 4.11). In DLD-1 cells, there was a marked increase in G1 arrest in 5-FU resistant cells (61%) compared to parental (44.5%) and oxaliplatin resistant cells (43.6%), consistent with the data presented in Figure 4.11.

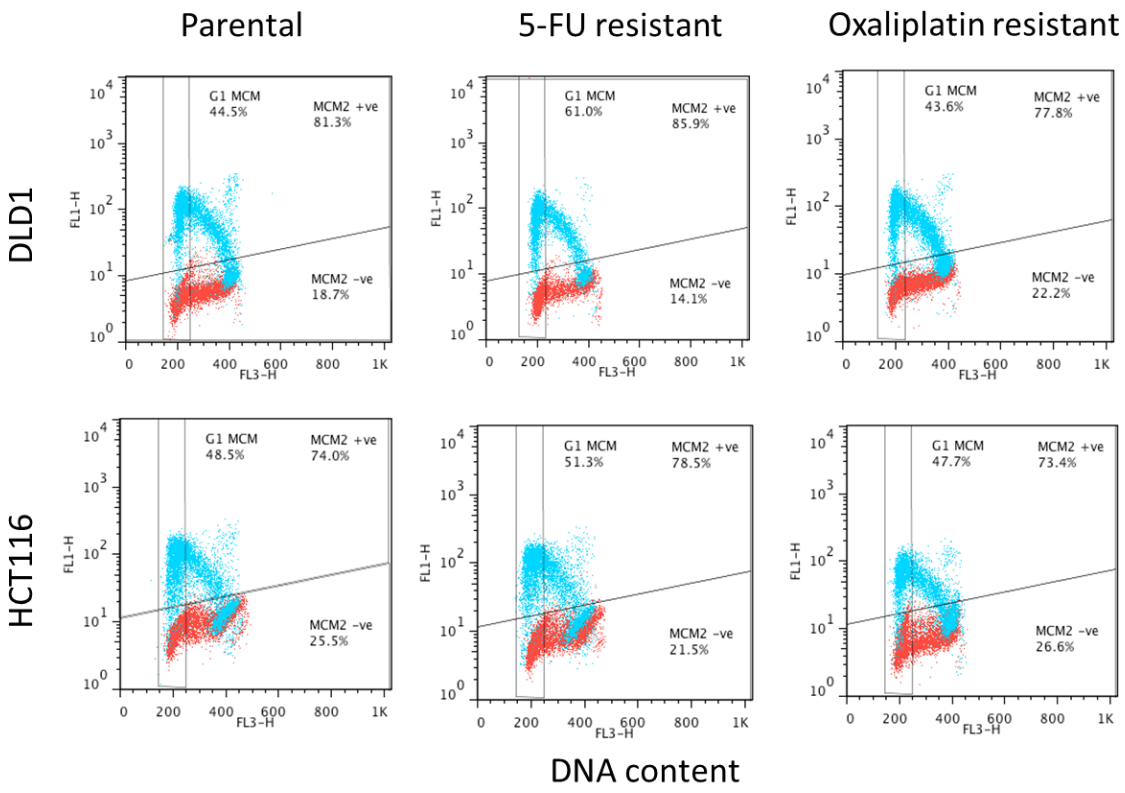

Figure 4.12: ***The cell cycle kinetics and MCM2 loading profile of 5-FU and oxaliplatin resistant HCT116 and DLD-1 cells.*** *Cells were labelled with Propidium iodide and fluorescently tagged MCM2 antibody. DNA content and MCM2 was then analysed by flow cytometry to determine the percentage of cells in the defined phases of the cell cycle, as described in Section 2.2.14.1. Experiment was performed once.*

Figure 4.13 shows that when cells in phase G1 were gated and plotted against MCM2 levels, the proportion of MCM2-positive cells in G1 did not significantly change between HCT116 parental cells (93.8%) and 5-FU (94.4%) and oxaliplatin resistant cells (93.8%; Figure 4.13 A). The same observation was noted in DLD-1 parental cells (96.6%) compared to 5-FU (97.9%) and oxaliplatin resistant cells (96.6%; Figure 4.13 B). This suggests that the G0/G1 arrest highlighted in HCT116 and DLD-1 5-FU resistant cells are unlikely to be due to a tendency for the cells to enter G0.

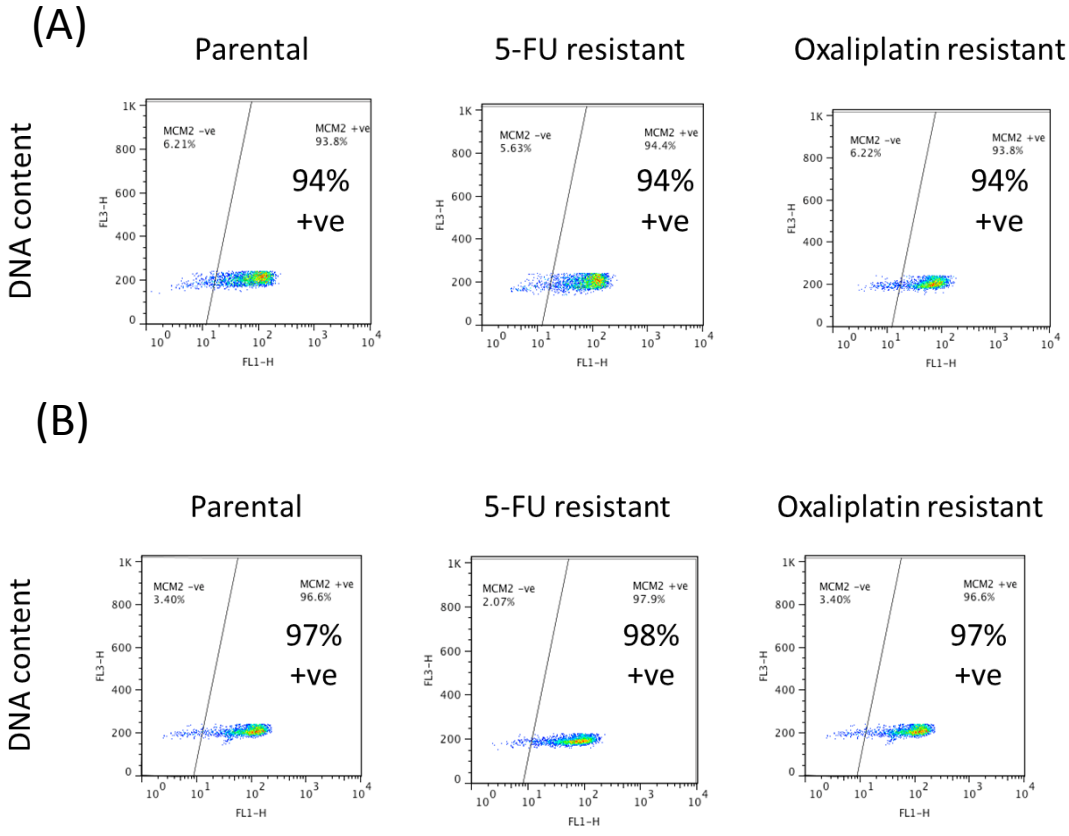

Figure 4.13: ***The cell cycle kinetics and MCM2 loading profile of 5-FU and oxaliplatin resistant HCT116 and DLD-1 cells. A)*** *HCT116 and* ***B)*** *DLD-1 cells were labelled with Propidium iodide and fluorescently tagged MCM2 antibody and then analysed by flow cytometry to determine the percentage of cells in the defined phases of the cell cycle, as described in Section 2.2.14.1. The DNA content of cells in G0/G1 phase was then plotted against MCM2 levels to determine the proportion of cells in G0 in comparison to cells in G1. Experiment was performed once.*

It was speculated that the increase in G1 arrest in 5-FU resistant HCT116 and DLD-1 cells may therefore be due to a delay in the commitment of cells entering late G1. The $p21^{cip21}$ protein is a cyclin dependent kinase (CDK) inhibitor which functions as a cell cycle regulator particularly in the transition from early to mid-phase G1 to late G1/S phase. It is able to cause cell cycle arrest in response to DNA damage or other types of stress if their levels are increased.

Taqman qRT-PCR analysis was performed to assess the expression of *CDKN1A*, the gene that codes $p21^{cip21}$, in the drug resistant cells compared to their respective parental cells. *CDKN1A* expression was significantly increased (1.68 fold; p=0.001) in HCT116 5-FU resistant cells compared to HCT116 parental cells. There was no significant difference in *CDKN1A* expression between HCT116 parental cells and HCT116 oxaliplatin resistant cells (p=0.1; Figure 4.14 A). This increase in p21 is consistent with the cell cycle kinetics showing that HCT116 5-FU resistant cells spend longer in G1. *CDNK1A* expression was significantly increased in DLD-1 5-FU resistant cells (6.3 fold; p=0.03) compared to parental cells and also significantly increased in DLD-1 oxaliplatin resistant cells (28.8 fold; p=0.04). Whilst the cell cycle kinetics and *CDNK1A* expression is consistent in DLD-5-FU resistant cells, this is not the case in DLD-1 oxaliplatin resistant cells. However, this could be a reflection of DLD-1 harbouring mutant p53 and thus not reflecting a normal p53 response to cellular stress whereas HCT116 has WT p53.

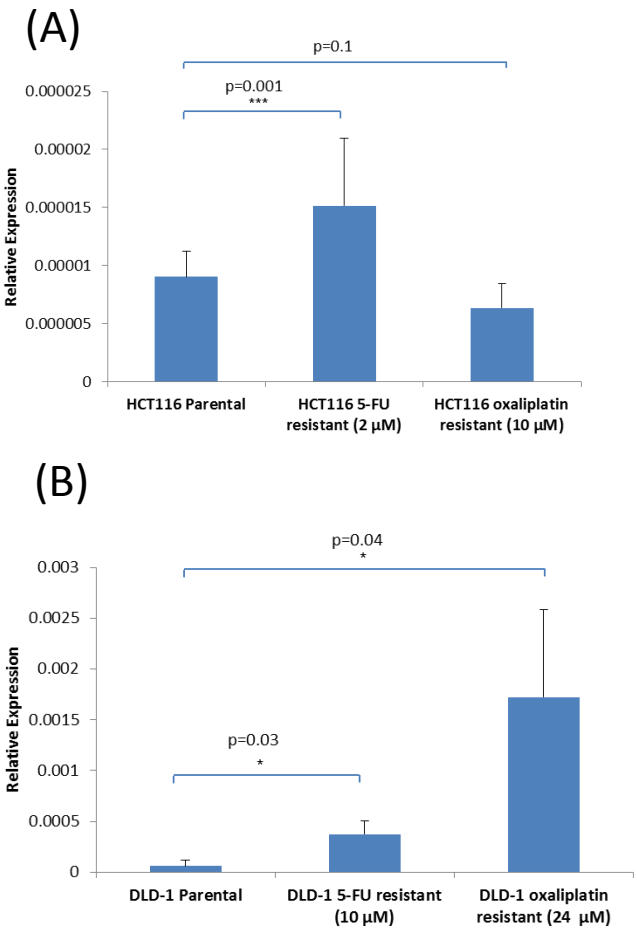

Figure 4.14: ***The expression of CDKN1A in 5-FU and oxaliplatin resistant cells.*** *The expression of CDKN1A was assessed, relative to the control gene 18S ribosomal RNA, in* ***A)*** *HCT116 5-FU resistant, oxaliplatin resistant and parental cells and* ***B)*** *DLD-1 5-FU resistant, oxaliplatin resistant and parental cells, as detailed in section 2.2.9.4. Each sample was assessed in triplicate and the errors were determined by calculating* $2^{(-\delta Ct + sd\ \delta Ct)}$ *and* $2^{(-\delta Ct - sd\ \delta Ct)}$*, as detailed in section 2.2.9.5. Statistical significance* ($p \leq 0.05$) *was determined by performing independent T-tests.*

4.3.6. The relationship between cancer cell glycolysis and drug resistance

Tables 4.2 - 4.5 show that genes coding for enzymes involved in glycolysis are amongst the top 20 differentially over and under-expressed genes in HCT116 and DLD-1 drug resistant cells. In particular, we show that *PGAM1* (phosphoglycerate mutase) was under-expressed in HCT116 5-FU resistant cells

(11.05-fold), DLD-1 5-FU resistant cells (31.64-fold) and DLD-1 oxaliplatin resistant cells (37.84-fold). *ALDOA* (Aldolase A), another enzyme involved in glycolysis, was under-expressed in HCT116 5-FU resistant cells (21.25-fold) and DLD-1 5-FU resistant cells (31.6-fold).

Therefore to explore the effect of acquired drug resistance on cell glycolysis, the Seahorse Bioanalyser and XF glycolysis stress test kit was used to investigate the extracellular acidification rate (ECAR) in response to glucose in DLD-1 parental and drug resistant cells as described Section 2.2.15.

Following the injection of glucose, the ECAR was increased 5-fold from baseline (100%) to 500% in DLD-1 parental cells at the first measurement (44 minutes; Figure 4.15). The fold change in ECAR was lower in 5-FU resistant cells (4-fold) and oxaliplatin resistant cells (3.5-fold). This suggests that 5-FU and oxaliplatin resistant cells lower their glycolytic activity which is consistent with the marked under-expression of glycolytic enzymes such as PGAM1 and ALDOA. However this is very preliminary data and further studies would be required to better understand this relationship.

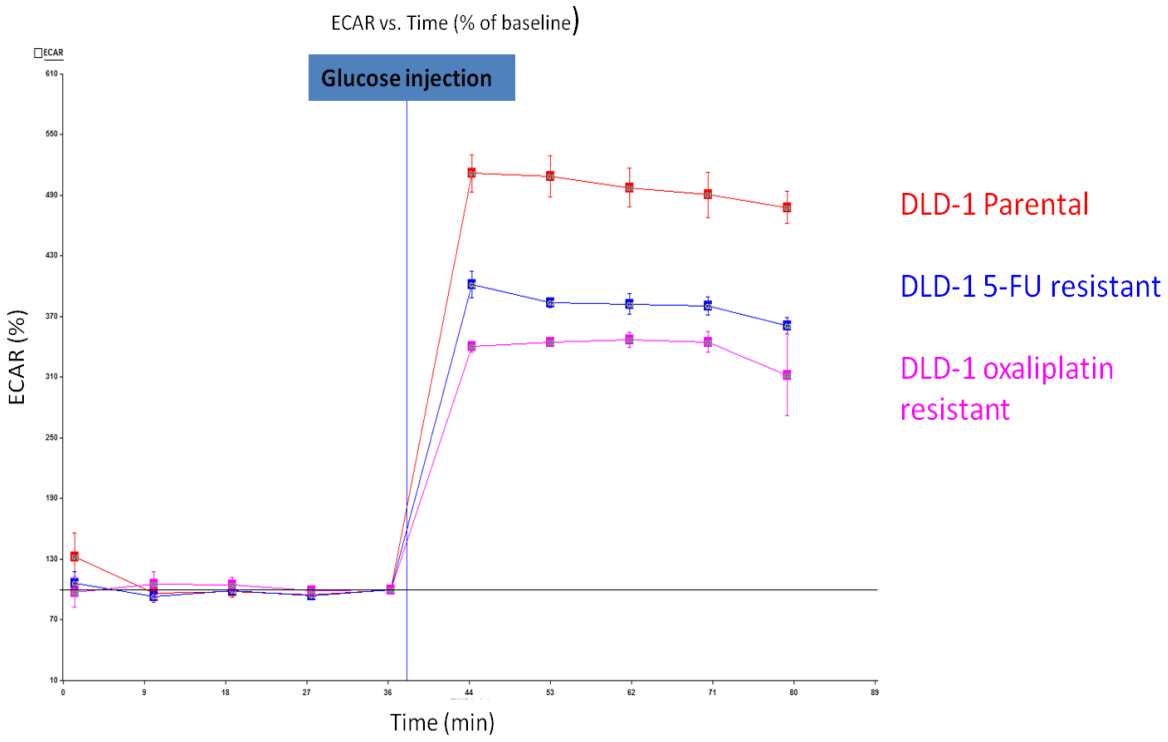

Figure 4.15: ***The ECAR of DLD-1 parental and drug resistant cells in response to glucose.*** *The Seahorse Bioanalyser and XF glycolysis stress test kit was used to compare the ECAR of DLD-1 parental, 5-FU resistant and oxaliplatin resistant cells in response to 20 µM glucose, as described in Section 2.2.15. The blue horizontal line indicates the point at which glucose was injected. Experiment was performed once.*

4.3.7. Signalling pathways affected by 5-FU and oxaliplatin resistance

To investigate the effect of 5-FU and oxaliplatin resistance in HCT116 and DLD-1 cells on downstream signalling pathways, a PathScan intracellular signalling array which detects the phosphorylation or cleavage of 18 well characterised signalling molecules was used as described in Section 2.2.13.

In the HCT116 cell line background, the acquisition of 5-FU and oxaliplatin resistance led to a decrease in the phosphorylation of ERK 1/2, p70 S6 kinase, and PRAS40 and a decreased cleavage of PARP (Figure 4.16; Figure 4.17). HCT116 5-FU resistant cells showed a decrease in the phosphorylation of Stat3 and S6 (Figure 4.16) whereas in HCT116 oxaliplatin resistant cells, there was a decreased phosphorylation of the pro-apoptotic protein Bad and an increased phosphorylation of p53 at serine 15 (Figure 4.17).

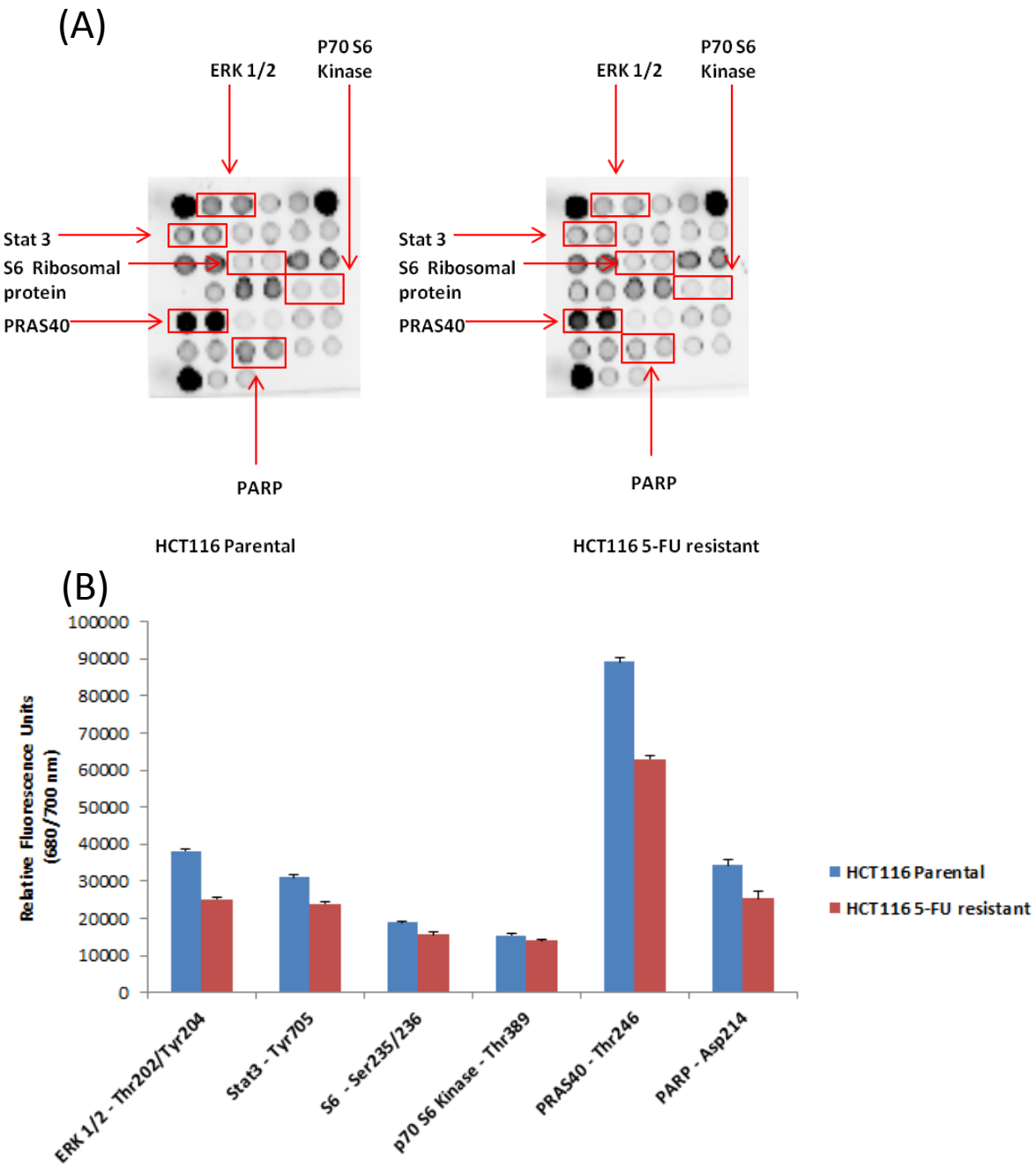

Figure 4.16: ***Signalling pathways affected by 5-FU resistance in HCT116 cells.*** ***A)*** *The PathScan intracellular signalling array and LiCor Odyssey fluorescence imaging system was used to assess the effect of 5-FU resistance in HCT116 cells on the phosphorylation or cleavage of 18 signalling molecules compared to HCT116 parental cells as detailed in Section 2.2.13. Each signalling molecule is represented in duplicate.* ***B)*** *The fluorescent signals at wavelength 680/700 nm as determined by LiCor Image Studio are represented graphically. Experiment was performed once and error bars represent the technical replictates.*

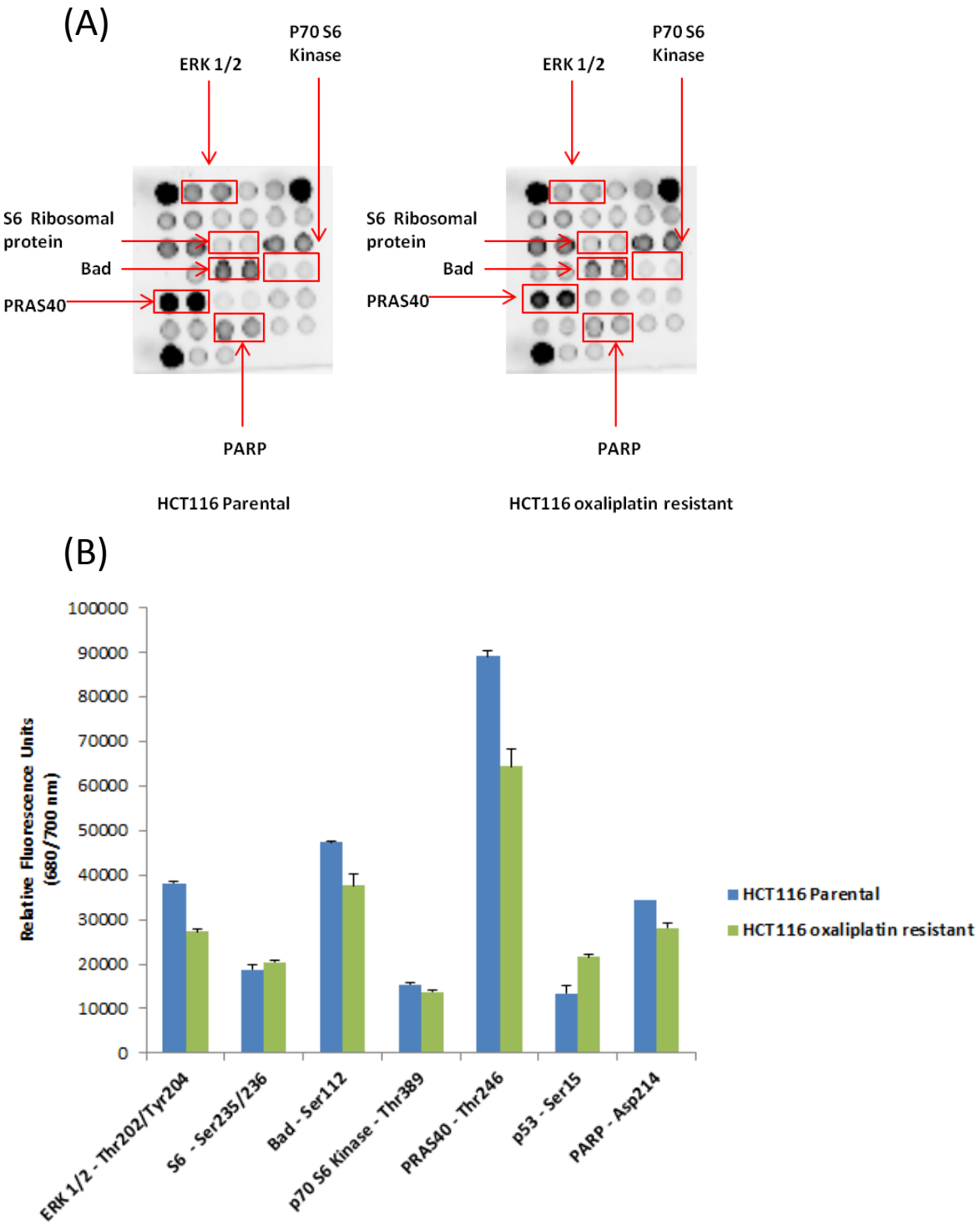
(A)
ERK 1/2
P70 S6 Kinase
S6 Ribosomal protein
Bad
PRAS40
PARP
HCT116 Parental
HCT116 oxaliplatin resistant
(B)
Relative Fluorescence Units (680/700 nm)
100000
90000
80000
70000
60000
50000
40000
30000
20000
10000
0
ERK 1/2 - Thr202/Tyr204
S6 - Ser235/236
Bad - Ser112
p70 S6 Kinase - Thr389
PRAS40 - Thr246
p53 - Ser15
PARP - Asp214
HCT116 Parental
HCT116 oxaliplatin resistant

Figure 4.17

Figure 4.17: ***Signalling pathways affected by oxaliplatin resistance in HCT116 cells.*** ***A)*** *The PathScan intracellular signalling array and LiCor Odyssey fluorescence imaging system was used to assess the effect of oxaliplatin resistance in HCT116 cells on the phosphorylation or cleavage of 18 signalling molecules compared to HCT116 parental cells as detailed in Section 2.2.13. Each signalling molecule is represented in duplicate.* ***B)*** *The fluorescent signals at wavelength 680/700 nm as determined by LiCor Image Studio are represented graphically. Experiment was performed once and error bars represent the technical replictates.*

Interestingly, in the DLD-1 cell line background, 5-FU and oxaliplatin resistance affected distinctly different pathways. In response to DLD-1 5-FU resistance there was a decrease in the phosphorylation of Stat1 but an increase in the phosphorylation of S6 ribosomal protein and PRAS40 (Figure 4.18). In contrast, in DLD-1 oxaliplatin resistant cells, there was a decrease in the phosphorylation of AMPK, mTOR, HSP27, Bad, PRAS40, p38 and SAPK/JNK and a decreased cleavage of caspase 3 (Figure 4.19).

This suggests that HCT116 and DLD-1 cells develop resistance to 5-FU and oxaliplatin by affecting different signalling pathways. Intriguingly, the data suggests that in HCT116 cells the development of 5-FU and oxaliplatin may be mediated by similar pathways whereas 5-FU and oxaliplatin resistance in DLD-1 cells may be mediated by very different pathways. This could be part of the reason why there was no cross-resistance to 5-FU and oxaliplatin in DLD-1 oxaliplatin and DLD-1 5-FU resistant cells and *vice versa*, and why there was cross-resistance to 5-FU in HCT116 oxaliplatin resistant cells (Section 4.3.1). Thus this analysis identifies potential signalling molecules and pathways that could be investigated further using Western blots.

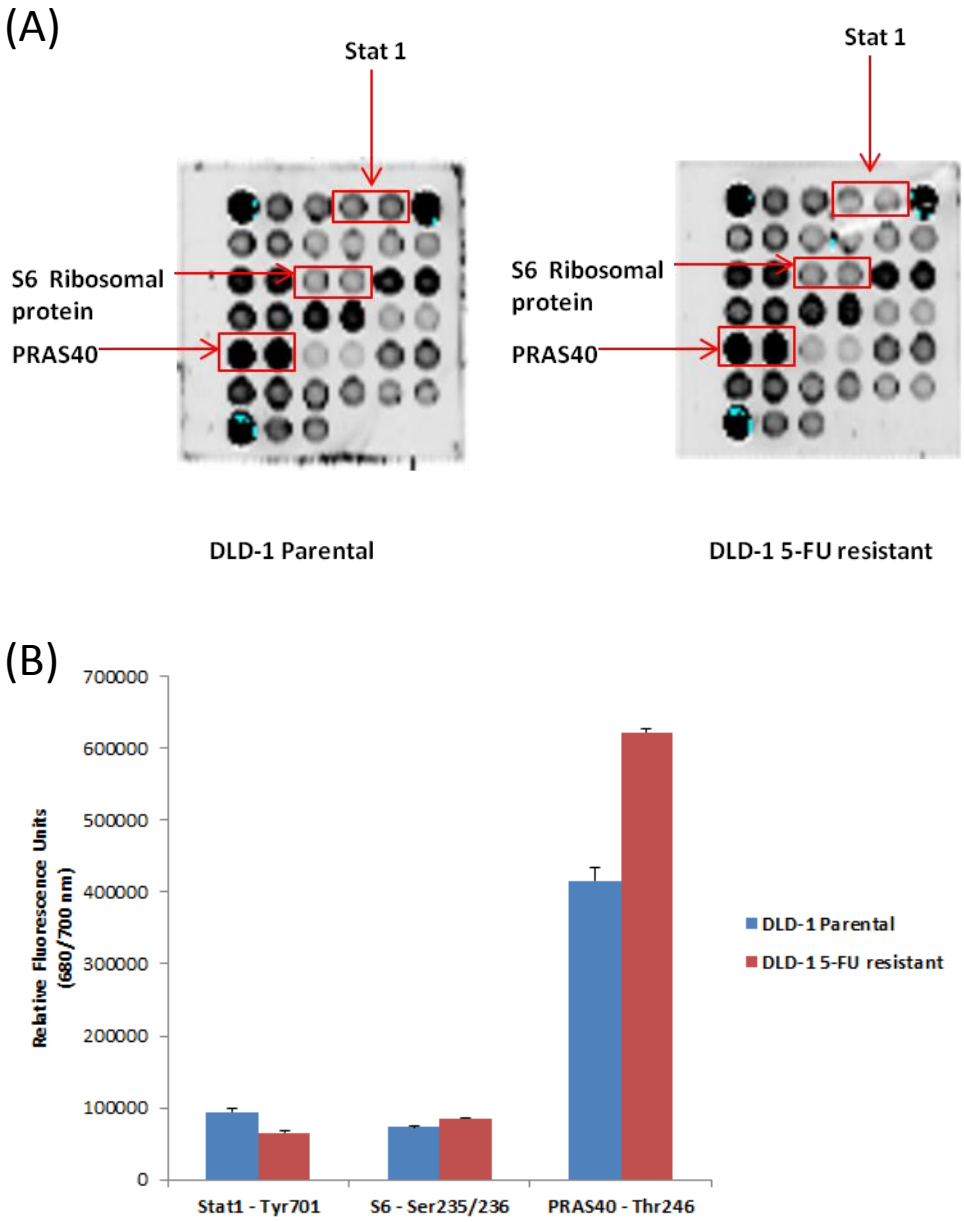

Figure 4.18: ***Signalling pathways affected by 5-FU resistance in DLD-1 cells.*** ***A)*** *The PathScan intracellular signalling array and LiCor Odyssey fluorescence imaging system was used to assess the effect of 5-FU resistance in DLD-1 cells on the phosphorylation or cleavage of 18 signalling molecules compared to DLD-1 parental cells as detailed in Section 2.2.13. Each signalling molecule is represented in duplicate.* ***B)*** *The fluorescent signals at wavelength 680/700 nm as determined by LiCor Image Studio are represented graphically. Experiment was performed once and error bars represent the technical replictates.*

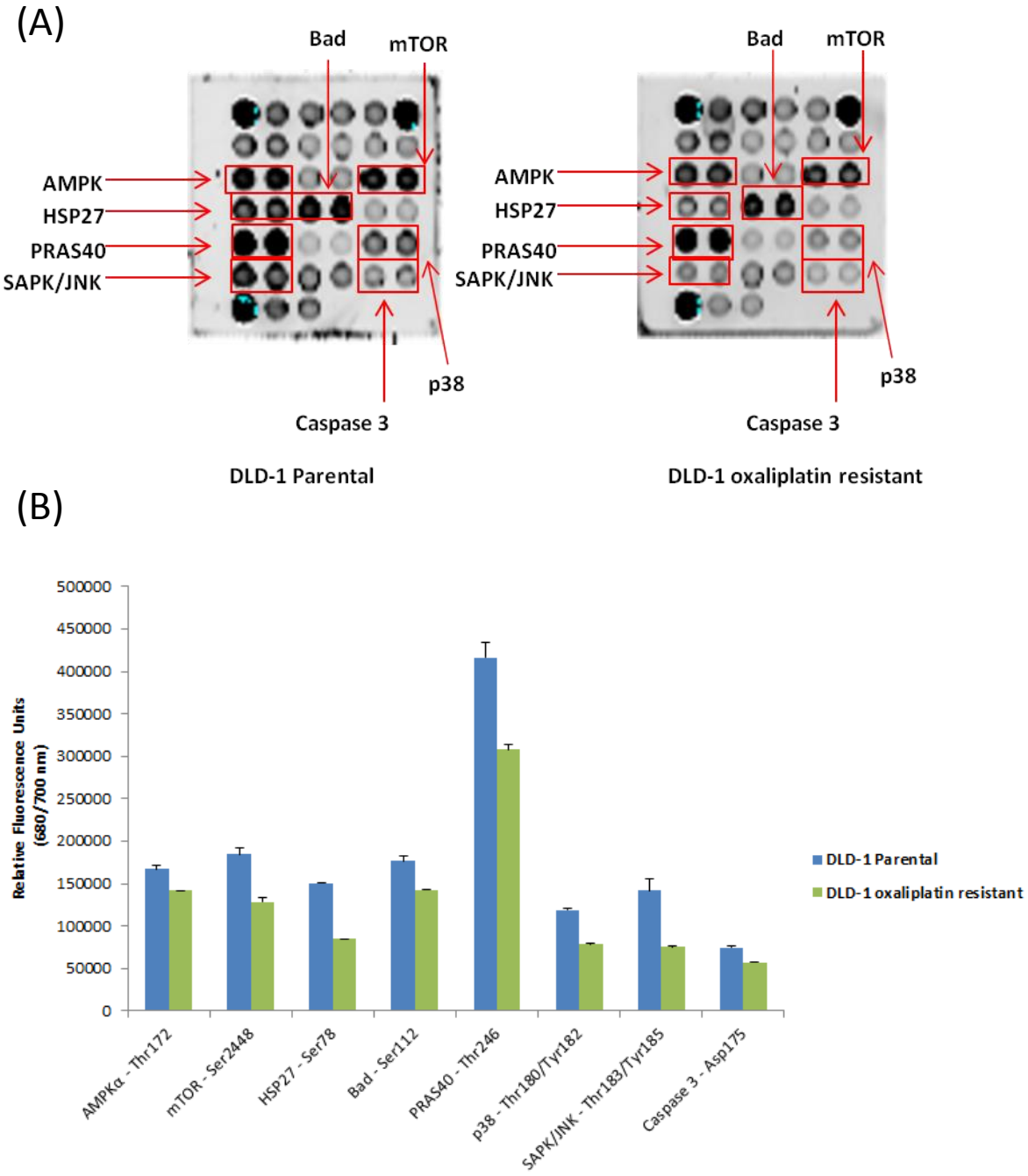

Figure 4.19: ***Signalling pathways affected by oxaliplatin resistance in DLD-1 cells.*** ***A)*** *The PathScan intracellular signalling array and LiCor Odyssey fluorescence imaging system was used to assess the effect of oxaliplatin resistance in DLD-1 cells on the phosphorylation or cleavage of 18 signalling molecules compared to DLD-1 parental cells as detailed in Section 2.2.13. Each signalling molecule is represented in duplicate.* ***B)*** *The fluorescent signals at wavelength 680/700 nm as determined by LiCor Image Studio are represented graphically. Experiment was performed once and error bars represent the technical replictates.*

4.3.8. The effect of drug resistance on drug metabolism genes

Having explored the drug resistance phenotypes predicted from our bioinformatics data, we next investigated whether HCT116 and DLD-1 cells developed resistance to 5-FU or oxaliplatin by affecting the gene expression of 5-FU metabolising enzymes and DNA repair proteins.

The expression of *TYMS*, *TYMP* and *DPYD* was assessed in HCT116 and DLD-1 5-FU and oxaliplatin resistant cells compared to their respective drug sensitive parental cells using Taqman qRT-PCR analysis as described in Section 2.2.9.4. The expression of *TYMP* was significantly increased in HCT116 5-FU resistant (1.4 fold, p=0.013) and oxaliplatin resistant (2.5 fold, p=0.001) compared to HCT116 parental cells (Figure 4.20 A). *TYMP* was not expressed in DLD-1 cells (data not shown).

In HCT116 cells, *TYMS* expression levels were decreased in 5-FU resistant cells (3.4 fold; $p=6.4x10^{-5}$) and to a lesser extent also decreased in oxaliplatin resistant cells (1.5 fold, p=0.0003; Figure 4.20 B). Similarly, *TYMS* expression was significantly decreased in both DLD-1 5FU resistant (5.4 fold; $p=1.6x10^{-5}$) and oxaliplatin resistant (4.2 fold; $p=2.6x10^{-6}$) cells (Figure 4.20 C). These results were unexpected as the overexpression of *TYMS* and under-expression of *TYMP* has been associated with a 5-FU resistant phenotype in patients (Goto *et al*, 2012). *DPYD* expression was as expected increased in 5-FU resistant HCT116 cells (1.9 fold, p=0.0027) and in oxaliplatin resistant cells (1.3 fold, p=0.03; Figure

4.20 D). *DPYD* was not expressed in DLD-1 cells (data not shown). Further protein expression experiments would help to confirm these results.

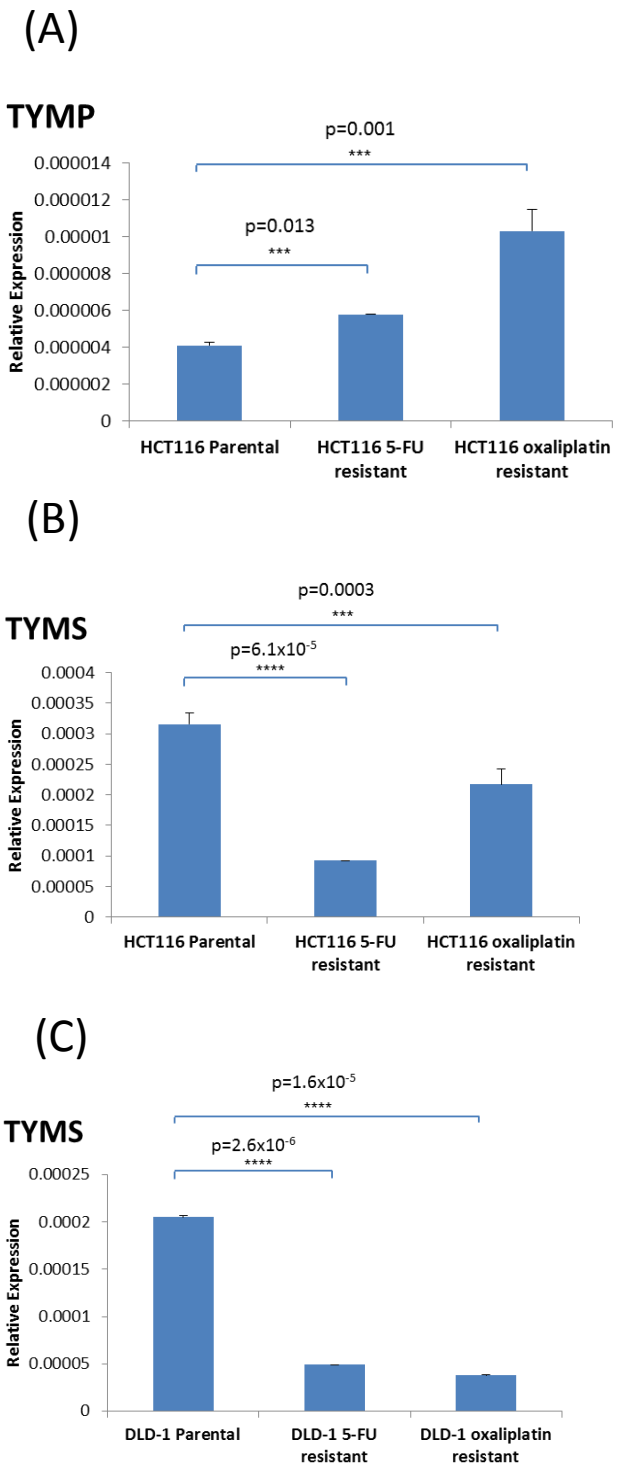

Figure 4.20

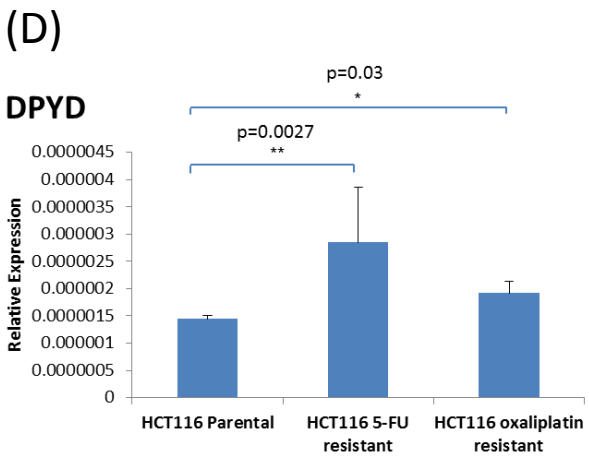

Figure 4.20: ***The expression of 5-FU drug metabolising enzymes in 5-FU and oxaliplatin resistant cells.*** *The mRNA expression of* ***A)*** *TYMP in HCT116 5-FU resistant, oxaliplatin resistant and parental cells, TYMS in* ***B)*** *HCT116 5-FU resistant, oxaliplatin resistant and parental cells and in* ***C)*** *DLD-1 5-FU resistant, oxaliplatin resistant and parental cells and* ***D)*** *DPYD in HCT116 5-FU resistant, oxaliplatin resistant and parental cells was assessed, relative to the control gene 18S ribosomal RNA, as detailed in Section 2.2.9.4. Each sample was assessed in triplicate and the errors were determined by calculating* $2^{(-\delta Ct + sd\ \delta Ct)}$ *and* $2^{(-\delta Ct - sd\ \delta Ct)}$*, as detailed in Section 2.2.9.5. Statistical significance (p≤0.05) was determined by performing independent T-tests.*

The expression of *ERCC1* and *TOPO1* was also assessed in HCT116 and DLD-1 drug resistant and parental cells by Taqman qRT-PCR analysis. *ERCC1* expression was unchanged in HCT116 5-FU resistant cells and increased in oxaliplatin resistant cells (2.3 fold; p=0.02; Figure 4.21 A). Similarly, in DLD-1 cells the expression of *ERCC1* was increased in 5-FU resistant cells (1.4 fold; p=0.002) and oxaliplatin resistant cells (2.1 fold. p=0.0006; Figure 4.21 B), consistent with the findings of Seetharam *et al* (2010).

TOPO1 expression was increased in both HCT116 5-FU and oxaliplatin resistant cells compared to their drug sensitive parental cells (Figure 4.21 C). Conversely, consistent with our Illumina microarray data analysis (Appendix J, Table J3 and

J4), *TOPO1* expression was decreased in both DLD-1 5-FU and oxaliplatin resistant cells compared to their parental cells (Figure 4.21 D). Future work would, once again, be directed towards performing Western blots to assess relative protein expression of ERCC1 and TOPO1 in the drug resistant cell lines compared to their parental cells.

(A)

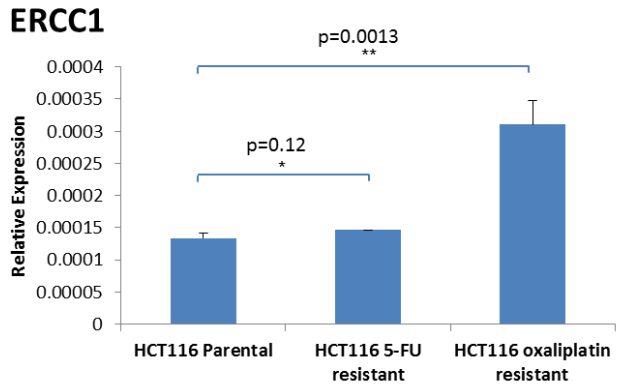

(B)

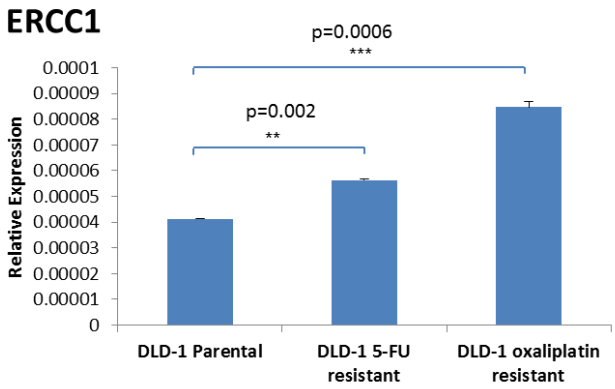

Figure 4.21

(C)

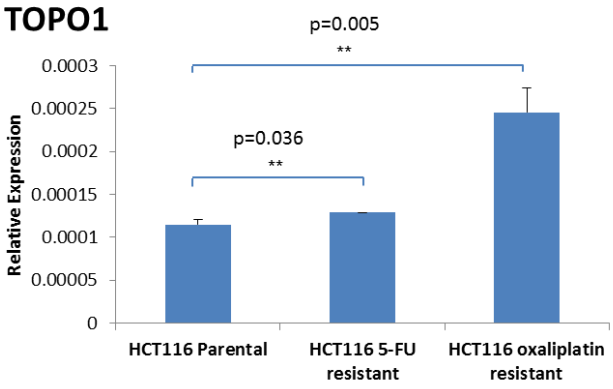

(D)

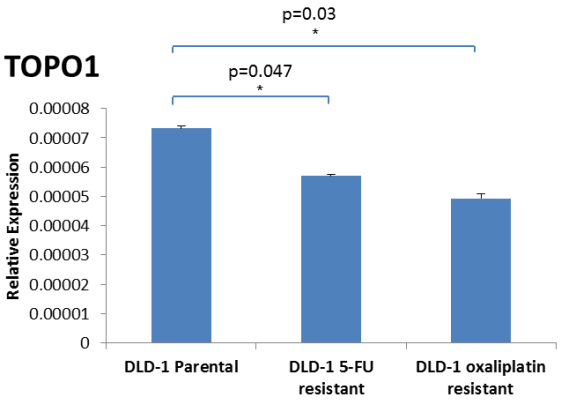

Figure 4.21: The expression of ERCC1 and TOPO1 in 5-FU and oxaliplatin resistant cells. *The mRNA expression of in ERCC1* ***A)*** *HCT116 5-FU resistant, oxaliplatin resistant and parental cells and* ***B)*** *DLD-1 5-FU resistant, oxaliplatin resistant and parental cells and TOPO1 in* ***C)*** *HCT116 5-FU resistant, oxaliplatin resistant and parental cells and* ***D)*** *DLD-1 5-FU resistant, oxaliplatin resistant and parental cells was assessed, relative to the control gene 18S ribosomal RNA, as detailed in Section 2.2.9.4. Each sample was assessed in triplicate and the errors were determined by calculating* $2^{(-\delta Ct + sd\ \delta Ct)}$ *and* $2^{(-\delta Ct - sd\ \delta Ct)}$*, as detailed in Section 2.2.9.5. Statistical significance (p≤0.05) was determined by performing independent T-tests.*

4.3.9. The expression of miR-224 in 5-FU and oxaliplatin resistant cells

Chapter 3 discussed the role of miR-224 in promoting tumorigenesis and metastasis in colorectal cancer. I also discussed how miR-224 modulates 5-FU

sensitivity possibly through the regulation of KRAS pathways or by affecting the expression of 5-FU metabolising enzymes.

The present study therefore investigated how acquired 5-FU or oxaliplatin resistance would affect miR-224 expression. The expression of miR-224 was compared in 5-FU and oxaliplatin resistant HCT116 and DLD-1 cells and their respective drug sensitive parental cells.

MiR-224 was initially eliminated from the analysis presented in Tables 4.16 – 4.19 as TLDA analysis suggested that the miR-224 had a CT value greater than 35 in 5-FU and oxaliplatin resistant cell lines whereas miR-224 expression was marked as 'undetermined' or unexpressed in DLD-1 5-FU and oxaliplatin resistant cells.

Single-probe qRT-PCR Taqman analysis showed that miR-224 expression was significantly decreased in HCT116 5-FU resistant (2.9-fold, p=0.001), HCT116 oxaliplatin resistant cells (2.7-fold, p=0.002) compared to HCT116 parental cells. The expression of miR-224 was also significantly decreased in DLD-1 5-FU resistant (5.9-fold, p=0.0002) and oxaliplatin resistant cells (6.1-fold, p=0.0002 Figure 4.22).

Rossi *et al* (2007) have previously reported decreased expression of miR-224 in HCT116 and HT29 colorectal cancer cells following treatment with 10 μM 5-FU for 6 days. MiR-224 expression has also been shown to be decreased in methotrexate resistant HT29 cells (Mencia *et al*, 2011). This suggests that under-

expression of miR-224 may be involved in stress-response and resistance mechanisms to a number of chemotherapeutic drugs.

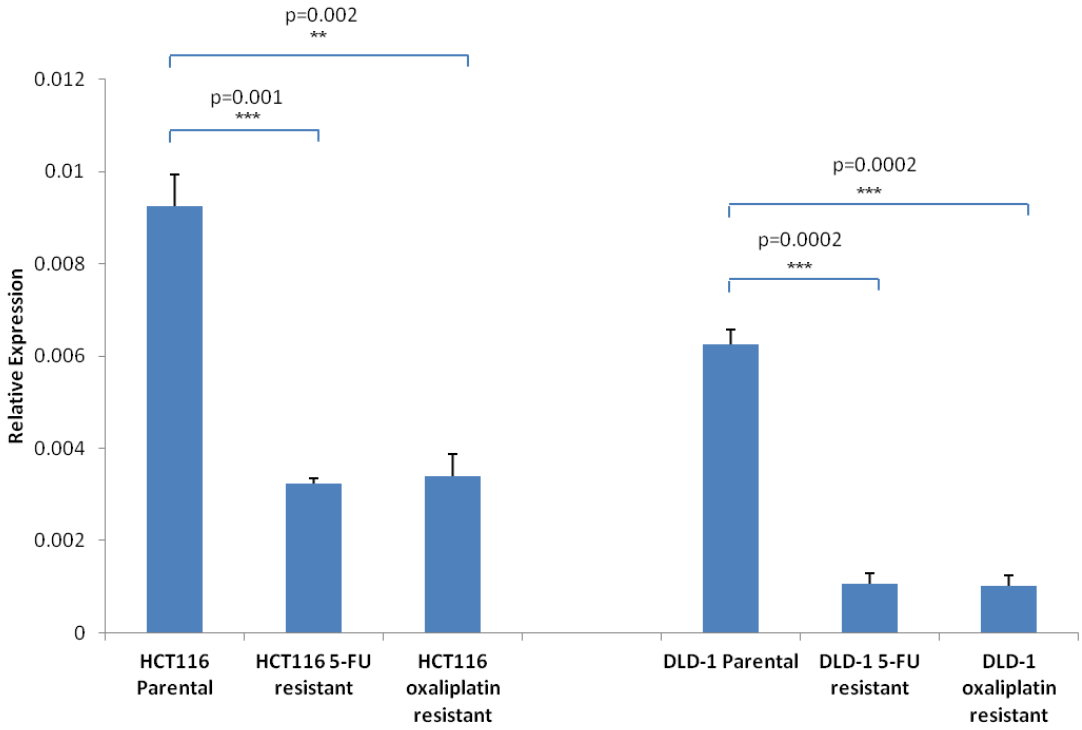

Figure 4.22: ***The expression of miR-224 in 5-FU and oxaliplatin resistant cells.*** *The expression of miR-224, relative to the control U6, was assessed in HCT116 5-FU and oxaliplatin resistant cells compared to HCT116 parental cells and in DLD-1 5-FU and oxaliplatin resistant cells compared to DLD-1 parental cells as detailed in Section 2.2.9.2. Each sample was assessed in triplicate and the errors were determined by calculating* $2^{(-\delta Ct + sd\ \delta Ct)}$ *and* $2^{(-\delta Ct - sd\ \delta Ct)}$*, as detailed in Section 2.2.9.5. Statistical significance (p≤0.05) was determined by performing independent T-tests.*

4.4. Discussion

The aim of the present study was to generate 5-FU and oxaliplatin resistant colorectal cancer cell lines and to use miRNA and mRNA expression profiling to identify 5-FU, oxaliplatin or common drug resistant signatures and predict mechanisms of drug resistance.

In the present study, we have established using MTT cytotoxicity assays that all drug resistant cells were resistant to their selection drug. Additionally, we have shown that HCT116 oxaliplatin resistant cells were also cross-resistant to 5-FU whereas neither DLD-1 drug resistant cell line showed cross-resistance. We also show that both 5-FU and oxaliplatin resistant DLD-1 cells were not cross-resistant to irinotecan. Chemosensitivity to irinotecan in 5-FU and oxaliplatin resistant HCT116 cells was not assessed in the present study. However, it is interesting that previous studies have shown cross-resistance to irinotecan in HCT116 oxaliplatin resistant cells (Gourdier *et al*, 2002) and HCT116 5-FU resistant cells (Boyer *et al*, 2004).

HCT116 cells were also more sensitive to 5-FU and oxaliplatin (2 µM 5-FU and 10 µM oxaliplatin) than DLD-1 cells (10 µM 5-FU and 24 µM oxaliplatin). The two cell lines, amongst other factors, differ in their p53 mutation status with DLD-1 cells harbouring a mutation p53 $Ser^{241}Phe$ mutation compared to WT in HCT116. Loss of functional p53 is associated with resistance to both 5-FU and oxaliplatin (Violette *et al*, 2002, Boyer *et al*, 2004) which could partly explain the higher resistance of DLD-1 cells to 5-FU and oxaliplatin.

The present study also used mRNA and miRNA profiling to independently predict mechanisms of 5-FU and/or oxaliplatin resistance which were then experimentally validated in the drug resistant cell lines.

We firstly identified genes that were specifically differentially expressed in 5-FU resistant cells, oxaliplatin resistant cells or that were commonly differentially expressed in both 5-FU and oxaliplatin resistant cells and therefore may represent a general drug resistance expression signature. Bioinformatics analysis of genes differentially under-expressed in each drug resistant cell line compared to their respective parental cell line, showed an enrichment of cell cycle regulation pathways. Bioinformatics analysis also showed an enrichment of pathways involved in cytoskeleton remodelling and immune or inflammatory response with differentially over-expressed genes. This was irrespective of whether the cells were resistant to 5-FU and oxaliplatin suggesting similar resistance mechanisms.

Previous studies have described a link between chronic inflammation and cancer development (Chen *et al*, 2007). The activation of the transcription factor NF-kB, a key event in the inflammatory response, has been reported to lead to the production of pro-inflammatory cytokines, chemokines, growth factors, and the expression of anti-apoptotic genes, thus giving a survival advantage to cells and aiding in their resistance to chemotherapy (Chen *et al*, 2007). NF-kB has been reported to contribute to resistance to 5-FU in gastric and colorectal cancer (Camp *et al*, 2003; Voboril *et al*, 2006).

In the present study, amongst the most abundantly differentially expressed genes in all four drug resistant cells compared to their respective parental cells were genes that were commonly differentially expressed in both 5-FU and oxaliplatin resistant cells. Included were genes coding for cytoskeletal actin and tubulin proteins (*TUBA1A, TUBA1C, TUBB, ACTB, ACTG1*) as well as genes involved in glycolysis (*PGAM1, ALDOA, TPI1*), cell cycle progression (*MCM4*), multidrug resistance (*ABCC3*), metastasis (*ANGPTL4*) and steroidogenesis (*AKR1C3*).

Beta-actin (*ACTB*) is a highly conserved cytoskeleton structural protein that is widely distributed in all eukaryotic cells and plays critical roles in cell migration, cell division, embryonic development, wound healing, immune response and gene expression (Guo *et al*, 2013). In colorectal cancer, *ACTB* expression has been shown to be increased in colorectal cancers compared to matched normal mucosa and a role for *ACTB* in promoting cell motility, invasiveness and metastasis has been suggested (Guo *et al*, 2013). Tubulin beta chain protein (*TUBB*), which is one of the tubulin proteins that make up microtubules, has also been shown to be differentially over-expressed in colorectal cancers compared to normal mucosa (Yang *et al*, 2012*a*). The cytoskeleton proteins, though prominently decreased in 5-FU and oxaliplatin resistant cells in the present study, have not been previously associated with a role in conferring drug resistance.

Assessing the expression of EMT genes did not show what would have been expected if the cells were actively undergoing EMT. Furthermore, a decrease in the expression of actin and tubulin proteins also indicates less cell motility. Therefore, the invasive phenotype that was observed in oxaliplatin resistant cells could occur through another mechanism such as the overexpression of Angiopoetin-like protein 4 (*ANGPTL4*).

ANGPTL4 is a glycosylated, secreted protein that functions as a serum hormone that regulates glucose homeostasis, lipid metabolism, and insulin sensitivity. It has also been shown to be involved with promoting an invasive phenotype in colorectal cancer cells (Nakayama *et al*, 2011; Huang *et al*, 2012*b*). This could possibly be through the disruption of adhesion molecules in the vasculature, as suggested earlier by Huang *et al* (2011) who showed that ANGPTL4 contributed to metastasis in lung cancer by disrupting VE-cadherin and claudin-5. However, it has not been previously linked to having a role in 5-FU or oxaliplatin resistance in cancer.

MCM4 is a licensing factor protein that is involved in the initiation and regulation of the cell cycle. An increased expression of *MCM4* is shown to increase cell proliferation (Kikuchi *et al*, 2010) and *MCM4* has also been found to be increased in a number of cancers including colorectal cancer (Fijneman *et al*, 2012). We show that *MCM4* is prominently decreased in 5-FU and oxaliplatin resistant cells. This decrease is consistent with the cell cycle arrest and lower proliferation observed in the cells, particularly in the DLD-1 5-FU resistant cells.

The glycolytic enzyme Aldolase A (ALDOA), catalyses the breakdown of fructose 1,6-bisphosphate to glyceraldehyde 3-phosphate in one of the many steps of glycolysis. Increased *ALDOA* expression has previously been associated with an aggressive phenotype in hepatocellular carcinoma (Hamaguchi *et al*, 2008) and breast cancer (Migneco *et al*, 2010). ALDOA has not been previously suggested to be linked with 5-FU or oxaliplatin resistance.

Phosphoglycerate mutase 1 (PGAM1) is also a glycolytic enzyme and catalyses the conversion of 3-phosphoglycerate (3PG) to 2-phosphoglycerate (2PG), downstream in the glycolytic pathway to ALDOA. Similarly to ALDOA, PGAM1 expression is increased in a number of cancers including hepatocellular carcinoma (Ren *et al*, 2010) and glioma (Gao *et al*, 2013). Moreover, Chen *et al* (2014) recently reported *PGAM1* to be decreased in methotrexate resistant breast cancer cells.

The decrease in *ALDOA* and *PGAM1* expression is therefore consistent with our preliminary data suggesting that DLD-1 5-FU and oxaliplatin resistant cells had lower glycolytic activity than DLD-1 parental cells. An increase in glycolysis is commonly seen in cancer, as they try to support their rapid growth, sometimes in hypoxic conditions, by switching from aerobic to anaerobic glycolysis in a phenomenon known as the Warburg effect (Vander Heiden *et al*, 2009). However, decreased expression of these genes in drug resistance cell lines could be a consequence of the decrease in proliferation.

We also showed that AKR1C3, an enzyme involved in steroidogenesis and the control of growth and differentiation, is increased 5-FU and oxaliplatin

resistance. It has previously been found to be enhanced in cisplatin resistance in colorectal cancer cells (Matsunga *et al*, 2013). Additionally, the ATP-cassette drug transporter, ABCC3 is reported to be involved in multi-drug resistance. It has been shown to be increased in doxorubicin-resistant breast cancer cells (Liu *et al*, 2005), 5-FU resistant pancreatic cancer cells and adriamycin resistant HCC cells (Wang *et al*, 2010*b*).

The PathScan signalling array suggested that in HCT116 5-FU and oxaliplatin resistant lines there was a reduction in ERK 1/2 phosphorylation which may indicate a less active RAS/MAPK pathway and reduced proliferation as has been demonstrated in HCT116 oxaliplatin resistant cells. Future experiments measuring GTP-bound activated KRAS in drug resistant cells compared to parental cells, as described in Section 2.2.12, could test this hypothesis. There was also a significant decrease in the activation of p70 S6 kinase. P70 S6 kinase is one of the downstream targets of the MAPK pathway and causes the phosphorylation of the ribosomal protein S6 allowing for protein synthesis to occur at this site and promotes cell growth (Harada *et al*, 2001). This also suggests that a major mechanism in the resistance 5-FU and oxaliplatin is through slowing cell cycle progression.

The present study also identified a miRNA signature of acquired drug resistance in colorectal cancer cell lines. Previous studies had investigated the acute effect of 5-FU and oxaliplatin treatment on miRNA expression (Rossi *et al*, 2007; Zhou *et al*, 2010) creating a possible acute drug response signature that may contribute to the pharmacodynamics of the drug.

To date, only three other studies have performed miRNA profiling in 5-FU or oxaliplatin resistant colorectal cancer cells. Consistent with the present study, Akao *et al* (2011) and Kurokawa *et al* (2012) associate 5-FU resistance with the increased differential expression of miR-92 and miR-19b respectively. Furthermore miR-20a, the most abundantly overexpressed miRNA in 5-FU resistant DLD-1 cells in the present study, has previously been shown to contribute to 5-FU resistance by targeting BCL2/adenovirus E1B 19 kDa protein-interacting protein 2 (BNIP2) in SW480 and SW620 colorectal cancer cells (Chai *et al*, 2011).

In a recent study, Zhou *et al* (2014) generated oxaliplatin resistant cells in HCT116, RKO and HT29 colorectal cancer cell backgrounds. The differentially expressed miRNAs in their HCT116 oxaliplatin resistant cells did not match miRNAs differentially expressed in the HCT116 oxaliplatin resistant cells generated in the present study. However, Zhou *et al* (2014) show that differential expression of miRNAs such as miR-31, miR-200a and miR-93 was associated with an oxaliplatin resistance phenotype, consistent with some of the differentially expressed miRNAs expressed in our DLD-1 oxaliplatin resistant cells.

Having identified potential mRNA and miRNA expression signatures of drug resistance, it is important to understand how miRNAs may mediate the drug resistant phenotypes that have been predicted from bioinformatics analysis and experimentally validated.

The miR-200 family and miR-31, which were differently expressed in the present study, have recently been shown to regulate cytoskeleton remodelling and cell invasion through the targeting of WAVE3, an actin remodelling protein, in a number of cancers (Sossey-Alaoui *et al*, 2009; Sossey-Alaoui *et al*, 2011). Moreover, miR-93, which was over-expressed in DLD-1 5-FU and oxaliplatin resistant cells in the present study, has been reported to target p21 and cause G2 arrest in colorectal cancer cells (Yang *et al*, 2012*b*).

Using the online bioinformatics tool TargetScan (http://www.targetscan.org/vert_61/) to predict which of our differentially expressed miRNAs may target the 3'UTR of some of genes mentioned above, may allow us to understand the role of miRNAs in mediating drug resistance mechanisms. Table 4.25 show examples of possible inverse relationships between drug resistance genes and miRNAs.

Table 4.25: The inverse relationship between candidate drug resistance genes and miRNAs as predicted by TargetScan

Differentially expressed gene	**Differentially expressed miRNAs predicted to target gene**
ABCC3	↓ miR-197
MCM4	↑ miR-24, miR-17, miR-20a, miR-93, miR-106a, miR-186
ACTG1	↑ miR-186, miR-10a
ACTB	↑ miR-31, miR-19b
TUBA1A	↑ miR-221, miR-222, miR-15b, miR-16
PGAM1	↑ miR-92, miR-200a, miR-494

The overexpression of miR-20a in DLD-1 5-FU resistant cells may contribute to resistance, in part, through the down-regulation of the cell cycle regulator, MCM4. In another example, the over-expression of miR-494 in HCT116 and DLD-1 5-FU resistant cells may also contribute to resistance through the down-regulation of the glycolytic enzyme PGAM1. However, as discussed previously miRNAs have many targets due to imperfect complementarity that could in theory have opposing effects on a particular pathway or process. Therefore the prominent over or under-expression of mRNA genes may be more informative in how they would mediate drug resistance. However, miRNAs have the potential to be very useful as markers of drug resistance in colorectal cancer. A recent study by Kjersem *et al* (2014), for example, shows that the increased expression of miR-106a, miR-484 and 130b in the plasma of colorectal cancer patients, is associated with patients described as non-responders to 5-FU and oxaliplatin-based therapy.

The present study also showed that miR-224 expression was decreased in 5-FU and oxaliplatin resistant cells in both cell line backgrounds compared to their respective parental cells. As discussed in Chapter 3, we show that the increased expression of miR-224 is an early and persistent feature of colorectal cancer development. MiR-224 may also modulate 5-FU chemosensitivity through the regulation of KRAS pathways and by indirectly affecting the expression of 5-FU metabolising enzymes.

In the drug resistant cell model, the cells have adapted and developed resistance to 5-FU and oxaliplatin partly through decreased expression of miR-224. MiR-

224 has been experimentally validated to target the genes coding for p21 and p27, therefore, in theory, the decrease in miR-224 expression would lead to an increase in $p21^{cip1}$ and $p27^{kip1}$ and thus cell cycle arrest. However, there are many other factors that affect the expression of $p21^{cip1}$ and $p27^{kip1}$ and this relationship would need to be experimentally validated.

4.5. Conclusions and future work

4.5.1. Conclusions

We have successfully created 5-FU and oxaliplatin resistant cells in HCT116 and DLD-1 colorectal backgrounds. We have also identified 5-FU and oxaliplatin mRNA and miRNA expression signatures that independently predict resistance mechanisms involving cell cycle progression, glycolysis, cytoskeleton remodelling and invasion. We also suggest, from a miRNA target prediction database, that miRNAs differentially expressed in the present study may mediate the aforementioned resistance mechanisms through targeting key genes highlighted in our study as having key roles in the development of drug resistance.

4.5.2. Future work

In further studies, it will be important to validate the expression of our candidate genes and miRNAs in paired drug sensitive and drug resistant cell lines. Our work would also progress through experimentally validating which of our candidate miRNAs, if any, may directly target the 3'UTR of one or more of our proposed candidate genes.

Ultimately, our aim is to investigate whether differential expression of our candidate mRNAs or miRNAs is associated with drug resistance in colorectal cancer patients. Professor Alastair Munro and colleagues have identified a cohort of over 200 colorectal cancer patients who have received 5-FU-based therapy. Future work would also be directed towards correlating some candidate drug resistance miRNAs (including miR-224) and genes with prognosis and treatment response in colorectal cancer patient samples.

Chapter 5

The role of microRNAs in radiation response

5.1. Introduction

5.1.1. Cellular response to radiation treatment

The aim of radiation treatment is to eradicate or to reduce the size of cancers. Ionising radiation damages cancer cells through the production of free radicals, in particular the hydroxyl radical (OH·), which causes injury to cellular components including DNA (Hu & Gatti, 2010). DNA damage, and in particular double-stranded breaks (DSB), are considered to be the most detrimental to cell survival. Cells respond to this kind of injury by activating the ATM pathway, eventually causing cell cycle arrest and allowing for DSB repair though non-homologous end joining (NHEJ) during the G0/G1 phase of the cell cycle or by homologous recombination during the S/G2 phase (Hu & Gatti, 2010). However, should radiation dose and cellular damage be too high, cancer cells undergo cell death by apoptosis or mitotic catastrophe hence the reduction of cancer mass (Figure 5.1; Hu & Gatti, 2010).

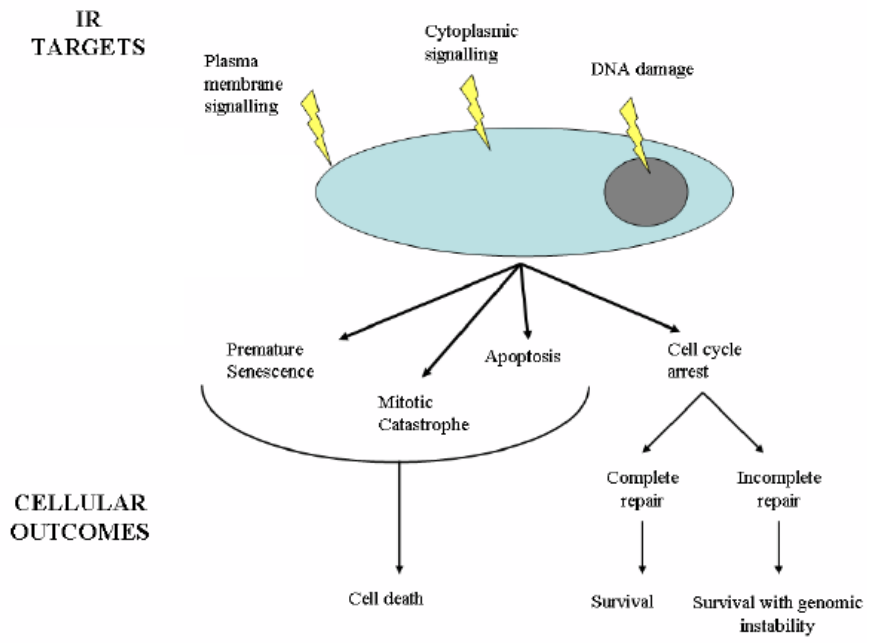

Figure 5.1: ***The cellular response to radiation.*** *Radiation targets and causes injury to a number of cellular components including DNA. This leads to cell cycle arrest and DNA damage repair. However it may also lead it cell death through a number of mechanisms (Sanders, 2011).*

Radiation resistance remains a challenge to radiation treatment in many cancers, including rectal cancer. Factors including intrinsic radiation resistance, increased cancer cell proliferation, hypoxia and enhanced DNA damage repair have been suggested to contribute to radiation resistance (Pajonk *et al*, 2010). A number of pathways that regulate the cell cycle, proliferation and apoptosis have also been shown to be induced in response to radiation and to also have a role in radiation resistance (Dent *et al*, 2003).

Studies have shown that radiation exposure can lead to the activation of the ERK pathway through the activation of EGFR (Schmidt-Ullrich *et al*, 1997; Kavanagh et al, 1998). It was reported that radiation doses of 1-2 Gy led to the same level

of activation as with physiological growth factors such as EGF at a concentration of approximately 0.1 nM (Dent *et al*, 1999). The activation of the ERK pathway and the subsequent activation of PI3K/Akt pathways following radiation have thus been linked to the ability of cells to proliferate and survive despite irradiation.

The present study has previously highlighted the importance of *KRAS* mutation status in colorectal cancer patients. *KRAS* mutant patients have significantly reduced survival and higher resistance to cetuximab than *KRAS* WT patients (Andreyev *et al*, 1998; Andreyev *et al,* 2001; Conlin *et al*, 2005; Lievre *et al*, 2006; Bokemeyer *et al*, 2008; Amado *et al*, 2008). Many studies have also shown a role for activated or mutant KRAS signalling in radiation resistance.

5.1.2. KRAS-mediated radiation resistance

The observation that activated RAS mediates radiation resistance is well established and was first described in NIH3T3 mouse fibroblast cells (Fitzgerald, 1985; Sklar, 1988). McKenna *et al* (1990) subsequently showed in primary rat cells that activated HRAS transformation induced radiation resistance. However, they also showed that the v-myc oncogene, which had no effect on radiation resistance itself, was required for a synergistic induction of radiation resistance by HRAS.

The blockage of post-translational farnesylation of HRAS, and thus HRAS processing, by the farnesylation inhibitor FTI-277 resulted in increased apoptosis

following irradiation and increased radio-sensitivity in HRAS-transformed rat embryos (Bernhard *et al*, 1996).

In human cancer cell lines, both the presence of an activated NRAS allele and re-introduction of an activated NRAS allele after loss were shown to increase clonogenic survival and radiation resistance in HT1080 fibrosarcoma cells (Bernhard *et al*, 2000). Bernhard *et al* (2000) also showed that the presence of a *KRAS* mutant allele contributed to radiation resistance in DLD-1 colorectal cancer cells.

Gupta *et al* (2001) reported that the inhibition of the PI3K pathway by the inhibitor LY294002 selectively sensitised RAS-mutant cells, whilst having no effect on WT cells. Furthermore the induction of the PI3K pathway in RAS-WT cells increased radio-resistance which was subsequently reversed following treatment with LY294002. Additionally, Grana *et al* (2002) suggested that RAS-mediated radio-resistance in rat intestinal epithelial cells was PI3K/Akt and RAF-1 dependent but MEK independent, as the blockage of MEK using the inhibitor UO126 resulted in no change in survival, as determined by clonogenic survival assays, following irradiation.

Despite these advances in knowledge, the molecular mechanisms governing response to radiation is poorly understood and there remains a great need to identify ways to manipulate these pathways for greater irradiation efficacy. MiRNAs, as described previously, are additional regulators of gene expression. Several miRNAs, with roles in controlling cell proliferation, cell cycle, apoptosis and DNA damage repair pathways, have been shown to be differentially

expressed in a number of cancer cell lines following irradiation (Metheetrairut & Slack, 2013). In particular, members of the let-7 family, which target *KRAS*, have been shown to be differentially over-expressed in response to radiation in glioblastomas (Chaudhry *et al*, 2010) but under-expressed in lung cancer (Weidhass *et al*, 2007). Saleh *et al* (2011) also showed that the expression of let-7a and let-7b was decreased in HCT116 colorectal cancer cells after irradiation, and suggested that this was p53-dependent, as determined using HCT116 $p53^{(+/+)}$ and p53-null cells. This shows that differential let-7 expression after radiation could be cancer cell-type and genotype dependent.

Increased expression of let-7g was reported to be associated with a radio-sensitive phenotype in non-small cell lung carcinoma cells (Jeong *et al*, 2009). The study also showed that LIN28, a posttranscriptional repressor of let-7 biogenesis, increased *KRAS* expression through the repression of let-7g. The findings from Jeong *et al* (2009) suggest that post-transcriptional activation of KRAS may also regulate response to radiotherapy. Similarly, Oh *et al* (2010) found that the silencing of LIN28 led to the up-regulation of let-7a, a decrease in *KRAS* expression and thus KRAS signalling. This lead to radio-sensitisation in lung and pancreatic cancer cells, an effect that was not seen in *KRAS* WT SQ20B head and neck carcinoma cells or normal fibroblast cells.

A recent study by Luu *et al* (2013) also showed in HCT116 cells that functional p53 was required for let-7-dependent repression of KRAS activity and sensitisation to chemo-radiotherapy (3 μM 5-FU and 2 Gy radiation). The cells subsequently became resistant to therapy when let-7 expression was inhibited.

The studies by Jeong *et al* (2009), Oh *et al* (2010) and Luu *et al* (2013) thus strengthen the notion that increased KRAS signalling through increased *KRAS* expression or the presence of mutant *KRAS* increases radiation resistance. They also suggest that manipulating the expression of miRNAs that target KRAS and its downstream targets provides an additional method of overcoming KRAS-mediated radiation resistance. To date however, miRNA expression profiling has not been performed on isogenic *KRAS* WT and mutant colorectal cancer cells following irradiation. This would aid in the understanding of the role of miRNAs in KRAS-mediated radiation resistance.

5.1.3. Aims and objectives

The aims of the present study were firstly to identify miRNAs that were differentially expressed in colorectal cancer cell lines in response to radiation, and predict pathways and processes that they may regulate. Secondly, the study aimed to explore how the radiation response miRNA signature changed with *KRAS* mutation status. Thirdly, the present study aimed to identify miRNAs that may modulate radiation response in a KRAS-dependent manner.

5.3. Results

5.3.1. Laboratory cell irradiator

The present study used a laboratory irradiator to investigate the role of miRNAs in modulating response to radiotherapy in colorectal cancer cell lines, as described in Section 2.2.16. The laboratory irradiator was previously used by Dr Ian Sanders and Professor Alastair Munro (University of Dundee) as an *in vitro* simulation of rectal intraoperative radiotherapy (IORT) to identify biological markers of IORT response.

Sanders (2011) showed that the expression of 3 proteins involved in the DNA double-strand break repair pathway, phosphorylated H_2AX, ATM and p53 (serine 15), were induced and detected by Western blotting 5 minutes after 5 Gy of radiation in a number of colorectal cancer cell lines. Sanders (2011) cites a study by Vaidya *et al* (2010) as being representative of the breast cancer IORT protocol used in the Targit trial and therefore was the basis of why 5 Gy of irradiation was used throughout his study. Based on this, the present study therefore irradiated HCT116 colorectal cancer cells at a dose of 5 Gy of radiation and confirmed that γH_2AX was induced, after 5 minutes incubation, in treated cells compared to non-treated control cells (Figure 5.2).

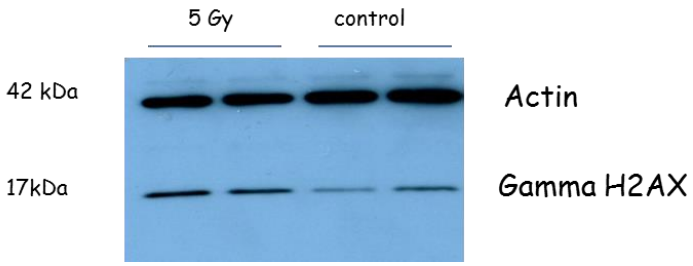

Figure 5.2: ***The induction of gamma (γ-) H_2AX in response to 5 Gy of radiation in HCT116 colorectal cancer cells.*** *HCT116 cells were irradiated in duplicate with 5 Gy of radiation using a laboratory in vitro cell irradiator, as described in Section 2.2.16. A Western blot was performed to quantify the protein expression of γH_2AX in irradiated treated cells in comparison to untreated control cells. Actin was used as the loading control.*

5.3.2. Optimisation of maximum microRNA induction or inhibition time following radiation treatment

To understand the role of miRNAs in the biological response to radiation in colorectal cancer, TLDA miRNA cards were used to identify miRNAs that were differentially expressed in response to 5 Gy of radiation as described in Section 2.2.16.1. Whereas only 5 minutes was required for the induction of proteins such as γH_2AX, it was speculated that the time required for optimum miRNA induction or inhibition may be considerably longer.

Taqman qRT-PCR analysis was therefore used to assess the expression of miR-24, miR-100 and miR-125b, which have previously been shown to be induced or decreased in response to radiation (Hu & Gatti, 2011), at 10, 30, 60 and 180 minutes after treatment. From 10 minutes to 60 minutes, miR-24, miR-100 and miR-125 showed a time dependent decrease in expression followed by an increase in expression after 180 minutes. Expression levels for all three miRNAs

were at their lowest at 60 minutes. MiR-24 expression was significantly decreased 2.1-fold (p=0.0007) 60 minutes after irradiation. The expression of miR-100 and miR-125b were also decreased 5.4-fold ($p=5.8x10^{-7}$) and 2.8-fold ($p=1.6x10^{-5}$) respectively 60 minutes after irradiation (Figure 5.3). Thus for the following experiments with TLDA miRNA cards, cells were placed in an incubator for 60 minutes after radiation treatment before RNA was extracted for further analysis.

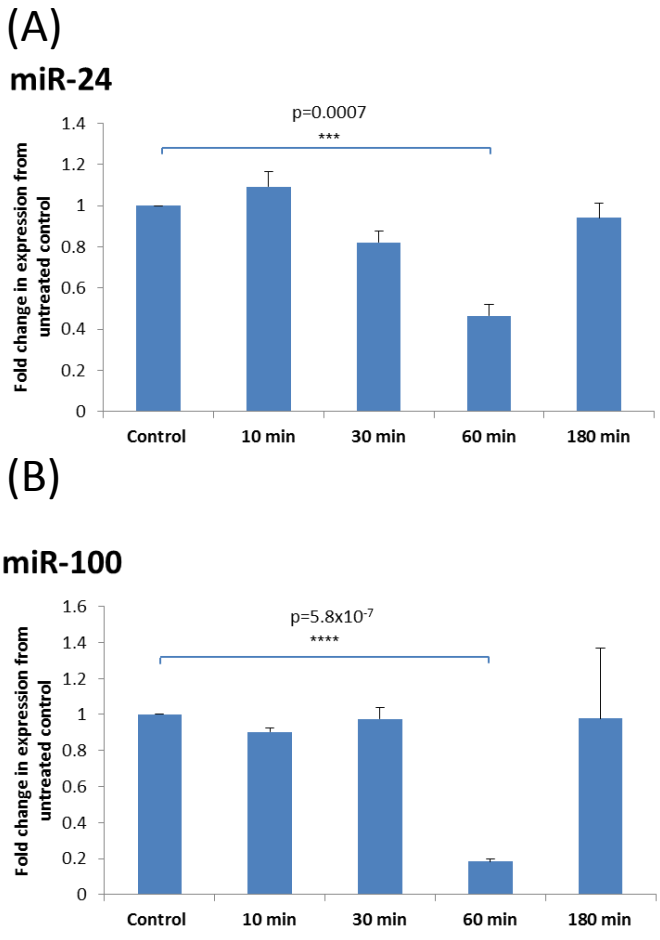

Figure 5.3

(C)

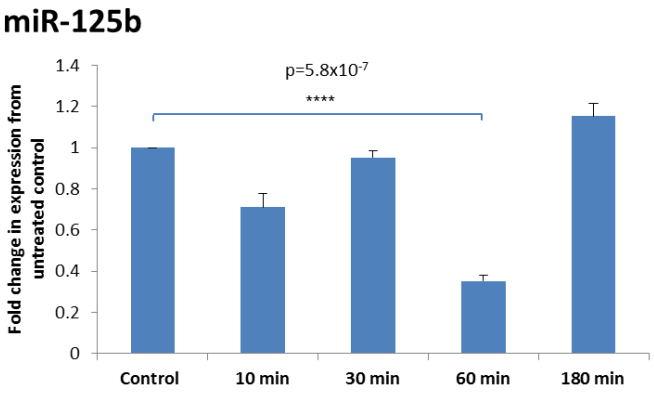

Figure 5.3: ***The expression of miR-24, miR-100 and miR-125b at different time points following irradiation.*** *The expression of* ***A)*** *miR-24,* ***B)*** *miR-100 and* ***C)*** *miR-125b, relative to the control U6, was assessed, as described in Section 2.2.9.2, 10, 30, 60 and 180 minutes after treatment of HCT116 cells with 5 Gy of radiation as described in Section 2.2.16. Data is represented as the fold change in relative expression in treated cells compared to non-treated control cells. Each sample was assessed in triplicate and the errors represent the SEM. Statistical significance (p≤0.05) was determined by performing Independent T-tests.*

5.3.3. MicroRNA profiling of irradiated isogenic *KRAS* mutant and WT cells

Next, TLDA miRNA profiling was used to explore how differential miRNA expression following irradiation changed depending on *KRAS* mutation status. Following irradiation, 16 miRNAs were differentially expressed (14 up, 2 down) in treated cells compared to untreated HCT116 *KRAS* mutant cells. MiR-15b and let-7a were the most abundantly over and under-expressed miRNAs respectively in HCT116 *KRAS* mutant cells following treatment (Table 5.1).

Table 5.1: MicroRNAs differentially expressed in irradiated HCT116 *KRAS* mutant cells compared to non-treated control cells

microRNA	Fold Change	Adjusted value
miR-15b	3.45	0.021
miR-454	2.69	0.043
let-7d	2.67	0.009
miR-29a	**2.62**	**0.006**
miR-886-3p	**2.52**	**0.006**
miR-100	**2.15**	**0.014**
miR-93	2.14	0.017
miR-221	**2.01**	**0.008**
miR-886-5p	1.99	0.022
miR-30b	1.94	0.033
miR-30c	1.87	0.009
miR-17	**1.84**	**0.004**
miR-16	**1.80**	**0.026**
miR-200b	**1.72**	**0.046**
miR-197	-1.82	0.008
let-7a	-3.06	0.008

The miRNAs in bold were induced in both KRAS mutant and KRAS WT HCT116 cells in response to radiation

As previously described in Section 2.2.17, the bioinformatic tool, Metacore was used to identify pathways and processes predicted to be enriched and significantly associated with the predicted targets of the miRNAs listed in Table 5.1.

Cancer related pathways and processes involved in cytoskeleton remodelling, development of EMT, cell adhesion and the immune response were prominently enriched (Table 5.2).

Table 5.2: Pathways and processes associated with the predicted targets of miRNAs differentially expressed in HCT116 *KRAS* mutant cells after irradiation

	Pathway name	p value	Ratio
1	Cytoskeleton remodeling_TGF, WNT and cytoskeletal remodeling	2.00E-24	90/111
2	Cytoskeleton remodeling_Cytoskeleton remodelling	2.67E-19	79/102
3	Development_Regulation of epithelial-to-mesenchymal transition (EMT)	1.13E-17	55/64
4	Cell adhesion_Chemokines and adhesion	3.16E-16	74/100
5	Cardiac Hypertrophy_NF-AT signaling in Cardiac Hypertrophy	4.90E-16	54/65
6	Normal and pathological TGF-beta-mediated regulation of cell proliferation	2.31E-14	32/33
7	Development_TGF-beta receptor signalling	4.22E-14	43/50
8	Development_TGF-beta-dependent induction of EMT via MAPK	5.93E-14	41/47
9	Cell cycle_Regulation of G1/S transition (part 1)	1.03E-13	35/38
10	Immune response_HSP60 and HSP70/ TLR signaling pathway	1.15E-13	45/54

	Process name	p value	Ratio
1	Development_Neurogenesis_Synaptogenesis	2.26E-13	150/180
2	Signal transduction_WNT signalling	2.45E-12	146/177
3	Signal transduction_NOTCH signalling	2.38E-11	185/236
4	Cytoskeleton_Regulation of cytoskeleton rearrangement	3.49E-11	148/183
5	Cell adhesion_Synaptic contact	1.86E-09	145/184
6	Development_Ossification and bone remodelling	2.66E-09	126/157
7	Development_EMT_Regulation of epithelial-to-mesenchymal transition	4.27E-09	172/225
8	Cytoskeleton_Actin filaments	8.48E-09	138/176
9	Development_Hedgehog signalling	1.37E-08	190/254
10	Cell adhesion_Cadherins	1.73E-08	140/180

Similarly, HCT116 *KRAS* WT cells were treated with 5 Gy of radiation. Following treatment, 11 miRNAs were differentially expressed in treated cells compared to untreated HCT116 *KRAS* WT cells. All 11 miRNAs were significantly overexpressed in response to treatment, with miR-20a the most abundantly over-expressed miRNA (Table 5.3).

Table 5.3: MicroRNAs differentially expressed in irradiated HCT116 *KRAS* WT cells compared to its non-treated control

microRNA	Fold Change	Adjusted p value
miR-20a	4.43	0.010
miR-19b	3.08	0.029
miR-29a	**2.38**	**0.019**
miR-126	2.35	0.008
miR-200b	**2.11**	**0.008**
miR-16	**2.03**	**0.020**
miR-100	**1.99**	**0.047**
miR-17	**1.81**	**0.037**
miR-221	**1.80**	**0.016**
miR-886-3p	**1.76**	**0.038**
miR-125b	1.72	0.033

The miRNAs in bold were induced in both KRAS mutant and KRAS WT HCT116 cells in response to radiation

Metacore bioinformatics analysis also suggested that pathways and processes predicted to be enriched by the predicted targets of the miRNAs listed in Table 5.3 included those involved in cytoskeleton remodelling, cell adhesion, EMT and an immune response. This suggests that HCT116 *KRAS* WT and *KRAS* mutant cells respond to the stress induced by radiation by activating similar pathways and by mediating similar phenotypes.

Table 5.4: Pathways and processes associated with the predicted targets of miRNAs differentially expressed in HCT116 *KRAS* WT cells after irradiation

	Pathway name	p value	Ratio
1	Cytoskeleton remodeling_TGF, WNT and cytoskeletal remodeling	2.69E-25	98/111
2	Cytoskeleton remodeling_Cytoskeleton remodelling	2.86E-22	89/102
3	Development_TGF-beta-dependent induction of EMT via MAPK	4.25E-17	46/47
4	Transport_Clathrin-coated vesicle cycle	6.32E-17	63/71
5	Development_TGF-beta receptor signaling	2.61E-15	47/50
6	Development_Regulation of epithelial-to-mesenchymal transition (EMT)	1.42E-14	56/64
7	Immune response_HSP60 and HSP70/ TLR signaling pathway	2.53E-14	49/54
8	Cell adhesion_Chemokines and adhesion	4.57E-14	78/100
9	Cardiac Hypertrophy_NF-AT signaling in Cardiac Hypertrophy	6.17E-14	56/65
10	Immune response_IL-2 activation and signaling pathway	1.02E-13	45/49

	Process name	p value	Ratio
1	Development_Neurogenesis_Synaptogenesis	1.26E-14	167/180
2	Signal transduction_NOTCH signaling	7.08E-11	206/236
3	Development_Neurogenesis_Axonal guidance	9.53E-11	201/230
4	Cell adhesion_Cadherins	1.52E-09	159/180
5	Cytoskeleton_Regulation of cytoskeleton rearrangement	2.37E-08	159/183
6	Signal transduction_WNT signalling	3.20E-08	154/177
7	Transcription_mRNA processing	6.15E-08	140/160
8	Cytoskeleton_Actin filaments	1.18E-07	152/176
9	Cell adhesion_Attractive and repulsive receptors	1.48E-07	151/175
10	Cytoskeleton_Cytoplasmic microtubules	2.49E-07	103/115

Despite the similarities, the bioinformatics analysis does not indicate the extent to which the two cell lines respond to ionising radiation. Seven miRNAs, miR-16, miR-17, miR-29a, miR-100, miR-200b, miR-221 and miR-886-3p, were similarly overexpressed in both cell lines in response to radiation, suggesting that they may represent a common stress response signature to radiation. Although not in colorectal cancer cells, the expression of miR-100 (Simone *et al*, 2009; Mueller *et al*, 2013), miR-17 (Weidhass *et al*, 2007; Chaudrey et al, 2010; John-Aryankalayil

et al, 2012) and miR-16 (Wagner-Ecker *et al*, 2010; Chaudrey *et al*, 2010) have previously been reported to be altered in response to radiation. MiR-221 was also shown to affect radiation resistance in gastric cancer (Chun-Zhi *et al*, 2010). The differential expression of miR-29a, miR-200b and miR-886-3p in response to irradiation has not been previously reported.

We then compared irradiated HCT116 *KRAS* mutant cells to irradiated HCT116 *KRAS* WT cells. This analysis allowed for identification of miRNAs that may mediate a KRAS pathway-dependent response to radiation. All 22 miRNAs were significantly over-expressed in *KRAS* mutant cells compared to *KRAS* WT HCT116 cells, with miR-328 the most abundantly overexpressed miRNA (Table 5.5). The list includes 3 of the miRNAs (miR-17, miR-29a and miR-100) that were commonly differentially expressed in *KRAS* WT and mutant cells compared to their respective non-treated controls. Interestingly, the list also includes two members of the let-7 family (let-7e and let-7g). However, in contrast to previously discussed studies in lung cancer cells (Jeong *et al*, 2009; Oh *et al*, 2010), increased expression of let-7e and let-7g appear to be associated with a mutant KRAS signalling and therefore possibly KRAS-dependent radiation resistance. The list also comprises miR-30c which has been experimentally validated to target KRAS in breast cancer (Tanic *et al*, 2012).

Table 5.5: MicroRNAs differentially expressed in irradiated HCT116 *KRAS* mutant cells compared to irradiated *KRAS* WT wells.

microRNA	Fold Change	Adjusted p value
miR-328	5.58	0.004
miR-197	3.32	0.005
miR-20a	3.21	0.014
miR-186	3.15	0.003
miR-126	2.90	0.001
miR-574-3p	2.87	0.005
miR-532-3p	2.74	0.009
let-7e	2.66	0.003
miR-29a	2.43	0.013
miR-92a	2.34	0.008
miR-320	2.29	0.001
miR-191	2.17	0.001
miR-149	2.13	0.010
let-7g	2.10	0.018
miR-145	1.85	0.008
miR-100	1.78	0.041
miR-19b	1.73	0.048
miR-106a	1.70	0.035
miR-30c	1.64	0.022
miR-17	1.60	0.011
miR-342-3p	1.42	0.049
miR-200c	1.38	0.025

Increased miRNA expression in irradiated *KRAS* mutant cells compared to irradiated *KRAS* WT cells therefore leads to the question of whether reducing the expression of miR-328 or any of the miRNAs listed in Table 5.5 would have a role in sensitising HCT116 *KRAS* mutant cells to radiation through regulating KRAS expression and signalling.

Once again, bioinformatics analysis of the predicted targets of the miRNAs listed in Table 5.5 suggested associations with pathways and processes involved with

cytoskeleton remodelling, the immune response, cell adhesion, EMT and cell cycle regulation (Table 5.6).

Table 5.6: Pathways and processes associated with the predicted targets of miRNAs differentially expressed in irradiated HCT116 *KRAS* mutant cells compared to irradiated *KRAS* WT cells

	Pathway name	p value	Ratio
1	Cytoskeleton remodeling_TGF, WNT and cytoskeletal remodeling	1.46E-21	93/111
2	Development_Regulation of epithelial-to-mesenchymal transition (EMT)	1.55E-18	59/64
3	Immune response_HSP60 and HSP70/ TLR signaling pathway	2.24E-17	51/54
4	Cytoskeleton remodeling_Cytoskeleton remodelling	3.26E-16	81/102
5	Neurophysiological process_Receptor-mediated axon growth repulsion	2.40E-15	43/45
6	Immune response_IL-1 signaling pathway	5.77E-15	42/44
7	Cell adhesion_Chemokines and adhesion	7.34E-15	78/100
8	Transport_Clathrin-coated vesicle cycle	1.07E-14	60/71
9	Cardiac Hypertrophy_NF-AT signaling in Cardiac Hypertrophy	1.27E-13	55/65
10	Development_WNT signaling pathway. Part 2	2.00E-12	46/53

	Process name	p value	Ratio
1	Signal transduction_WNT signalling	5.95E-10	155/177
2	Signal transduction_NOTCH signalling	1.26E-09	200/236
3	Development_Neurogenesis_Synaptogenesis	2.96E-09	156/180
4	Cell adhesion_Cadherins	9.17E-09	155/180
5	Cell cycle_G1-S Interleukin regulation	1.29E-08	114/128
6	Cell cycle_G1-S Growth factor regulation	1.69E-08	166/195
7	Cell adhesion_Attractive and repulsive receptors	3.17E-08	150/175
8	Development_EMT_Regulation of epithelial-to-mesenchymal transition	4.05E-08	188/225
9	Transcription_mRNA processing	4.89E-08	138/160
10	Cell adhesion_Synaptic contact	2.21E-07	155/184

Additionally, we found that 6 miRNAs (miR-203, miR-224, miR-422a, miR-455-3p, miR-494 and miR-636) were expressed in irradiated HCT116 *KRAS* WT cells but expression was completely abolished in irradiated HCT116 *KRAS* mutant cells.

The expression of 5 of the above miRNAs (all but miR-636) were also completely abolished in irradiated *KRAS* mutant cells but expressed in non-radiated *KRAS* mutant cells.

MiR-224 has been previously shown in Chapter 3 to be 3.3 times more highly expressed in HCT116 *KRAS* WT cells compared to *KRAS* mutant cells. TLDA profiling data suggests that the expression of the six miRNAs, including miR-224, was reduced in response to radiation in both *KRAS* WT and mutant cells. However, as the miRNA expression levels were so low in mutant cells, they were effectively abolished in response to radiation.

These observations would need to be validated using single probe qRT-PCR Taqman analysis. However, it raises the question of whether reducing the expression of miR-203, miR-224, miR-422a, miR-455-3p, miR-494 or miR-636 in HCT116 *KRAS* WT cells would lead to a more mutant-*KRAS* radiation response phenotype. If this was the case then the increased expression of these miRNAs may be indicative of a radiation sensitive phenotype and the over-expression of the specific miRNA (e.g. by transfection of a specific miRNA mimic) in mutant cells would also sensitise *KRAS* mutant cells to radiation.

Bioinformatics analysis also showed that pathways and processes involved in cytoskeleton remodelling, EMT, cell adhesion as well as TGF-β signalling were enriched and predicted to be significantly associated with the predicted targets of the six aforementioned miRNAs (Table 5.7).

Table 5.7: Pathways and processed associated with the predicted targets of the six miRNAs abolished in HCT116 *KRAS* mutant cells in response to radiation

	Pathway name	p value	Ratio
1	Cytoskeleton remodeling_TGF, WNT and cytoskeletal remodeling	1.09E-12	62/111
2	Cytoskeleton remodeling_Cytoskeleton remodeling	3.55E-11	56/102
3	Development_Regulation of epithelial-to-mesenchymal transition (EMT)	4.39E-11	41/64
4	IGF family signaling in colorectal cancer	4.30E-10	38/60
5	Cell adhesion_Chemokines and adhesion	4.30E-10	53/100
6	Development_Thrombopoietin-regulated cell processes	1.19E-09	31/45
7	Development_TGF-beta-dependent induction of EMT via SMADs	3.29E-09	26/35
8	Development_BMP signalling	3.37E-09	25/33
9	Development_TGF-beta receptor signaling	7.27E-09	32/50
10	Stimulation of TGF-beta signaling in lung cancer	9.20E-09	31/48

	Process name	p value	Ratio
1	Development_Hedgehog signaling	1.28E-08	139/254
2	Reproduction_FSH-beta signaling pathway	1.31E-07	93/160
3	Signal Transduction_TGF-beta, GDF and Activin signaling	1.31E-07	90/154
4	Signal Transduction_BMP and GDF signaling	2.80E-07	59/91
5	Development_EMT_Regulation of epithelial-to-mesenchymal transition	4.03E-07	120/225
6	Development_Blood vessel morphogenesis	4.28E-07	121/228
7	Signal transduction_NOTCH signaling	1.11E-06	123/236
8	Development_Neurogenesis_Synaptogenesis	3.32E-06	97/180
9	Cell cycle_G1-S Growth factor regulation	4.59E-06	103/195
10	Cardiac development_FGF_ErbB signaling	5.84E-06	71/124

5.3.4. The role of miR-224 in the modulation of radiation response

The knockdown of miR-224 in HCT116 *KRAS* WT cells has previously been shown, in Chapter 3, to increase KRAS activation and ERK 1/2 phosphorylation and switch the phenotype of *KRAS* WT cells to a more mutant-like phenotype. We therefore hypothesised that the knockdown of miR-224 in *KRAS* WT cells would increase radiation resistance.

Flow cytometry was used to determine the proportion of cells with reduced viability in response to 5 Gy of radiation, as determined by the SYTOX AADvanced Dead Cell Stain kit and described in Section 2.2.16.3.

The percentage of non-viable cells in irradiated samples compared to non-treated controls was increased by 1.75-fold (p=0.09) in HCT116 *KRAS* WT cells compared to *KRAS* mutant cells (Figure 5.4). An increased fold-change indicates higher sensitivity to radiation as a higher proportion of cells have lost viability. The knockdown of miR-224 in *KRAS* WT cells did not significantly change cell viability compared to untransfected *KRAS* WT cells in response to radiation (Figure 5.4). This suggests that miR-224 may not have a role in regulating radiation response in colorectal cancer. Future studies would be directed towards testing this relationship using γH_2AX Western blots and clonogenic survival assays.

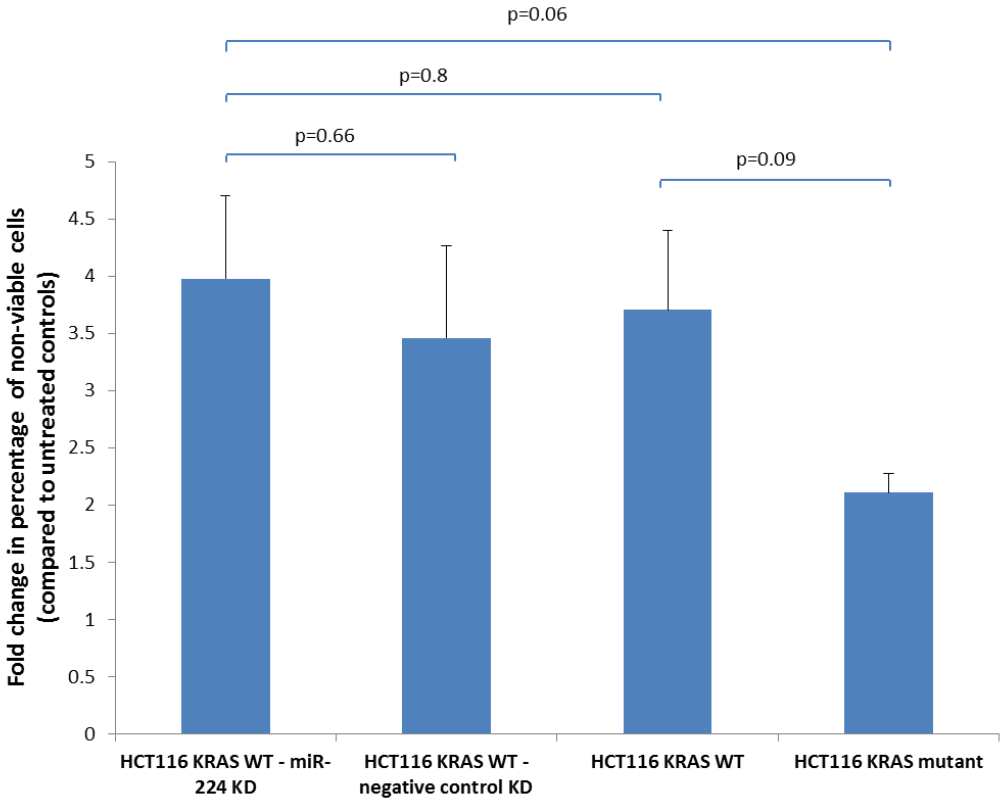

Figure 5.4: ***The effect of miR-224 knockdown on radiation response.*** *HCT116 KRAS WT miR-224 knockdown cells, HCT116 KRAS WT negative control miRNA knockdown cells and untransfected HCT116 KRAS WT and mutant cells were seeded at a density of 2.5 x 10^4 cells per 3.5 cm diameter plate and irradiated in triplicate at 5 Gy, as described in Section 2.2.16.3. The SYTOX AADvanced Dead Cell Stain kit was used to assess changes in cell viability in treated cells compared to non-treated controls using a flow cytometer. Graph represents the fold change in percentage of non-viable cells from untreated to treated cells and the errors represent the SEM of three separate experiments. Significance ($p \leq 0.05$) was determined using independent T tests.*

5.4. Discussion

In colorectal cancer, a small number of studies have explored the role of miRNAs in radiation response and resistance. Svoboda *et al* (2008) analysed miRNA expression in cancer biopsies from rectal cancer patients before and 2 weeks after capecitabine-based chemo-radiotherapy. The study reports the consistent over-expression of miR-125b and miR-137 in cancer biopsies after therapy. A later clinical study profiled miRNAs in good and poor responders to 5-FU or capecitabine-based chemo-radiotherapy (Svoboda *et al*, 2012). Svoboda *et al* (2012) showed that the expression of miR-215, miR-190b and miR-29b were increased in non-responders whereas let-7e, miR-196b, miR-450a, miR-450b-5p and miR-99a were decreased.

Recent studies have reported that miR-21 increased resistance to both 5-FU and radiation (Deng *et al*, 2014) and that miR-124 sensitised colorectal cells to radiation through targeting PPRX1, a new EMT inducer and stemness regulator (Zhang *et al*, 2014). The work by Saleh *et al* (2011) and Luu *et al* (2013) showing the role of let-7 in modulating radiation response in HCT116 colorectal cancer cells have been previously discussed.

The aim of the present study was firstly to identify miRNAs that were differentially expressed in HCT116 *KRAS* WT and mutant cell lines following radiation, and the predicted pathways and processes that they may mediate. There were 16 and 11 miRNAs that were differentially expressed in response to radiation in *KRAS* mutant and *KRAS* WT cells compared to their non-treated controls. Bioinformatics analysis showed that, despite differences in *KRAS*

mutation status, very similar pathways and processes were predicted to be associated with response to radiation in both cell lines.

The predicted role of cytoskeleton remodelling, EMT and increased cell adhesion is consistent with previous studies showing cell phenotypes mediated in response to radiation. Radiation has been shown to enhance migration and invasiveness in colorectal cancer, alongside the up-regulation of MMPs (Kumar *et al*, 2000; Speake *et al*, 2005) and the molecular and morphological changes associated with EMT, including the remodelling of the cytoskeleton (Andarawewa *et al*, 2007; Kawamoto *et al*, 2012).

The bioinformatics data predicted an involvement of TGF-β signalling in EMT, especially with the miRNAs involved in radiation response in *KRAS* mutant cells and the six miRNAs that were abolished in *KRAS* mutant cells following irradiation. This is consistent with the findings of Andarawewa *et al* (2007), who specifically showed that both TGF-β and irradiation was required to induce EMT in human mammary epithelial cells (HMEC). It is well established that TGF-β is a tumour suppressor during the early stages of carcinogenesis, but has the ability to switch to a cancer promoter in the latter stages (Bierie & Moses, 2006). Gene profiling data from Andarawewa *et al* (2007) suggested that ERK/MAPK activation may be important in inducing TGF-β and radiation induced EMT. They confirmed that the phosphorylation of ERK 1/2 and MEK 1/2 was markedly increased in response to TGF-β and radiation and that the blockage of MEK by UO126 decreased ERK activation, reversed EMT and decreased cell migration

(Andarawewa *et al*, 2007). This indicates the cross-talk between two different pathways that may occur during KRAS-mediated radiation resistance.

The bioinformatics data also suggested a role for the immune response in radiation response. As discussed in Chapter 4, previous studies have described a link between the activation of immune and inflammatory mediators and cancer development (Chen *et al*, 2007). The activation of transcription factors such as NF-kB, Stat3 and HIF1α are known to play key roles in radiation-induced inflammatory responses (Multhoff & Radons, 2012). The activation of these transcription factors causes the recruitment of immune cells to the cancer microenvironment and leads to the production of pro-inflammatory cytokines, chemokines, growth factors, and the expression of anti-apoptotic genes, allowing cancer cells to gain a survival advantage (Multhoff & Radons, 2012). The induction of EMT and immune responses shows that through the normal mechanisms of cell survival, radiation treatment can also induce increased cell proliferation and cancer growth as well as cancer metastasis, thus contributing to radiation resistance.

The present study also identified a possible common radiation response miRNA expression signature. In both HCT116 *KRAS* mutant and WT cells, 7 miRNAs (miR-16, miR-17, miR-29a, miR-100, miR-200b, miR-221, miR-886-3p) were commonly over-expressed in response to radiation. The increased expression of miR-29a, miR-221 and miR-17 has already been shown to promote colorectal cancer progression. The present study has previously shown in Chapter 3 (Section 3.1.2, Table 3.2) that miR-29a is one of the most consistently reported over-expressed

miRNA in colorectal cancer. MiR-29a has been reported as a novel serum marker for early detection of liver metastasis (Wang & Gu, 2012) and has recently been shown to promote cell invasion in colorectal cancer cells (Tang *et al*, 2014). Additionally miR-17, a member of the miR-17-92 cluster, is reported to be over-expressed in colorectal cancer and to contribute to colorectal cancer cell invasion (Zhang *et al*, 2014). Qin *et al* (2014) also recently report the involvement of miR-221 in promoting colorectal cancer cell invasion and metastasis by directly targeting and repressing the metastasis suppressor, RECK. Thus, there are many ways by which miRNAs that are induced by radiation can mediate the aforementioned predicted radiation-response phenotypes. The transcription and expression of miRNAs is known to be caused by the action of transcription factors (Chang *et al*, 2007; Chang *et al*, 2008). Further work could therefore be directed towards exploring whether the increased transcription and expression of the miRNA highlighted in the present study in response to radiation is, for example, p53 or Nf-kB dependent.

The present study also aimed to identify miRNAs that may, in addition to the let-7 family as previously reported, have important roles in modulating KRAS-mediated radiation resistance. We have identified a group of 22 miRNAs that were induced in irradiated *KRAS* mutant cells compared to irradiated *KRAS* WT cells and may possibly be associated with a radiation resistant phenotype. We have also identified a group of 6 miRNAs, which included miR-224, that were abolished in irradiated *KRAS* mutant cells. The knockdown of miR-224 in HCT116 *KRAS* WT cells however did not mediate a KRAS-mediated resistant phenotype in

KRAS WT cells. However, miR-224 has been shown to be associated with a radiation sensitive phenotype in medulloblastomas (Gokhake *et al*, 2010) and glioblastomas (Upraity *et al*, 2014). The data in the present study does provide a starting point from which candidate miRNAs can be explored further for their role in radiation response in future studies.

5.5. Conclusions and Future work

5.5.1. Conclusions

The present study has identified a common miRNA radiation response expression signature, where the miRNAs may have roles in mediating radiation-induced inflammation and cancer invasion. The study has also suggested miRNAs that may play a role in regulating KRAS-mediated radiation resistance.

5.5.2. Future work

Future work would be directed towards exploring the role of some of the other listed miRNAs in radiation response in colorectal cancer *in vitro* and determining any association with regulating *KRAS* expression and signalling. There is also a need for more detailed time course experiments to determine the extent of miRNA induction or inhibition at different radiation doses.

Radiotherapy is usually administered in a regimen involving 5-FU-based chemotherapy. A major priority will be to conduct detailed chemo-radiation experiments in isogenic *KRAS* WT and mutant cells colorectal cancer cells to investigate the links between miRNAs and KRAS signalling in response to both 5-

FU and radiation. Moreover, using the drug resistant cell lines generated and described in Chapter 4, future work would also be directed towards investigating the miRNAs and pathways involved in cross-resistance to radiation treatment.

Chapter 6

Conclusions and future perspectives

The present study set out to add to ongoing research into the molecular and genetic basis of colorectal cancer development and the mechanisms of resistance to commonly administered chemotherapeutic drugs and radiotherapy. Colorectal cancer remains a major cause of cancer-related death in the UK and is partly attributed to a failure to detect the disease at its early stages and also to inherent and acquired resistance to current drug and radiation treatment.

Previous studies have shown at a molecular level variability amongst colorectal cancer patients in disease progression and prognosis as well as in response to treatment. Inter-patient differences in *KRAS* mutation status in colorectal cancers have been shown to impact patient survival (Andreyev *et al*, 1998; Andreyev *et al,* 2001; Conlin *et al*, 2005) and response to therapy such as the anti-EGFR monoclonal antibody drug cetuximab (Lievre *et al*, 2006; Bokemeyer *et al*, 2008; Amado *et al*, 2008). Mutant *KRAS* has also been shown in colorectal cancer cell lines to affect resistance to radiation (Jeong *et al*, 2009; Oh *et al*, 2010; Luu *et al*, 2013). Moreover, inter-patient differences in p53 status or the expression of genes encoding drug transporters, for example, have been shown to impact both inherent and acquired drug resistance (Boyer *et al*, 2004; Gazzaniga *et al*, 2010).

MiRNAs, which were first discovered in the early nineties (Lee *et al*, 1993), have emerged as additional regulators of gene expression. Calin *et al* (2002) first reported a role for miRNAs in the development of cancer and subsequent studies have also reported on the integral role miRNAs play in modulating

cellular drug and radiation response and resistance in a number of cancers (Hummel *et al*, 2010). The general aims of the present study were therefore to explore the potential of miRNAs as biomarkers of disease progression and treatment response in colorectal cancer.

Given the importance of *KRAS* mutation status in patient survival as reported previously in our research group (Conlin *et al*, 2005), the present study aimed to firstly explore how inter-patient variability in miRNAs regulating KRAS and its signalling pathways affected disease progression and their potential to further sub-classify colorectal cancers. My data showed the over-expression of miR-224 in colorectal cancer to be an early and persistent event in colorectal cancer as it was one of 7 miRNAs found to be increased in colorectal adenomas and cancers compared to patient-matched normal tissue. My study also showed that miR-224 was the most abundantly differentially expressed miRNA in isogenic *KRAS* WT and mutant HCT116 colorectal cancer cell lines, with a higher expression of miR-224 in *KRAS* WT cells. The knockdown of miR-224 in *KRAS* WT cells increased the amount of GTP-bound activated KRAS and also increased ERK 1/2 phosphorylation, thus increasing KRAS signalling and mimicking a *KRAS* mutant phenotype. Furthermore, miR-224 expression was found to be under-expressed in *BRAF* mutant colorectal cancers compared to *KRAS* and *BRAF* WT cancers. This suggests that the expression of miR-224 was suppressed by a currently unknown factor downstream of RAF-1 in both the *KRAS* mutant cell lines and *BRAF* mutant colorectal cancers.

Additionally, miR-224 regulated 5-FU sensitivity by indirectly affecting expression of 5-FU metabolising enzymes and perhaps through the regulation of KRAS signalling, although more work is required to further explore and verify this relationship.

MiR-224 knockdown also reduced cell invasion *in vitro* and miR-224 expression was shown to be decreased in lymph node metastases but increased in liver metastases assessed in comparison to patient-matched primary colorectal cancers. Inter-patient differences in miR-224 expression in liver metastases suggest that miR-224 may have an important role in driving metastasis in some patients whereas in other patients, other mechanisms may dominate.

In the wider context, the present study has for the first time showed that miR-224 regulates KRAS signalling. It also suggests that miR-224 may have an important role in driving disease progression in colorectal cancer, although it is too early to state whether this is likely to be directly through KRAS-mediated tumorigenesis. Taken together, miR-224 could be a useful disease progression biomarker in conjunction with other markers to aid in determining patient prognosis. MiRNAs in blood serum have been shown to be stable biomarkers of disease progression in colorectal cancer (Chen *et al*, 2008; Mitchell *et al*, 2008), and thus exploring the potential of miR-224 as a non-invasive serum biomarker would be a future objective. Our close links with the Scottish National Bowel Screening Programme, directed by Professor Steele, will greatly facilitate these studies.

I have highlighted that a single miRNA can target a multitude of genes due to imperfect complementarity. Therefore miRNAs can in theory target and repress the translation of genes that have opposing effects on a particular pathway. Previous studies have, for example, shown an oncogenic role for miR-224 through its repression of the tumour suppressor *SMAD4* (Wang *et al*, 2013; Zhang *et al*, 2013*a*) and a pro-apoptotic role through the repression of the apoptosis inhibitor *API5* (Wang *et al*, 2008). This shows that the miRNA-mRNA network within a given pathway is tightly controlled and that the net effect of modulating the expression of a miRNA can be tipped in favour of proliferation or apoptosis depending on certain external selective pressures. It also demonstrates the complexities of trying to elucidate how miRNAs regulate particular cellular phenotypes. MiRNAs are, however, better placed than protein coding genes to aid as biomarkers. The differential expression of a single miRNA may occur as a result of many upstream molecular events and represents an easier marker to exploit and detect.

My second aim was to generate 5-FU and oxaliplatin resistant cell lines by incremental drug selection and to further investigate the role of miRNAs in the mechanism of acquired resistance. My findings show that miRNA and mRNA profiling and bioinformatics analysis predicted cancer-related pathways and processes involved with cell invasion, cell cycle regulation and glycolysis as drug resistance mechanisms, which were then experimentally validated in paired 5-FU and oxaliplatin resistant and sensitive cell lines. The study also identified candidate drug resistance genes that were some of the most abundantly over or

under-expressed genes in drug resistant cell lines and were reported to be involved in the aforementioned cancer-related pathways and processes (*ACTB, TUBB, ANGPTL4, MCM4, ALDOA, PGAM1, and AKR1C3*). A miRNA target prediction database was then used to predict how my proposed candidate drug resistance miRNAs could regulate the expression of my proposed candidate genes and thus modulate drug resistance mechanisms. The expression of the DNA replication licensing factor, MCM4 which was under-expressed in my drug resistant cell lines could, for example, be regulated by candidate drug resistance miRNAs such as miR-24 or miR-93 which were overexpressed in drug resistant cells. The under-expression of miR-224 was also shown to be associated with a drug resistance phenotype.

This work was one of four studies conducted concurrently in colorectal cancer where miRNAs had been profiled in paired 5-FU or oxaliplatin resistant and sensitive cell lines (Akao *et al*, 2011; Kurokawa *et al*, 2012; Zhou *et al*, 2014). This work benefits from the use of controlled, cell line backgrounds to identify novel miRNA and mRNA markers of 5-FU and/or oxaliplatin drug resistance in colorectal cancer that could then be tested in patients to determine whether they discriminate between good and poor responders to drug treatment.

Thirdly, the present study aimed to further investigate the molecular basis of radiation response and KRAS-mediated radiation resistance using miRNA expression profiling in isogenic *KRAS* WT and mutant colorectal cancer cells following irradiation. Bioinformatics analysis predicted that pathways and processes involved in radiation response were similar to those predicted in

acquired drug resistance. Adding to previous studies describing a role for members of the let-7 family in regulating KRAS signalling and radiation response, the present study also identified a number of miRNAs, including miR-224, that were differentially expressed in irradiated *KRAS* WT and mutant cells and that may modulate KRAS-mediated radiation resistance. A major priority to this work is also to conduct more detailed chemo-radiation experiments in isogenic *KRAS* WT and mutant colorectal cancer cells and paired 5-FU or oxaliplatin resistant and sensitive colorectal cancer cells.

The similarities in the pathways and processes associated with miRNAs differentially expressed in acquired 5-FU and oxaliplatin resistance, and also in the acute response to radiation suggest that cells undergo a similar stress response (long term or acute) in both experiments. However, it does also raise questions on whether these pathways and processes are enriched as a result of the predicted targets of a specific list of miRNAs, or whether it is likely that most miRNA lists would lead to similar enrichment of the aforementioned pathways and processes, perhaps due to the large number of genes that a single miRNA can target. Nevertheless, as discussed previously, many of the aforementioned pathways and processes have been experimentally validated in previous studies.

The present study has suggested some potential markers and modulators of disease progression and resistance to drug and radiotherapy. The natural progression of this work will be to validate the most promising candidates in cancers from cohorts of colorectal patients who have received chemotherapy

and/or radiotherapy. The identification of these cohorts is a task that is already underway.

References

1. Acloque H, Thiery JP & Nieto MA (2008). The physiology and pathology of the EMT. Meeting on the epithelial-mesenchymal transition. *EMBO Rep* **9,** 322–326.

2. Akao Y, Noguchi S, Iio A, Kojima K, Takagi T & Naoe T (2011). Dysregulation of microRNA-34a expression causes drug-resistance to 5-FU in human colon cancer DLD-1 cells. *Cancer Lett* **300,** 197–204.

3. Amado RG, Wolf M, Peeters M, Van Cutsem E, Siena S, Freeman DJ, Juan T, Sikorski R, Suggs S, Radinsky R, Patterson SD & Chang DD (2008). Wild-type KRAS is required for panitumumab efficacy in patients with metastatic colorectal cancer. *J Clin Oncol* **26,** 1626–1634.

4. Andarawewa KL, Erickson AC, Chou WS, Costes SV, Gascard P, Mott JD, Bissell MJ & Barcellos-Hoff MH (2007). Ionizing radiation predisposes nonmalignant human mammary epithelial cells to undergo transforming growth factor beta induced epithelial to mesenchymal transition. *Cancer Res* **67,** 8662–8670.

5. Andreyev HJ et al. (2001). Kirsten ras mutations in patients with colorectal cancer: the "RASCAL II" study. *Br J Cancer* **85,** 692–696.

6. Andreyev HJ, Norman AR, Cunningham D, Oates JR & Clarke PA (1998). Kirsten ras mutations in patients with colorectal cancer: the multicenter "RASCAL" study. *J Natl Cancer Inst* **90,** 675–684.

7. De Angelis PM, Svendsrud DH, Kravik KL & Stokke T (2006). Cellular response to 5-fluorouracil (5-FU) in 5-FU-resistant colon cancer cell lines during treatment and recovery. *Mol Cancer* **5,** 20.

8. Arndt GM, Dossey L, Cullen LM, Lai A, Druker R, Eisbacher M, Zhang C, Tran N, Fan H, Retzlaff K, Bittner A & Raponi M (2009). Characterization of global microRNA expression reveals oncogenic potential of miR-145 in metastatic colorectal cancer. *BMC Cancer* **9,** 374.

9. Arnold CN, Goel A & Boland CR (2003). Role of hMLH1 promoter hypermethylation in drug resistance to 5-fluorouracil in colorectal cancer cell lines. *Int J Cancer* **106,** 66–73.

10. Arnould S, Hennebelle I, Canal P, Bugat R & Guichard S (2003). Cellular determinants of oxaliplatin sensitivity in colon cancer cell lines. *European Journal of Cancer* **39,** 112–119.

11. Asangani IA, Rasheed SAK, Nikolova DA, Leupold JH, Colburn NH, Post S & Allgayer H (2008). MicroRNA-21 (miR-21) post-transcriptionally downregulates tumor suppressor Pdcd4 and stimulates invasion, intravasation and metastasis in colorectal cancer. *Oncogene* **27,** 2128–2136.

12. Balaguer F, Link A, Lozano JJ, Cuatrecasas M, Nagasaka T, Boland CR & Goel A (2010). Epigenetic silencing of miR-137 is an early event in colorectal carcinogenesis. *Cancer Res* **70,** 6609–6618.

13. Bandres E, Agirre X, Bitarte N, Ramirez N, Zarate R, Roman-Gomez J, Prosper F & Garcia-Foncillas J (2009). Epigenetic regulation of microRNA expression in colorectal cancer. *Int J Cancer* **125,** 2737–2743.

14. Bandrés E, Cubedo E, Agirre X, Malumbres R, Zárate R, Ramirez N, Abajo A, Navarro A, Moreno I, Monzó M & García-Foncillas J (2006). Identification by Real-time PCR of 13 mature microRNAs differentially expressed in colorectal cancer and non-tumoral tissues. *Mol Cancer* **5,** 29.

15. Barbacid M (1990). Ras oncogenes: their role in neoplasia. *European Journal of Clinical Investigation* **20,** 225–235.

16. Barski OA, Tipparaju SM & Bhatnagar A (2008). The aldo-keto reductase superfamily and its role in drug metabolism and detoxification. *Drug Metab Rev* **40,** 553–624.

17. Bartel DP (2004). MicroRNAs: genomics, biogenesis, mechanism, and function. *Cell* **116,** 281–297.

18. Bartley AN, Yao H, Barkoh BA, Ivan C, Mishra BM, Rashid A, Calin GA, Luthra R & Hamilton SR (2011). Complex patterns of altered MicroRNA expression during the adenoma-adenocarcinoma sequence for microsatellite-stable colorectal cancer. *Clin Cancer Res* **17,** 7283–7293.

19. Battle TE, Lynch RA & Frank DA (2006). Signal transducer and activator of transcription 1 activation in endothelial cells is a negative regulator of angiogenesis. *Cancer Res* **66,** 3649–3657.

20. Benjamini Y & Hochberg Y (1995). Controlling the False Discovery Rate: A Practical and Powerful Approach to Multiple Testing. *Journal of the Royal Statistical Society Series B (Methodological)* **57,** 289–300.

21. Bernhard EJ, Kao G, Cox AD, Sebti SM, Hamilton AD, Muschel RJ & McKenna WG (1996). The farnesyltransferase inhibitor FTI-277 radiosensitizes H-ras-transformed rat embryo fibroblasts. *Cancer Res* **56,** 1727–1730.

22. Bernhard EJ, Stanbridge EJ, Gupta S, Gupta AK, Soto D, Bakanauskas VJ, Cerniglia GJ, Muschel RJ & McKenna WG (2000). Direct evidence for the contribution of activated N-ras and K-ras oncogenes to increased intrinsic radiation resistance in human tumor cell lines. *Cancer Res* **60,** 6597–6600.

23. Bese NS, Sut PA & Ober A (2005). The effect of treatment interruptions in the postoperative irradiation of breast cancer. *Oncology* **69,** 214–223.

24. Bierie B & Moses HL (2006). TGF-beta and cancer. *Cytokine Growth Factor Rev* **17,** 29–40.

25. Blower PE, Verducci JS, Lin S, Zhou J, Chung J-H, Dai Z, Liu C-G, Reinhold W, Lorenzi PL, Kaldjian EP, Croce CM, Weinstein JN & Sadee W (2007). MicroRNA expression profiles for the NCI-60 cancer cell panel. *Mol Cancer Ther* **6,** 1483–1491.

26. Bojmar L, Karlsson E, Ellegård S, Olsson H, Björnsson B, Hallböök O, Larsson M, Stål O & Sandström P (2013). The role of microRNA-200 in progression of human colorectal and breast cancer. *PLoS ONE* **8,** e84815.

27. Bokemeyer C, Bondarenko I, Hartmann JT, De Braud FG, Volovat C, Nippgen J, Stroh C, Celik I & Koralewski P (2008). KRAS status and efficacy of first-line treatment of patients with metastatic colorectal cancer (mCRC) with FOLFOX with or without cetuximab: The OPUS experience. *ASCO Meeting Abstracts* **26,** 4000.

28. Boni V, Bitarte N, Cristobal I, Zarate R, Rodriguez J, Maiello E, Garcia-Foncillas J & Bandres E (2010). miR-192/miR-215 influence 5-fluorouracil resistance through cell cycle-mediated mechanisms complementary to its post-transcriptional thymidilate synthase regulation. *Mol Cancer Ther* **9,** 2265–2275.

29. Borralho PM, Kren BT, Castro RE, da Silva IBM, Steer CJ & Rodrigues CMP (2009). MicroRNA-143 reduces viability and increases sensitivity to 5-fluorouracil in HCT116 human colorectal cancer cells. *FEBS J* **276,** 6689–6700.

30. Boyer J, McLean EG, Aroori S, Wilson P, McCulla A, Carey PD, Longley DB & Johnston PG (2004). Characterization of p53 Wild-Type and Null Isogenic Colorectal Cancer Cell Lines Resistant to 5-Fluorouracil, Oxaliplatin, and Irinotecan. *Clin Cancer Res* **10,** 2158–2167.

31. Brattain MG, Fine WD, Khaled FM, Thompson J & Brattain DE (1981). Heterogeneity of malignant cells from a human colonic carcinoma. *Cancer Res* **41,** 1751–1756.

32. Brueckner B, Stresemann C, Kuner R, Mund C, Musch T, Meister M, Sültmann H & Lyko F (2007). The Human let-7a-3 Locus Contains an Epigenetically Regulated MicroRNA Gene with Oncogenic Function. *Cancer Res* **67,** 1419–1423.

33. Brunet Vega A, Pericay C, Moya I, Ferrer A, Dotor E, Pisa A, Casalots À, Serra-Aracil X, Oliva J-C, Ruiz A & Saigí E (2013). microRNA expression profile in stage III colorectal cancer: circulating miR-18a and miR-29a as promising biomarkers. *Oncol Rep* **30,** 320–326.

34. Burk U, Schubert J, Wellner U, Schmalhofer O, Vincan E, Spaderna S & Brabletz T (2008). A reciprocal repression between ZEB1 and members of the miR-200 family promotes EMT and invasion in cancer cells. *EMBO Rep* **9,** 582–589.

35. Calin GA, Dumitru CD, Shimizu M, Bichi R, Zupo S, Noch E, Aldler H, Rattan S, Keating M, Rai K, Rassenti L, Kipps T, Negrini M, Bullrich F & Croce CM (2002). Frequent deletions and down-regulation of micro- RNA genes miR15 and miR16 at 13q14 in chronic lymphocytic leukemia. *Proc Natl Acad Sci USA* **99,** 15524–15529.

36. Calin GA, Liu C-G, Sevignani C, Ferracin M, Felli N, Dumitru CD, Shimizu M, Cimmino A, Zupo S, Dono M, Dell'Aquila ML, Alder H, Rassenti L, Kipps TJ, Bullrich F, Negrini M & Croce CM (2004*a*). MicroRNA profiling reveals distinct signatures in B cell chronic lymphocytic leukemias. *PNAS* **101,** 11755–11760.

37. Calin GA, Sevignani C, Dumitru CD, Hyslop T, Noch E, Yendamuri S, Shimizu M, Rattan S, Bullrich F, Negrini M & Croce CM (2004*b*). Human microRNA genes are frequently located at fragile sites and genomic regions involved in cancers. *Proc Natl Acad Sci USA* **101,** 2999–3004.

38. Camp ER, Li J, Minnich DJ, Brank A, Moldawer LL, MacKay SLD & Hochwald SN (2004). Inducible nuclear factor-kappaB activation contributes to chemotherapy resistance in gastric cancer. *J Am Coll Surg* **199,** 249–258.

39. Cancer Research UK (2014). Bowel cancer statistics. Available at: http://www.cancerresearchuk.org/cancer-info/cancerstats/types/bowel/ [Accessed June 29, 2014].

40. Chai H, Liu M, Tian R, Li X & Tang H (2011). miR-20a targets BNIP2 and contributes chemotherapeutic resistance in colorectal adenocarcinoma SW480 and SW620 cell lines. *Acta Biochim Biophys Sin (Shanghai)* **43,** 217–225.

41. Chang KH, Miller N, Kheirelseid EAH, Lemetre C, Ball GR, Smith MJ, Regan M, McAnena OJ & Kerin MJ (2011). MicroRNA signature analysis in colorectal cancer: identification of expression profiles in stage II tumors associated with aggressive disease. *Int J Colorectal Dis* **26,** 1415–1422.

42. Chang T-C, Wentzel EA, Kent OA, Ramachandran K, Mullendore M, Lee KH, Feldmann G, Yamakuchi M, Ferlito M, Lowenstein CJ, Arking DE, Beer MA, Maitra A & Mendell JT (2007). Transactivation of miR-34a by p53 broadly influences gene expression and promotes apoptosis. *Mol Cell* **26,** 745–752.

43. Chang T-C, Yu D, Lee Y-S, Wentzel EA, Arking DE, West KM, Dang CV, Thomas-Tikhonenko A & Mendell JT (2008). Widespread microRNA repression by Myc contributes to tumorigenesis. *Nat Genet* **40,** 43–50.

44. De la Chapelle A (2004). Genetic predisposition to colorectal cancer. *Nat Rev Cancer* **4,** 769–780.

45. Chaudhry MA, Sachdeva H & Omaruddin RA (2010). Radiation-Induced Micro-RNA Modulation in Glioblastoma Cells Differing in DNA-Repair Pathways. *DNA and Cell Biology* **29,** 553–561.

46. Chen ML, Liang LS & Wang XK (2012). miR-200c inhibits invasion and migration in human colon cancer cells SW480/620 by targeting ZEB1. *Clin Exp Metastasis* **29,** 457–469.

47. Chen R, Alvero AB, Silasi D-A & Mor G (2007). Inflammation, cancer and chemoresistance: taking advantage of the toll-like receptor signaling pathway. *Am J Reprod Immunol* **57,** 93–107.

48. Chen S, Cai J, Zhang W, Zheng X, Hu S, Lu J, Xing J & Dong Y (2014). Proteomic identification of differentially expressed proteins associated with the multiple drug resistance in methotrexate-resistant human breast cancer cells. *Int J Oncol* **45,** 448–458.

49. Chen X et al. (2008). Characterization of microRNAs in serum: a novel class of biomarkers for diagnosis of cancer and other diseases. *Cell Res* **18,** 997–1006.

50. Chen X, Guo X, Zhang H, Xiang Y, Chen J, Yin Y, Cai X, Wang K, Wang G, Ba Y, Zhu L, Wang J, Yang R, Zhang Y, Ren Z, Zen K, Zhang J & Zhang C-Y (2009). Role of miR-143 targeting KRAS in colorectal tumorigenesis. *Oncogene* **28,** 1385–1392.

51. Christoffersen NR, Silahtaroglu A, Orom UA, Kauppinen S & Lund AH (2007). miR-200b mediates post-transcriptional repression of ZFHX1B. *RNA* **13,** 1172–1178.

52. Chun-Zhi Z, Lei H, An-Ling Z, Yan-Chao F, Xiao Y, Guang-Xiu W, Zhi-Fan J, Pei-Yu P, Qing-Yu Z & Chun-Sheng K (2010). MicroRNA-221 and microRNA-222 regulate gastric carcinoma cell proliferation and radioresistance by targeting PTEN. *BMC Cancer* **10,** 367.

53. Climent J, Dimitrow P, Fridlyand J, Palacios J, Siebert R, Albertson DG, Gray JW, Pinkel D, Lluch A & Martinez-Climent JA (2007). Deletion of chromosome 11q predicts response to anthracycline-based chemotherapy in early breast cancer. *Cancer Res* **67,** 818–826.

54. Conlin A, Smith G, Carey FA, Wolf CR & Steele RJC (2005). The prognostic significance of K-ras, p53, and APC mutations in colorectal carcinoma. *Gut* **54,** 1283–1286.

55. Croce CM (2009). Causes and consequences of microRNA dysregulation in cancer. *Nat Rev Genet* **10,** 704–714.

56. Cunningham D, Humblet Y, Siena S, Khayat D, Bleiberg H, Santoro A, Bets D, Mueser M, Harstrick A, Verslype C, Chau I & Van Cutsem E (2004). Cetuximab monotherapy and cetuximab plus irinotecan in irinotecan-refractory metastatic colorectal cancer. *N Engl J Med* **351,** 337–345.

57. Dallas NA, Xia L, Fan F, Gray MJ, Gaur P, van Buren G 2nd, Samuel S, Kim MP, Lim SJ & Ellis LM (2009). Chemoresistant colorectal cancer cells, the cancer stem cell phenotype, and increased sensitivity to insulin-like growth factor-I receptor inhibition. *Cancer Res* **69,** 1951–1957.

58. Deng J, Lei W, Fu J-C, Zhang L, Li J-H & Xiong J-P (2014). Targeting miR-21 enhances the sensitivity of human colon cancer HT-29 cells to chemoradiotherapy in vitro. *Biochem Biophys Res Commun* **443,** 789–795.

59. Deng S, Calin GA, Croce CM, Coukos G & Zhang L (2008). Mechanisms of microRNA deregulation in human cancer. *Cell Cycle* **7,** 2643–2646.

60. Dent P, Reardon DB, Park JS, Bowers G, Logsdon C, Valerie K & Schmidt-Ullrich R (1999). Radiation-induced Release of Transforming Growth Factor ? Activates the Epidermal Growth Factor Receptor and Mitogen-activated Protein Kinase Pathway in Carcinoma Cells, Leading to Increased Proliferation and Protection from Radiation-induced Cell Death. *Mol Biol Cell* **10,** 2493–2506.

61. Dent P, Yacoub A, Fisher PB, Hagan MP & Grant S (2003). MAPK pathways in radiation responses. *Oncogene* **22,** 5885–5896.

62. Dexter DL, Spremulli EN, Fligiel Z, Barbosa JA, Vogel R, VanVoorhees A & Calabresi P (1981). Heterogeneity of cancer cells from a single human colon carcinoma. *Am J Med* **71,** 949–956.

63. Diosdado B, van de Wiel MA, Terhaar Sive Droste JS, Mongera S, Postma C, Meijerink WJHJ, Carvalho B & Meijer GA (2009). MiR-17-92 cluster is associated with 13q gain and c-myc expression during colorectal adenoma to adenocarcinoma progression. *Br J Cancer* **101,** 707–714.

64. Douillard JY, Cunningham D, Roth AD, Navarro M, James RD, Karasek P, Jandik P, Iveson T, Carmichael J, Alakl M, Gruia G, Awad L & Rougier P (2000). Irinotecan combined with fluorouracil compared with fluorouracil alone as first-line treatment for metastatic colorectal cancer: a multicentre randomised trial. *Lancet* **355,** 1041–1047.

65. Downward J (2003). Targeting RAS signalling pathways in cancer therapy. *Nat Rev Cancer* **3,** 11–22.

66. Dukes CE (1932). The classification of cancer of the rectum. *J Pathol* **35,** 323–332.

67. Earle JSL, Luthra R, Romans A, Abraham R, Ensor J, Yao H & Hamilton SR (2010). Association of microRNA expression with microsatellite instability status in colorectal adenocarcinoma. *J Mol Diagn* **12,** 433–440.

68. Edge S., Byrd D., Compton C., Fritz A., Greene F. & Trotti A (2010). *AJCC Cancer Staging Manual*, 7th Edition. Springer, New York, N.Y.

69. Ellis CA & Clark G (2000). The importance of being K-Ras. *Cell Signal* **12,** 425–434.

70. Esquela-Kerscher A & Slack FJ (2006). Oncomirs - microRNAs with a role in cancer. *Nat Rev Cancer* **6,** 259–269.

71. Etienne-Grimaldi M-C, Formento J-L, Francoual M, François E, Formento P, Renée N, Laurent-Puig P, Chazal M, Benchimol D, Delpero J-R, Letoublon C, Pezet D, Seitz J-F & Milano G (2008). K-Ras mutations and treatment outcome in colorectal cancer patients receiving exclusive fluoropyrimidine therapy. *Clin Cancer Res* **14,** 4830–4835.

72. Faltejskova P, Svoboda M, Srutova K, Mlcochova J, Besse A, Nekvindova J, Radova L, Fabian P, Slaba K, Kiss I, Vyzula R & Slaby O (2012). Identification and functional screening of microRNAs highly deregulated in colorectal cancer. *J Cell Mol Med* **16,** 2655–2666.

73. Fernández-Peralta AM, Nejda N, Oliart S, Medina V, Azcoita MM & González-Aguilera JJ (2005). Significance of mutations in TGFBR2 and BAX in neoplastic progression and patient outcome in sporadic colorectal tumors with high-frequency microsatellite instability. *Cancer Genet Cytogenet* **157,** 18–24.

74. Fijneman RJA et al. (2012). Proximal fluid proteome profiling of mouse colon tumors reveals biomarkers for early diagnosis of human colorectal cancer. *Clin Cancer Res* **18,** 2613–2624.

75. FitzGerald TJ, Daugherty C, Kase K, Rothstein LA, McKenna M & Greenberger JS (1985). Activated human N-ras oncogene enhances x-irradiation repair of mammalian cells in vitro less effectively at low dose rate. Implications for increased therapeutic ratio of low dose rate irradiation. *Am J Clin Oncol* **8,** 517–522.

76. Di Francesco AM, Ruggiero A & Riccardi R (2002). Cellular and molecular aspects of drugs of the future: oxaliplatin. *Cell Mol Life Sci* **59,** 1914–1927.

77. Frattini M, Balestra D, Suardi S, Oggionni M, Alberici P, Radice P, Costa A, Daidone MG, Leo E, Pilotti S, Bertario L & Pierotti MA (2004). Different genetic features associated with colon and rectal carcinogenesis. *Clin Cancer Res* **10,** 4015–4021.

78. Fu J, Tang W, Du P, Wang G, Chen W, Li J, Zhu Y, Gao J & Cui L (2012). Identifying microRNA-mRNA regulatory network in colorectal cancer by a combination of expression profile and bioinformatics analysis. *BMC Syst Biol* **6,** 68.

79. Fukuda T, Yamagata K, Fujiyama S, Matsumoto T, Koshida I, Yoshimura K, Mihara M, Naitou M, Endoh H, Nakamura T, Akimoto C, Yamamoto Y, Katagiri T, Foulds C, Takezawa S, Kitagawa H, Takeyama K, O'Malley BW & Kato S (2007). DEAD-box RNA helicase subunits of the Drosha complex are required for processing of rRNA and a subset of microRNAs. *Nat Cell Biol* **9,** 604–611.

80. Gao H, Yu B, Yan Y, Shen J, Zhao S, Zhu J, Qin W & Gao Y (2013). Correlation of expression levels of ANXA2, PGAM1, and CALR with glioma grade and prognosis. *J Neurosurg* **118,** 846–853.

81. Gastaldi C, Bertero T, Xu N, Bourget-Ponzio I, Lebrigand K, Fourre S, Popa A, Cardot-Leccia N, Meneguzzi G, Sonkoly E, Pivarcsi A, Mari B, Barbry P, Ponzio G & Rezzonico R (2014). miR-193b/365a cluster controls progression of epidermal squamous cell carcinoma. *Carcinogenesis* **35,** 1110–1120.

82. Gazzaniga P, Gradilone A, Petracca A, Nicolazzo C, Raimondi C, Iacovelli R, Naso G & Cortesi E (2010). Molecular markers in circulating cancer cells from metastatic colorectal cancer patients. *J Cell Mol Med* **14,** 2073–2077.

83. Gentleman RC et al. (2004). Bioconductor: open software development for computational biology and bioinformatics. *Genome Biol* **5,** R80.

84. Gmeiner WH, Reinhold WC & Pommier Y (2010). Genome-Wide mRNA and microRNA Profiling of the NCI 60 Cell-Line Screen and Comparison of FdUMP[10] with Fluorouracil, Floxuridine, and Topoisomerase 1 Poisons. *Mol Cancer Ther* **9,** 3105–3114.

85. Gokhale A, Kunder R, Goel A, Sarin R, Moiyadi A, Shenoy A, Mamidipally C, Noronha S, Kannan S & Shirsat NV (2010). Distinctive microRNA signature of medulloblastomas associated with the WNT signaling pathway. *J Cancer Res Ther* **6,** 521–529.

86. Goto T, Shinmura K, Yokomizo K, Sakuraba K, Kitamura Y, Shirahata A, Saito M, Kigawa G, Nemoto H, Sanada Y & Hibi K (2012). Expression levels of thymidylate synthase, dihydropyrimidine dehydrogenase, and thymidine phosphorylase in patients with colorectal cancer. *Anticancer Res* **32,** 1757–1762.

87. Gourdier I, Del Rio M, Crabbé L, Candeil L, Copois V, Ychou M, Auffray C, Martineau P, Mechti N, Pommier Y & Pau B (2002). Drug specific resistance to oxaliplatin is associated with apoptosis defect in a cellular model of colon carcinoma. *FEBS Lett* **529,** 232–236.

88. De Gramont A, Figer A, Seymour M, Homerin M, Hmissi A, Cassidy J, Boni C, Cortes-Funes H, Cervantes A, Freyer G, Papamichael D, Le Bail N, Louvet C, Hendler D, de Braud F, Wilson C, Morvan F & Bonetti A (2000). Leucovorin and fluorouracil with or without oxaliplatin as first-line treatment in advanced colorectal cancer. *J Clin Oncol* **18,** 2938–2947.

89. Grana TM, Rusyn EV, Zhou H, Sartor CI & Cox AD (2002). Ras mediates radioresistance through both phosphatidylinositol 3-kinase-dependent and Raf-dependent but mitogen-activated protein kinase/extracellular signal-regulated kinase kinase-independent signaling pathways. *Cancer Res* **62,** 4142–4150.

90. Gray LH, Conger AD, Ebert M, Hornsey S & Scott OCA (1953). The Concentration of Oxygen Dissolved in Tissues at the Time of Irradiation as a Factor in Radiotherapy. *The British Journal of Radiology* **26,** 638–648.

91. Guo C, Liu S, Wang J, Sun M-Z & Greenaway FT (2013). ACTB in cancer. *Clin Chim Acta* **417,** 39–44.

92. Gupta AK, Bakanauskas VJ, Cerniglia GJ, Cheng Y, Bernhard EJ, Muschel RJ & McKenna WG (2001). The Ras radiation resistance pathway. *Cancer Res* **61,** 4278–4282.

93. Hamaguchi T, Iizuka N, Tsunedomi R, Hamamoto Y, Miyamoto T, Iida M, Tokuhisa Y, Sakamoto K, Takashima M, Tamesa T & Oka M (2008). Glycolysis module activated by hypoxia-inducible factor 1alpha is related to the aggressive phenotype of hepatocellular carcinoma. *Int J Oncol* **33,** 725–731.

94. Hamfjord J, Stangeland AM, Hughes T, Skrede ML, Tveit KM, Ikdahl T & Kure EH (2012). Differential expression of miRNAs in colorectal cancer: comparison of paired tumor tissue and adjacent normal mucosa using high-throughput sequencing. *PLoS ONE* **7,** e34150.

95. Harada H, Andersen JS, Mann M, Terada N & Korsmeyer SJ (2001). p70S6 kinase signals cell survival as well as growth, inactivating the pro-apoptotic molecule BAD. *Proc Natl Acad Sci USA* **98,** 9666–9670.

96. Harris AL (2002). Hypoxia--a key regulatory factor in cancer growth. *Nat Rev Cancer* **2,** 38–47.

97. Hashimoto Y, Akiyama Y & Yuasa Y (2013). Multiple-to-multiple relationships between microRNAs and target genes in gastric cancer. *PLoS ONE* **8,** e62589.

98. Hatley ME, Patrick DM, Garcia MR, Richardson JA, Bassel-Duby R, van Rooij E & Olson EN (2010). Modulation of K-Ras-dependent lung tumorigenesis by MicroRNA-21. *Cancer Cell* **18,** 282–293.

99. Horikawa Y, Wood CG, Yang H, Zhao H, Ye Y, Gu J, Lin J, Habuchi T & Wu X (2008). Single Nucleotide Polymorphisms of microRNA Machinery Genes Modify the Risk of Renal Cell Carcinoma. *Clin Cancer Res* **14,** 7956–7962.

100. Hu H & Gatti RA (2011). MicroRNAs: new players in the DNA damage response. *J Mol Cell Biol* **3,** 151–158.

101. Huang L, Dai T, Lin X, Zhao X, Chen X, Wang C, Li X, Shen H & Wang X (2012*a*). MicroRNA-224 targets RKIP to control cell invasion and expression of metastasis genes in human breast cancer cells. *Biochem Biophys Res Commun* **425,** 127–133.

102. Huang R-L, Teo Z, Chong HC, Zhu P, Tan MJ, Tan CK, Lam CRI, Sng MK, Leong DTW, Tan SM, Kersten S, Ding JL, Li HY & Tan NS (2011). ANGPTL4 modulates vascular junction integrity by integrin signaling and disruption of intercellular VE-cadherin and claudin-5 clusters. *Blood* **118,** 3990–4002.

103. Huang X-F, Han J, Hu X-T & He C (2012*b*). Mechanisms involved in biological behavior changes associated with Angptl4 expression in colon cancer cell lines. *Oncol Rep* **27,** 1541–1547.

104. Huang Z, Huang D, Ni S, Peng Z, Sheng W & Du X (2010). Plasma microRNAs are promising novel biomarkers for early detection of colorectal cancer. *Int J Cancer* **127,** 118–126.

105. Hummel R, Hussey DJ & Haier J (2010). MicroRNAs: Predictors and modifiers of chemo- and radiotherapy in different cancer types. *European Journal of Cancer* **46,** 298–311.

106. Hurteau GJ, Carlson JA, Spivack SD & Brock GJ (2007). Overexpression of the microRNA hsa-miR-200c leads to reduced expression of transcription factor 8 and increased expression of E-cadherin. *Cancer Res* **67,** 7972–7976.

107. Illemann M, Bird N, Majeed A, Sehested M, Laerum OD, Lund LR, Danø K & Nielsen BS (2006). MMP-9 is differentially expressed in primary human colorectal adenocarcinomas and their metastases. *Mol Cancer Res* **4,** 293–302.

108. Jeong S-H, Wu H-G & Park W-Y (2009). LIN28B confers radio-resistance through the posttranscriptional control of KRAS. *Exp Mol Med* **41,** 912–918.

109. Jiang W, Kahn SM, Guillem JG, Lu SH & Weinstein IB (1989). Rapid detection of ras oncogenes in human tumors: applications to colon, esophageal, and gastric cancer. *Oncogene* **4,** 923–928.

110. John-Aryankalayil M, Palayoor ST, Makinde AY, Cerna D, Simone CB, Falduto MT, Magnuson SR & Coleman CN (2012). Fractionated radiation alters oncomir and tumor suppressor miRNAs in human prostate cancer cells. *Radiat Res* **178,** 105–117.

111. Johnston PG & Kaye S (2001). Capecitabine: a novel agent for the treatment of solid tumors. *Anticancer Drugs* **12,** 639–646.

112. Kavanagh BD, Dent P, Schmidt-Ullrich RK, Chen P & Mikkelsen RB (1998). Calcium-dependent stimulation of mitogen-activated protein kinase activity in A431 cells by low doses of ionizing radiation. *Radiat Res* **149,** 579–587.

113. Kawamoto A, Yokoe T, Tanaka K, Saigusa S, Toiyama Y, Yasuda H, Inoue Y, Miki C & Kusunoki M (2012). Radiation induces epithelial-mesenchymal transition in colorectal cancer cells. *Oncol Rep* **27,** 51–57.

114. Kearsey SE & Labib K (1998). MCM proteins: evolution, properties, and role in DNA replication. *Biochim Biophys Acta* **1398,** 113–136.

115. Kikuchi J, Kinoshita I, Shimizu Y, Kikuchi E, Takeda K, Aburatani H, Oizumi S, Konishi J, Kaga K, Matsuno Y, Birrer MJ, Nishimura M & Dosaka-Akita H (2011). Minichromosome maintenance (MCM) protein 4 as a marker for proliferation and its clinical and clinicopathological significance in non-small cell lung cancer. *Lung Cancer* **72,** 229–237.

116. Kim I-J, Kang HC, Park J-H, Shin Y, Ku J-L, Lim S-B, Park SY, Jung S-Y, Kim HK & Park J-G (2003). Development and applications of a beta-catenin oligonucleotide microarray: beta-catenin mutations are dominantly found in the proximal colon cancers with microsatellite instability. *Clin Cancer Res* **9,** 2920–2925.

117. Kim J-S, Choi YY, Jin G, Kang H-G, Choi J-E, Jeon H-S, Lee W-K, Kim D-S, Kim CH, Kim YJ, Son J-W, Jung TH & Park JY (2010). Association of a common AGO1 variant with lung cancer risk: a two-stage case-control study. *Mol Carcinog* **49,** 913–921.

118. Kinzler KW & Vogelstein B (1996). Lessons from hereditary colorectal cancer. *Cell* **87,** 159–170.

119. Kjersem JB, Ikdahl T, Lingjaerde OC, Guren T, Tveit KM & Kure EH (2014). Plasma microRNAs predicting clinical outcome in metastatic colorectal cancer patients receiving first-line oxaliplatin-based treatment. *Mol Oncol* **8,** 59–67.

120. Klampfer L, Swaby L-A, Huang J, Sasazuki T, Shirasawa S & Augenlicht L (2005). Oncogenic Ras increases sensitivity of colon cancer cells to 5-FU-induced apoptosis. *Oncogene* **24,** 3932–3941.

121. Konishi F & Morson BC (1982). Pathology of colorectal adenomas: a colonoscopic survey. *J Clin Pathol* **35,** 830–841.

122. Kumar A, Collins HM, Scholefield JH & Watson SA (2000). Increased type-IV collagenase (MMP-2 and MMP-9) activity following preoperative radiotherapy in rectal cancer. *Br J Cancer* **82,** 960–965.

123. Kurokawa K, Tanahashi T, Iima T, Yamamoto Y, Akaike Y, Nishida K, Masuda K, Kuwano Y, Murakami Y, Fukushima M & Rokutan K (2012). Role of miR-19b and its target mRNAs in 5-fluorouracil resistance in colon cancer cells. *J Gastroenterol* **47,** 883–895.

124. Kusaba T, Nakayama T, Yamazumi K, Yakata Y, Yoshizaki A, Inoue K, Nagayasu T & Sekine I (2006). Activation of STAT3 is a marker of poor prognosis in human colorectal cancer. *Oncol Rep* **15,** 1445–1451.

125. Lamouille S, Xu J & Derynck R (2014). Molecular mechanisms of epithelial-mesenchymal transition. *Nat Rev Mol Cell Biol* **15,** 178–196.

126. Landi D, Gemignani F, Naccarati A, Pardini B, Vodicka P, Vodickova L, Novotny J, Försti A, Hemminki K, Canzian F & Landi S (2008). Polymorphisms within micro-RNA-binding sites and risk of sporadic colorectal cancer. *Carcinogenesis* **29,** 579–584.

127. Lanza G, Ferracin M, Gafà R, Veronese A, Spizzo R, Pichiorri F, Liu C, Calin GA, Croce CM & Negrini M (2007). mRNA/microRNA gene expression profile in microsatellite unstable colorectal cancer. *Mol Cancer* **6,** 54.

128. Lee RC, Feinbaum RL & Ambros V (1993). The C. elegans heterochronic gene lin-4 encodes small RNAs with antisense complementarity to lin-14. *Cell* **75,** 843–854.

129. Leslie A, Stewart A, Baty DU, Mechan D, McGreavey L, Smith G, Wolf CR, Sales M, Pratt NR, Steele RJC & Carey FA (2006). Chromosomal changes in colorectal adenomas: relationship to gene mutations and potential for clinical utility. *Genes Chromosomes Cancer* **45,** 126–135.

130. Lewis BP, Burge CB & Bartel DP (2005). Conserved seed pairing, often flanked by adenosines, indicates that thousands of human genes are microRNA targets. *Cell* **120,** 15–20.

131. Li Q, Ding C, Chen C, Zhang Z, Xiao H, Xie F, Lei L, Chen Y, Mao B, Jiang M, Li J, Wang D & Wang G (2014). miR-224 promotion of cell migration and invasion by targeting Homeobox D 10 gene in human hepatocellular carcinoma. *J Gastroenterol Hepatol* **29,** 835–842.

132. Li Q, Wang G, Shan J-L, Yang Z-X, Wang H-Z, Feng J, Zhen J-J, Chen C, Zhang Z-M, Xu W, Luo X-Z & Wang D (2010). MicroRNA-224 is upregulated in HepG2 cells and involved in cellular migration and invasion. *J Gastroenterol Hepatol* **25,** 164–171.

133. Li X, Shen Y, Ichikawa H, Antes T & Goldberg GS (2009). Regulation of miRNA expression by Src and contact normalization: effects on nonanchored cell growth and migration. *Oncogene* **28,** 4272–4283.

134. Li X, Zhang G, Luo F, Ruan J, Huang D, Feng D, Xiao D, Zeng Z, Chen X & Wu W (2012). Identification of aberrantly expressed miRNAs in rectal cancer. *Oncol Rep* **28,** 77–84.

135. Liang M, Yao G, Yin M, Lü M, Tian H, Liu L, Lian J, Huang X & Sun F (2013). Transcriptional cooperation between p53 and NF-κB p65 regulates microRNA-224 transcription in mouse ovarian granulosa cells. *Mol Cell Endocrinol* **370,** 119–129.

136. Liao W-T, Li T-T, Wang Z-G, Wang S-Y, He M-R, Ye Y-P, Qi L, Cui Y-M, Wu P, Jiao H-L, Zhang C, Xie Y-J, Wang J-X & Ding Y-Q (2013). microRNA-224 promotes cell proliferation and tumor growth in human colorectal cancer by repressing PHLPP1 and PHLPP2. *Clin Cancer Res* **19,** 4662–4672.

137. Lièvre A, Bachet J-B, Le Corre D, Boige V, Landi B, Emile J-F, Côté J-F, Tomasic G, Penna C, Ducreux M, Rougier P, Penault-Llorca F & Laurent-Puig P (2006). KRAS mutation status is predictive of response to cetuximab therapy in colorectal cancer. *Cancer Res* **66,** 3992–3995.

138. Lin J, Horikawa Y, Tamboli P, Clague J, Wood CG & Wu X (2010). Genetic variations in microRNA-related genes are associated with survival and recurrence in patients with renal cell carcinoma. *Carcinogenesis* **31,** 1805–1812.

139. Liu K, Li G, Fan C, Zhou X, Wu B & Li J (2011). Increased expression of microRNA-21and its association with chemotherapeutic response in human colorectal cancer. *J Int Med Res* **39,** 2288–2295.

140. Liu Y, Peng H & Zhang J-T (2005). Expression profiling of ABC transporters in a drug-resistant breast cancer cell line using AmpArray. *Mol Pharmacol* **68,** 430–438.

141. Liu Z, Qiu M, Tang Q-L, Liu M, Lang N & Bi F (2010). Establishment and biological characteristics of oxaliplatin-resistant human colon cancer cell lines. *Chin J Cancer* **29,** 661–667.

142. Longley DB, Allen WL & Johnston PG (2006). Drug resistance, predictive markers and pharmacogenomics in colorectal cancer. *Biochim Biophys Acta* **1766,** 184–196.

143. Longley DB, Harkin DP & Johnston PG (2003). 5-fluorouracil: mechanisms of action and clinical strategies. *Nat Rev Cancer* **3,** 330–338.

144. Lutgens MWMD, van Oijen MGH, van der Heijden GJMG, Vleggaar FP, Siersema PD & Oldenburg B (2013). Declining risk of colorectal cancer in inflammatory bowel disease: an updated meta-analysis of population-based cohort studies. *Inflamm Bowel Dis* **19,** 789–799.

145. Luu C, Heinrich EL, Duldulao M, Arrington AK, Fakih M, Garcia-Aguilar J & Kim J (2013). TP53 and let-7a micro-RNA regulate K-Ras activity in HCT116 colorectal cancer cells. *PLoS ONE* **8,** e70604.

146. Ma D, Tao X, Gao F, Fan C & Wu D (2012). miR-224 functions as an onco-miRNA in hepatocellular carcinoma cells by activating AKT signaling. *Oncol Lett* **4,** 483–488.

147. Ma Y, Yang Y, Wang F, Zhang P, Shi C, Zou Y & Qin H (2013). Obesity and Risk of Colorectal Cancer: A Systematic Review of Prospective Studies. *PLoS ONE* **8,** e53916.

148. Marchand LL (1999). Combined Influence of Genetic and Dietary Factors on Colorectal Cancer Incidence in Japanese Americans. *J Natl Cancer Inst Monogr* **1999,** 101–105.

149. Markowitz S, Hines null, Lutterbaugh null, Myeroff null, Mackay null, Gordon null, Rustum null, Luna null & Kleinerman null (1995). Mutant K-ras oncogenes in colon cancers Do not predict Patient's chemotherapy response or survival. *Clin Cancer Res* **1,** 441–445.

150. Matsunaga T, Hojo A, Yamane Y, Endo S, El-Kabbani O & Hara A (2013). Pathophysiological roles of aldo-keto reductases (AKR1C1 and AKR1C3) in development of cisplatin resistance in human colon cancers. *Chem Biol Interact* **202,** 234–242.

151. McKenna WG, Weiss MC, Endlich B, Ling CC, Bakanauskas VJ, Kelsten ML & Muschel RJ (1990). Synergistic effect of the v-myc oncogene with H-ras on radioresistance. *Cancer Res* **50,** 97–102.

152. Mees ST, Mardin WA, Sielker S, Willscher E, Senninger N, Schleicher C, Colombo-Benkmann M & Haier J (2009). Involvement of CD40 targeting miR-224 and miR-486 on the progression of pancreatic ductal adenocarcinomas. *Ann Surg Oncol* **16,** 2339–2350.

153. Mencia N, Selga E, Noé V & Ciudad CJ (2011). Underexpression of miR-224 in methotrexate resistant human colon cancer cells. *Biochem Pharmacol* **82,** 1572–1582.

154. Metheetrairut C & Slack FJ (2013). MicroRNAs in the ionizing radiation response and in radiotherapy. *Curr Opin Genet Dev* **23,** 12–19.

155. Meyers M, Wagner MW, Hwang HS, Kinsella TJ & Boothman DA (2001). Role of the hMLH1 DNA mismatch repair protein in fluoropyrimidine-mediated cell death and cell cycle responses. *Cancer Res* **61,** 5193–5201.

156. Michael MZ, O' Connor SM, van Holst Pellekaan NG, Young GP & James RJ (2003). Reduced accumulation of specific microRNAs in colorectal neoplasia. *Mol Cancer Res* **1,** 882–891.

157. Migneco G, Whitaker-Menezes D, Chiavarina B, Castello-Cros R, Pavlides S, Pestell RG, Fatatis A, Flomenberg N, Tsirigos A, Howell A, Martinez-Outschoorn UE, Sotgia F & Lisanti MP (2010). Glycolytic cancer associated fibroblasts promote breast cancer tumor growth, without a measurable increase in angiogenesis: evidence for stromal-epithelial metabolic coupling. *Cell Cycle* **9,** 2412–2422.

158. Mitchell PS et al. (2008). Circulating microRNAs as stable blood-based markers for cancer detection. *Proc Natl Acad Sci USA* **105,** 10513–10518.

159. Monzo M, Navarro A, Bandres E, Artells R, Moreno I, Gel B, Ibeas R, Moreno J, Martinez F, Diaz T, Martinez A, Balagué O & Garcia-Foncillas J (2008). Overlapping expression of microRNAs in human embryonic colon and colorectal cancer. *Cell Res* **18,** 823–833.

160. Morikawa T, Baba Y, Yamauchi M, Kuchiba A, Nosho K, Shima K, Tanaka N, Huttenhower C, Frank DA, Fuchs CS & Ogino S (2011). STAT3 expression, molecular features, inflammation patterns, and prognosis in a database of 724 colorectal cancers. *Clin Cancer Res* **17,** 1452–1462.

161. Mosakhani N, Sarhadi VK, Borze I, Karjalainen-Lindsberg M-L, Sundström J, Ristamäki R, Osterlund P & Knuutila S (2012). MicroRNA profiling differentiates colorectal cancer according to KRAS status. *Genes Chromosomes Cancer* **51,** 1–9.

162. Mosmann T (1983). Rapid colorimetric assay for cellular growth and survival: application to proliferation and cytotoxicity assays. *J Immunol Methods* **65,** 55–63.

163. Motoyama K, Inoue H, Takatsuno Y, Tanaka F, Mimori K, Uetake H, Sugihara K & Mori M (2009). Over- and under-expressed microRNAs in human colorectal cancer. *Int J Oncol* **34,** 1069–1075.

164. Mueller AC, Sun D & Dutta A (2013). The miR-99 family regulates the DNA damage response through its target SNF2H. *Oncogene* **32,** 1164–1172.

165. Al-Mulla F, Hagan S, Behbehani AI, Bitar MS, George SS, Going JJ, García JJC, Scott L, Fyfe N, Murray GI & Kolch W (2006). Raf kinase inhibitor protein expression in a survival analysis of colorectal cancer patients. *J Clin Oncol* **24,** 5672–5679.

166. Multhoff G & Radons J (2012). Radiation, inflammation, and immune responses in cancer. *Front Oncol* **2,** 58.

167. Nakajima G, Hayashi K, Xi Y, Kudo K, Uchida K, Takasaki K, Yamamoto M & Ju J (2006). Non-coding MicroRNAs hsa-let-7g and hsa-miR-181b are Associated with Chemoresponse to S-1 in Colon Cancer. *Cancer Genomics Proteomics* **3,** 317–324.

168. Nakayama T, Hirakawa H, Shibata K, Nazneen A, Abe K, Nagayasu T & Taguchi T (2011). Expression of angiopoietin-like 4 (ANGPTL4) in human colorectal cancer: ANGPTL4 promotes venous invasion and distant metastasis. *Oncol Rep* **25,** 929–935.

169. Di Nicolantonio F, Martini M, Molinari F, Sartore-Bianchi A, Arena S, Saletti P, De Dosso S, Mazzucchelli L, Frattini M, Siena S & Bardelli A (2008). Wild-type BRAF is required for response to panitumumab or cetuximab in metastatic colorectal cancer. *J Clin Oncol* **26,** 5705–5712.

170. Nishida N, Nagahara M, Sato T, Mimori K, Sudo T, Tanaka F, Shibata K, Ishii H, Sugihara K, Doki Y & Mori M (2012). Microarray analysis of colorectal cancer stromal tissue reveals upregulation of two oncogenic miRNA clusters. *Clin Cancer Res* **18,** 3054–3070.

171. Nita ME, Nagawa H, Tominaga O, Tsuno N, Fujii S, Sasaki S, Fu CG, Takenoue T, Tsuruo T & Muto T (1998). 5-Fluorouracil induces apoptosis in human colon cancer cell lines with modulation of Bcl-2 family proteins. *Br J Cancer* **78,** 986–992.

172. Oberg AL, French AJ, Sarver AL, Subramanian S, Morlan BW, Riska SM, Borralho PM, Cunningham JM, Boardman LA, Wang L, Smyrk TC, Asmann Y, Steer CJ & Thibodeau SN (2011). miRNA expression in colon polyps provides evidence for a multihit model of colon cancer. *PLoS ONE* **6,** e20465.

173. Oh J-S, Kim J-J, Byun J-Y & Kim I-A (2010). Lin28-let7 modulates radiosensitivity of human cancer cells with activation of K-Ras. *Int J Radiat Oncol Biol Phys* **76,** 5–8.

174. Olaru AV, Yamanaka S, Vazquez C, Mori Y, Cheng Y, Abraham JM, Bayless TM, Harpaz N, Selaru FM & Meltzer SJ (2013). MicroRNA-224 negatively regulates p21 expression during late neoplastic progression in inflammatory bowel disease. *Inflamm Bowel Dis* **19,** 471–480.

175. Pajonk F, Vlashi E & McBride WH (2010). Radiation Resistance of Cancer Stem Cells: The 4 R's of Radiobiology Revisited. *Stem Cells* **28,** 639–648.

176. Pawlik TM & Keyomarsi K (2004). Role of cell cycle in mediating sensitivity to radiotherapy. *Int J Radiat Oncol Biol Phys* **59,** 928–942.

177. Peltier HJ & Latham GJ (2008). Normalization of microRNA expression levels in quantitative RT-PCR assays: identification of suitable reference RNA targets in normal and cancerous human solid tissues. *RNA* **14,** 844–852.

178. Poma P, Labbozzetta M, Vivona N, Porcasi R, D'Alessandro N & Notarbartolo M (2012). Analysis of possible mechanisms accounting for raf-1 kinase inhibitor protein downregulation in hepatocellular carcinoma. *OMICS* **16,** 579–588.

179. Pommier Y, Leo E, Zhang H & Marchand C (2010). DNA Topoisomerases and Their Poisoning by Anticancer and Antibacterial Drugs. *Chemistry & Biology* **17,** 421–433.

180. Popat S, Hubner R & Houlston RS (2005). Systematic review of microsatellite instability and colorectal cancer prognosis. *J Clin Oncol* **23,** 609–618.

181. Pratt S, Shepard RL, Kandasamy RA, Johnston PA, Perry W 3rd & Dantzig AH (2005). The multidrug resistance protein 5 (ABCC5) confers resistance to 5-fluorouracil and transports its monophosphorylated metabolites. *Mol Cancer Ther* **4,** 855–863.

182. Qin J & Luo M (2014). MicroRNA-221 promotes colorectal cancer cell invasion and metastasis by targeting RECK. *FEBS Lett* **588,** 99–104.

183. R Development Core Team (2008). *R: a language and environment for statistical computing*. R Foundation for Statistical Computing, Vienna, Austria.

184. Ragusa M et al. (2010). Specific alterations of microRNA transcriptome and global network structure in colorectal carcinoma after cetuximab treatment. *Mol Cancer Ther* **9,** 3396–3409.

185. Rajagopalan H, Bardelli A, Lengauer C, Kinzler KW, Vogelstein B & Velculescu VE (2002). Tumorigenesis: RAF/RAS oncogenes and mismatch-repair status. *Nature* **418,** 934.

186. Reid JF, Gariboldi M, Sokolova V, Capobianco P, Lampis A, Perrone F, Signoroni S, Costa A, Leo E, Pilotti S & Pierotti MA (2009). Integrative approach for prioritizing cancer genes in sporadic colon cancer. *Genes Chromosomes Cancer* **48,** 953–962.

187. Reid JF, Sokolova V, Zoni E, Lampis A, Pizzamiglio S, Bertan C, Zanutto S, Perrone F, Camerini T, Gallino G, Verderio P, Leo E, Pilotti S, Gariboldi M & Pierotti MA (2012). miRNA profiling in colorectal cancer highlights miR-1 involvement in MET-dependent proliferation. *Mol Cancer Res* **10,** 504–515.

188. Ren F, Wu H, Lei Y, Zhang H, Liu R, Zhao Y, Chen X, Zeng D, Tong A, Chen L, Wei Y & Huang C (2010). Quantitative proteomics identification of phosphoglycerate mutase 1 as a novel therapeutic target in hepatocellular carcinoma. *Mol Cancer* **9,** 81.

189. Ribic CM, Sargent DJ, Moore MJ, Thibodeau SN, French AJ, Goldberg RM, Hamilton SR, Laurent-Puig P, Gryfe R, Shepherd LE, Tu D, Redston M & Gallinger S (2003). Tumor microsatellite-instability status as a predictor of benefit from fluorouracil-based adjuvant chemotherapy for colon cancer. *N Engl J Med* **349,** 247–257.

190. Rossi L, Bonmassar E & Faraoni I (2007). Modification of miR gene expression pattern in human colon cancer cells following exposure to 5-fluorouracil in vitro. *Pharmacol Res* **56,** 248–253.

191. Saleh AD, Savage JE, Cao L, Soule BP, Ly D, DeGraff W, Harris CC, Mitchell JB & Simone NL (2011). Cellular stress induced alterations in microRNA let-7a and let-7b expression are dependent on p53. *PLoS ONE* **6,** e24429.

192. Samowitz WS, Holden JA, Curtin K, Edwards SL, Walker AR, Lin HA, Robertson MA, Nichols MF, Gruenthal KM, Lynch BJ, Leppert MF & Slattery ML (2001). Inverse relationship between microsatellite instability and K-ras and p53 gene alterations in colon cancer. *Am J Pathol* **158,** 1517–1524.

193. Samowitz WS, Slattery ML, Sweeney C, Herrick J, Wolff RK & Albertsen H (2007). APC mutations and other genetic and epigenetic changes in colon cancer. *Mol Cancer Res* **5,** 165–170.

194. Sanders I (2011). *Practical and Scientific Aspects of IORT for Rectal Cancer* (PhD thesis). University of Dundee.

195. Sarver AL, French AJ, Borralho PM, Thayanithy V, Oberg AL, Silverstein KAT, Morlan BW, Riska SM, Boardman LA, Cunningham JM, Subramanian S, Wang L, Smyrk TC, Rodrigues CMP, Thibodeau SN & Steer CJ (2009). Human colon cancer profiles show differential microRNA expression depending on mismatch repair status and are characteristic of undifferentiated proliferative states. *BMC Cancer* **9,** 401.

196. Schepeler T, Reinert JT, Ostenfeld MS, Christensen LL, Silahtaroglu AN, Dyrskjøt L, Wiuf C, Sørensen FJ, Kruhøffer M, Laurberg S, Kauppinen S, Ørntoft TF & Andersen CL (2008). Diagnostic and prognostic microRNAs in stage II colon cancer. *Cancer Res* **68,** 6416–6424.

197. Schetter AJ, Leung SY, Sohn JJ, Zanetti KA, Bowman ED, Yanaihara N, Yuen ST, Chan TL, Kwong DLW, Au GKH, Liu C-G, Calin GA, Croce CM & Harris CC (2008). MicroRNA expression profiles associated with prognosis and therapeutic outcome in colon adenocarcinoma. *JAMA* **299,** 425–436.

198. Schmidt-Ullrich RK, Mikkelsen RB, Dent P, Todd DG, Valerie K, Kavanagh BD, Contessa JN, Rorrer WK & Chen PB (1997). Radiation-induced proliferation of the human A431 squamous carcinoma cells is dependent on EGFR tyrosine phosphorylation. *Oncogene* **15,** 1191–1197.

199. Schmitz KJ, Hey S, Schinwald A, Wohlschlaeger J, Baba HA, Worm K & Schmid KW (2009). Differential expression of microRNA 181b and microRNA 21 in hyperplastic polyps and sessile serrated adenomas of the colon. *Virchows Arch* **455,** 49–54.

200. Schubbert S, Shannon K & Bollag G (2007). Hyperactive Ras in developmental disorders and cancer. *Nat Rev Cancer* **7,** 295–308.

201. Scisciani C, Vossio S, Guerrieri F, Schinzari V, De Iaco R, D'Onorio de Meo P, Cervello M, Montalto G, Pollicino T, Raimondo G, Levrero M & Pediconi N (2012). Transcriptional regulation of miR-224 upregulated in human HCCs by NFκB inflammatory pathways. *J Hepatol* **56,** 855–861.

202. Scottish Bowel Screening Programme (2014). Why is screening important? Available at: http://www.bowelscreening.scot.nhs.uk/why-is-screening-important [Accessed June 29, 2014].

203. Scottish Intercollegiate Guidelines Network (2014). Diagnosis and management of colorectal cancer.

204. Seetharam RN, Sood A, Basu-Mallick A, Augenlicht LH, Mariadason JM & Goel S (2010). Oxaliplatin resistance induced by ERCC1 up-regulation is abrogated by siRNA-mediated gene silencing in human colorectal cancer cells. *Anticancer Res* **30,** 2531–2538.

205. Semenza GL (2004). Intratumoral hypoxia, radiation resistance, and HIF-1. *Cancer Cell* **5,** 405–406.

206. Shen S, Wang L, Jia Y, Hao Y, Zhang L & Wang H (2013). Upregulation of microRNA-224 is associated with aggressive progression and poor prognosis in human cervical cancer. *Diagn Pathol* **8,** 69.

207. Shirasawa S, Furuse M, Yokoyama N & Sasazuki T (1993). Altered growth of human colon cancer cell lines disrupted at activated Ki-ras. *Science* **260,** 85–88.

208. Shirota Y, Stoehlmacher J, Brabender J, Xiong Y-P, Uetake H, Danenberg KD, Groshen S, Tsao-Wei DD, Danenberg PV & Lenz H-J (2001). ERCC1 and Thymidylate Synthase mRNA Levels Predict Survival for Colorectal Cancer Patients Receiving Combination Oxaliplatin and Fluorouracil Chemotherapy. *JCO* **19,** 4298–4304.

209. Shuck SC, Short EA & Turchi JJ (2008). Eukaryotic nucleotide excision repair: from understanding mechanisms to influencing biology. *Cell Res* **18,** 64–72.

210. Simone NL, Soule BP, Ly D, Saleh AD, Savage JE, DeGraff W, Cook J, Harris CC, Gius D & Mitchell JB (2009). Ionizing Radiation-Induced Oxidative Stress Alters miRNA Expression. *PLoS ONE* **4,** e6377.

211. Sklar MD (1988). The ras oncogenes increase the intrinsic resistance of NIH 3T3 cells to ionizing radiation. *Science* **239,** 645–647.

212. Slattery ML, Wolff E, Hoffman MD, Pellatt DF, Milash B & Wolff RK (2011). MicroRNAs and colon and rectal cancer: differential expression by tumor location and subtype. *Genes Chromosomes Cancer* **50,** 196–206.

213. Smith G, Bounds R, Wolf H, Steele RJC, Carey FA & Wolf CR (2010). Activating K-Ras mutations outwith "hotspot" codons in sporadic colorectal cancers - implications for personalised cancer medicine. *Br J Cancer* **102,** 693–703.

214. Song B, Wang Y, Xi Y, Kudo K, Bruheim S, Botchkina GI, Gavin E, Wan Y, Formentini A, Kornmann M, Fodstad O & Ju J (2009). Mechanism of chemoresistance mediated by miR-140 in human osteosarcoma and colon cancer cells. *Oncogene* **28,** 4065–4074.

215. Soong R, Shah N, Salto-Tellez M, Tai BC, Soo RA, Han HC, Ng SS, Tan WL, Zeps N, Joseph D, Diasio RB & Iacopetta B (2008). Prognostic significance of thymidylate synthase, dihydropyrimidine dehydrogenase and thymidine phosphorylase protein expression in colorectal cancer patients treated with or without 5-fluorouracil-based chemotherapy. *Ann Oncol* **19,** 915–919.

216. Söreide K, Janssen E a. M, Söiland H, Körner H & Baak JPA (2006). Microsatellite instability in colorectal cancer. *Br J Surg* **93,** 395–406.

217. Sossey-Alaoui K, Bialkowska K & Plow EF (2009). The miR200 family of microRNAs regulates WAVE3-dependent cancer cell invasion. *J Biol Chem* **284,** 33019–33029.

218. Sossey-Alaoui K, Downs-Kelly E, Das M, Izem L, Tubbs R & Plow EF (2011). WAVE3, an actin remodeling protein, is regulated by the metastasis suppressor microRNA, miR-31, during the invasion-metastasis cascade. *Int J Cancer* **129,** 1331–1343.

219. Speake WJ, Dean RA, Kumar A, Morris TM, Scholefield JH & Watson SA (2005). Radiation induced MMP expression from rectal cancer is short lived but contributes to in vitro invasion. *Eur J Surg Oncol* **31,** 869–874.

220. Steel GG, McMillan TJ & Peacock JH (1989). The 5Rs of radiobiology. *Int J Radiat Biol* **56,** 1045–1048.

221. Svoboda M, Izakovicova Holla L, Sefr R, Vrtkova I, Kocakova I, Tichy B & Dvorak J (2008). Micro-RNAs miR125b and miR137 are frequently upregulated in response to capecitabine chemoradiotherapy of rectal cancer. *Int J Oncol* **33,** 541–547.

222. Svoboda M, Sana J, Fabian P, Kocakova I, Gombosova J, Nekvindova J, Radova L, Vyzula R & Slaby O (2012). MicroRNA expression profile associated with response to neoadjuvant chemoradiotherapy in locally advanced rectal cancer patients. *Radiat Oncol* **7,** 195.

223. Tang W, Zhu Y, Gao J, Fu J, Liu C, Liu Y, Song C, Zhu S, Leng Y, Wang G, Chen W, Du P, Huang S, Zhou X, Kang J & Cui L (2014). MicroRNA-29a promotes colorectal cancer metastasis by regulating matrix metalloproteinase 2 and E-cadherin via KLF4. *Br J Cancer* **110,** 450–458.

224. Tanic M, Yanowsky K, Rodriguez-Antona C, Andrés R, Márquez-Rodas I, Osorio A, Benitez J & Martinez-Delgado B (2012). Deregulated miRNAs in hereditary breast cancer revealed a role for miR-30c in regulating KRAS oncogene. *PLoS ONE* **7,** e38847.

225. Thiery JP (2002). Epithelial-mesenchymal transitions in cancer progression. *Nat Rev Cancer* **2,** 442–454.

226. Thiery JP & Sleeman JP (2006). Complex networks orchestrate epithelial-mesenchymal transitions. *Nat Rev Mol Cell Biol* **7,** 131–142.

227. Tominaga S & Kuroishi T (1997). An ecological study on diet/nutrition and cancer in Japan. *Int J Cancer* **Suppl 10,** 2–6.

228. Torrance CJ, Agrawal V, Vogelstein B & Kinzler KW (2001). Use of isogenic human cancer cells for high-throughput screening and drug discovery. *Nat Biotechnol* **19,** 940–945.

229. Toyota M, Suzuki H, Sasaki Y, Maruyama R, Imai K, Shinomura Y & Tokino T (2008). Epigenetic Silencing of MicroRNA-34b/c and B-Cell Translocation Gene 4 Is Associated with CpG Island Methylation in Colorectal Cancer. *Cancer Res* **68,** 4123–4132.

230. Tsuchida A, Ohno S, Wu W, Borjigin N, Fujita K, Aoki T, Ueda S, Takanashi M & Kuroda M (2011). miR-92 is a key oncogenic component of the miR-17-92 cluster in colon cancer. *Cancer Sci* **102,** 2264–2271.

231. Upraity S, Kazi S, Padul V & Shirsat NV (2014). MiR-224 expression increases radiation sensitivity of glioblastoma cells. *Biochem Biophys Res Commun* **448,** 225–230.

232. Vaidya JS et al. (2010). Targeted intraoperative radiotherapy versus whole breast radiotherapy for breast cancer (TARGIT-A trial): an international, prospective, randomised, non-inferiority phase 3 trial. *Lancet* **376,** 91–102.

233. Valeri N, Gasparini P, Braconi C, Paone A, Lovat F, Fabbri M, Sumani KM, Alder H, Amadori D, Patel T, Nuovo GJ, Fishel R & Croce CM (2010). MicroRNA-21 induces resistance to 5-fluorouracil by down-regulating human DNA MutS homolog 2 (hMSH2). *Proc Natl Acad Sci USA* **107,** 21098–21103.

234. Vander Heiden MG, Cantley LC & Thompson CB (2009). Understanding the Warburg effect: the metabolic requirements of cell proliferation. *Science* **324,** 1029–1033.

235. Violette S, Poulain L, Dussaulx E, Pepin D, Faussat A-M, Chambaz J, Lacorte J-M, Staedel C & Lesuffleur T (2002). Resistance of colon cancer cells to long-term 5-fluorouracil exposure is correlated to the relative level of Bcl-2 and Bcl-X(L) in addition to Bax and p53 status. *Int J Cancer* **98,** 498–504.

236. Viswanathan SR, Daley GQ & Gregory RI (2008). Selective blockade of microRNA processing by Lin28. *Science* **320,** 97–100.

237. Voboril R, Hochwald SN, Li J, Brank A, Weberova J, Wessels F, Moldawer LL, Camp ER & MacKay SLD (2004). Inhibition of NF-kappa B augments sensitivity to 5-fluorouracil/folinic acid in colon cancer. *J Surg Res* **120,** 178–188.

238. Vogelstein B, Fearon ER, Hamilton SR, Kern SE, Preisinger AC, Leppert M, Smits AMM & Bos JL (1988). Genetic Alterations during Colorectal-Tumor Development. *New England Journal of Medicine* **319,** 525–532.

239. Volinia S, Calin GA, Liu C-G, Ambs S, Cimmino A, Petrocca F, Visone R, Iorio M, Roldo C, Ferracin M, Prueitt RL, Yanaihara N, Lanza G, Scarpa A, Vecchione A, Negrini M, Harris CC & Croce CM (2006). A microRNA expression signature of human solid tumors defines cancer gene targets. *Proc Natl Acad Sci USA* **103,** 2257–2261.

240. Wagner-Ecker M, Schwager C, Wirkner U, Abdollahi A & Huber PE (2010). MicroRNA expression after ionizing radiation in human endothelial cells. *Radiat Oncol* **5,** 25.

241. Walther A, Johnstone E, Swanton C, Midgley R, Tomlinson I & Kerr D (2009). Genetic prognostic and predictive markers in colorectal cancer. *Nat Rev Cancer* **9,** 489–499.

242. Wang C-J, Stratmann J, Zhou Z-G & Sun X-F (2010*a*). Suppression of microRNA-31 increases sensitivity to 5-FU at an early stage, and affects cell migration and invasion in HCT-116 colon cancer cells. *BMC Cancer* **10,** 616.

243. Wang D & DuBois RN (2009). The role of COX-2 in intestinal inflammation and colorectal cancer. *Oncogene* **29,** 781–788.

244. Wang L-G & Gu J (2012). Serum microRNA-29a is a promising novel marker for early detection of colorectal liver metastasis. *Cancer Epidemiol* **36,** e61–67.

245. Wang X-B, Wang S-S, Zhang Q-F, Liu M, Li H-L, Liu Y, Wang J-N, Zheng F, Guo L-Y & Xiang J-Z (2010*b*). Inhibition of tetramethylpyrazine on P-gp, MRP2, MRP3 and MRP5 in multidrug resistant human hepatocellular carcinoma cells. *Oncol Rep* **23,** 211–215.

246. Wang Y, Lee ATC, Ma JZI, Wang J, Ren J, Yang Y, Tantoso E, Li K-B, Ooi LLPJ, Tan P & Lee CGL (2008). Profiling microRNA expression in hepatocellular carcinoma reveals microRNA-224 up-regulation and apoptosis inhibitor-5 as a microRNA-224-specific target. *J Biol Chem* **283,** 13205–13215.

247. Wang Y, Ren J, Gao Y, Ma JZI, Toh HC, Chow P, Chung AYF, Ooi LLPJ & Lee CGL (2013). MicroRNA-224 targets SMAD family member 4 to promote cell proliferation and negatively influence patient survival. *PLoS ONE* **8,** e68744.

248. Wang Y, Toh HC, Chow P, Chung AYF, Meyers DJ, Cole PA, Ooi LLPJ & Lee CGL (2012). MicroRNA-224 is up-regulated in hepatocellular carcinoma through epigenetic mechanisms. *FASEB J* **26,** 3032–3041.

249. Wang YX, Zhang XY, Zhang BF, Yang CQ, Chen XM & Gao HJ (2010*c*). Initial study of microRNA expression profiles of colonic cancer without lymph node metastasis. *J Dig Dis* **11,** 50–54.

250. Weidhaas JB, Babar I, Nallur SM, Trang P, Roush S, Boehm M, Gillespie E & Slack FJ (2007). MicroRNAs as potential agents to alter resistance to cytotoxic anticancer therapy. *Cancer Res* **67,** 11111–11116.

251. White NMA, Chow T-FF, Mejia-Guerrero S, Diamandis M, Rofael Y, Faragalla H, Mankaruous M, Gabril M, Girgis A & Yousef GM (2010). Three dysregulated miRNAs control kallikrein 10 expression and cell proliferation in ovarian cancer. *Br J Cancer* **102,** 1244–1253.

252. Wicki A, Herrmann R & Christofori G (2010). Kras in metastatic colorectal cancer. *Swiss Med Wkly* **140,** w13112.

253. Winter J, Jung S, Keller S, Gregory RI & Diederichs S (2009). Many roads to maturity: microRNA biogenesis pathways and their regulation. *Nat Cell Biol* **11,** 228–234.

254. Withers H. (1975). The four R's of radiotherapy. In *Advances in Radiation Biology*. Academic Press, New York.

255. Xi Y, Formentini A, Chien M, Weir DB, Russo JJ, Ju J, Kornmann M & Ju J (2006*a*). Prognostic Values of microRNAs in Colorectal Cancer. *Biomark Insights* **2,** 113–121.

256. Xi Y, Shalgi R, Fodstad O, Pilpel Y & Ju J (2006*b*). Differentially regulated micro-RNAs and actively translated messenger RNA transcripts by tumor suppressor p53 in colon cancer. *Clin Cancer Res* **12,** 2014–2024.

257. Xiong B, Cheng Y, Ma L & Zhang C (2013). MiR-21 regulates biological behavior through the PTEN/PI-3 K/Akt signaling pathway in human colorectal cancer cells. *Int J Oncol* **42,** 219–228.

258. Yang AD, Fan F, Camp ER, van Buren G, Liu W, Somcio R, Gray MJ, Cheng H, Hoff PM & Ellis LM (2006). Chronic oxaliplatin resistance induces epithelial-to-mesenchymal transition in colorectal cancer cell lines. *Clin Cancer Res* **12,** 4147–4153.

259. Yang H-Y, Kwon J, Park H-R, Kwon S-O, Park Y-K, Kim H-S, Chung Y-J, Chang Y-J, Choi H-I, Chung K-J, Lee D-S, Park B-J, Jeong S-H & Lee T-H (2012*a*). Comparative proteomic analysis for the insoluble fractions of colorectal cancer patients. *J Proteomics* **75,** 3639–3653.

260. Yang I-P, Tsai H-L, Hou M-F, Chen K-C, Tsai P-C, Huang S-W, Chou W-W, Wang J-Y & Juo S-HH (2012*b*). MicroRNA-93 inhibits tumor growth and early relapse of human colorectal cancer by affecting genes involved in the cell cycle. *Carcinogenesis* **33,** 1522–1530.

261. Yao G, Yin M, Lian J, Tian H, Liu L, Li X & Sun F (2010). MicroRNA-224 is involved in transforming growth factor-beta-mediated mouse granulosa cell proliferation and granulosa cell function by targeting Smad4. *Mol Endocrinol* **24,** 540–551.

262. Yu G, Tang J-Q, Tian M-L, Li H, Wang X, Wu T, Zhu J, Huang S-J & Wan Y-L (2012). Prognostic values of the miR-17-92 cluster and its paralogs in colon cancer. *J Surg Oncol* **106,** 232–237.

263. Yuan K, Xie K, Fox J, Zeng H, Gao H, Huang C & Wu M (2013). Decreased levels of miR-224 and the passenger strand of miR-221 increase MBD2, suppressing maspin and promoting colorectal tumor growth and metastasis in mice. *Gastroenterology* **145,** 853–864.e9.

264. Zhang G-J, Zhou H, Xiao H-X, Li Y & Zhou T (2013*a*). Up-regulation of miR-224 promotes cancer cell proliferation and invasion and predicts relapse of colorectal cancer. *Cancer Cell Int* **13,** 104.

265. Zhang J, Xiao Z, Lai D, Sun J, He C, Chu Z, Ye H, Chen S & Wang J (2012). miR-21, miR-17 and miR-19a induced by phosphatase of regenerating liver-3 promote the proliferation and metastasis of colon cancer. *Br J Cancer* **107,** 352–359.

266. Zhang Y, Takahashi S, Tasaka A, Yoshima T, Ochi H & Chayama K (2013*b*). Involvement of microRNA-224 in cell proliferation, migration, invasion, and anti-apoptosis in hepatocellular carcinoma. *J Gastroenterol Hepatol* **28,** 565–575.

267. Zhang Y, Wang X, Xu B, Wang B, Wang Z, Liang Y, Zhou J, Hu J & Jiang B (2013*c*). Epigenetic silencing of miR-126 contributes to tumor invasion and angiogenesis in colorectal cancer. *Oncol Rep* **30,** 1976–1984.

268. Zhang Y, Zheng L, Huang J, Gao F, Lin X, He L, Li D, Li Z, Ding Y & Chen L (2014). MiR-124 Radiosensitizes Human Colorectal Cancer Cells by Targeting PRRX1. *PLoS ONE* **9,** e93917.

269. Zhao X, Sun T, Che N, Sun D, Zhao N, Dong X, Gu Q, Yao Z & Sun B (2011). Promotion of hepatocellular carcinoma metastasis through matrix metalloproteinase activation by epithelial-mesenchymal transition regulator Twist1. *J Cell Mol Med* **15,** 691–700.

270. Zhou J, Zhou Y, Yin B, Hao W, Zhao L, Ju W & Bai C (2010). 5-Fluorouracil and oxaliplatin modify the expression profiles of microRNAs in human colon cancer cells in vitro. *Oncol Rep* **23,** 121–128.

271. Zhou T, Zhang G, Liu Z, Xia S & Tian H (2013). Overexpression of miR-92a correlates with tumor metastasis and poor prognosis in patients with colorectal cancer. *Int J Colorectal Dis* **28,** 19–24.

272. Zhou Y, Wan G, Spizzo R, Ivan C, Mathur R, Hu X, Ye X, Lu J, Fan F, Xia L, Calin GA, Ellis LM & Lu X (2014). miR-203 induces oxaliplatin resistance in colorectal cancer cells by negatively regulating ATM kinase. *Mol Oncol* **8,** 83–92.

273. Zhu S, Sachdeva M, Wu F, Lu Z & Mo Y-Y (2010). Ubc9 promotes breast cell invasion and metastasis in a sumoylation-independent manner. *Oncogene* **29,** 1763–1772.

Appendix

Please see accompanying CD ROM for Appendices A, E, G, H, I, J and K

Appendix A: TLDA microRNA 'A' layout

Appendix E: List of miRNAs expressed in colorectal cancers, normal mucosa and adenomas

Appendix G: The correlation of miR-224 expression with gene expression data from Affymetrix data in 41 colorectal cancers analysed in Section 3.3.3

Appendix H: Predicted gene targets of the 12 miRNAs differentially expressed in HCT116 *KRAS* WT and mutant cells

Appendix I: Predicted miR-224 target genes

Appendix J: Over and under-expressed genes in HCT116 and DLD-1 drug resistant cells relative to their respective parental cells

Appendix K: Genes commonly or uniquely differentially expressed in drug resistant cells compared to parental cells.

Appendix B: Inter-patient variability in the expression of individual miRNAs

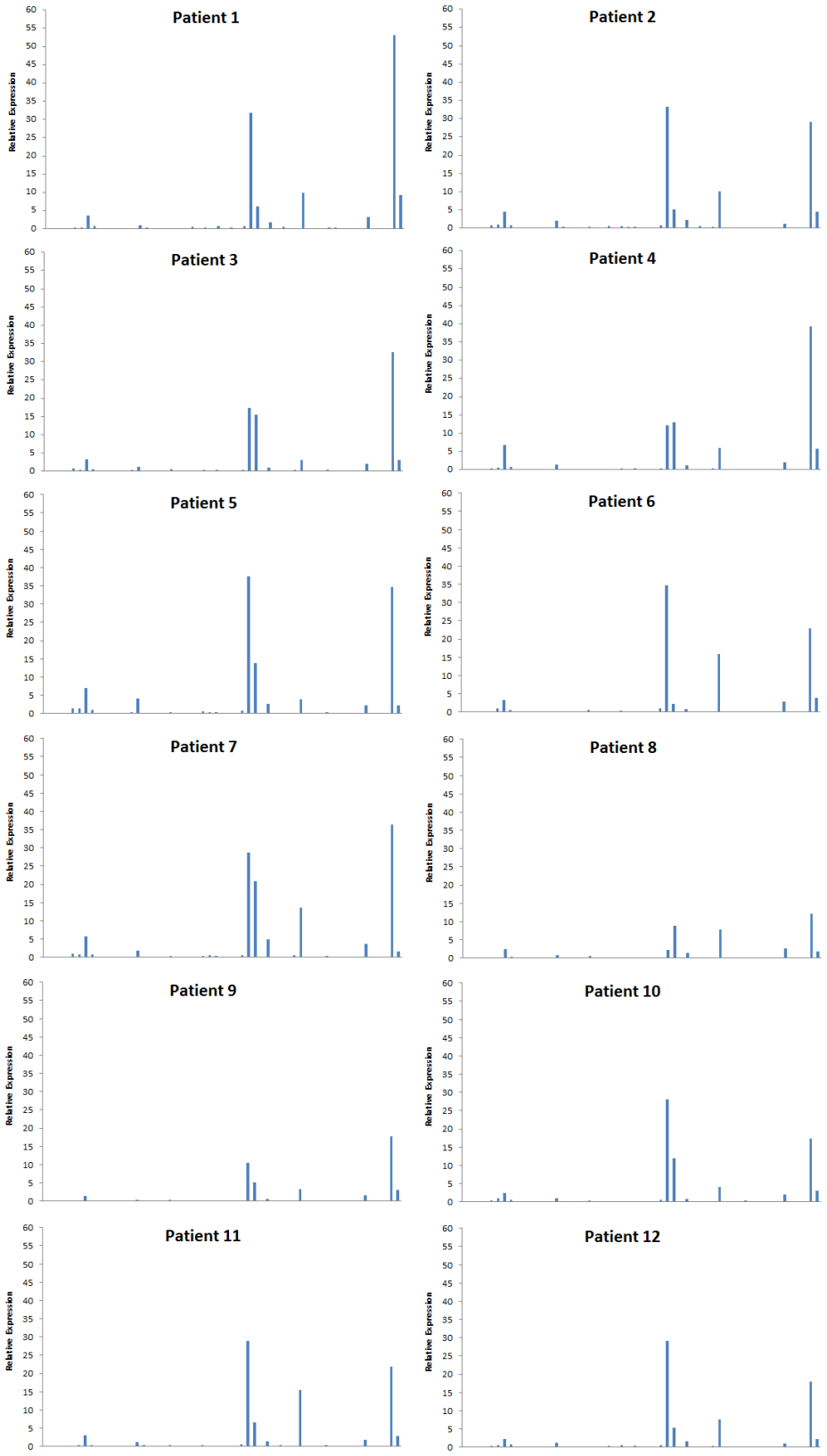

Figure B1

Figure B1: ***Inter-patient variability in the expression of individual miRNAs.*** *TLDA miRNA 'A' cards (Life Technologies) were used to profile the expression of 377 miRNAs in 12 colorectal cancers, as detailed in Section 2.2.9.8. The expression of the second set of 55 miRNAs on the TLDA card, relative to the control miRNA let-7a, is shown. Each bar represents a single point determinant of relative expression.*

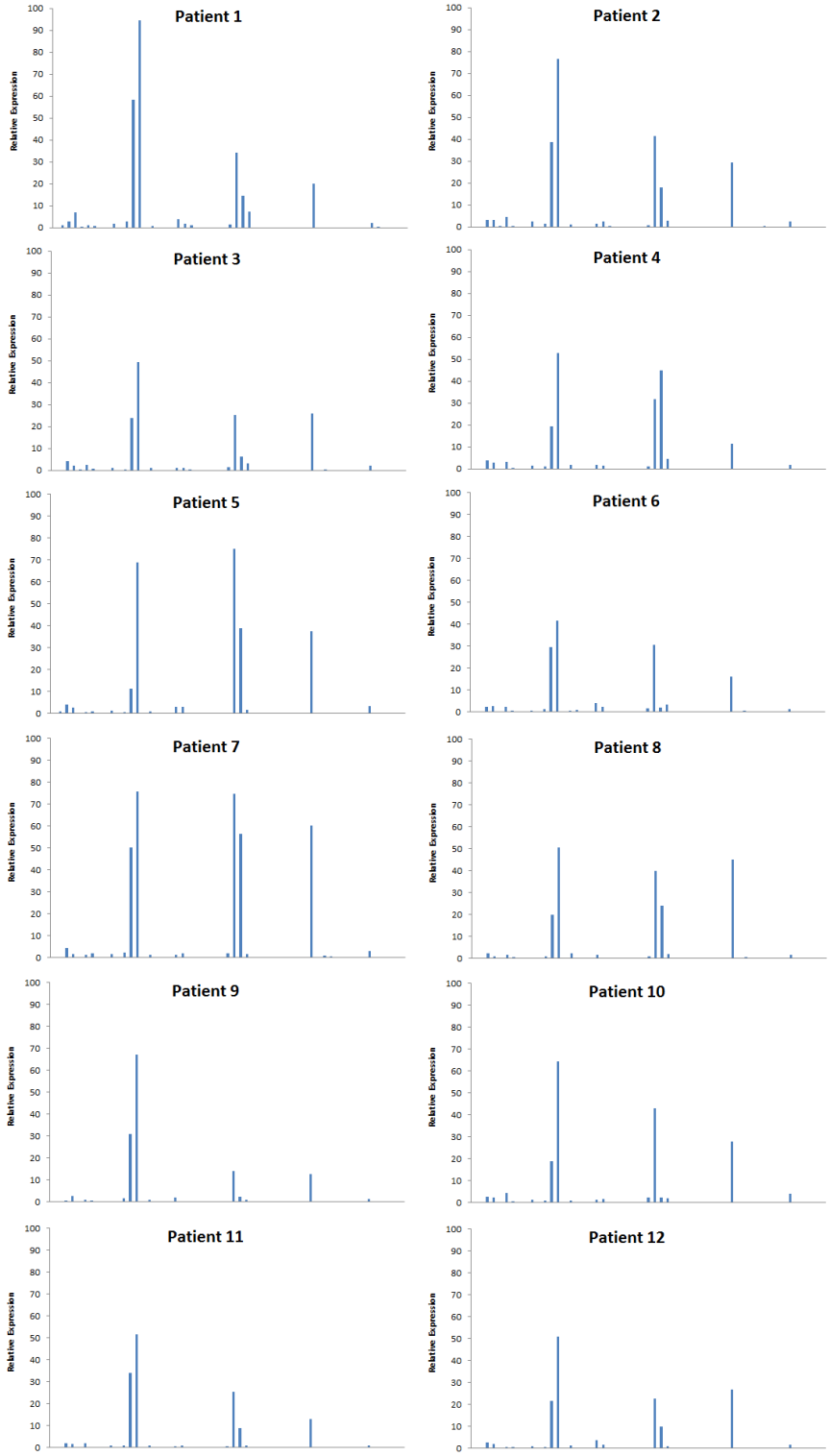

Figure B2: ***Inter-patient variability in the expression of individual miRNAs.*** *TLDA miRNA 'A' cards (Life Technologies) were used to profile the expression of 377 miRNAs in 12 colorectal cancers, as detailed in Section 2.2.9.8. The expression of the third set of 55 miRNAs on the TLDA card, relative to the control miRNA let-7a, is shown. Each bar represents a single point determinant of relative expression.*

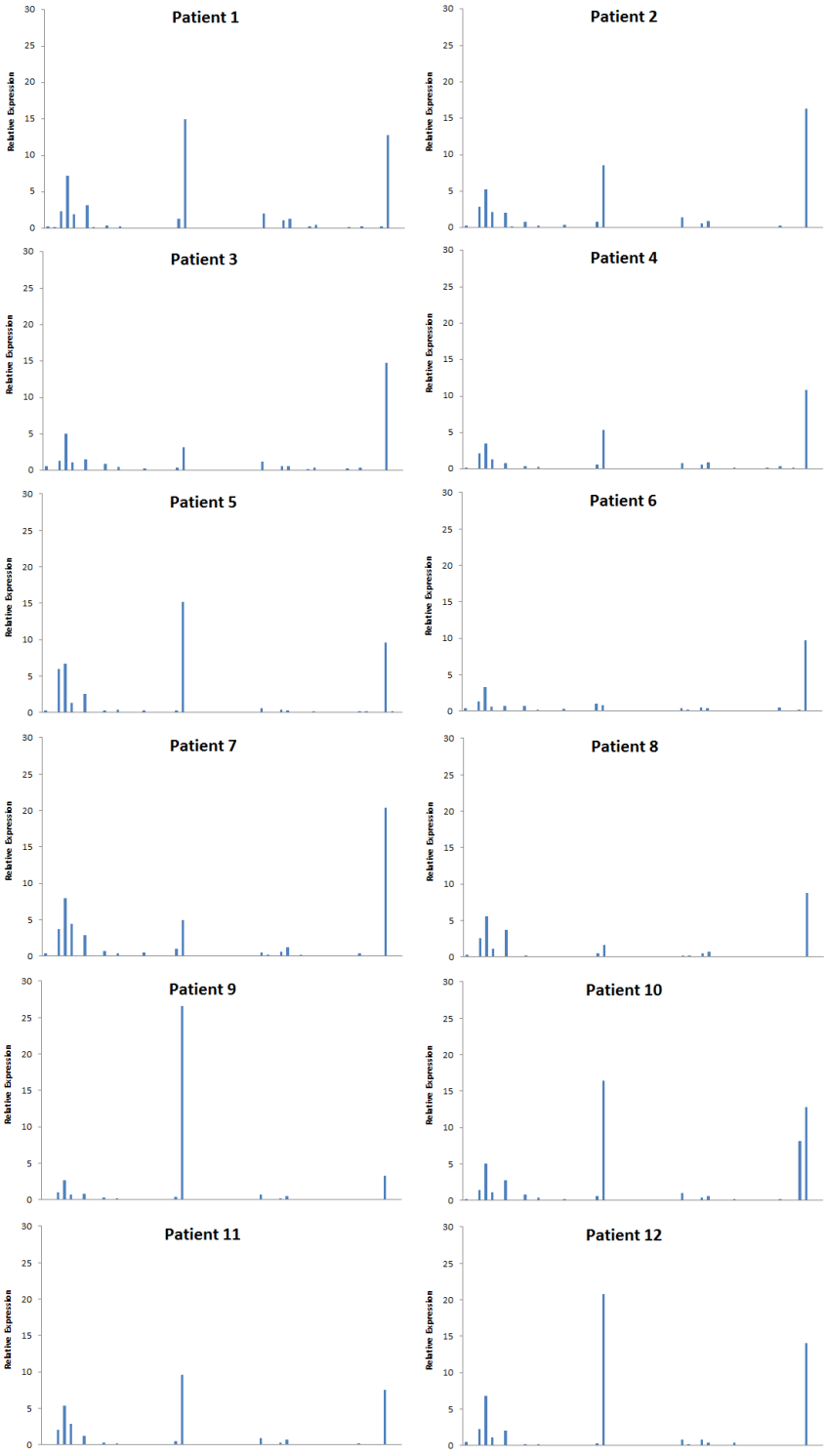

Figure B3: ***Inter-patient variability in the expression of individual miRNAs.*** *TLDA miRNA 'A' cards (Life Technologies) were used to profile the expression of 377 miRNAs in 12 colorectal cancers, as detailed in Section 2.2.9.8. The expression of the fourth set of 55 miRNAs on the TLDA card, relative to the control miRNA let-7a, is shown. Each bar represents a single point determinant of relative expression.*

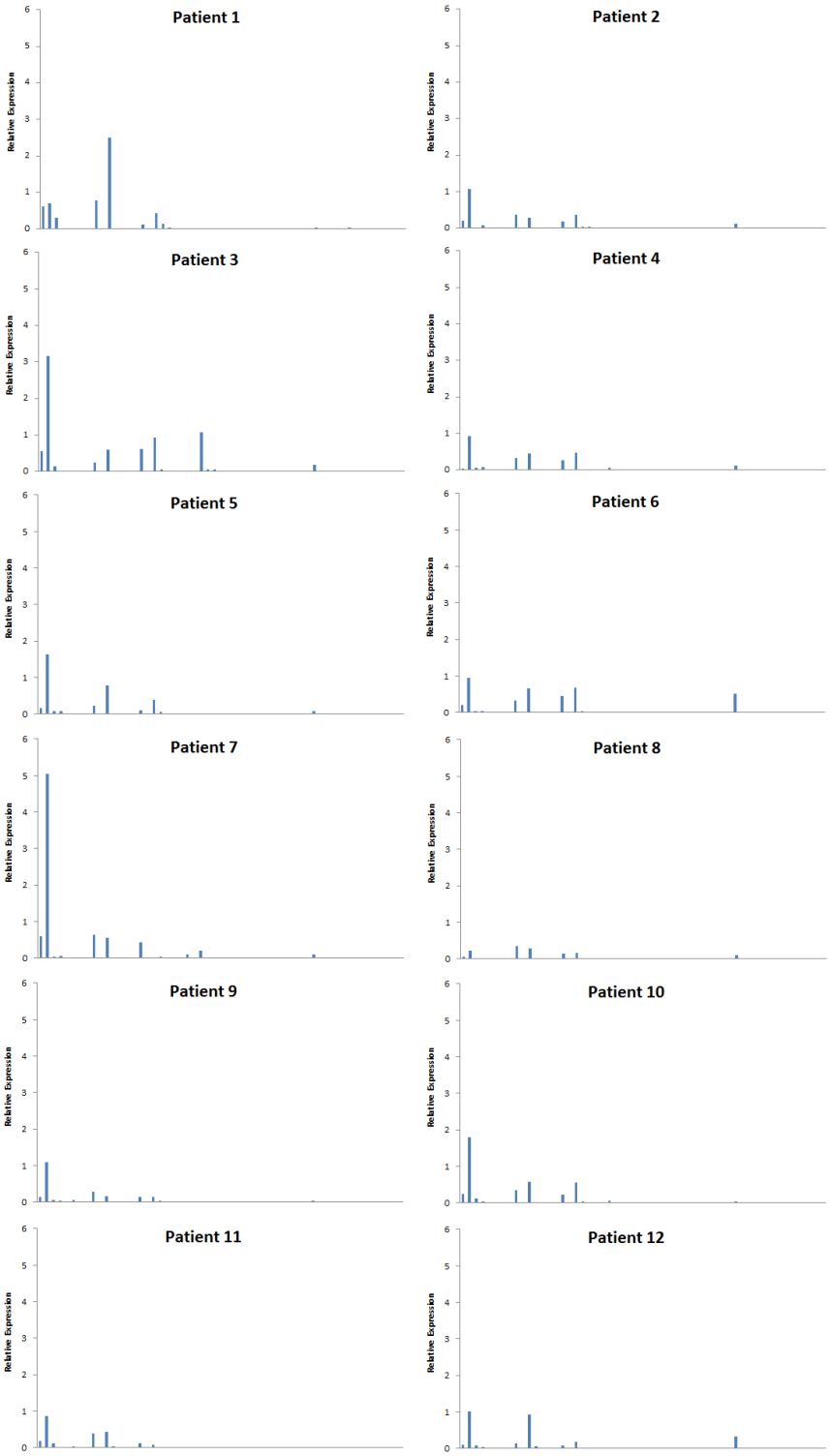

Figure B4: ***Inter-patient variability in the expression of individual miRNAs.*** *TLDA miRNA 'A' cards (Life Technologies) were used to profile the expression of 377 miRNAs in 12 colorectal cancers, as detailed in Section 2.2.9.8. The expression of the fifth set of 55 miRNAs on the TLDA card, relative to the control miRNA let-7a, is shown. Each bar represents a single point determinant of relative expression.*

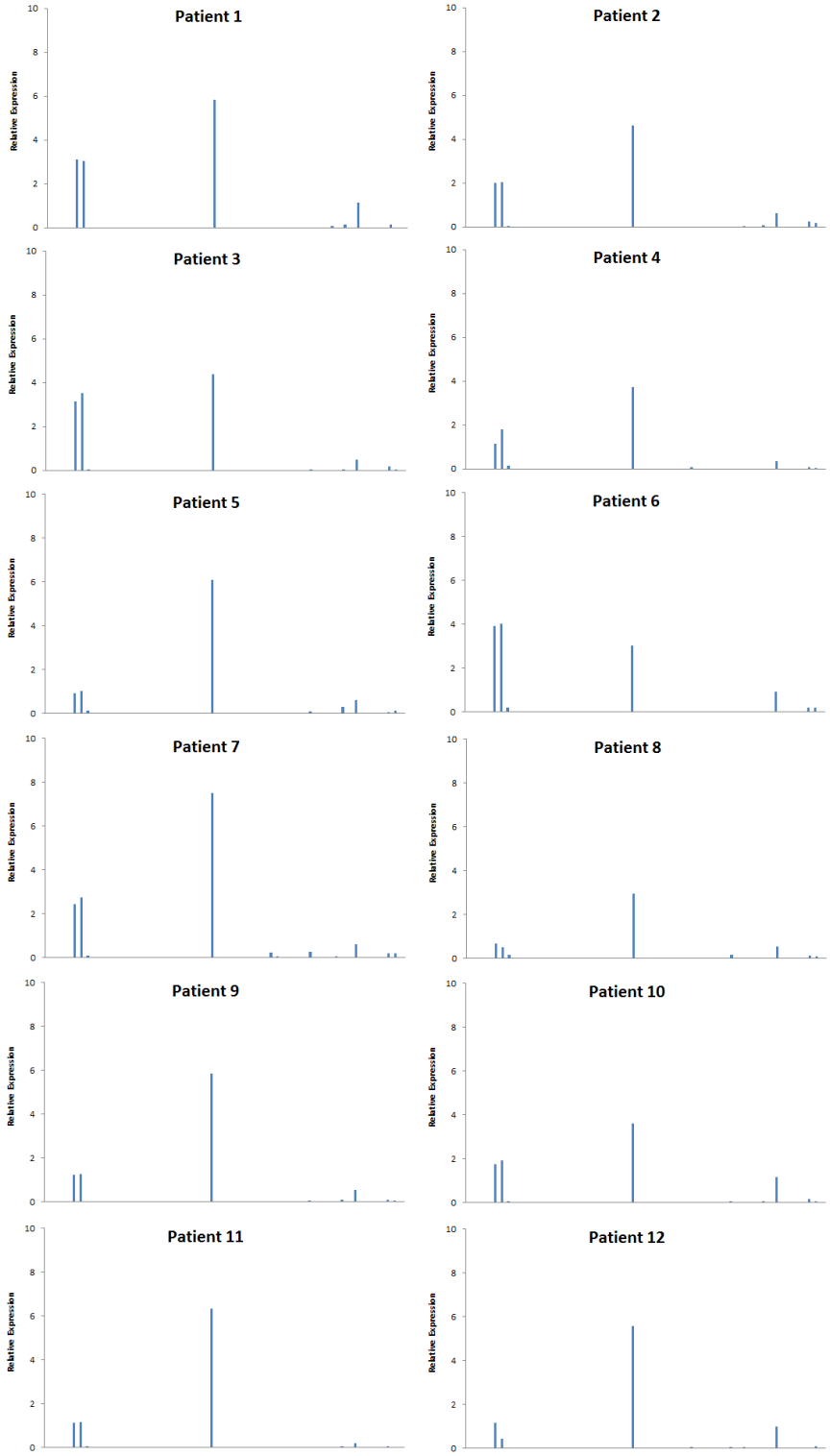

Figure B5: ***Inter-patient variability in the expression of individual miRNAs.*** *TLDA miRNA 'A' cards (Life Technologies) were used to profile the expression of 377 miRNAs in 12 colorectal cancers, as detailed in Section 2.2.9.8. The expression of the sixth set of 55 miRNAs on the TLDA card, relative to the control miRNA let-7a, is shown. Each bar represents a single point determinant of relative expression.*

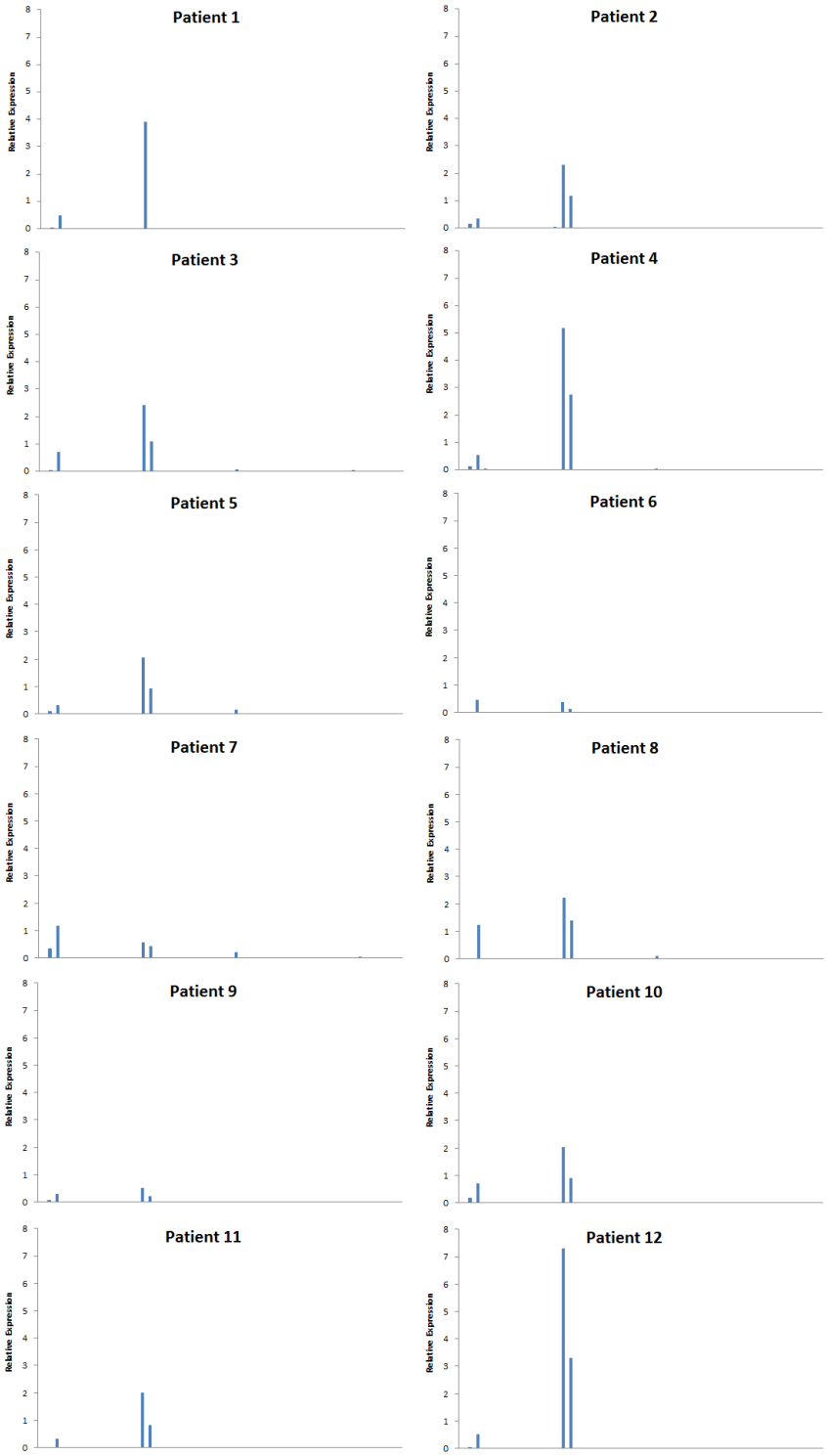

Figure B6: ***Inter-patient variability in the expression of individual miRNAs.*** *TLDA miRNA 'A' cards (Life Technologies) were used to profile the expression of 377 miRNAs in 12 colorectal cancers, as detailed in Section 2.2.9.8. The expression of the final set of 47 miRNAs on the TLDA card, relative to the control gene let-7a, is shown. Each bar represents a single point determinant of relative expression.*

Appendix C: Electropherograms generated from the 12 normal colorectal mucosa samples obtained from Tayside Tissue bank

RNA was extracted from 12 normal colorectal mucosa samples, patient-matched to colorectal cancers described in Table F1 (Appendix F). The 3 normal mucosa samples used for TLDA miRNA profiling were chosen based on their high RNA yield and integrity (RIN) relative to other samples following RNA extraction as assessed by methods described in Section 2.2.8.4. The electropherograms below were generated by the Bioanalyzer 2100 and display RNA concentration (ng/µl), the 18s and 28s ribosomal subunit ratios (28s/18s) and RNA integrity number (RIN).

In the present study, patient samples 3356 (Patient 3; RIN of 10), 3362 (Patient 4; RIN of 10) and 3371 (Patient 9; RIN of 9.8) were used due to their very high RIN. Sample 4324 (Patient 12) which also had a RIN of 10 was not used due to the low RNA concentration (44 ng/µl).

Patient 1

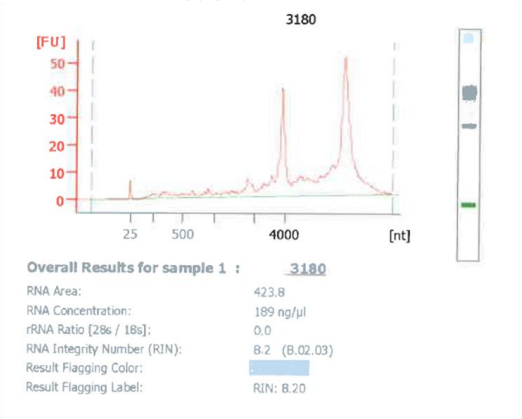

Overall Results for sample 1 : 3180

RNA Area:	423.8
RNA Concentration:	189 ng/µl
rRNA Ratio [28s / 18s]:	0.0
RNA Integrity Number (RIN):	8.2 (B.02.03)
Result Flagging Color:	
Result Flagging Label:	RIN: 8.20

Patient 2

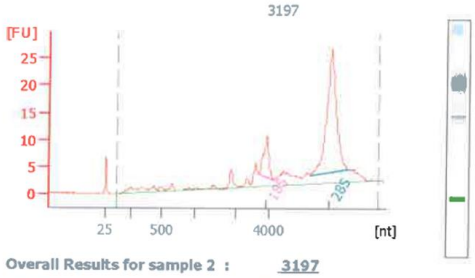

Overall Results for sample 2 : 3197

RNA Area:	163.1
RNA Concentration:	73 ng/µl
rRNA Ratio [28s / 18s]:	4.9
RNA Integrity Number (RIN):	8.8 (B.02.03)
Result Flagging Color:	
Result Flagging Label:	RIN: 8.80

Patient 3

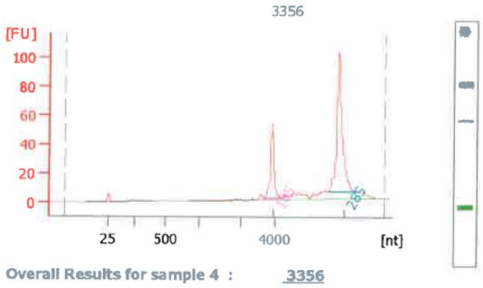

Overall Results for sample 4 : 3356

RNA Area:	318.4
RNA Concentration:	142 ng/µl
rRNA Ratio [28s / 18s]:	2.4
RNA Integrity Number (RIN):	10.0 (B.02.03)
Result Flagging Color:	
Result Flagging Label:	RIN:10

Patient 4

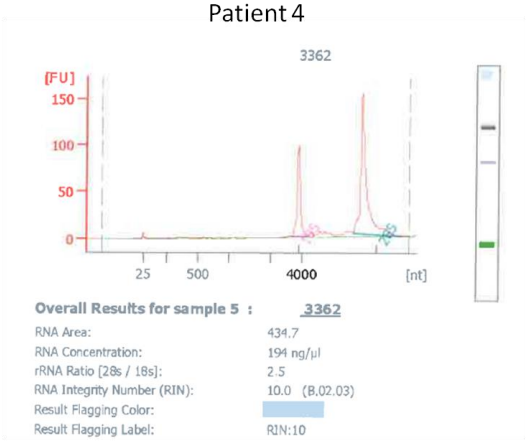

Overall Results for sample 5 :	3362
RNA Area:	434.7
RNA Concentration:	194 ng/µl
rRNA Ratio [28s / 18s]:	2.5
RNA Integrity Number (RIN):	10.0 (B.02.03)
Result Flagging Color:	
Result Flagging Label:	RIN:10

Patient 5

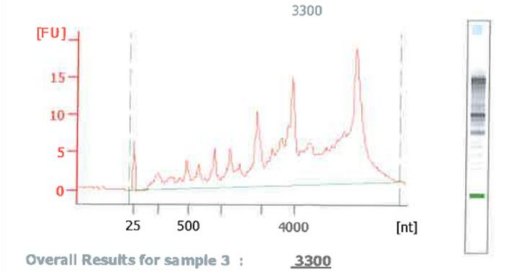

Overall Results for sample 3 :	3300
RNA Area:	294.2
RNA Concentration:	131 ng/µl
rRNA Ratio [28s / 18s]:	0.0
RNA Integrity Number (RIN):	5.2 (B.02.03)
Result Flagging Color:	
Result Flagging Label:	RIN: 5.20

Patient 6

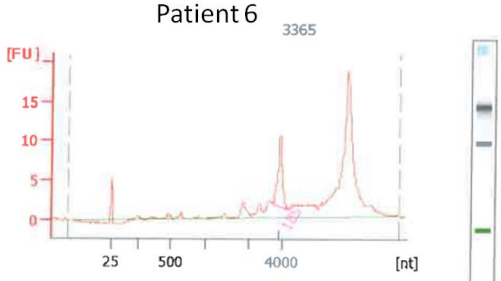

Overall Results for sample 6 :	3365
RNA Area:	112.7
RNA Concentration:	50 ng/µl
rRNA Ratio [28s / 18s]:	0.0
RNA Integrity Number (RIN):	8.7 (B.02.03)
Result Flagging Color:	
Result Flagging Label:	RIN: 8.70

Patient 7

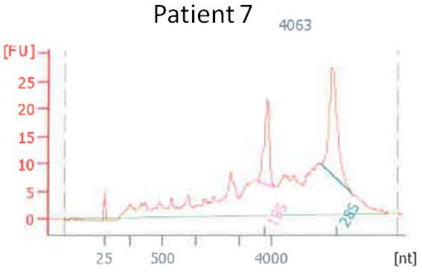

Overall Results for sample 10 : 4063

RNA Area:	403.2
RNA Concentration:	180 ng/µl
rRNA Ratio [28s / 18s]:	1.7
RNA Integrity Number (RIN):	6.3 (B.02.03)
Result Flagging Color:	
Result Flagging Label:	RIN: 6.30

Patient 8

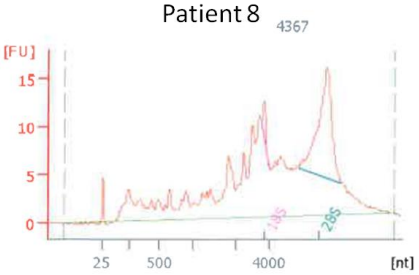

Overall Results for sample 12 : 4367

RNA Area:	327.8
RNA Concentration:	146 ng/µl
rRNA Ratio [28s / 18s]:	11.6
RNA Integrity Number (RIN):	5.9 (B.02.03)
Result Flagging Color:	
Result Flagging Label:	RIN: 5.90

Patient 9

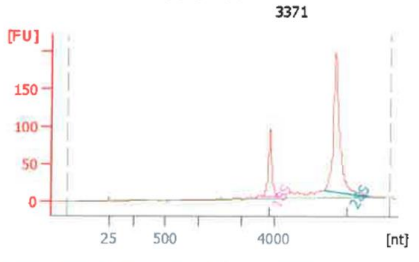

Overall Results for sample 7 : 3371

RNA Area:	675.4
RNA Concentration:	301 ng/µl
rRNA Ratio [28s / 18s]:	2.9
RNA Integrity Number (RIN):	9.8 (B.02.03)
Result Flagging Color:	
Result Flagging Label:	RIN: 9.80

Patient 10

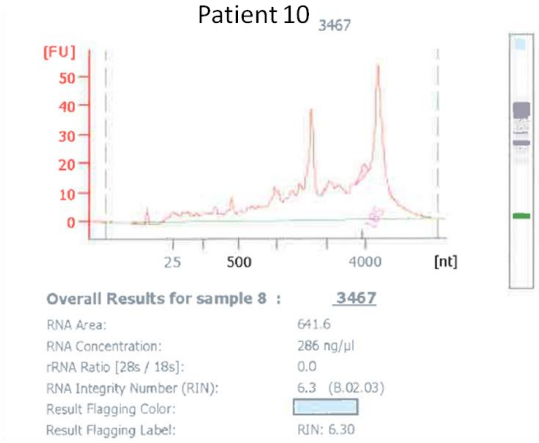

Overall Results for sample 8 : 3467

RNA Area:	641.6
RNA Concentration:	286 ng/µl
rRNA Ratio [28s / 18s]:	0.0
RNA Integrity Number (RIN):	6.3 (B.02.03)
Result Flagging Color:	
Result Flagging Label:	RIN: 6.30

Patient 11

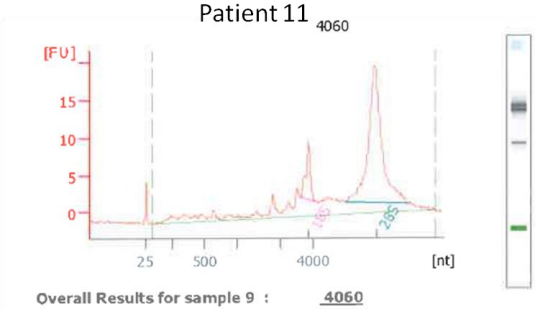

Overall Results for sample 9 : 4060

RNA Area:	172.4
RNA Concentration:	77 ng/µl
rRNA Ratio [28s / 18s]:	5.8
RNA Integrity Number (RIN):	8.9 (B.02.03)
Result Flagging Color:	
Result Flagging Label:	RIN: 8.90

Patient 12

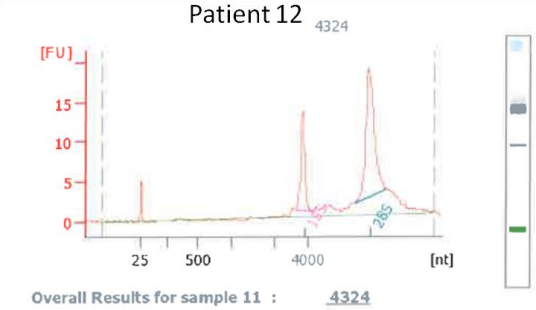

Overall Results for sample 11 : 4324

RNA Area:	99.8
RNA Concentration:	44 ng/µl
rRNA Ratio [28s / 18s]:	2.4
RNA Integrity Number (RIN):	10.0 (B.02.03)
Result Flagging Color:	
Result Flagging Label:	RIN:10

Appendix D: Electropherograms generated from the 12 colorectal adenomas obtained from Tayside Tissue bank

RNA was extracted from 12 colorectal adenoma samples that displayed low or high grades of dysplasia as described in Table D1. The six samples (3 low grade, 3 high grade) used for TLDA miRNA profiling were chosen based on their high RNA yield and integrity (RIN) relative to other samples following RNA extraction as assessed by methods described in Section 2.2.8.4. The electropherograms below were generated by the Bioanalyzer 2100 and display RNA concentration (ng/µl), the 18s and 28s ribosomal subunit ratios (28s/18s) and RNA integrity number (RIN).

In the present study, patient samples 5932 (RIN of 8.2), 5472 (RIN of 8.1) and 5284 (RIN of 7.8) were chosen from the low grade adenoma group. Patient samples 3817 (RIN of 5.3), 3904 (RIN of 8.9) and 3680 (RIN of 5.7) were chosen from the high grade adenoma group.

Table D1: List of colorectal adenomas received from Tayside Tissue Bank

Patient ID	Histology	Grade of dysplasia
2419	Tubulovillous	High
3680	Tubulovillous	High
3817	Tubulovillous	High
3904	Tubulovillous	High
4601	Tubulovillous	Low
4682	Tubulovillous	High
5284	Tubulovillous	Low
5472	Tubulovillous	Low
5918	Tubular/Tubulovillous	Low
5932	Tubular	Low
6002	Tubulovillous	Low
6301	Tubulovillous	High

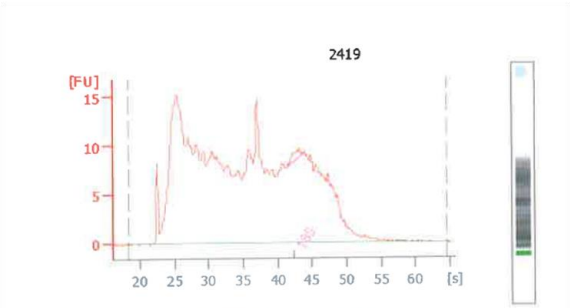

Overall Results for sample 1 : **2419**

RNA Area:	648.4
RNA Concentration:	376 ng/µl
rRNA Ratio [28s / 18s]:	0.0
RNA Integrity Number (RIN):	2.3 (B.02.03)
Result Flagging Color:	
Result Flagging Label:	RIN: 2.30

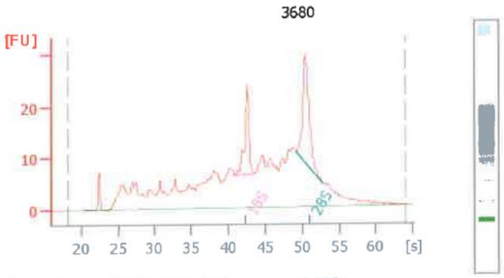

Overall Results for sample 2 : **3680**

RNA Area:	509.3
RNA Concentration:	296 ng/µl
rRNA Ratio [28s / 18s]:	1.6
RNA Integrity Number (RIN):	5.7 (B.02.03)
Result Flagging Color:	
Result Flagging Label:	RIN: 5.70

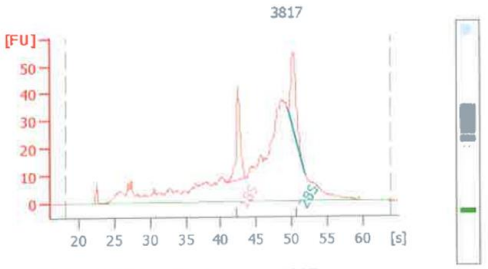

Overall Results for sample 3 : **3817**

RNA Area:	799.6
RNA Concentration:	464 ng/µl
rRNA Ratio [28s / 18s]:	0.9
RNA Integrity Number (RIN):	5.3 (B.02.03)
Result Flagging Color:	
Result Flagging Label:	RIN: 5.30

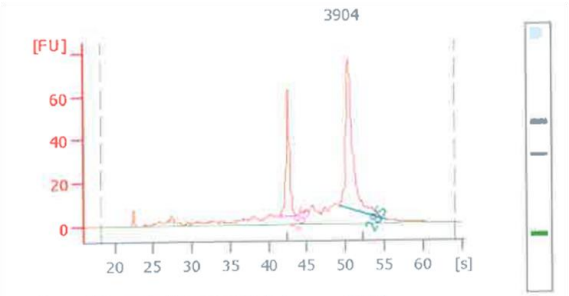

Overall Results for sample 4 : 3904

RNA Area:	482.5
RNA Concentration:	280 ng/µl
rRNA Ratio [28s / 18s]:	1.9
RNA Integrity Number (RIN):	8.9 (B.02.03)
Result Flagging Color:	
Result Flagging Label:	RIN: 8.90

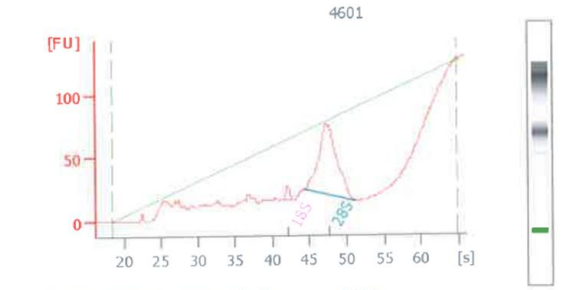

Overall Results for sample 5 : 4601

RNA Area:	0.8
RNA Concentration:	0 ng/µl
rRNA Ratio [28s / 18s]:	19.3
RNA Integrity Number (RIN):	N/A (B.02.03)
Result Flagging Color:	
Result Flagging Label:	RIN N/A

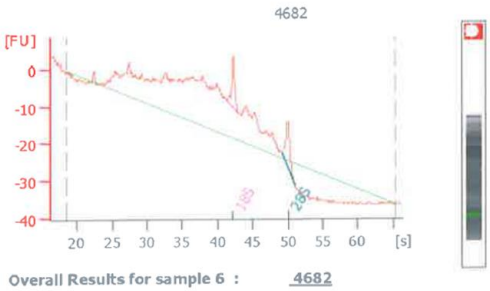

Overall Results for sample 6 : 4682

RNA Area:	584.9
RNA Concentration:	339 ng/µl
rRNA Ratio [28s / 18s]:	1.0
RNA Integrity Number (RIN):	N/A (B.02.03)
Result Flagging Color:	
Result Flagging Label:	RIN N/A

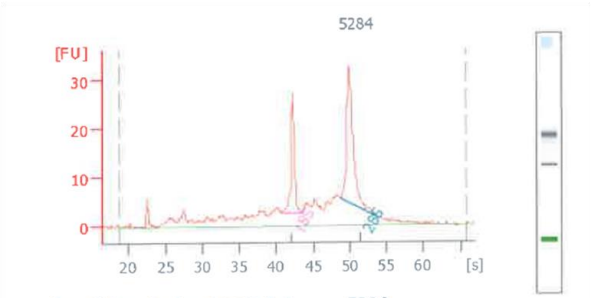

Overall Results for sample 7 : 5284

RNA Area:	292.0
RNA Concentration:	169 ng/µl
rRNA Ratio [28s / 18s]:	1.8
RNA Integrity Number (RIN):	7.8 (B.02.03)
Result Flagging Color:	
Result Flagging Label:	RIN: 7.80

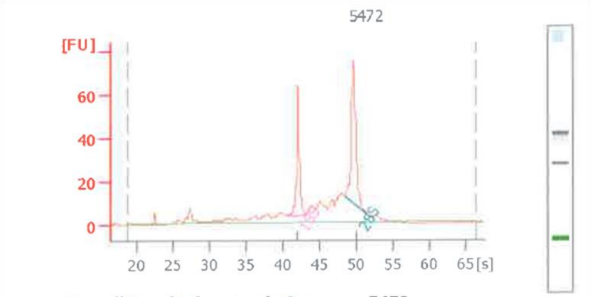

Overall Results for sample 8 : 5472

RNA Area:	460.3
RNA Concentration:	267 ng/µl
rRNA Ratio [28s / 18s]:	1.6
RNA Integrity Number (RIN):	8.1 (B.02.03)
Result Flagging Color:	
Result Flagging Label:	RIN: 8.10

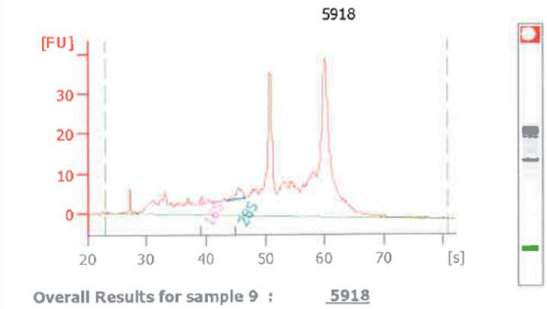

Overall Results for sample 9 : 5918

RNA Area:	495.9
RNA Concentration:	288 ng/µl
rRNA Ratio [28s / 18s]:	2.8
RNA Integrity Number (RIN):	N/A (B.02.03)
Result Flagging Color:	
Result Flagging Label:	RIN N/A

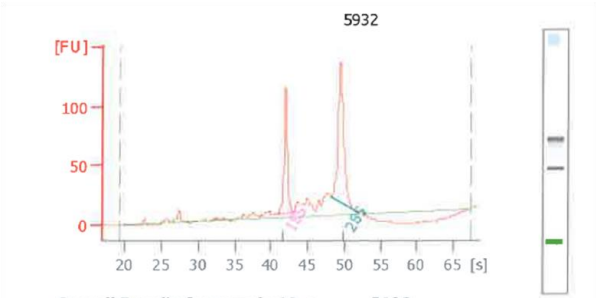

Overall Results for sample 10 : 5932

RNA Area:	631.4
RNA Concentration:	366 ng/µl
rRNA Ratio [28s / 18s]:	1.6
RNA Integrity Number (RIN):	8.2 (B.02.03)
Result Flagging Color:	
Result Flagging Label:	RIN: 8 20

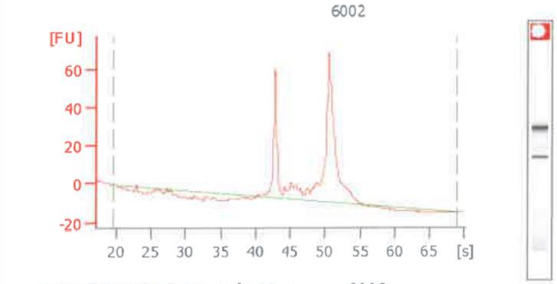

Overall Results for sample 11 : 6002

RNA Area:	381.1
RNA Concentration:	221 ng/µl
rRNA Ratio [28s / 18s]:	0.0
RNA Integrity Number (RIN):	N/A (B.02.03)
Result Flagging Color:	
Result Flagging Label:	RIN N/A

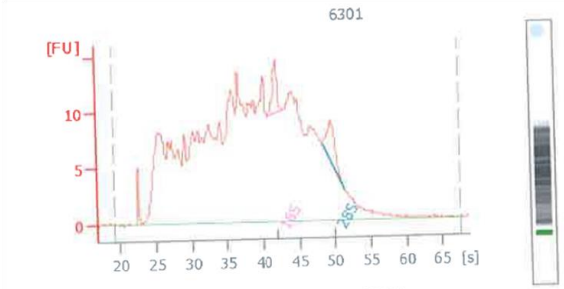

Overall Results for sample 12 : 6301

RNA Area:	641.8
RNA Concentration:	373 ng/µl
rRNA Ratio [28s / 18s]:	1.2
RNA Integrity Number (RIN):	2.9 (B.02.03)
Result Flagging Color:	
Result Flagging Label:	RIN: 2.90

Appendix F: The patient details and *KRAS/BRAF* mutation status of colorectal cancers used in the present study

Table F1: Patient details and the staging and *KRAS/BRAF* mutation status of colorectal cancers described and analysed in Section 3.3.3 (Figure 3.3)

Patient	Patient ID	Age	Sex	Dukes' Stage	TMN Stage	*KRAS/BRAF* mutation status
1	3180	76	F	B	T3 N0 MX	WT
2	3197	83	M	C	T3 N1 MX	WT
3	3356	78	M	B	T4 N0 MX	WT
4	3362	63	F	A	T1 N0 MX	WT
5	3300	72	F	B	T3 N0 MX	*BRAF* mutant
6	3365	74	M	C1	T4 N2 MX	*BRAF* mutant
7	4063	85	F	B	T3 N0 MX	*BRAF* mutant
8	4367	87	F	C1	T4 N1 MX	*BRAF* mutant
9	3371	69	F	C	T3 N2 MX	*KRAS* mutant
10	3467	71	M	B	T3 N0 MX	*KRAS* mutant
11	4060	54	M	A	T1 N0 MX	*KRAS* mutant
12	4324	69	F	C1	T3 N2 MX	*KRAS* mutant

Colorectal cancers and matched normal mucosa from patients 3, 4 and 9 used for TLDA analysis

Table F2: Patient details and the staging and *KRAS/BRAF* mutation status of colorectal cancers described and analysed in Section 3.3.3 (Figure 3.4)

Patient ID	Age	Sex	Dukes' Stage	TMN Stage	*KRAS/BRAF* mutation status
3605	65	M	C1	T4 N1 MX	WT
4036	79	F	B	Not known	WT
4124	53	F	B	T3 N0 MX	WT
4216	82	M	B	T3 N0 MX	WT
4223	80	F	B	T3 N0 MX	WT
4248	83	F	C2	T4 N2 MX	WT
4257	68	F	A	T2 N0 MX	WT
4327	76	M	A	T2 N0 MX	WT
4388	75	F	C	T4 N1 MX	WT
4431	78	F	B	T4 N0 MX	WT
3433	81	F	B	T3 N0 MX	*BRAF* mutant
3828	79	M	C	T3 N1 MX	*BRAF* mutant
4335	76	M	B	T3 N0 MX	*BRAF* mutant
4562	63	F	B	T3 N0 MX	*BRAF* mutant
4576	60	M	B	T3 N0 MX	*BRAF* mutant
3143	63	M	B	T3 N0 MX	*KRAS* mutant
3216	75	M	C1	T3 N1 MX	*KRAS* mutant
3462	79	F	B	T3 N0 MX	*KRAS* mutant
3686	82	M	C	T4 N2 MX	*KRAS* mutant
3759	80	F	C1	T3 N1 MX	*KRAS* mutant
3829	74	M	C	T3 N1 MX	*KRAS* mutant
4076	83	F	B	T2 N0 MX	*KRAS* mutant
4113	82	M	C	T4 N1 MX	*KRAS* mutant
4238	64	F	C	T3 N1 MX	*KRAS* mutant
4349	73	M	C1	T2 N1 MX	*KRAS* mutant
4392	83	F	C1	T3 N1 MX	*KRAS* mutant
4426	88	F	B	T3 N0 MX	*KRAS* mutant
4439	47	F	B	T3 N0 MX	*KRAS* mutant
4467	77	M	B	T3 N0 MX	*KRAS* mutant

Appendix L: Pathways and processes associated with differentially expressed genes in drug resistant cells

Table L1: Pathways and processes associated with genes under-expressed in both 5-FU and oxaliplatin resistant DLD-1 cells

	Pathway Name	p value	Ratio
1	Cell cycle_Role of APC in cell cycle regulation	5.10E-09	17/31
2	Cell cycle_Start of DNA replication in early S phase	4.62E-08	16/31
3	Cell cycle_Spindle assembly and chromosome separation	4.62E-08	16/31
4	Cell cycle_Chromosome condensation in prometaphase	2.64E-07	12/20
5	Cell cycle_Role of Nek in cell cycle regulation	5.49E-07	14/28
6	Cell cycle_The metaphase checkpoint	2.56E-06	15/35
7	LRRK2 in neurons in Parkinson's disease	4.14E-06	14/32
8	Cell cycle_Role of 14-3-3 proteins in cell cycle regulation	9.46E-06	11/22
9	dATP/dITP metabolism	1.33E-05	18/53
10	ATP/ITP metabolism	1.50E-05	24/84

	Process Name	p value	Ratio
1	Cell cycle_Mitosis	1.07E-16	60/174
2	Cell cycle_Core	1.85E-15	45/113
3	Cell cycle_S phase	1.93E-13	49/145
4	Cell cycle_G2-M	1.09E-12	59/203
5	Translation_Translation initiation	2.48E-12	50/159
6	Cytoskeleton_Spindle microtubules	7.20E-08	32/106
7	Cell cycle_G1-S	6.17E-07	40/161
8	DNA damage_DBS repair	1.09E-06	30/107
9	DNA damage_Checkpoint	1.16E-06	33/124
10	Cytoskeleton_Intermediate filaments	1.25E-05	23/80

Table L2: Pathways and processes associated with genes over-expressed in both 5-FU and oxaliplatin resistant DLD-1 cells

	Pathway Name	p value	Ratio
1	Protein folding and maturation_Angiotensin system maturation	1.20E-04	9/31

	Process Name	p value	Ratio
1	Signal transduction_Leptin signaling	1.75E-04	15/86

Table L3: Pathways associated with genes under-expressed in both 5-FU and oxaliplatin resistant HCT116 cells

	Pathway Name	p value	Ratio
1	Development_Role of IL-8 in angiogenesis	4.10E-05	4/52
2	G-protein signaling_G-Protein alpha-i signaling cascades	8.77E-05	3/23
3	Transport_ACM3 in salivary glands	1.00E-04	3/24
4	Transport_Alpha-2 adrenergic receptor regulation of ion channels	1.60E-04	3/28
5	Regulation of lipid metabolism_Regulation of lipid metabolism via LXR, NF-Y and SREBP	1.78E-04	3/29
6	Membrane-bound ESR1: interaction with G-proteins signaling	3.15E-04	3/35
7	Muscle contraction_Relaxin signaling pathway	3.72E-04	3/37
8	Amitraz-induced inhibition of Insulin secretion	4.10E-04	2/8
9	Regulation of lipid metabolism_Insulin regulation of fatty acid metabolism	5.82E-04	3/43

No significantly associated processes

Table L4: Pathways associated with genes over-expressed in both 5-FU and oxaliplatin resistant HCT116 cells

	Pathway Name	p value	Ratio
1	Cell adhesion_ECM remodeling	2.20E-06	6/51
2	Transcription_Role of AP-1 in regulation of cellular metabolism	2.02E-04	4/38
3	Immune response_IL-1 signaling pathway	3.29E-04	4/43
4	Regulation of lipid metabolism_Stimulation of Arachidonic acid production by ACM receptors	4.27E-04	4/46

	Process Name	p value	Ratio
1	Proteolysis_Connective tissue degradation	2.19E-05	7/119
2	Inflammation_Kallikrein-kinin system	6.27E-05	7/140
3	Reproduction_Feeding and Neurohormone signaling	9.04E-05	8/201
4	Proteolysis_ECM remodeling	3.27E-04	5/83
5	Inflammation_Amphoterin signaling	1.34E-03	5/113
6	Cell cycle_G1-S Interleukin regulation	1.89E-03	5/122
7	Immune response_Th17-derived cytokines	3.09E-03	4/83